Author:
Ince, Rachel Jane

Title:
Sensitivity and temporal resolution of the eyes of mesopelagic and coastal malacostracans.

SENSITIVITY AND TEMPORAL RESOLUTION OF THE EYES OF MESOPELAGIC AND COASTAL MALACOSTRACANS

Rachel Jane Ince

School of Biological Sciences

University of Bristol

A dissertation submitted to the University of Bristol in accordance with the requirements of the degree of Doctor of Philosophy in the Faculty of Science

December 2001

Word count: 70,658.

ABSTRACT

Visual sensitivity and temporal resolution can be related to species' visual ecology. This thesis describes measurements of the sensitivities and temporal resolving powers of the compound eyes of mesopelagic and shallow-water, marine malacostracan crustaceans, and relates these to aspects of their visual ecology. Mesopelagic and coastal species are compared because they inhabit environments with quite different optical properties. Mesopelagic species inhabit an unique light environment typified by dim shortwave sunlight and bioluminescence, and little is known of the visual behaviour of these animals due to difficulties in observing these animals *in situ* under natural conditions. Extracellular electrophysiology is used to record electroretinograms (ERGs) from the eyes of mesopelagic and coastal malacostracans to assess both the relative sensitivities of the eyes, and the speed of the visual response to light stimuli with different temporal properties. This thesis includes discussion of the technical problems associated with ERG recordings from mesopelagic animals at sea, the technical problems associated with producing sinusoidal light output from an LED, and the use of the impulse response methods to determine temporal resolution, making this the first study to use such a methodology on mesopelagic animals. Visual sensitivity and temporal resolving power of the eyes of both mesopelagic and coastal malacostracan species can be related to the light environments inhabited by these animals. Visual sensitivity is not always correlated with temporal resolving power for the mesopelagic species studied, and this may be explained by the visual requirements of hunting bioluminescent prey.

Dedicated to Len

ACKNOWLEDGEMENTS

Sincere thanks to Julian Partridge for his guidance, support and advice during my four years in Bristol.

Many thanks also to Peter Shelton, Ted Gaten and Peter Herring for their expert advice and encouragement throughout my Ph.D.

Thank you to Tammy Frank, Edie Widder and Jose Torres for allowing me to participate in their cruises. A special thank you goes to Tammy Frank for her generosity in sharing her expertise, and providing both support and friendship during my Ph.D. Thank you also for reassuring me that making successful ERG recordings at sea is possible!

This work would not have been possible without the Captains and crew of the RRS Discovery, the R/V Edwin Link, the R/V Pelican and the R/V Seadiver, all of whom helped to make my sea-going experiences unforgettable. A large proportion of this Ph.D. involved assembling and maintaining electrophysiological equipment and I have to express my gratitude to Linda Teagle, Steve Soffe, Paul Chappell and Dave Edge for their technical advice and assistance.

Thank you to Stuart Church for advice on statistical analysis and thank you to Stuart Parsons for his help with Matlab programming and advice on digital signal processing.

The Vision Group at Bristol have shared both their knowledge and good humour with me throughout my Ph.D. Liz White and Kate Buchanan deserve a special mention for keeping me sane (ish) and for continuously supplying tea and coffee.

Thank you to my friends for maintaining my sense of humour and self-esteem, you are all brilliant, and special thanks to Liz Smith for her solid friendship, great sense of humour and unending support over the past four years.

Thanks to Mum, Dad and Andrew, for their undeviating support and encouragement, and for consistently reminding me that anything is possible providing you are prepared to work hard for it!

And finally, thank you Barry, for your strength, tolerance, support, and love, throughout the past 7 years.

The work in this thesis was supported by NERC (grant GR3/A1212).

AUTHOR'S DECLARATION

I declare that the work in this dissertation was carried out in accordance with the Regulations of the University of Bristol. The work is original except where indicated by special reference in the text and no part of the dissertation has been submitted for any other degree.

Any views expressed in the dissertation are those of the author and in no way represent those of the University of Bristol.

The dissertation has not been presented to any other University for examination either in the United Kingdom or overseas.

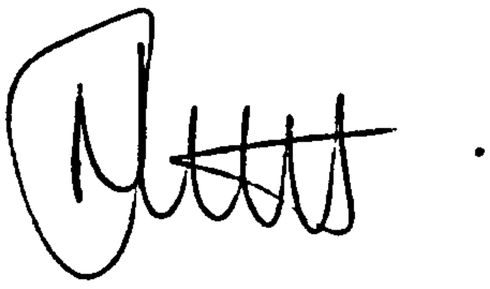

Rachel Jane Ince

December 2001

TABLE OF CONTENTS

CHAPTER 1: GENERAL INTRODUCTION

1.1 An Introduction to Vision

Sensory systems are vital to animals, enabling them to interact with their environment. Vision allows animals to detect, perceive and identify objects within their environment: for example, to judge potential threats from predators, to capture prey, or to find a mate. A light source is fundamental to vision and the sun is the primary source of this light. Moonlight and starlight contribute to illumination during the night, but these light sources are in the order of 6-9 log units less bright than sunlight (Dusenbery, 1992). The spectral composition and distribution of sunlight can be quite different within different habitats, depending on the particulate matter present, as this matter will preferentially absorb and scatter different wavelengths of electromagnetic radiation. This is reflected in the fact that there is a wide diversity of eye types in the animal kingdom, with differing optical structures to optimise vision according to both behavioural requirements and the light environment inhabited.

The laws of optics govern vision in all animals and this prevents the visual sense from being infinitely versatile. Every animal's visual sense has to function within the same set of rules, and so the more fundamental mechanisms of the visual process differ only in detail across the animal kingdom (Lythgoe, 1979). Consequently, although there is a wide diversity of optical mechanisms adopted by different animals, they all function in accordance with the nature of light, for example, they are all ultimately limited by diffraction and spherical and chromatic aberration. Under circumstances in which there is a shortage of available light (for example in the deep-sea or at night), the visual systems of animals show various adaptations (e.g. sensitivity and acuity, see sections *1.5.4-1.5.6*) in order to maximise sensitivity to light.

1.1.1 Why study Crustacean vision?

There are in excess of 30,000 known species within the subphylum Crustacea, and the majority of these species are aquatic, inhabiting marine, brackish and freshwater environments. Different aquatic environments experience different mean intensities and spectral distributions of ambient light (see section *1.2, 1.3* and *1.4* for examples), which impose specific requirements on the visual systems of animals inhabiting these environments. The Crustacea

are a very diverse group of animals in terms of habitats occupied and this is reflected in the diversity of morphology seen within this group. Land (1984) states "there is a much greater diversity of eye types in the Crustacea than in the insects or any other invertebrate group"; several different eye design 'strategies' are found within the subphylum Crustacea. Marine crustaceans are found with functional visual systems in habitats ranging from the rocky shore to the ocean floor (at depths of 5,000 metres or more below sea level); providing an opportunity for a comparative study of aspects of the vision of crustacean species that differ in their ecology.

1.2 The Aquatic Photic Environment

1.2.1 Electromagnetic radiation

The sun emits vast amounts of electromagnetic radiation that travels in waveforms to our atmosphere. The electromagnetic spectrum of radiation emitted by the sun comprises photons with frequencies ranging from 10^3 to 10^{22} Hz (Campbell and Dwek, 1984, from Partridge and Cummings, 1999). When we refer to 'light' we generally consider those frequencies of electromagnetic radiation that are visible to humans, *ca.* $7.5x10^{14}$ and $4.3x10^{14}$ Hz, equivalent to wavelengths in a vacuum of 400-700nm (Partridge and Cummings, 1999). However, the spectral sensitivities of the eyes of other animals extend into the ultra-violet, i.e. 300-400nm, and into the near infrared i.e. wavelengths of *ca.* 800nm (Partridge and Cummings, 1999). Generally, the wavelengths that animals can detect are related to the spectrum of light available in their habitat, and also their requirements of perception (see section *1.6.2*). As light passes through the earth's atmosphere it is scattered and absorbed by particles in the air, and thus its spectral distribution is altered to an extent dependent on factors such as altitude, solar elevation, season, latitude, and weather conditions (Partridge and Cummings, 1999).

1.2.2 The air-water interface

Light reaching the air-water interface of a water body is reflected and refracted. Reflection of light with an angle of incidence of less than 45° at the water surface is low, and only approximately 2% of this light is reflected (Sathyendranath and Platt, 1990). However, as the

angle of incidence becomes more than 45°, reflection increases until reflection becomes total (Sathyendranath and Platt, 1990).

Light not reflected at the water surface is refracted due to the difference in the refractive indices of air (1.00) and water (1.33). The refraction of light at the air-water interface forces the angular distribution of light entering the water to a solid angle of 97° (Partridge, 1990). This angle is referred to as Snell's window as it is predicted using Snell's Law. Snell's Law is a simple formula used to calculate the refraction of light travelling between two media of differing refractive indices and is given below:

$$\frac{n_1}{\sin(\theta_1)} = \frac{n_2}{\sin(\theta_2)}$$

where:

θ_1 is the angle of incidence of a light ray at the interface between the media of differing refractive index (n_1 and n_2),

θ_2 is the angle of refraction of a light ray as it passes through the interface between the media.

In calm water, therefore, an animal just below the surface looking upwards will see the entire above-water hemisphere within a 97° solid angle (a rough sea surface will degrade the boundaries of Snell's window). Outside this angle, the animal will only see reflections from the sea beneath it, due to total internal reflection at the water surface (Partridge, 1990). Snell's window therefore causes discontinuity in both the brightness and the spectral distribution of light available to an animal living just below the water surface. The light penetrating through the water surface within Snell's window will have a relatively broad spectral distribution and high irradiance compared with light that is reflected from deeper water (Partridge, 1990). The angle of Snell's window remains constant with increasing depth, but scattering of light by water molecules and particles in the water degrades the boundaries of the window and the radiance distribution becomes increasingly symmetrical about the vertical axis (see *1.2.3*). These effects are apparent at as little as 1m depth from the surface in turbid water, and *ca.* 40m in clear ocean water (Lythgoe, 1979).

1.2.3 Radiance distribution of light underwater

Just below the surface of the water, the sun has a strong influence on the underwater radiance distribution of light and it is slightly asymmetrical (see Fig. 1.1). Radiance is defined as "radiant flux at that point in a given direction per unit solid angle per unit area at right angles to the direction of propagation" (Kirk, 1994) and is given in units of watts per square metre per steradian (a steradian is the S.I. unit of solid angle enclosing a surface on a sphere equal to the square of the radius of the sphere). However, with increasing depth the radiance distribution becomes increasingly symmetrical around the vertical axis, as a result of both absorption and scatter of light by particles in the water (see Fig. 1.1). As depth increases the radiance distribution of light eventually reaches an asymptotic radiance distribution around the vertical axis (Kirk, 1994; Partridge, 1990). Thus with increasing depth the radiance distribution of light in the water column becomes uniform about the vertical axis.

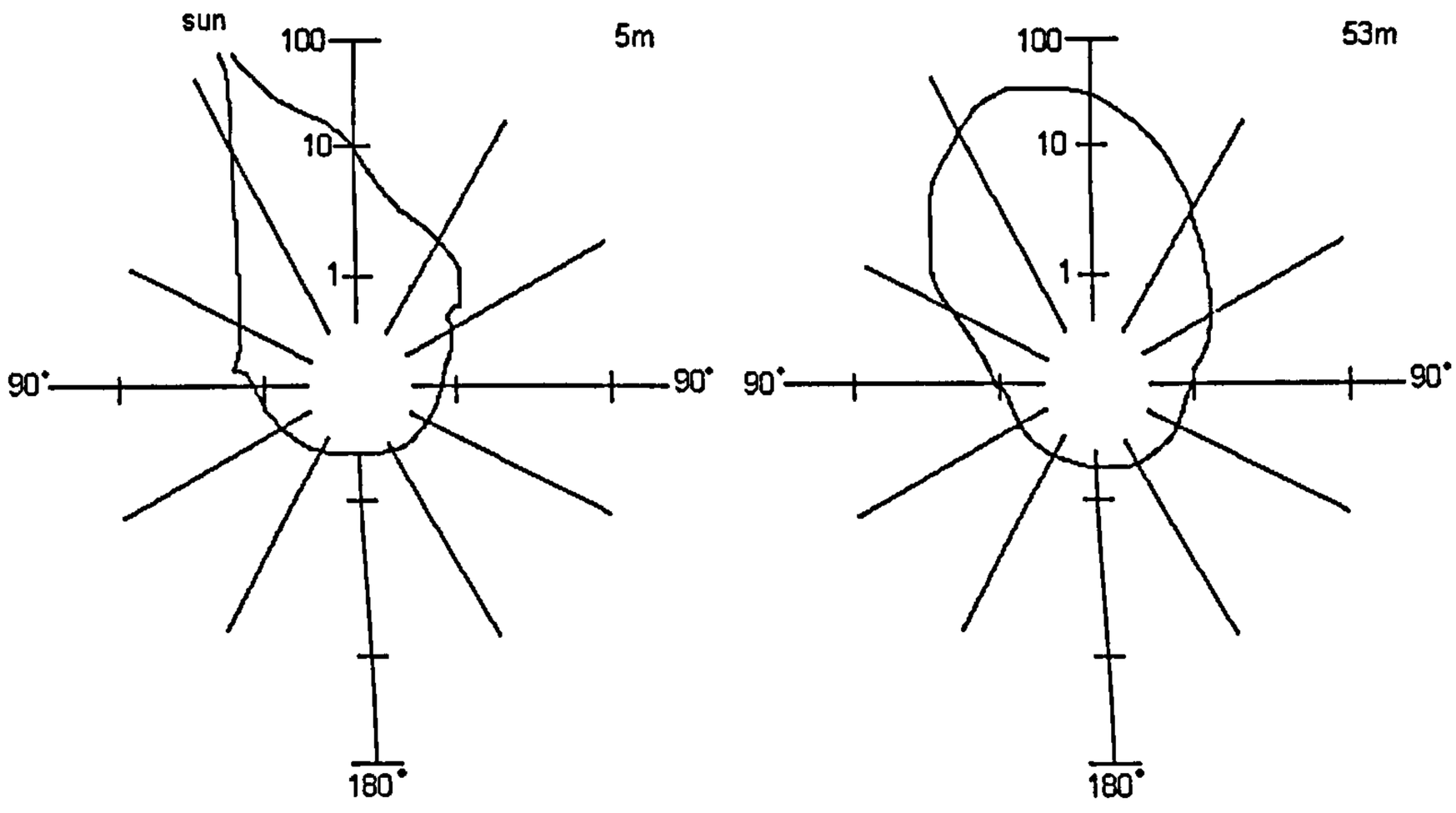

Figure 1.1. The angular distribution of sunlight just below the water surface (5m) and at greater depth (53m). The logarithmic scales on the axes indicate relative radiance, normalized for horizontal light in one direction. At a depth of 5m, the position of the sun in the sky has a marked effect on the angular distribution of light, causing an asymmetrical distribution with 'shoulders' that mark the edge of Snell's window. At a depth of 53m it is clear that neither the sun nor Snell's window have a dramatic effect on the angular distribution of light, scatter and selective absorption of light in the water leads to a symmetrical angular distribution of light, and at 53m the angular distribution of light is approaching it's asymptotic distribution (redrawn from Partridge, 1990, data obtained from Smith, 1974, cited in Partridge, 1990).

1.2.4 Spectral composition of light in water

Light is scattered and selectively absorbed during its passage through air. This also occurs as light passes through water, but to a much greater extent, such that light is attenuated rapidly with depth in the ocean. Attenuation of light in water has "visually significant effects over a few metres path length (Duntley, 1962, 1963)" (Partridge and Cummings, 1999). Absorption and scattering have significant effects on both the spatial (radiance) distribution of light in deep water (see section *1.2.3*), and also on the spectral composition of light in the water. Three principle factors absorb and scatter light underwater: 1) water itself (water molecules), 2) chlorophyll, and 3) the breakdown products of plants, known variously as Gelbstoffe, yellow substances, gilvins or Dissolved Organic Matter (Partridge, 1990). The relative contribution of each of the above in an aquatic environment affects the light transmission of the spectral irradiance at depth (irradiance is defined as the "radiant flux per unit area of a surface" [Kirk, 1994] and has units of photons s^{-1} cm^{-2}). "Differences in the colour of littoral seas are common because dissolved and particulate materials change with time and vary geographically, modifying the extinction properties of these seas" (McFarland and Munz, 1975). In coastal waters or inland freshwater lakes, where phytoplankton is dense and there is run-off from the land, the proportions of chlorophyll and Gelbstoffe are high enough to dominate the spectral irradiance of the water. Such bodies of water appear green or yellow as the chlorophyll and Gelbstoffe selectively reflect the wavelengths that appear green and yellow respectively, and those wavelengths of light that we perceive as blue[1] are strongly attenuated as they are absorbed by phytoplankton pigments (Kirk, 1994; Partridge and Cummings, 1999). In pure water, open oceans or tropical seas, where productivity is low and there is less particulate matter in the water, it is predominantly water molecules that affect the composition of light. Water molecules absorb long wavelength (red) light strongly and therefore red light is attenuated rapidly. However, these waters are 'transparent' to blue wavelengths and blue light penetrates deeply, thus oligotrophic waters tend to appear blue (McFarland and Munz, 1975; Kirk, 1994; Partridge, 1990).

---

[1]Wavelengths are often referred to in terms of the colour perceived when they are reflected from a given surface. Whilst there may be reference in this thesis to coloured wavelengths it is acknowledged that this terminology should be used with care, as wavelengths are not coloured, "if at any time I speak of Light and Rays as coloured or endued with colours, I would be understood to speak not philosophically and properly, but grossly, and accordingly to such conceptions as vulgar People...." (Newton, cited in Wright, 1967).

In order to divide coastal and open ocean waters on the basis of their spectral transmission, Jerlov (1976) devised a classification system with associated attenuation data. Open ocean water is classified into five types, types I, IA, IB, II and III based on differences in spectral transmittance of downward irradiance at high solar altitudes (Jerlov, 1976). The shapes of the spectral transmittance curves for these five water types are similar (i.e. they have similar wavelengths of maximum transmission). However, the spectral transmittance of these water types differs in the extent of attenuation at specific wavelengths. For example, type I oceanic water has relatively high transmission at a wavelength of 475nm, as does type III oceanic water, however, type I water transmits 98.2% of light at this wavelength, whereas type III water transmits just 89% of light at this wavelength (Jerlov, 1976). Therefore it may be stated that water types IA, IB, II and III become progressively less transparent to light in the order that they are written here. Jerlov (1976) also classified coastal water into five types (J1,3,5,7,9), again based on the spectral transmittance of the water. For these coastal waters, the wavelength of maximum transmission ranges from approximately 550nm for type 1 coastal water to 600nm for type 9 coastal water (Jerlov, 1976).

Although this classification system is now over 20 years old it is still used in generalized descriptions of the transmission properties of water bodies. However, the spectral transmittance curves generated by Jerlov (1976) were calculated using attenuation coefficients that were determined for surface waters, and thus may not be relevant to downwelling spectral irradiance at depth (where there is less phytoplankton, for example). Recent advances in technology have allowed *in situ* measurements of the spectrum of downwelling irradiance at depth in the ocean and thus direct quantification of the downwelling spectral irradiance. However, few such measurements have been made, and data are only available for certain locations: e.g. type IA water, Northwest Providence Channel, Bahamas (Frank and Widder, 1996); type IB, Wilkinsons Basin, Gulf of Maine (Frank and Widder, 1997); type IB water, Oceanographers Canyon, Gulf of Maine (Widder and Frank, 2001).

1.3 The Light Environment of the Open Ocean

In the open ocean, downwelling light from the sun is strongly attenuated with depth; below 200m depth in the clearest tropical water (Jerlov type I), there is approximately a one tenth decrease in downwelling light intensity for every 75m increase in depth (Jerlov, 1976; Denton,

1990). At a depth of 1000 metres (even in the clearest ocean water), the absolute threshold of vision during daylight (when viewing downwellling light) for deep-sea fish is reached (Denton, 1990). Below 200m the light environment becomes progressively more monochromatic. Wavelengths outside the range 430 to 530nm are preferentially absorbed and scattered leading to a relatively narrow waveband of light in the open ocean (Denton, 1990). The wavelength of maximum transmission at a depth of 200m in clear oceanic water (Jerlov type I) is *ca.* 460nm (Jerlov, 1976). It is important to note that although the light environment in the open ocean becomes both increasingly monochromatic and symmetrical about the vertical axis with depth, those organisms living in the mid-water do not experience even illumination over their three-dimensional space. The levels of irradiance vary depending on the direction of viewing, i.e. upward irradiance (generated by the back-scatter of downwelling irradiance) is only about 0.5% of vertical downwelling irradiance, and horizontal irradiance (generated from the scatter of photons in the water) is only 3% of vertical downwelling irradiance (Denton, 1990). Consequently animals inhabiting the mid-water environment may be conspicuous as a silhouette when viewed from below against the relatively bright downwelling irradiance.

For epipelagic animals (inhabiting depths between the surface and 200m), downwelling irradiance levels are high, which is reinforced by the presence of phytoplankton up to depths of 150m. For mesopelagic animals (inhabiting depths of 200-1000m), the level of downwelling irradiance available for vision is strongly dependent on the daytime depth range inhabited. These animals are also exposed to bioluminescence as a visual stimulus (see section *1.3.1*) and the relative importance of downwelling light and bioluminescence to vision for mesopelagic animals varies depending depth distribution, the time of day and solar elevation (Herring and Roe, 1988). For bathypelagic animals (inhabiting depths greater than 1000m) ambient light is too low to be useful in vision (Denton, 1990), and bioluminescence becomes the most important light source in this environment. The fact that there are bathypelagic animals with functioning visual systems indicates the importance of bioluminescence as a light source for vision.

1.3.1 Bioluminescence

Many oceanic organisms are capable of generating their own light through bioluminescence. Bioluminescence emitted as point sources, or diffusely, becomes equal to or is more intense

than ambient light as depth increases (Clarke and Wertheim, 1956, from Hiller-Adams and Case, 1984). In the mesopelagic zone (200-1000m), bioluminescence is very common, for example approximately 79% of malacostracan decapod species are bioluminescent (Herring, 1976). Studies of marine bioluminescence spectra (Herring, 1983; Widder *et. al.*, 1983) show that the wavelength of bioluminescent peak emission of mesopelagic decapod shrimps ranges from 440nm-490nm. Therefore, this emission is well matched to the spectral distribution of ambient light in the mesopelagic environment.

Certain species of mesopelagic malacostracan use bioluminescent emissions from photophores distributed on the ventral surface for purposes of camouflage. Those shrimps that possess ventral photophores (e.g. *Sergestes similis*) are able to dynamically match diffuse photophore emission with the intensity and spectral content of downwelling light (Warner *et al.* 1979; Lindsay *et al.* 1999). The result is that these animals become camouflaged against the relatively bright downwelling light and therefore are not conspicuous when viewed from beneath. Other forms of bioluminescent emission include diffuse defensive secretions (exuded to confuse the predator and so aid escape) and point source flashes (that may be used in signalling and congener recognition; Herring, 1976, 1983). The spatial and temporal pattern of light production depends on the function of the signal in communication. In fireflies, for example, the temporal pattern of long and short flashes is species-specific to ensure conspecific mating (Lloyd, 1983, from Bradbury and Vehrencamp, 1998), and shallow-water ostracod crustaceans (*Vargula* spp.) use complex bioluminescent patterns in (presumably) mating displays (Herring, 2000a). It is likely, therefore, that equivalent communication systems have evolved in the deep-sea.

1.3.2 Diel vertical migration

Bioluminescent signalling may also play a role in vertical migration as bioluminescent emissions may aid in guiding congeners in vertical migrations (Frank and Case, 1988a). Diel vertical migrations within the ocean involve mostly mesopelagic and some shallow living bathypelagic organisms, which move *en masse* towards the surface at night to feed in the relatively productive shallower waters under the cover of darkness. Vertical migrations begin before sunset and can involve such numbers that sonic scattering layers are formed, which are detectable on shipboard sonar systems (Frank and Widder, 1997). The diel migration involves

animals moving from depth to the surface after sunset and returning back to depth as sunrise approaches. It is generally accepted that light is a 'cue' for vertical migrations, but the actual characteristics of the light field in the mesopelagic zone that trigger the migrations are not yet known (Frank and Widder, 1997).

1.4 The Coastal Shallow-water Light Environment

Animals inhabiting shallow, coastal waters are potentially exposed to large diurnal changes in light intensity, and during the daytime, habitats such as estuaries and the intertidal zone will have relatively high levels of irradiance, as attenuation with depth is not an issue. However, in estuarine habitats light can be strongly attenuated due to high concentrations of suspended sediment particles (Kirk, 1994). Estuaries are dynamic habitats, and therefore the turbidity of the water can vary longitudinally along the estuary (Kirk, 1994). Similarly, in coastal waters, wave action can stir up sediment and increase levels of suspended sediment, which can increase the turbidity of the water. Forward *et al.* (1988) have measured the downwelling quantal irradiance spectra in estuarine and coastal waters of the Newport River estuary (North Carolina, USA) under various conditions of rainfall and tidal cycle. Bottom measurements at midday during normal rainfall from two stations in the estuary (upper estuary and lower estuary) and from two offshore stations (2.5 and 4.5km offshore) reveal that water clarity increases upon moving from the highest point in the estuary to the furthest point offshore (Forward *et al.* 1988). In terms of spectral transmission, it was found that spectral irradiance at the top of the estuary (furthest from the sea) is maximum at wavelengths between 570 and 700nm (Forward *et al.* 1988). This is dependent on the weather conditions as increased rainfall leads to increased run-off from the land and spectral irradiance is pushed to longer wavelengths (700nm) due to higher concentration of Gelbstoffe in the water (Forward *et al.* 1988, see section *1.2.4*). In near shore coastal waters spectral irradiance was greatest between 500 and 570nm, again depending on weather conditions (Forward *et al.* 1988). Consequently there is a progressive shift from transmission of relatively longer wavelengths at the highest point in the estuary to shorter wavelengths in the coastal waters. Spectral irradiance measurements made at twilight in estuary waters show a significant shift in wavelengths of maximum transmission to shorter wavelengths and the downwelling irradiance spectrum spans approximately 490-520nm (Forward *et al.* 1988). Similar short wavelength shifts also occur in atmospheric spectral transmission at twilight (see Rozenberg, 1966).

In summary, animals inhabiting coastal waters are exposed to a much more dynamic and 'photon-rich' light environment in comparison with mesopelagic animals. Evolutionary adaptations in the optics, morphology and spectral sensitivity of the compound eyes of both coastal and mesopelagic malacostracan species that are related to the respective light environments inhabited have been identified and some of these adaptations are reviewed in section *1.6*.

1.5 The Invertebrate Compound Eye

Compound eyes are not the only eye type found in the Crustacea, and for a review of crustacean eye types the reader is referred to Land (1981, 1984). However, the compound eye is the dominant eye type of most arthropods (Nilsson, 1989). There are two basic types of compound eye, the apposition compound eye and the superposition compound eye, and these are described in sections *1.5.2* and *1.5.3*.

1.5.1 The ommatidium

The compound eye is composed of a large number of individual units called ommatidia. The surface of a compound eye is divided into a regular array of hexagonal or square facets. Each facet is the external face of the cornea of each ommatidium. Fig. 1.2 shows a schematical ommatidium.

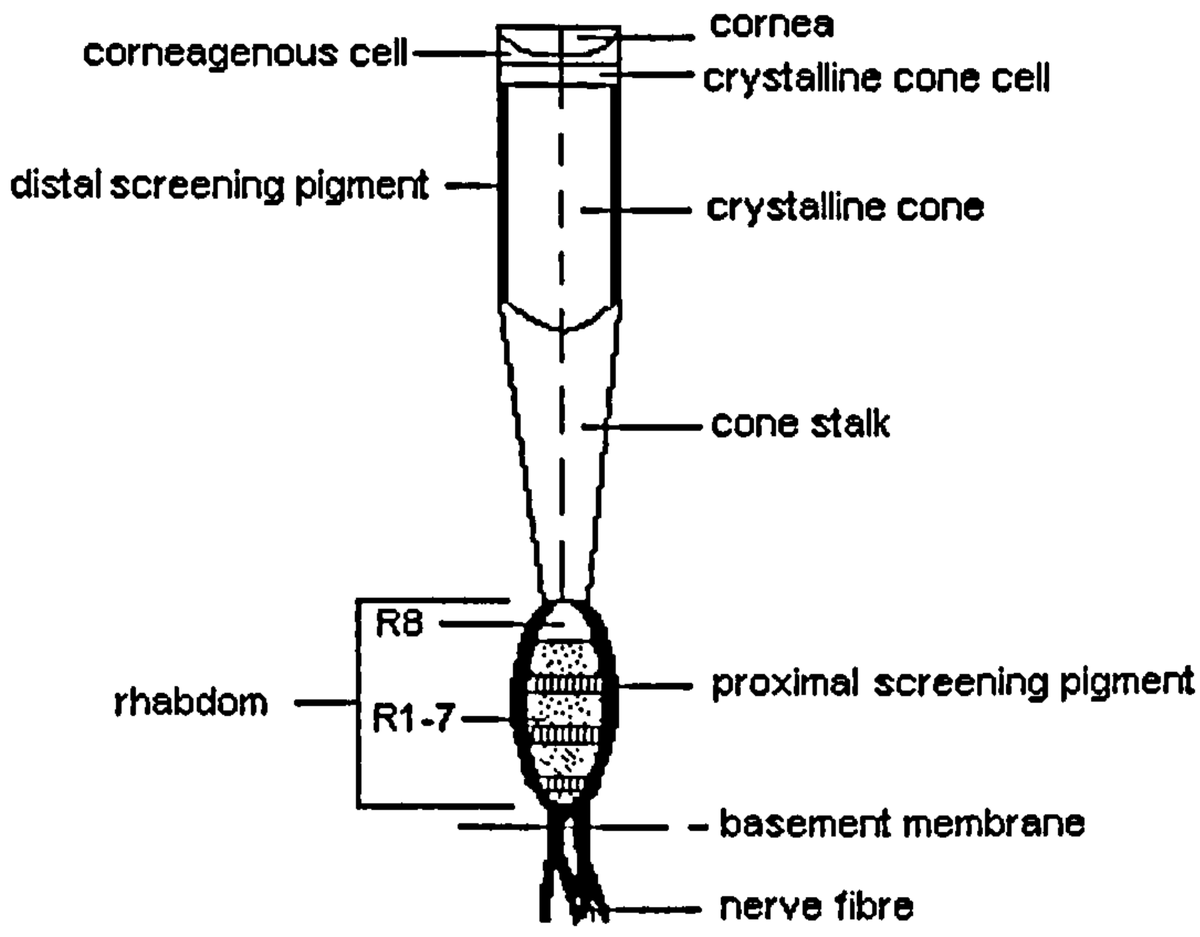

Figure 1.2. A diagrammatical longitudinal section of an individual ommatidium. The cornea, crystalline cone and cone stalk comprise the dioptric apparatus and the rhabdom is the photoreceptive portion of the ommatidium. The rhabdom comprises 8 retinular cells; R1-7 are proximal retinula cells, and R8 is a distal retinula cell. Both the distal and proximal screening pigments (see section *1.5.4*) act to optically isolate the ommatidial unit from neighbouring units.

The cornea is secreted by the underlying corneagenous cells, and whilst it functions to focus light at the facet in insect species, it generally has no dioptric function in crustacean species (Nilsson, 1989, see section *1.5.2*), as most are aquatic species and the similarity between the refractive indices of water and the outer face of the corneal facet render its focussing power useless. Four crystalline cone cells beneath the corneagenous cells are responsible for secreting the crystalline cone structure and the cone stalk. The cone stalk connects the dioptric apparatus to the photoreceptive rhabdom. Light rays pass through the cornea and the crystalline cone and are directed to the centre of the rhabdom via the cone stalk in apposition eyes (in superposition eyes the clear zone replaces the cone stalks, see section *1.5.3*). The rhabdom consists of photoreceptors called retinular cells. Each retinular cell has an extensive array of microvilli over the cell surface closest to the ommatidial axis, and these are the sites at which the visual pigments (rhodopsins or porphyropsins) are located. The distribution of visual pigment throughout the microvillus structure of the retinular cell maximizes the concentration of visual pigment per retinular cell and hence sites for photon absorption. For most crustacean species there are 8 retinular cells that form a two-tiered structure within the rhabdom (Eakin, 1972). The retinular cells R1-7 are proximally situated within the rhabdom and contain blue-green sensitive, rhodopsin (wavelength of maximum absorption between 480 and 540nm). Some

species of freshwater crustacean, e.g. the crayfish *Procambarus clarkii*, have visual pigments known as porphyropsins (as opposed to rhodopsins). The wavelengths of maximum absorption of porphyropsins are shifted to relatively longer wavelengths than rhodopsins to match the spectral distribution of the light environment inhabited (Bridges and Yoshikama, 1970, cited in Kent, 1997). The retinular cell R8 is distally situated and contains near-ultraviolet sensitive rhodopsin (λ_{max} near 400nm) (Marshall *et al.* 1999). The axons of the retinular cells exit the ommatidium at the proximal end; pass through the basal membrane, and transverse tens of micrometers before synapsing with second-order neurons. The axons of the R1-7 cells terminate in the medulla externa, whilst the R8 axons terminate in a separate neuropile, the lamina ganglionaris (Cummins and Goldsmith, 1982, cited in Kent, 1997).

1.5.2 Apposition optics

Fig. 1.3a shows the image formation mechanism of the apposition eye. The apposition compound eye is the most common type of compound eye possessed by arthropods (Land, 1984; Nilsson, 1989). In the apposition eye each ommatidial unit is optically isolated and therefore has its own 'private' lens system with which it forms its own image of a sector of the environment. In terrestrial animals, the cornea of each ommatidium acts to focus the light rays along the axis of the ommatidium. However, for aquatic species, the refractive properties of the outer surface of the cornea are insignificant in water due to the similarities in the refractive indices of the cornea and water (Land, 1984, Nilsson, 1989). Each crystalline cone therefore contains a lens cylinder with a gradient of refractive index (high refractive index along the cylinder axis falling parabolically as a function of radius to lower refractive index laterally). Light rays are thus brought to a focus along the axis of the lens cylinder, and an inverted image is formed at the proximal end of each crystalline cone (Land, 1984). The light intensity information in this focused inverted image is then passed along the cone stalk, which acts as a waveguide, and is delivered to the centre of the rhabdom. The image is not resolved by the individual photoreceptors and each ommatidium samples its own section of the visual field (the angle of the visual field sampled by each ommatidium is determined by the ommatidial acceptance angle see section *1.5.6*). The neural image of the eye is formed from an amalgamation of the information obtained by each rhabdom (Nilsson, 1989). Distal screening pigments are used in apposition optics to prevent the spread of light rays between adjacent ommatidia. These screening pigments improve image resolution as they reduce light scatter

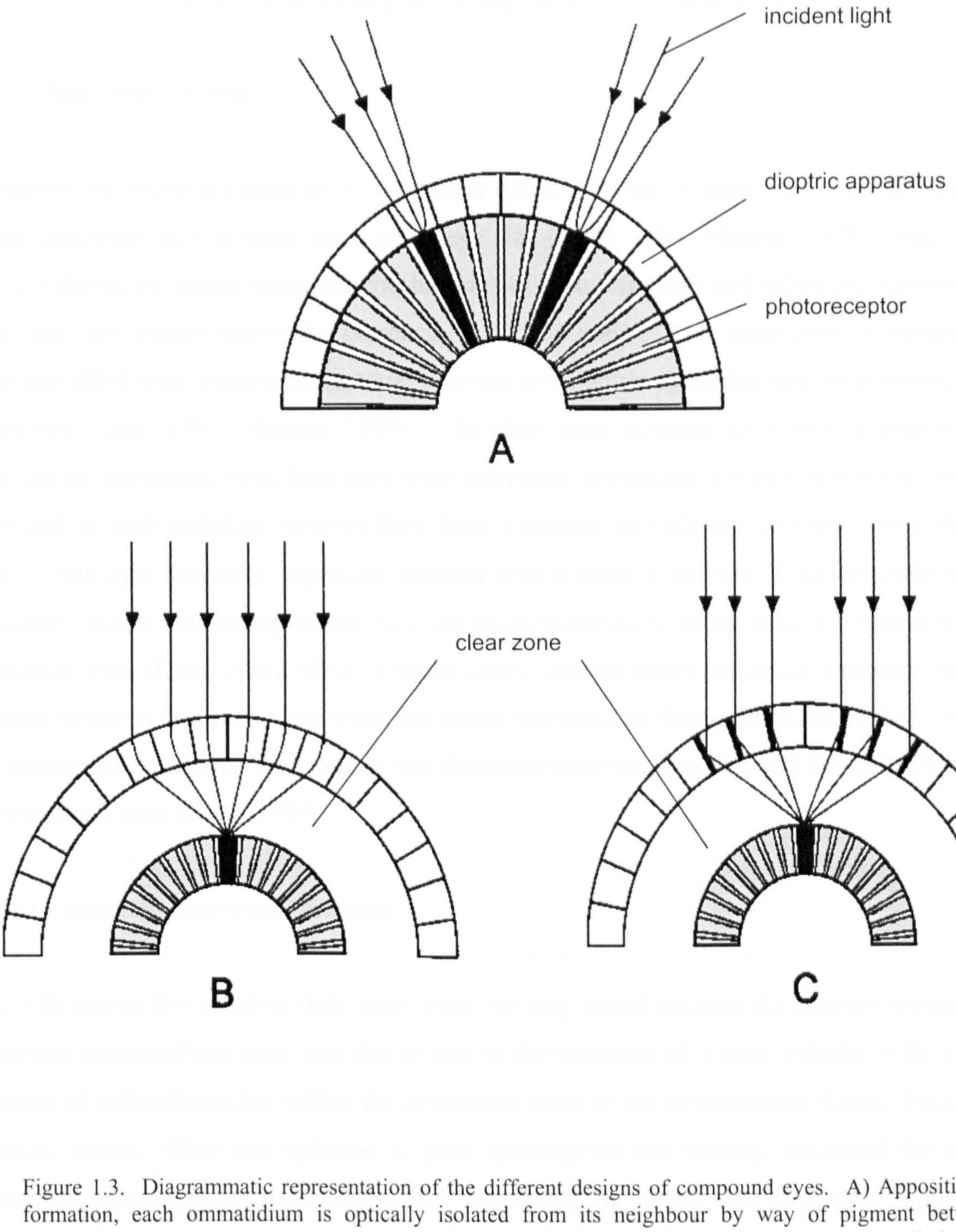

Figure 1.3. Diagrammatic representation of the different designs of compound eyes. A) Apposition image formation, each ommatidium is optically isolated from its neighbour by way of pigment between the ommatidia (shown above as white). B) Refracting superposition image formation, lens cylinders with a refractive gradient in the dioptric apparatus act to focus light from a number of ommatidia onto a single rhabdom. The presence of the clear zone allows light rays to cross from the crystalline cone of one ommatidium to the rhabdom of another. C) Reflecting superposition image formation, this design functions in the same way as that of the refracting superposition design but light is reflected within the dioptric apparatus due to the presence of mutlilayer interference mirrors (redrawn from Kent, 1997; all after Land, 1981).

within the ommatidium (Land, 1999). Among the Malacostraca, isopods, amphipods, stomatopods and brachyuran crabs all possess apposition eyes (Land, 1984).

1.5.3 Superposition optics

Superposition optics are superior to apposition optics in terms of sensitivity, i.e. superposition optics maximise photon catch for a given eye size (Land, 1984; Nilsson, 1989; Land, 1999). Fig. 1.3 shows the image formation mechanisms of both refracting and reflecting superposition eyes, and also clearly shows the presence of a 'clear zone'. This clear zone is essentially a wide gap filled with transparent material between the dioptric apparatus and the photoreceptive rhabdoms (Land, 1981; Nilsson, 1989). The clear zone contains no screening pigment and thus, unlike apposition eyes, light rays from individual ommatidia are able to traverse the clear zone and so each rhabdom receives light from a number of different ommatidia (see Fig. 1.3 b&c). This light gathering capability coupled with a small F-number (focal length/facet lens diameter), means that superposition eyes can be approximately 1000 times more sensitive than apposition eyes (Land 1981, 1984). Consequently, superposition optics are generally found in animals living in dim light conditions, including mesopelagic decapods (Land, 1984). Among the Malacostraca, mysids, euphausiids and decapods (shrimps, crayfish and lobsters) all possess superposition eyes (Land, 1984).

1.5.3.1 Refracting superposition optics

Fig. 1.3b shows that incident light rays 'bend' as they travel through the dioptric apparatus of refracting superposition eyes and this is due to the presence of a lens cylinder with a radial gradient of refractive index within the crystalline cone of the ommatidium (Land, 1981,1984; Nilsson, 1989). This lens cylinder is quite different to that already described for aquatic animals possessing apposition eyes in that it is twice the length, and functions in a manner analogous to two lenses in series: i.e. the light rays are bought to a focus in the middle of the lens cylinder and the rays emerge parallel to one another (Land, 1981). The consequence of this is that whilst apposition optics generate an inverted image at the proximal end of each crystalline cone, superposition optics generate a single upright image at the retinula cell level that is contributed to by a large number of ommatidia. Light rays entering the distal end of a crystalline cone at a given angle of incidence, exit the proximal end of the cone at the same

angle relative to the axis after being bent through twice the angle of incidence (Land, 1981, 1984). Mysids and euphausiids possess refracting superposition eyes (Land, 1984).

1.5.3.2 Reflecting superposition optics

Reflecting superposition eyes may be diagnosed by presence of square facets across the eye as opposed to the closely packed hexagonal facets often seen that are indicative of apposition or refracting superposition compound eyes. Behind these square facets reside square-sided crystalline cones that are twice as long as they are wide. The four sides of each cone are coated with mutlilayers of pteridine crystals and thus function as radially arranged plane mirrors (Land, 1984). The dioptric apparatus of the reflecting superposition eye thus uses the 'corner reflector principle' (Vogt, 1975, cited in Land, 1976, 1981), and behaves like a flat mirror at right angles to the plane of the ray. The mirror box in the crystalline cone causes light rays to be reflected through twice their angle of incidence and emerge from the dioptric apparatus at an equal, but opposite angle to the incident ray (Land, 1981; Nilsson, 1989). Therefore the light rays emerge from the crystalline cone in parallel and are bought to an upright focus at a single point in the rhabdom array, as in the case of refracting superposition eyes. Malacostracan decapods (such as shrimps and lobsters) possess reflecting superposition eyes (Land, 1984).

1.5.4 Screening pigments

Fig. 1.2 shows the presence of both distal and proximal screening pigments within the ommatidial unit of a compound eye. These screening pigments are dark, usually dark brown or black and are comprised of ommochromes which are dark pigments derived from tryptophan (Autrum, 1981). Distal screening pigment is contained within two or more pigment cells and these can form a partial or complete sleeve distally around the ommatidium in order to absorb light rays that may be scattered out of the axial dioptric system (Autrum, 1981). Proximal screening pigment is contained within the rhabdom and can migrate distally to surround the retinula cells and thus prevent off-axis light from reaching the photoreceptive area (Autrum, 1981; Land, 1981). The migration of these pigments has a pupillary function and therefore provides dynamic stimulus control for the eye. The position of the pigments within the ommatidium controls retinal illuminance and consequently changes the sensitivity of the eye (Nilsson, 1989; Autrum, 1981). In some diurnal crustacean species screening pigment

migration is controlled by circadian rhythms and screening pigments change their position diurnally. During the day, when the eye is in a light-adapted state, the distal and proximal pigments surround the crystalline cones and rhabdoms respectively, thus limiting light flux to the photoreceptors. During the night, when the eye is in a dark-adapted state, the pigments withdraw from their positions so increasing light flux to the photoreceptors (Autrum, 1981). Pigment migrations can also be triggered in dark-adapted eyes when exposed to light, and conversely in light-adapted eyes when maintained in darkness (Autrum, 1981). Physiologically, the migrating pigments function to change the sensitivity of the eye and they also have an effect on the spatial acuity and hence resolution of the eye (see section *1.5.6* for detail of spatial resolution of compound eyes). In superposition eyes, during light adaptation, sensitivity is decreased when dark proximal pigment migrates distally and surrounds the rhabdoms and this is accompanied by an increase in visual acuity (Autrum, 1981). In apposition eyes, the movement of distal screening pigment to surround the distal portion of the ommatidium has a similar effect on visual acuity (Autrum, 1981). Thus the adaptation state of the eye has an effect on the receptive field of each rhabdom; in the superposition eye of *Cherax destructor* (crayfish) dark adaptation increases the acceptance angle (see section *1.5.6*) of the individual visual cells considerably, from 24° ±8° in the dark-adapted state to 4° ±2° in the light-adapted state (Autrum, 1981). Section *1.5.6* reviews the spatial acuity of compound eyes.

1.5.5 Reflecting pigment (the tapetum)

Reflecting pigment is white, light reflecting pigment composed of pteridines (Autrum, 1981). The reflecting pigment is responsible for the tapetum or 'eyeglow', which is apparent when eyes in the dark are illuminated with light. This pigment is situated proximal to the rhabdoms in association with the basement membrane and is ineffective when the eye is in a light adapted state when it is covered by the dark proximal screening pigment surrounding the rhabdoms (Nilsson, 1989). During dark-adaptation the reflecting pigment is exposed by the movement of dark proximal pigment (Autrum, 1981). Once the reflecting pigment layer is exposed it functions to increase the sensitivity of the eye as it reflects light diffusely back through the photoreceptive rhabdoms and effectively doubles the pathlength of light through the photoreceptive layer (Land, 1981). It is the diffuse reflection of light back through the photoreceptive layer that produces the eye glow seen when eyes are illuminated in the dark.

1.5.6 Spatial acuity of compound eyes

The spatial acuity, or resolution of compound eyes is the ability of the eye to resolve spatial detail within a visual image and it is this property of the compound eye that ultimately determines the overall resolution of the visual images generated. Each rhabdom has a restricted field of view that is ultimately determined by its acceptance angle [$\Delta\rho$] (Autrum, 1981). The acceptance angle of a given rhabdom is equal to the half width of the angular sensitivity function of that rhabdom. The angular sensitivity function is the relative sensitivity of the rhabdom to light incident from different directions and is represented in Fig. 1.4 (Autrum, 1981; Laughlin, 1981).

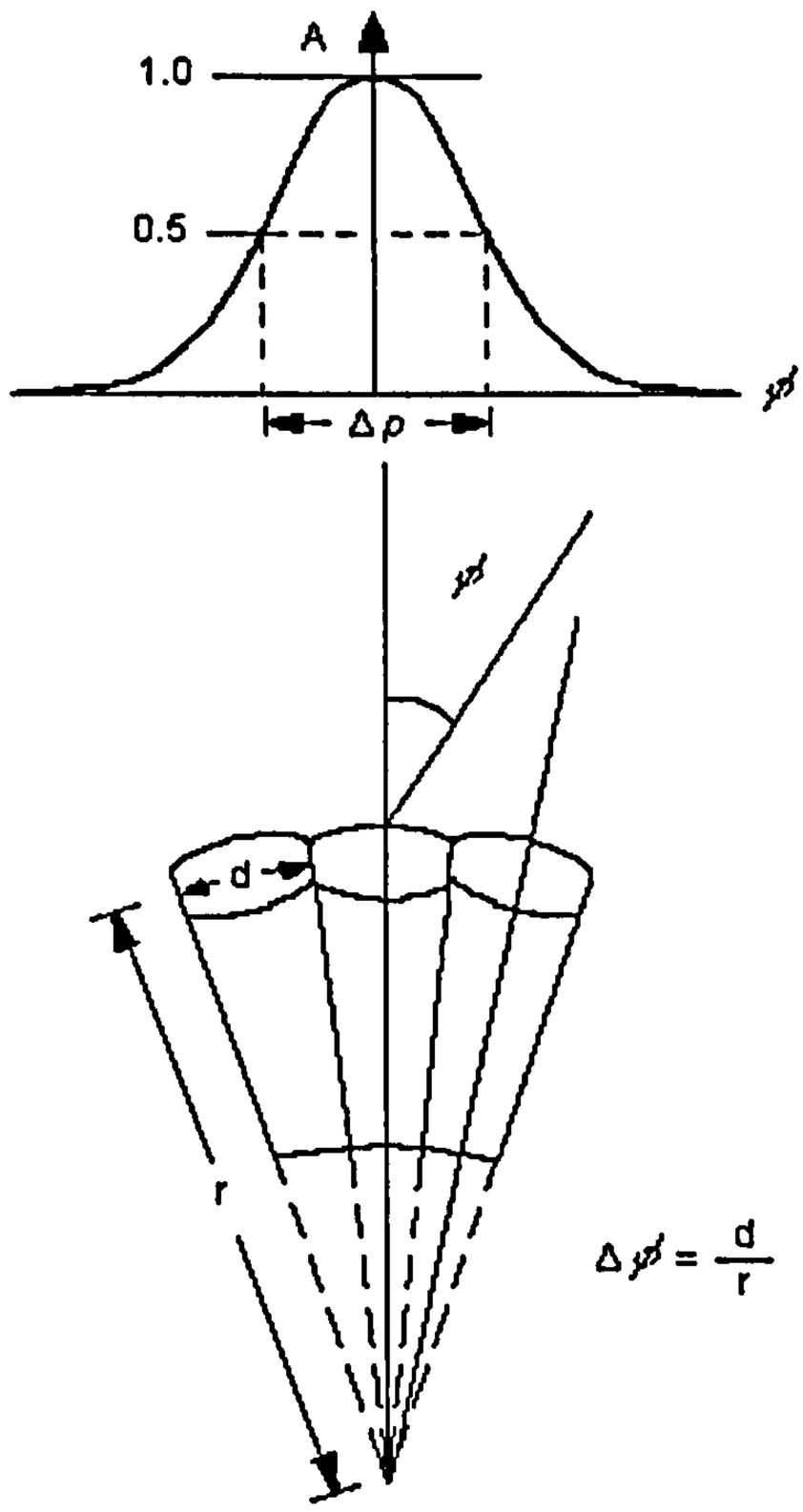

Figure 1.4. A diagrammatic representation of a cross-section through three ommatidia of a compound eye. d is the facet diameter, r is the radius of the eye and $\Delta\phi$ is the inter-ommatidial angle. The equation shown is an approximation of $\sin\Delta\phi = \Delta\phi = d/r$ since $\Delta\phi$ is small. Shown above this is the acceptance function of a retinula cell. This represents the relative sensitivity of the retinula cell response as a function of angle (ϕ) from the optical axis (A) of the ommatidium

The inter-ommatidial angle ($\Delta\phi$) of the eye is the angle between the ommatidial axes of neighbouring ommatidia and describes the angular separation of the rhabdoms in the eye (Land, 1984). A relatively small inter-ommatidial angle will potentially allow greater spatial resolving power. The equation shown in Fig. 1.4 indicates that the inter-ommatidial angle of an eye is approximately equal to the facet diameter divided by the radius of the eye. This is true for spherically symmetrical eyes, but for those eyes that are not spherically symmetrical and have regions of the eye with facets of differing size (see Land, 1999 for a review and section *1.6.1* for some examples) the interommatidial angle will depend upon the region of the eye in question (Snyder, 1979). Therefore the equation below is used to generate a value for eye parameter (p), which accounts for differences in facet diameter.

$$p = d\Delta\Phi = d^2 / r$$

where d is the facet diameter, r is the radius of the eye and ϕ is the inter-ommatidial angle.

In apposition eyes the values of $\Delta\rho$ and $\Delta\phi$ are similar due to the fact that if $\Delta\phi$ were greater than $\Delta\rho$ there would be holes in the visual field and conversely if $\Delta\rho$ were greater than $\Delta\phi$ there would be overlap in the visual field (Land, 1984). For superposition eyes this does not necessarily hold true as the spatial information from a number of ommatidia can fall onto a single rhabdom, consequently it is the acceptance angle of the retinula cells that determines the absolute spatial acuity of the visual image. This does not render the angular separation of the ommatidia entirely superfluous however, as the facet diameter of each ommatidium will set the resolution limit of the visual image in terms of the amount of diffraction incurred (Snyder, 1979; Land, 1981, 1999). The nature of compound eyes, in which there are a large number of small apertures through which light enters, leads to diffraction of light at each aperture (Snyder, 1979; Land, 1999). This leads to a loss of resolution of the visual image due to the interference of focused light waves and the severity of the problem varies inversely with the diameter of the facet (Land, 1999). Therefore, irrespective of the acceptance angle or inter-ommatidial angle of the eye, the facet diameter will set the absolute limits of resolution as diffraction cannot be corrected and will affect the acuity of vision.

As mentioned in section *1.5.4*, the acceptance angle of a retinula cell is generally decreased as luminance increases. Upon an increase in illumination, screening pigments are mobilized and migrate into position, thus reducing sensitivity of the eye and increasing acuity of vision. In compound eyes spatial resolution and sensitivity are therefore inversely related (Land, 1981, 1984).

1.6 The Visual Ecology of Crustaceans

Visual systems often show adaptations to achieve optimal function in both the light environment inhabited and in the visual tasks required. This section reviews some examples of adaptations in optical morphology and spectral sensitivity of the visual systems of marine crustaceans that are related to their visual ecology. Chapter 2 reviews visual adaptations in sensitivity and response dynamics at the neural level.

1.6.1 Optical adaptations to the aquatic environment

Superposition optics greatly improve the sensitivity of the visual system due to their photon gathering capability and the action of a tapetal reflecting layer when present (see sections *1.5.3* and *1.5.5*). Consequently most nocturnal and deep-water arthropods have superposition eyes with tapetal reflecting pigment (Land, 1999). Interestingly, in some mesopelagic decapod species there are ontogenetic changes in compound eye structure that can be associated with the differences in the habitat of the larvae and the adults (Land, 1984; Herring and Roe, 1988). In the genera *Acanthephyra* and *Sergestes*, the larval decapods have apposition optics as indicated by the presence of hexagonally packed facets, and the deep-living adults have reflecting superposition eyes as indicated by the presence of square facets across the eye surface (Herring and Roe, 1988). The larval decapods of these genera are shallow living, presumably because food supply is more abundant in the epipelagic zone. On maturing these animals move into deeper water and develop different ocular optics for vision in a photon-limited environment.

The shallow-living adult decapod, *Funchalia villosa*, has large reflecting superposition eyes with high concentrations of screening pigment and during the daytime the eyes presumably function as apposition eyes with screening pigment migrating to optically isolate each ommatidium (Herring and Roe, 1988). The inter-ommatidial angle of this species in the light-

adapted state is very low (1-2°) and similar to inter-ommatidial angles measured for shallow-water epibenthic crustacean species, indicating that the eye has high spatial acuity (Herring and Roe, 1988). It is the large size of the eye of *Funchalia villosa* that allows a large number of facets with small inter-ommatidial angles. Large eyes are also found in animals living at depth, and in benthic decapod species eye size increases with depth (Hiller-Adam and Case, 1985). The large eye size allows for both a smaller number of ommatidia with large facets, and for larger rhabdoms, which by virtue of their pathlengths, have high absorption and therefore overall greater capacity for collecting light (Hiller-Adams and Case, 1985; Herring and Roe, 1988).

The presence of mobile screening and reflecting pigments has been described in sections *1.5.4* and *1.5.5* and for most compound eyes these pigments are present and important in pupillary mechanisms during light exposure (Hallberg and Elofsson, 1989). Whilst the compound eyes of mesopelagic decapod species possess reflecting pigments (e.g. Shelton *et al.* 1992; Johnson *et al.* 2000b), there appears to be a lack of mobile screening pigment present (Land, 1976; Hallberg and Elofsson, 1989; Gaten *et al.* 1992). This observation suggests that pupillary mechanisms are not required in the vision of these animals, presumably because they are not exposed to large changes in light intensity in their natural environment. Further evidence to support this comes from the studies of Loew (1976), Nilsson and Lindström, (1983) and Shelton *et al.* (1985), which show that exposing deep-living crustacean species to daylight irradiance levels causes irreversible damage to the eyes.

The study of Gaten *et al.* (1992) describes regional morphological variation within the compound eyes of some mesopelagic decapod oplophorid species. This variation is evident as a difference in the rhabdom type found in the dorsal region of the eye relative to that found in the ventral region. Specifically, the two species *Oplophorus spinosus* and *Systellaspis debilis* have banded fusiform rhabdoms in the dorsal regions of the eyes and interdigitating rhabdoms in the ventral regions of the eyes (Gaten *et al.* 1992). The dorsally located fusiform rhabdoms are efficient in containing incident light and thus prevent the scatter of light across the rhabdom layer (Gaten *et al.* 1992). It is suggested that these rhabdoms are present to maintain the resolution of visual images when viewed against relatively bright downwelling irradiance (Gaten *et al.* 1992). Gaten *et al.* (1992) indicate that the ventrally located interdigitating rhabdoms are an adaptation to viewing objects under conditions of minimal irradiance.

Rhabdom morphology can also vary in terms of the relative sizes of the retinula cells. The study of Gaten *et al.* (1992) shows that for the oplophorid species *S. debilis*, the relative lengths of the R8 and R1-7 photoreceptors vary within the eye such that in dorsally located rhabdoms (i.e. those looking upwards), the R8 length to R1-7 length ratio is 0.15 whereas for ventrally located rhabdoms this ratio is 0.8. This is achieved by a relative shortening of the R1-7 and elongation of the R8 in the ventral retina and can be related to the fact that upwelling light contains a greater proportion of short wavelengths than downwelling light (Jerlov, 1976).

In hyperiid amphipods, euphausiids and mysids there are cases of morphological variation in eye structure in the form of specialized double eye structures (Land, 1984, 1999). The hyperiid amphipods have apposition optics and generally large eyes that can be divided into two distinct regions: dorsal and ventral e.g. *Phronima sedentaria* (Land, 1984). The dorsal region of these 'double-eyes' always has larger facets and smaller inter-ommatidial angles relative to the ventral region, presumably in order to both maximise sensitivity and resolution when viewing objects against the relatively bright downwelling light (Land 1984, 1999). In the dorsal eyes of the hyperiid amphipod *Phronima sedentaria*, the inter-ommitidal angle ($\Delta\phi$) is 0.25° and in the ventral eye it is 10° (Land, 1999).

The presence of double-eye structures in the superposition eyes of euphausiid and mysid species may be considered as even more surprising as spherical geometry is important in superposition eyes due to the shared optics (Land, 1984, 1999). However, the bilobed eyes of certain euphausiids (e.g. *Nematoscelis atlantica*, *Nematobrachion boopis*, *Stylocheiron maximum*) are composed of two essentially separate structures each with its own spherical geometry. Again, the acuity in the upper eye is generally greater than that in the lower eye for deep living species and the proposed function of this is to view objects against relatively bright downwelling light (Land, 1999).

This section has reviewed aspects of the optical morphology of marine malacostracans in relation to their visual ecology. Many more examples of adaptation of form to function in the compound eye exist; these are reviewed by Land (1984, 1999) and Herring and Roe (1988).

1.6.2 Spectral sensitivity and the aquatic environment

There are two general hypotheses that can describe the relationship between the spectral composition of an animal's environment and the spectral sensitivity of its visual system. The 'Sensitivity Hypothesis' states that the spectral position of the maximum absorbance of an animal's visual pigment/s will be matched to the wavelengths of maximum photon flux in the animal's visual environment (see Lythgoe, 1968; Partridge and Cummings, 1999). This is in order to provide the greatest sensitivity to light in the environment. The alternative hypothesis is the 'Contrast Hypothesis'. This hypothesis suggests that the spectral position of the maximum absorbance of an animal's visual pigment/s will be offset from the wavelengths of maximum photon flux in the environment in order to optimise the contrast between viewed objects and the background space light (see Lythgoe, 1968; Partridge and Cummings, 1999). Both hypotheses indicate that there is a strong relationship between the spectral sensitivity of the visual system of an animal and the spectral distribution of light in its environment. This section will review some examples of the relationship between spectral sensitivity and visual ecology in marine crustaceans.

The spectral sensitivities of various crustaceans have been studied using either electrophysiological recordings of the sensitivity of the visual response to light of different wavelengths, microspectrophotometric measurements of the absorption characteristics of the visual pigment *in situ*, i.e. within the rhabdom, or spectrophotometric measures of visual pigment extracts (Kampa, 1955, 1965, cited in Kent, 1997; Goldsmith and Fernandez, 1968; Wald and Seldin, 1968; Denys, 1982, cited in Kent, 1997; Denys and Brown, 1982; Martin and Mote, 1982; Widder *et al.* 1987, cited in Kent, 1997; Cronin and Forward, 1988; Frank and Case, 1988a, 1988b; Forward *et al.* 1988; Hiller-Adams *et al.* 1988; Cronin and Frank 1996; Kent, 1997; Johnson 1998). As a group, the Crustacea are quite conservative with respect to the wavelength of maximum absorbance (λ_{max}), of the visual pigments. This is surprising considering the diversity of habitats these animals inhabit in terms of the spectral distribution of light.

The majority of anomuran and brachyuran crab species inhabit shallow-water environments and consequently inhabit environments with relatively complex spectral distributions (see section *1.4*). However, the λ_{max} of the visual pigment within the R1-7 cells of 27 different crab

species averages 494nm with no more than a 20nm shift from this peak (Marshall *et al.* 1999). Forward *et al.* (1988) report that the λ_{max} of the visual pigments of 27 crab species studied, when compared with the spectral transmission of light in their respective habitats, do not conform to the sensitivity hypothesis despite the fact that a visual pigment with a λ_{max} matched to the wavelength of maximum photon flux in the visual environment would function optimally in the visual tasks required (see Marshall *et al.* 1999). In two species of crab, *Callinectes sapidus* and *Carcinus maenus* there is a second spectral sensitivity peak in the eye that is maximally sensitive to near-UV light (Martin and Mote, 1982). This is not surprising when one considers that the distal R8 retinula cell in most crustacean species contains shortwave length sensitive visual pigment, but the purpose of this additional spectral sensitivity is unclear. It is possible that this extra pigment is used in hue discrimination, contrast sensitivity or to broaden overall spectral sensitivity (Marshall *et al.* 1999).

The spectral sensitivities of some shallow-water, coastal species of decapod have also been determined (Goldsmith and Fernandez, 1968; Wald and Seldin, 1968; Johnson 1998). These studies indicate that there are dual pigment systems present in these animals with one spectral sensitivity peak at 520-550nm and one at around 400nm. The 520-550nm visual pigment is well matched to the chromatic content of the shallow-water coastal environment that is shifted toward longer wavelengths relative to open ocean water (see section *1.2.4*), suggesting some agreement with the sensitivity hypothesis. However, the role of the near-UV sensitivity is still uncertain (see Marshall *et al.* 1999).

There have also been a number of studies to determine the spectral sensitivities of various deep-sea species including euphausiids (Denys 1982, cited in Kent, 1997; Denys and Brown, 1982; Widder *et al.* 1987, cited in Kent, 1997); a mysid (Frank and Case, 1988b); oplophorids (Frank and Case, 1988a, Cronin and Frank, 1996); and sergestids (Hiller-Adams *et al.* 1988). These studies suggest that the spectral sensitivities of deep-sea crustaceans fall within the range of 470-500nm and that some oplophorid species e.g. *Systellaspis debilis* and *Oplophorous spinosus* have dual pigment systems with sensitivity to near-UV light at 400nm. The deep-sea environment has a relatively constant and narrow spectral distribution of downwelling light with a peak spectral transmission of 465-475nm depending on the water type in question (Jerlov, 1976, see section *1.3*). The spectral sensitivities of the deep-sea crustaceans are not exactly matched to the spectrum of downwelling light available and thus do not conform to the

sensitivity hypothesis. There is no match between spectral sensitivity and the spectral distribution of bioluminescent emissions of mesopelagic malacostracans either (440-490nm, Herring, 1983; Widder *et al.* 1983). It is suggested that the spectral sensitivities of the R1-R7 and R8 retinula cells of *S. debilis* are placed optimally for viewing bioluminescent emissions (Cronin *et al.* 1996, cited in Marshall *et al.* 1999).

1.7 Aims Of This Thesis

It is apparent that the visual systems of crustacean species show variation in both optical morphology and spectral sensitivity and that these variations are adaptations to the properties of the light environments inhabited.

The aim of this thesis is to determine whether there are differences in the visual systems of marine malacostracans at the neural level. Neural control of both visual sensitivity and the response dynamics of photoreceptors (temporal resolving power) are introduced in Chapter 2. There are relatively few comparative studies of the temporal resolving powers of the eyes of marine crustaceans despite the fact that other aspects of the visual systems of these animals have been so extensively studied. Consequently this thesis explores two methodologies used in determining the temporal resolution of photoreceptors in an eye when restricted to extracellular electrophysiological recordings in a shipboard laboratory.

Extracellular electrophysiological recording techniques are used to measure both the sensitivity and the temporal resolving power (see section *2.1.4*) of the eyes of mesopelagic and shallow-water coastal species of malacostracan crustaceans in order to determine if there are correlations between sensitivity, temporal resolving power and visual ecology.

CHAPTER 2: ELECTROPHYSIOLOGY OF INVERTEBRATE VISUAL SYSTEMS

2.1 ELECTROPHYSIOLOGY

2.1.1 The Electroretinogram

The electroretinogram (ERG) is a convenient and relatively simple method by which to assess the nature of events occurring at the earliest stages of the phototransduction process (the conversion of a light signal into a neural signal), and is a technique that has been used widely in the field of vision research. The ERG is a gross and non-selective measure of the response of the photoreceptor cells within the retina to a change in irradiance level falling on the eye. The ERG is recorded with electrodes that are placed some distance from the generating structures within the retina.

The ERG is recorded extracellularly. An electrode is inserted into the extracellular space in the eye, or, non-intrusively, the electrode can be placed on the outer surface of the eye by means of a salt bridge or a contact lens. The electrode picks up field potentials outside the photoreceptor cells. The field potentials are generated by the transient receptor potentials occurring within the photoreceptor cell. Because the ERG is recorded extracellularly, the polarity of the ERG is opposite to that of the internal receptor potential of the photoreceptor cell. Although advancement in technology has provided the opportunity for unitary analysis of photoreceptor function, i.e. resolving events within the single cell, (intracellular recording, voltage clamping, patch clamping), the ERG remains useful as a means of determining the gross response of an eye to a pre-defined stimulus. The electroretinogram becomes a particularly useful tool for assessing the visual capabilities of animals under conditions that will not allow intracellular recording. For example, obtaining electrophysiological recordings from deep-sea animals requires taking recordings on board ship, as the animals are not robust enough to survive transportation back to shore-based laboratories. The inherent problems of working on a moving vessel limit an electrophysiologist to making extracellular recordings only.

2.1.1.1 The electroretinogram of the invertebrate compound eye

The ERG is the summed mass response from a large number of photoreceptor cells in the eye. The relative simplicity of the compound eye of many invertebrates (e.g. *Limulus* lateral eye) has encouraged thorough investigation, with the intention of identifying parallels between relatively simple processes occurring within the invertebrate retina and the more complex interactions, which occur in the vertebrate retina.

2.1.2 Sensory Transduction in the Compound Eye

Sensory receptors are transducers (input-output devices), which are responsible for the conversion of the physical energy of a stimulus into ion movements and transmitter release characteristic of neural signals. Sensory receptors include: photoreceptors (which respond to electromagnetic energy), mechanoreceptors (which respond to mechanical stimuli), chemoreceptors (which respond to chemicals) and thermoreceptors (which respond to different levels of temperature). The term phototransduction specifically describes the conversion of light energy (photon absorption) into neural signals.

Each sensory modality has its own specific set of receptors and central pathways, as opposed to different modalities being signalled by a single system. However, the sequence of primary events leading to the perception of a sensory stimulus is the same for all sensory modalities. The sequence of events is as follows:

Receptor Activation ⟶ Receptor Potential ⟶ Generator Potential

Receptor activation is generally specific to the sensory modality in question, for example, photoreceptors respond primarily to electromagnetic energy and the mechanism for this is highly specific. A receptor potential is generated by changes in the conductance of the receptor cell membrane, which is in turn caused by a change in the ionic permeability of the receptor cell membrane. These dynamic membrane changes are a result of receptor activation, usually involving a conformational change in the membrane proteins of the receptor cell membrane.

The receptor potential of the invertebrate photoreceptor cell is generally a depolarisation, caused by an inward current into the cell. This receptor potential is a graded potential, which is a slow change in voltage across the cell membrane. A graded potential is localised and does not regeneratively propagate as action potentials do along neurons; but will spread electrotonically (with decrement) through cytoplasm or axoplasm to have significant effects at other locations within the receptor/receptor axon. The size of the graded potential is directly proportional to the amplitude and duration of the stimulus, although it does have a threshold level, which needs to be exceeded, and it can saturate if 'overloaded' with the stimulus. A graded potential lacks a refractory period and thus repeated depolarisations can summate.

The electrotonic spread of the receptor potential affects a 'trigger zone' (e.g. a neurotransmitter secreting synapse at the pre-synaptic membrane), which is located at a distance from the receptor activation site. At the 'trigger zone' release of neurotransmitter from the pre-synaptic membrane leads to the generation of a second depolarisation in a secondary neurone (at the post-synaptic membrane), termed a generator potential. This second graded potential leads to the generation of action potentials along an afferent nerve. The generator potential has the same properties as the receptor potential. Providing the generator potential exceeds threshold level, its electrotonic spread causes the generation of action potentials, or nerve impulses in the afferent neuron associated with the receptor, and the sensory signal is carried to the brain.

The stimulus intensity is coded in the amplitude of the receptor and generator potentials, so how is this intensity information relayed to the brain? The work of Adrian (1926 cited in Granit, 1955), revealed that nerve impulses propagating along the afferent neurons registered stimulus intensity by a variation in frequency. The application of unitary analysis (electrophysiological recordings from individual cells) to the receptors and neurons of the visual system of *Limulus* by Hartline in the late 1930's (cited in Hartline, 1969), revealed that higher stimulus intensities are signalled by higher frequencies of discharge of uniform impulses i.e. a simple frequency code is employed. (see Fig. 2.1a). The frequency of nerve impulse discharge is a linear function of the generator potential amplitude over a limited range, although saturation does occur (Fig. 2.1b).

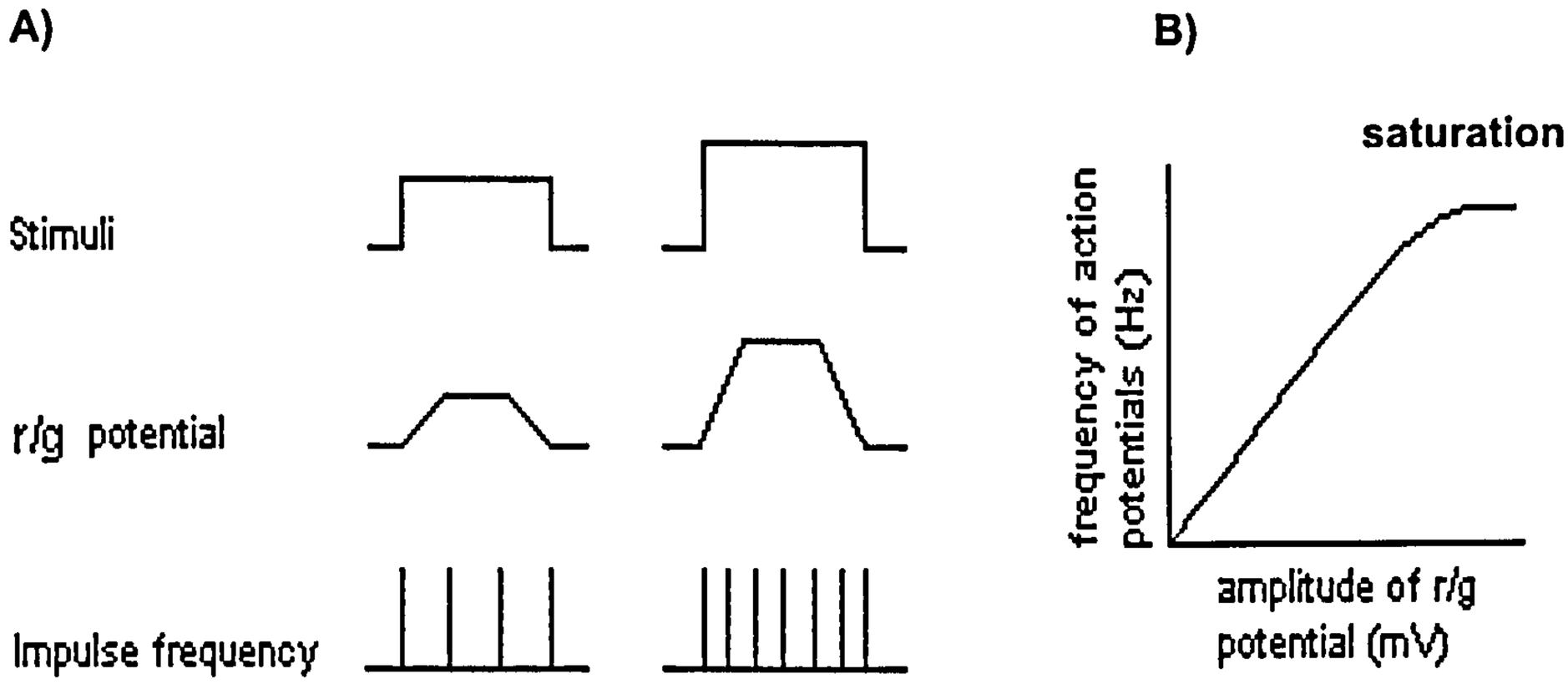

Figure 2.1. Illustration of the relationship between stimulus energy and sensory coding of the stimulus. A) shows the dependence of r/g (receptor/generator) potential amplitude on stimulus energy, also shows how r/g potential amplitude is coded by nerve impulse discharges (action potentials) which vary only in frequency. B) shows saturation of firing rate.

There exists an unequivocal relationship between stimulus intensity and response amplitude; an important general principle of sensory coding is that the output of the receptor is a function of the log of the stimulus intensity. This log response increases the range of stimulus intensities detectable and allows sensory receptors to respond with an approximate constant change to fractional changes in stimulus intensity.

The relationship between response amplitude and log stimulus intensity is sigmoidal, as is the relationship between amplitude of response and action potential frequency (see Fig. 2.2), and is characteristic of sensory receptors; this 'intensity-response' relationship is commonly used to describe the sensitivity of photoreceptor responses in a given adaptational state. Sensory receptors are required to respond to a wide range of stimulus intensities; particularly photoreceptors, which themselves typically have a dynamic response range of 4-5 log units (Laughlin and Hardie, 1978), as the ambient light levels in the visual field can potentially vary over 10 orders of magnitude (Laughlin, 1981).

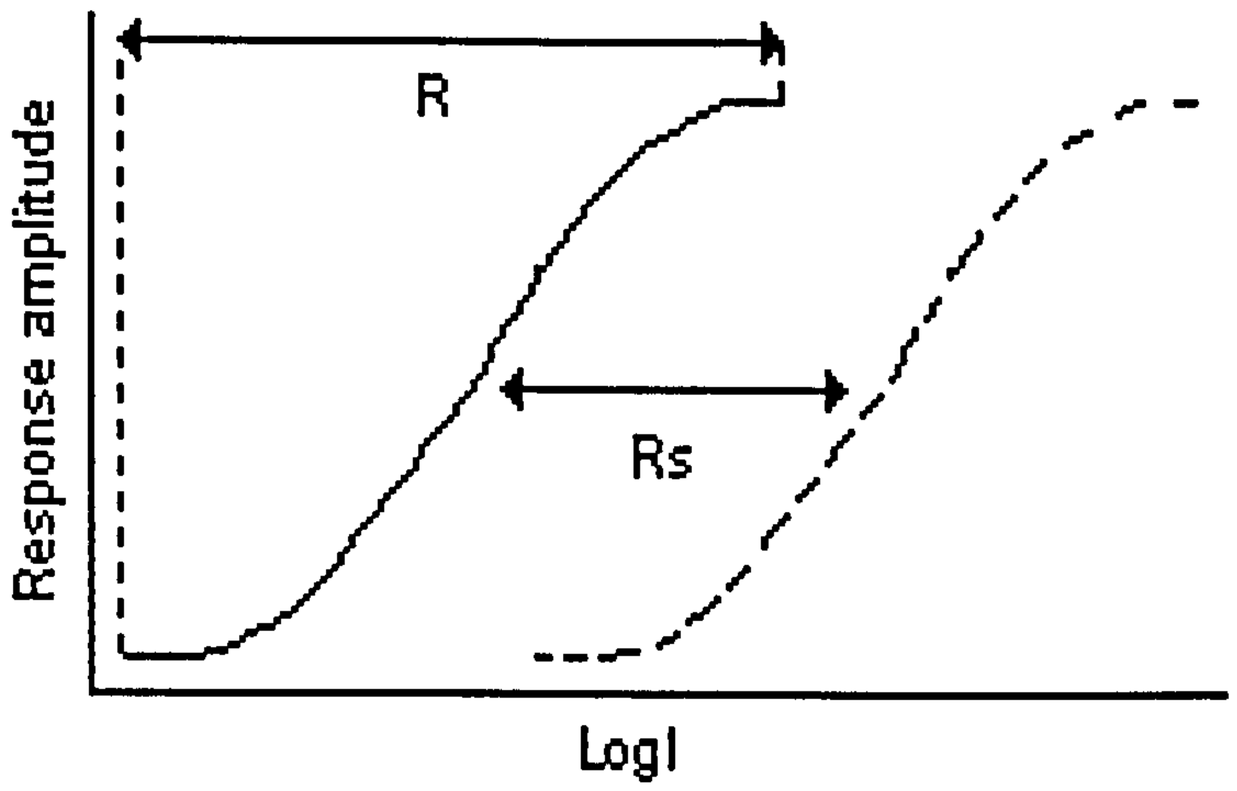

Figure 2.2. Illustration of the characteristic sigmoidal relationship between response amplitude and log stimulus intensity (LogI) in a photoreceptor. R = range sensitivity of the photoreceptor response, Rs= range shift, the range sensitivity is shifted along the logI axis during light adaptation.

Sensory adaptation prevents receptor saturation at high stimulus intensities and allows the receptor to function over a wide dynamic range. Hartline (1969) elegantly showed how discharge frequency of the eccentric cell is high at onset of illumination in *Limulus*, but that if the stimulus is maintained for any period, the discharge frequency is reduced to a more modest level. This is the effect of light adaptation "by virtue of this property, a receptor can signal even small changes in intensity while retaining its ability to function over a wide range of ambient illumination" (Hartline, 1969). Section *2.1.2.2* describes light adaptation in the invertebrate eye in more detail.

2.1.2.1 Physiology of phototransduction in the photoreceptor of the compound eye

The mechanism of phototransduction has been the focus of much research (see Fain and Lisman, 1981, for a review). For the purpose of this study, a relatively basic description of the physiology of the membrane processes within the photoreceptor cell during transduction will suffice. This is to provide a comprehensive background on invertebrate phototransduction; for a more detailed review, the reader is referred to Autrum (1979) and Fain and Lisman (1981).

The photoreceptor cells in the invertebrate compound eye are retinula cells. (see section *1.5* for review of compound eye structure). These cells have a resting membrane potential in the dark of around –60 to –80 mV, which is close to the equilibrium potential for potassium (E_k) (Autrum, 1979). In this state, the cell membrane has a high resistance and sodium (Na^+) conductance is low (Autrum, 1979). The visual pigment, rhodopsin, is photolabile, and is found in abundance within each retinula cell (see section *1.5.1*). Absorption of photons by this pigment brings about a conformational change in the rhodopsin molecule that triggers a cascade of events involving second messenger processes: this is receptor activation. A chemical signal, the end product of second messenger processes, causes changes in the conductance of the photoreceptor cell membrane. The invertebrate photoreceptor potential is generally a depolarisation (for exceptions see review by Autrum 1979). The first intracellular recordings from the lateral eye of *Limulus* by Hartline *et al.* (1952) revealed a depolarising receptor potential. This is in contrast to the receptor potential of the vertebrate cone photoreceptor, which is a hyperpolarisation (Autrum, 1979); the resting potential of the membrane of the vertebrate cone photoreceptors is maintained by high Na^+ conductance.

Dodge *et al.* (1968) present evidence obtained from intracellular recordings from the ventral photoreceptor of *Limulus,* suggesting that the receptor potential is a summation of discrete conductance changes in the photoreceptor membrane. Yeandle (1958) observed small, discrete depolarising potentials in *Limulus* photoreceptors during illumination with dim light or when dark-adapted (cited in Dowling, 1968). The occurrence of these discrete depolarising potentials follows Poisson statistics with a mean proportional to light intensity (Yeandle, 1958; Fuortes & Yeandle, 1964; cited in Laughlin, 1981). It is generally accepted that: a) in complete darkness, these discrete waves are generated randomly, due to spontaneous isomerisation of the visual pigment and this contributes to intrinsic photoreceptor noise (Laughlin, 1981); b) at low light levels these discrete waves (quantum/photon bumps) are responses to single photons, (Scholes, 1964, in a study on the photoreceptors of the locust, showed that one photon produces one bump and no more), and c) at higher light levels the summation of these events (so-called quantum bumps) produces larger sustained receptor potentials (Laughlin, 1981). The non-linear summation of these quantum bumps generates a sigmoidal intensity-response function (see section *2.1.2* Fig. 2.2).

Non-linear summation is an integral property of photoreceptors, and there are two components to it. Firstly, self-shunting occurs in membrane conductance channels, this being a property of all membrane responses generated by channels acting in parallel. Self-shunting occurs because the summed currents generated from photon absorption (quantum bumps) do not vary linearly with activated conductances; due to the fact that as total conductance increases, the receptor potential reduces the electromotive force (EMF) across the membrane (Laughlin, 1981). Secondly, the effectiveness of absorbed photons decreases, that is, photons become less effective at generating a voltage change. This could be due to one of two things: either a) the ratio of photons to activated channels decreases, or b) the action of antagonistic hyperpolarising potentials counteract depolarising potentials (Laughlin 1981). Whatever the mechanism is, the combined effects of these two non-linear components results in the non-linear response of photoreceptors (see Fig. 2.2, section *2.1.2*) (see Laughlin, 1981 for a review).

The depolarising receptor potential of the invertebrate retinula cell to a brief light stimulus, is typically a monophasic waveform which returns to the resting potential with a time course dependent on both the intensity of the stimulus and the adaptational state of the eye. The retinular cell response to a prolonged light stimulus typically shows an initial rapid transient depolarisation reaching maximum amplitude, which declines to a plateau level of depolarisation (see section *2.1.2.2 - physiology of light adaptation*), which is maintained for the duration of the stimulus.

The principle effect of light stimulation is to open Na^+ permeable channels in the invertebrate photoreceptor membrane, thus increasing the conductance to Na^+. As a result there is an influx of Na^+ into the cell. Substitution experiments in which Na^+ can be replaced (e.g. with Tris, an organic salt buffer) clearly show that at least part of the light-activated current is carried by Na^+ (Fain and Lisman, 1981). The light-activated increase in conductance of the cell membrane to Na^+ forces the membrane potential of the photoreceptor cell to move from resting potential (close to E_k) towards E_{Na} (the equilibrium potential of sodium). E_{Na} is at a positive potential, and therefore the membrane depolarises (see Fig. 2.3).

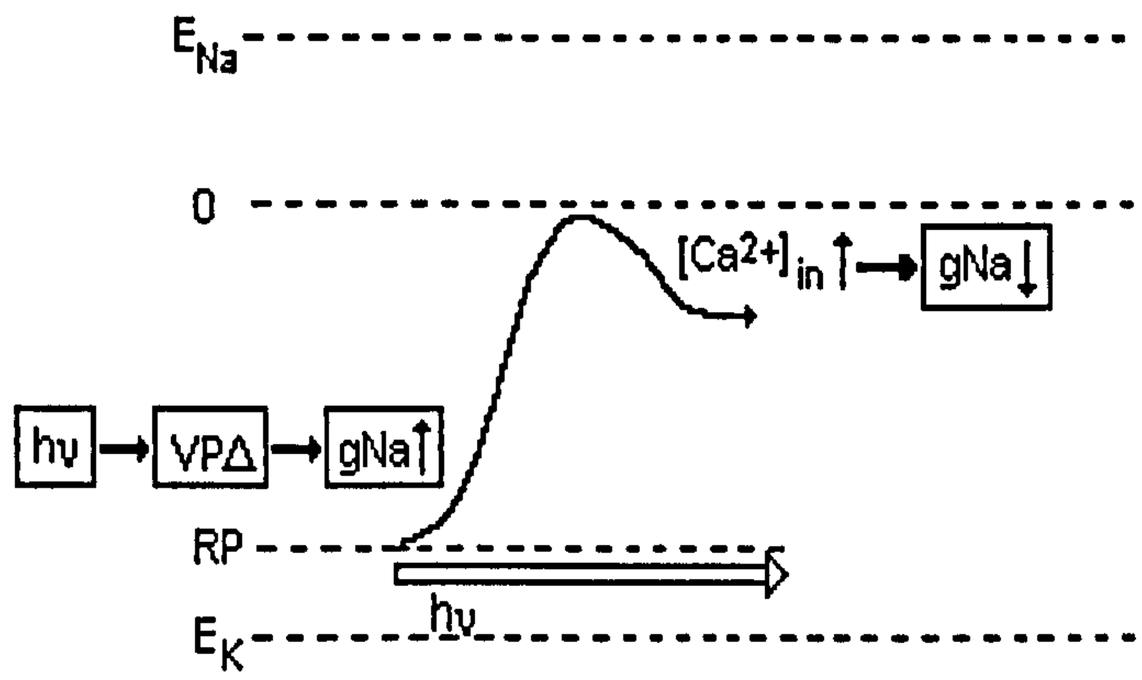

Figure 2.3. The depolarisation of the invertebrate photoreceptor cell in response to light stimulation (hν), which leads to a conformational change in the visual pigment molecules (VPΔ). Dotted lines show the relative positions of the equilibrium potentials of K^+ and Na^+ (E_K, E_{Na}), RP shows approximate position of photoreceptor cell resting potential. RP is close to E_K in the dark, light activation leads to increased Na^+ conductance (gNa) which causes depolarisation. Increased intracellular Ca^{2+} reduces gNa. Redrawn from Autrum (1979).

Although the principle effect of light is to increase sodium conductance into the photoreceptor cell, the depolarisation never reaches E_{Na}; before this can happen the cell begins to repolarise.

The light-activated depolarisation of the *Limulus* photoreceptor cell activates voltage-dependent conductances, including a calcium-sodium conductance (Ca^{2+}/Na^+), and two types of potassium (K^+) conductance with differing inactivation properties (Fain and Lisman, 1981; Weckström *et al.* 1991; Laughlin and Weckström, 1993; Weckström and Laughlin, 1995). The Ca^{2+}/Na^+ conductance plays a role in desensitising the retinula cell during light adaptation via negative feedback. This inward Ca^{2+}/Na^+ current increases intracellular calcium concentration $[Ca^{2+}]_i$ which in turn, reduces the light-activated sodium conductance, hence desensitising the cell (see *2.1.3.2* for more detail).

The two voltage-dependent K^+ conductances are outward currents that both act via negative feedback. These two outward currents include a transient and maintained current. In *Limulus*, the maintained current is conducted via delayed rectifying K^+ channels as it can be blocked by TEA (tetraethylammonium, a specific inhibitor of delayed rectifier K^+ channels) (Fain and Lisman, 1981). In the photoreceptors of the blowfly (*Calliphora vicina*), single-electrode voltage clamping reveals a voltage-sensitive outward current with the properties of a delayed rectifying K^+ conductance (Weckström *et al.* 1991).

In *Limulus* both the maintained and the transient conductances act to repolarise the cell once the depolarisation has reached a certain voltage. The type of voltage-dependent K^+ channel present in the photoreceptor cell membrane varies according to the temporal dynamics of the photoreceptors of certain arthropods Laughlin and Weckström (1993) (see *2.1.3*).

This voltage-dependent, repolarising K^+ conductance is itself attenuated by a light-activated, so-called 'slow process' in *Limulus* photoreceptors. The 'slow process' occurs during the depolarisation of the photoreceptor cell but is only observed when the stimulating light is of long duration, 30 seconds or more (Lisman and Brown, 1971, cited in Fain and Lisman, 1981). The exact mechanism behind the slow process is unclear but it plays an important role. As a prolonged stimulus falls on the photoreceptors, light-activated Na^+ conductance decreases with time (a consequence of light adaptation see *2.1.2.2*). If voltage-dependent K^+ conductance was not attenuated at this point, it would continue acting to repolarise the cell and the brain would receive information indicating that the eye was observing a dimming light source, as opposed to a constant one.

As the depolarising retinula cell potential is a graded potential (see section *2.1.2.1* for description), it is prominent as a slow potential that is easily distinguished from nerve spikes, or action potentials. The photoreceptor potential spreads electrotonically through the cytoplasm of the retinula cell and along the retinula cell axon. Generally, the eyestalks of crustaceans contain three successive neuropil regions, the lamina ganglionaris, the medulla externa and the medulla interna (Strausfel and Nässel, 1981). The retinula cells form axons that project from the proximal end of the rhabdom and through the basement membrane to form synapses in either the lamina (R 1-7, see section *1.5.1* for details), or the medulla (R8), (Laughlin, 1981). Therefore, the electrotonic spread of the graded retinula cell potential triggers a generator potential in the optic neuropil by means of a chemical synapse (Laughlin, 1981). As in the case of *Limulus*, once the generator potentials are summated such that they exceed threshold, action potential firing is triggered in the afferent neuron and the visual signal is propagated to the brain via the optic nerve.

2.1.2.2 Physiology of light adaptation in the photoreceptor of the compound eye

Dynamic control of photoreceptor sensitivity is fundamental in avoiding saturation of the visual response. "During maintained illumination of a visual cell, its sensitivity declines and its threshold rises (light adaptation). When the light intensity is reduced or the light is turned off, sensitivity increases (dark adaptation)." (Autrum, 1981).

The photomechanical changes that occur during light adaptation, providing effective dynamic stimulus control, have been discussed in section *1.5.4*, however the role of the photoreceptor in light adaptation i.e., neural adaptation will be discussed here. It was conventionally thought that light adaptation involved simply a desensitisation of the photoreceptor cell response induced by photopigment bleaching, thus reducing the amount of visual pigment available to initiate phototranduction (Glantz, 1972). However, a study of visual sensitivity in the rat (Dowling, 1963; cited in Glantz, 1972) revealed that variations in sensitivity could be observed in the absence of measurable pigment bleach. This directed study to potential adaptation processes occurring within the primary visual cells.

The relationship between receptor potential and stimulating light intensity, which exists over 4-5 log units of intensity (known as the dynamic range sensitivity of the photoreceptor), means that without a mechanism for shifting this relationship along the log irradiance axis (range shift), the photoreceptor would saturate over a relatively narrow range of stimulus irradiances. Sensitivity of the photoreceptor can be defined as the amount of change in membrane potential produced per incident photon (after Fain and Lisman, 1981).

Neural adaptation involves a change in gain control of the photoreceptor in response to light. This adaptation can occur at both the transducer (photoreceptor) level or at the level of subsequent neural processing. The electroretinogram will record only the effect of transducer light adaptation processes. During light adaptation, the amplitude of the ERG in response to criterion stimulus intensity decreases. Light adaptation modifies the intensity-response relationship of the photoreceptor (range shift, see Fig. 2.2, section *2.1.2*), such that photoreceptor sensitivity decreases. The shift of the intensity-response function along the logI axis has no effect on the shape or slope of the relationship – it is simply a horizontal shift.

The effect of light adaptation on photoreceptor response is also apparent as a change in the shape of the ERG waveform. When the photoreceptors are illuminated with prolonged high intensity stimuli, an initial transient response reaches maximum amplitude; this is followed by decay in the response amplitude to a steady plateau level, which is maintained until the stimulus is switched off (see Fig. 2.4).

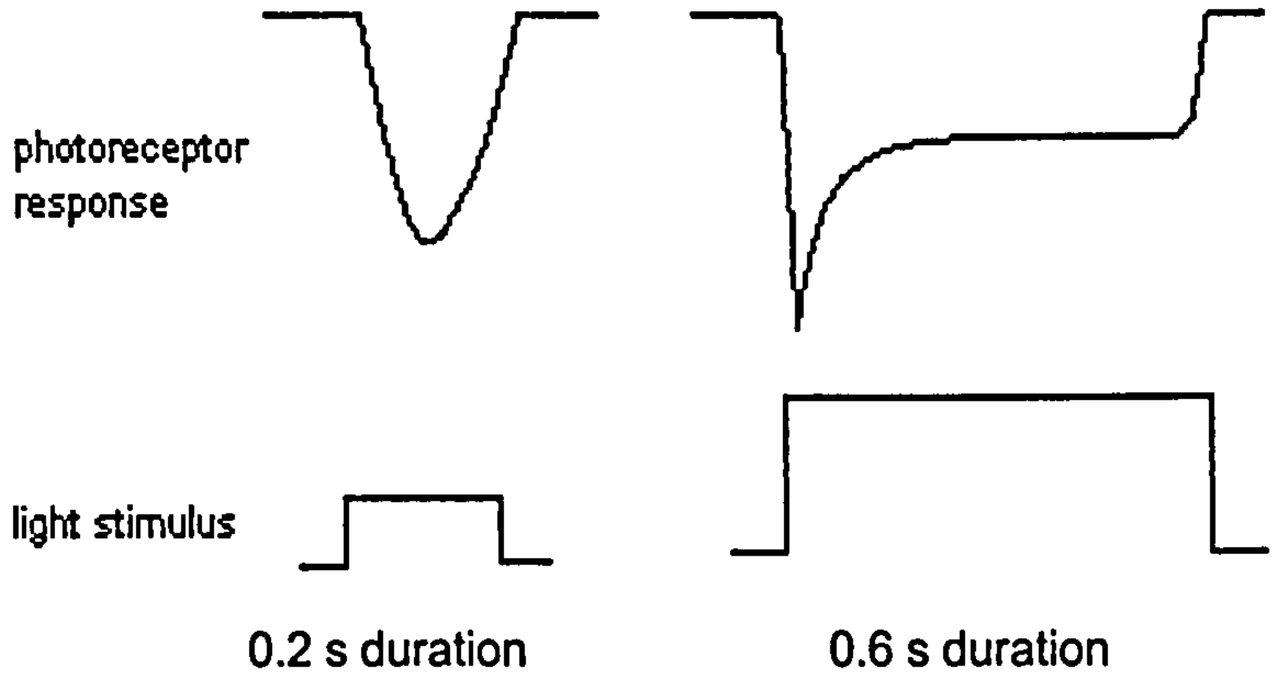

Figure 2.4. A diagrammatic representation of the response waveform of the ERG from an invertebrate compound eye. a) the response to a brief, dim light stimulus is typically monophasic, returning to pre-stimulus baseline once the stimulus is terminated; b) the response to a prolonged stimulus of higher intensity typically shows an initial rapid transient followed by decay to a plateau level, the response returns to pre-stimulus baseline on termination of the stimulus

In the transition between the peak amplitude transient phase and the maintained plateau phase, the conductance gain of the photoreceptor (transducer) changes and the ratio of activated depolarising conductances to photons falls, resulting in a situation where more photons are required to produce a criterion response.

The fundamental mechanism reducing conductance gain is a reduction in the inward (Na^+) current (see section *2.1.2.1*) across the photoreceptor cell membrane. The desensitising effect of intracellular calcium concentration ($[Ca^{2+}]_i$) on the retinula cell response has already been mentioned in section *2.1.2.1*. There is evidence that implicates the presence of intracellular Ca^{2+} in light adaptation desensitisation. For instance, the conductance increase of the photoreceptor membrane per absorbed photon is reduced during light adaptation in the ventral photoreceptors of *Limulus* (Lisman and Brown, 1975a) and intracellular injections of calcium buffers have been shown to reduce light-induced desensitisation (Lisman and Brown 1975b). Raising $[Ca^{2+}]_i$ in the dark produces a reversible desensitisation (Lisman and Brown, 1972,

cited in Fain and Lisman, 1981). Light adaptation affects the ratio between photons absorbed and conductance increase, and it is likely, although not certain, that the conductance decrease is due to a reduced number of opened channels per absorbed photon, and that this process is dependent on $[Ca^{2+}]_i$ in both *Limulus* and the honey bee drone (*Apis mellifera*) (Lisman and Brown, 1975b; Bader *et al.* 1976) (see Fain and Lisman, 1981, for a review).

The previously mentioned voltage-activated outward K^+ currents, (section *2.1.2.1*), act to repolarise the photoreceptor membrane. Therefore, they cannot be disregarded in a discussion of desensitising processes. Laughlin (1981) however, expresses doubt as to the prominence of these processes in light adaptation as it would be an energetically expensive means of desensitising the visual response, and therefore favours the importance of Ca^{2+} in desensitisation rather than K^+. In addition, the voltage-sensitive outward K^+ current is itself attenuated during prolonged stimuli so that as sodium conductance decreases, and thus the depolarisations become smaller (effect of light adaptation), the degree of repolarisation is also reduced so that brain does not receive messages indicating that the eye is observing a dimming stimulus.

2.1.3 Previous Electrophysiological Studies of the Invertebrate Visual System

Electrophysiology has been used in studies on invertebrate visual systems to investigate: light and dark adaptation; temporal dynamics; spectral sensitivity and polarised light sensitivity.

Light and Dark Adaptation

Electrophysiological approaches have been used to describe light adaptation in many different invertebrate species, these include: the crayfish, (*Procambarus clarki*), Glantz (1968); the drone bee (*Apis mellifera*), Bader *et al.* (1976); the fly (*Musca*), Laughlin and Hardie, (1978); the dragonfly (*Hemicordulia*), Laughlin and Hardie, (1978); and blowfly (*Calliphora*), Weckstrom *et al.* (1991). All of these studies are in agreement with the fact that adaptation to a background light of constant intensity shifts the intensity-response function of the photoreceptor parallel to the logarithmic intensity axis.

Glantz (1968) combines the use of intracellular recording from excised eyes of the crayfish with recordings of the ERG *in situ*. The latter technique is adopted in order that the preparation is useful for longer, the half lifetime of the excised preparation being only 3h. This was not long enough for a comprehensive study of light adaptation in which it is required that the eye return to a fully dark-adapted state at appropriate intervals. Glantz (1968) shows that dark-adaptation is a reversal of the light adaptation process, i.e. sensitivity is increased, and that the total time to complete dark-adaptation is a function of the intensity or duration of a preceding light stimulus.

Laughlin and Hardie (1978) use intracellular recording techniques to study light adaptation mechanisms of the visual system of the fly and dragonfly. The use of intracellular recording as opposed to recording the ERG has the advantage that one is recording the response of the penetrated cell alone, while the electroretinogram is a gross retinal response; and may therefore be 'contaminated' with signals from cells other than those of direct interest, the photoreceptors. This study reveals that there are two phases to light adaptation in the photoreceptors of the fly and dragonfly. A fast (duration 100ms) phase and a slow phase (duration up to 60s) shift the intensity-response relationship along the (log) intensity axis without changing the shape or slope of the relationship. The fast phase of light adaptation reduces the transient peak amplitude response to stimulation to a stable plateau. The authors suggest that the fast phase may be mediated by intracellular Ca^{2+} concentration as is suggested for the drone bee (Bader *et al.* 1976). The slow phase of light adaptation lasts for several seconds and it is suggested that this may be generated by a number of different components.

Weckström *et al.* (1991) investigated the role of voltage-sensitive conductances in the photoreceptors of the blowfly (*Calliphora vicina*) during light adaptation, using intracellular techniques. This study reveals that there are two light adaptation mechanisms occurring in blowfly photoreceptors: 1) the amplitude and duration of quantum bumps is reduced (probably as a result of an increase in $[Ca^{2+}]_i$ see section *2.1.2.2*), and 2) voltage-sensitive delayed rectifying K^+ channels reduce the amplitude of the sustained response to bright backgrounds and the responses to increments imposed on these backgrounds (see section *2.1.2.2*, Fig. 2.4). They conclude that the delayed rectifier (K^+ channel) in the photoreceptors of blowfly "regulates the cell's gain and frequency response so as to extend the photoreceptors operating range".

Autrum (1981) describes dark-adaptation as an "increase in sensitivity occurring as soon as ambient light decreases or is turned off", and is clear about the fact that dark-adaptation is not simply the converse of light adaptation. If light and dark-adapted responses of the same amplitude from the same eye/photoreceptor are compared, it is apparent that they differ in temporal dynamics. "Under constant adapting background light the latencies and time courses are shorter than when the same sensitivity is reached during dark adaptation". Studies specifically concerned with the temporal resolution of the response of photoreceptors in phototransduction are reviewed below.

Temporal Resolution

Since Autrum's extracellular work on insect photoreceptors in the 1950s, in which he measured the flicker fusion frequency (the frequency of a square wave stimulus at which the eye can no longer resolve the flicker/alternating pattern) of the visual response of various species, it has been generally accepted that photoreceptor response dynamics are tuned to the habitat and lifestyle of the animal. More recent studies utilising intracellular recording, on diurnal, terrestrial, and 'fast' and 'slow' insects (Howard *et al.* 1984; de Souza and Ventura, 1989; Laughlin and Weckström, 1993), have supported this concept. Photoreceptor response dynamics change according to the light level in the environment: diurnal species have a better temporal resolving power (i.e. they can resolve faster events) than arrhythmic and nocturnal species (Howard *et al.* 1984; deSouza and Ventura, 1989).

It has also been established that temporal resolution is associated with the speed at which insects move (Howard *et al.* 1984, deSouza and Ventura, 1989, Laughlin and Weckström, 1993). Laughlin and Weckström's (1993) experiments on the temporal response of the photoreceptors of dipteran species revealed that tipulids (crane flies) have slow photoreceptor cells (with light-adapted corner frequencies of 16-19Hz; the corner frequency is the frequency at which the signal power in the response from the eye falls to half maximum). This is in contrast to blowflies and flesh flies that show high temporal resolutions (with light-adapted corner frequencies of between 50 and 107Hz). The speed of the photoresponse is associated with the speed of image motion encountered on the retina. Long legs and weak flight prevent the slow-celled tipulids turning rapidly but the fast celled blowflies are notorious for their acrobatics (Laughlin and Weckström, 1993). For a description of techniques used to determine

temporal resolutions of photoreceptors e.g. flicker fusion frequency, the reader is referred to Chapter 4.

Experiments to determine the temporal dynamics of fly photoreceptors (e.g. Eckert and Bishop, 1975, cited in Laughlin, 1981) revealed that response dynamics are affected by adaptation state, i.e. the temporal resolution of the photoreceptor increases with light adaptation. A dark-adapted tipulid fly photoreceptor responds maximally to stimulation frequencies of 7Hz, but upon light adaptation, the response becomes maximally sensitive to frequencies of 16Hz (Laughlin, 1981), thus, light adaptation increases the speed of photoreceptor response.

Laughlin (1981) proposes that the time course of conductance changes, in the photoreceptor cell membrane, initiated by light stimulation may affect the response dynamics of the photoreceptor. Laughlin and Weckström (1993) used intracellular recording and current clamping to resolve the time constants across the photoreceptor membrane in dipteran species. They also determined the input resistance, rectification and conductance of photoreceptor membrane. From these measurements, they were able to determine that 'fast' and 'slow' cells produce voltage-gated outward (K^+) currents with different dynamics.

There are few studies of the temporal resolution of the visual systems of deep-sea animals and these are reviewed in section *4.1.2*.

For further detail regarding temporal resolution of the visual response, the reader is referred to Chapter 4.

Spectral Sensitivity

Electrophysiology can be used to determine the spectral sensitivity curve of the response of photoreceptors. All visual pigments have a major absorption peak at which they are most effective at absorbing photons; the wavelength at which this peak occurs is referred to as the λ_{max} (see section *1.6.2*). Electrophysiological recording (both extracellular and intracellular) can provide information about the spectral sensitivity of photoreceptors, and although this measurement may agree with the λ_{max} of the visual pigment measured spectrographically, this is not always the case due to distortion by selective filtering by the dioptric apparatus and

accessory pigments (Goldsmith and Fernandez, 1968; Marshall, *et al.* 1999). An argument can be made that it is more appropriate to measure the spectral response of the visual pigment itself; this can be done *in situ* using the technique of microspectrophotometry (MSP), whereby rhabdoms containing the visual pigment are isolated and tested. However, it may be more useful to record the response to light that the photoreceptor will produce *in situ* because such direct measurements include the effects of diverse factors such as screening pigments and intraocular filters for example.

Goldsmith and Fernandez (1968) used the ERG to measure the spectral sensitivities of the photoreceptor response from a number of species of crustacean; *Porcellio scaber* (woodlouse), *Paleomenetes paludosus* (prawn), *Callinectes sapidus* (blue crab) and *Orconectes virilis* (northern crayfish). The dark-adapted spectral sensitivity for each animal was established by determining the relative quantum flux required to evoke retinal potentials of constant size (Goldsmith and Fernandez, 1968). A plot of log sensitivity vs wavelength subsequently revealed any peak responses with respect to wavelength of stimulating light. In all species studied, the dark-adapted spectral sensitivity curve revealed a peak in the blue-green region of the spectrum (450-570nm); subsequently, each animal was adapted with long wavelength light (broadband red light) in order to preferentially bleach the longwave sensitive visual pigment, thus allowing any potential contribution of the unbleached visual pigment to be seen. Only in the prawn, *Paleomenetes paludosus* was this successful, and it is stated that this species has a dual pigment system in the photoreceptor (Goldsmith and Fernandez, 1968). It is concluded that the photoreceptors of *P. paludosus* contain a dominant pigment (dominant as it was prominent in the dark-adapted photoreceptor response) with a peak sensitivity of around 550nm and a second, less abundant pigment with a peak sensitivity of around 380nm.

Results of studies of the spectral sensitivities of marine crustaceans have already been reviewed in section *1.6.2*, and the reader is referred to this section.

Polarisation

A major discovery of visual function was made in the *Limulus* lateral eye using extracellular recording of the discharge rate from single visual units along the isolated afferent nerve for each unit. Waterman (1950) used light beams that were linearly polarised in varying planes of

polarisation to stimulate single visual units, and the discharge rate of the single visual units were examined in relation to the plane of polarisation of the stimulating light. The results of this investigation revealed that photoreceptor units in the *Limulus* eye were sensitive to the plane of polarisation of light. "It may thus be concluded that for this photoreceptor significant differences in the 'apparent brightness' of a stimulating light depend on the plane of its polarisation" (Waterman 1950).

2.2 RECORDING THE INVERTEBRATE ERG- MATERIALS AND METHODS

2.2.1 Animal Collection and Maintenance

2.2.1.1 Mesopelagic malacostracan crustaceans

Various species of mesopelagic decapod malacostracan were collected during RRS Discovery cruise 243, in the region of the Cape Verde Islands, Oct-Nov 1999. During this cruise, animals were collected in a closing cod-end used with a RMT 1+8 net. The closing cod-end functions as a light protected and thermally insulated container which is closed at depth (see Roe and Shale, 1979; Wild *et al.* 1985), thus animals are not exposed to ship lights or daylight irradiance levels on retrieval of the cod-end from the water. Exposure to these irradiance levels has been proven to cause irreversible damage to the physiology and structure of the photoreceptors of deep-sea species (Loew, 1976; Nilssön and Lindström, 1983; Shelton *et al.* 1985).

Specimens of the mesopelagic decapod malacostracan, *Systellaspis debilis*, were collected during a cruise on the R/V Seadiver (Harbor Branch Oceanographic Institution, Ft. Pierce, Fl.), in the region of the Northwest Providence Channel, Bahamas, March 2000. These animals were collected in a light protected and thermally insulated closing cod-end used with an opening/closing 2.4 x 1.8m Tucker Trawl.

One species of euphausiacean malacostracan, *Meganyctiphanes norvegica*, and two species of decapod malacostracan, *Pasiphaea multidentata* and *Sergestes arcticus*, were collected during two cruises on the R/V Edwin Link (Harbor Branch Oceanographic Institute, Ft. Pierce, Fl.) in the Gulf of Maine, June and September 2000. *M. norvegica* and *S. arcticus* were collected from Oceanographers Canyon, south edge of Georges Bank, Gulf of Maine. *P. multidentata* was collected from Wilkinsons Basin, Gulf of Maine. Once again, these animals were collected using the 2.4 x 1.8m Tucker Trawl with a closing cod-end.

In all cases of animal collection, once the closing cod-end was retrieved from the water it remained sealed until in a light protected environment. The cod-end was then opened and the catch sorted under dim-red light. Sorting was done under dim-red light (λ>600nm) to minimise

photoisomerisation of the short wavelength sensitive visual pigment, (Frank and Case 1988a, Hiller-Adams *et al.* 1988). The source of the dim red light was a Petzl Head Torch; light was made red by placing red filter (LEE filters, 106 primary red) in the light path (see Fig. 2.5)

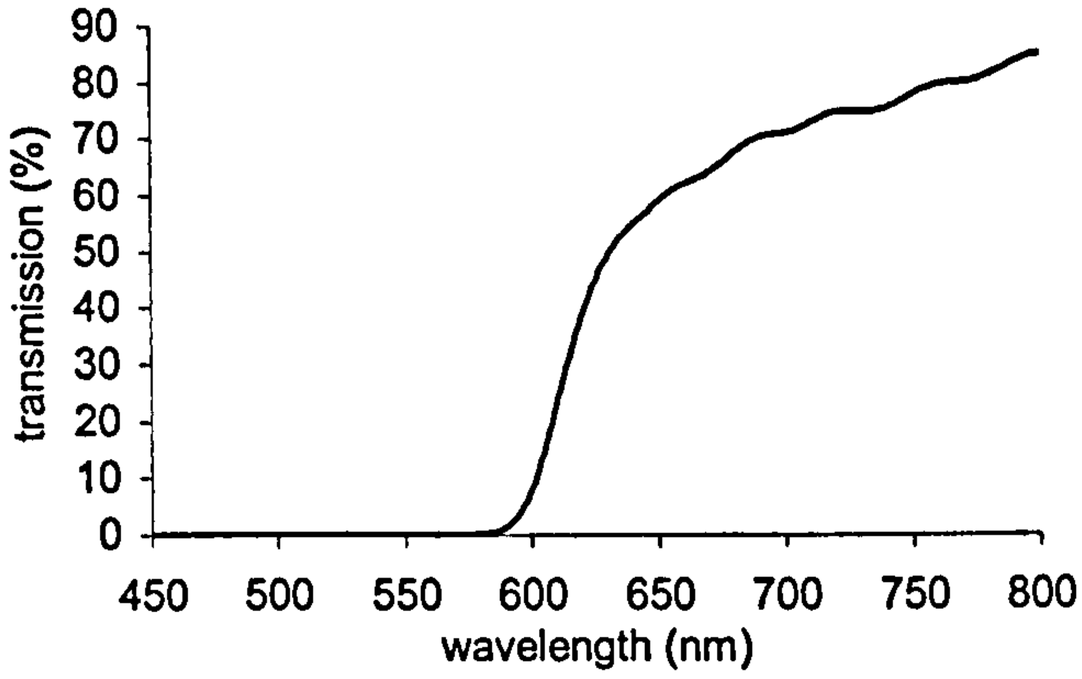

Figure 2.5. Transmission properties of red filter (LEE filters, 106 primary red) used to manipulate the output of a Petzl head torch and a dissecting microscope.

Once retrieved from the cod-end, animals were maintained at 5°C in light-protected tanks containing filtered seawater, which was aerated. Providing regular water changes were made, animals were maintained in good condition for up to one week. All electrophysiological recordings from mesopelagic malacostracans had to be carried out on board ship, as these animals do not survive transportation back to shore-based laboratories.

All animals were maintained in the dark for at least 24h prior to experimentation to allow the eyes to dark-adapt after exposure to bioluminescence in the cod-end. Hiller-Adams *et al.* (1988) present evidence for photoisomerisation of rhodopsin within the rhabdoms of mesopelagic decapod malacostracans, due to exposure to bioluminescence in the trawl. They also propose that these animals show regeneration of rhodopsin after periods of time in the dark. Circadian rhythm has no effect on the visual response of mesopelagic species (Moeller and Case, 1995; Frank, T., pers. comm.), therefore the time during the day at which the experiments were conducted was not controlled.

2.2.1.2 Coastal, shallow-water malacostracan crustaceans

Two species of decapod malacostracans, the coastal/estuarine species, *Crangon crangon* and the intertidal species *Palaeomon elegans*, were obtained from the University Marine Biological Station Millport (UMBSM), Scotland. Both species were maintained in aerated seawater tanks at 10°C at the University of Bristol. The animals were exposed to a 12h light:dark cycle. As both these species are shallow living (0-50m), the 12h light:dark cycle was used to imitate a diurnal change in irradiance levels. With weekly water changes and regular feeding the animals could be maintained in a healthy state for many months. All experimentation was performed on animals in the dark phase of the 12h light:dark cycle for two reasons: 1) to enable comparison with the dark-adapted visual response of the mesopelagic malacostracans; 2) to avoid any effect of circadian rhythm on the visual response (Aréchiga, 1977). Consequently, all animal handling was performed under dim red light (λ>600nm, see section *2.2.1.1*, Fig. 2.5) to avoid photoisomerisation of the visual pigment and to prevent the onset of pigment migration, a light adaptation mechanism, in the compound eyes of these animals (see section *1.5.4*).

The use of animals with intact visual systems was fundamental to this study. Only animals with undamaged eyes and bright eye-shine were used for experimentation. Eye-shine is caused by light entering the eye being reflected at the tapetal layer (see section *1.5.5* for description and function of the tapetum); all animals used in this study, with the exception of the euphausiid species, possessed a tapetum. It is often the case that an eye with internal damage shows dull or no eye shine (personal observation).

2.2.2 Apparatus

A considerable proportion of this study was concerned with the construction of experimental apparatus to record electroretinograms from malacostracans. The equipment had to be designed such that it would work equally effectively on a moving vessel at sea, and in a laboratory on land. Electrophysiological recording has a number of requirements, namely 1) a stable environment for the preparation to ensure it remains healthy; 2) reliable electronics to collect signals from the eye and amplify them to a usable size; and 3) a means of stimulating the preparation to provoke a response.

2.2.2.1 Electrical Recording

All electrophysiological recordings were made inside a light protected, metal-mesh Faraday cage. When connected to a common ground terminal, the Faraday Cage forms an extended electrical shield, reducing induced noise currents in the preparation from nearby electrical field sources in the laboratory. The cage was constructed with access holes to the interior to allow tubing and cables to reach into the cage. A single ground bolt within the cage was used to ground any equipment entering the cage. This bolt was subsequently attached to a common ground point to avoid the effects of ground loop currents (see section *2.2.3.2*).

All animals to be used for electrophysiological recordings were prepared in the same way. All preparation was carried out under dim red light (see section *2.2.1.1*). Each animal was mounted by the dorsal surface of the carapace/cephalothorax onto a perspex rod using a minimal quantity of superglue gel (Loctite). The animal was then suspended in a chamber filled with seawater within the Faraday cage, ensuring the ventral surface of the animal was submersed. This arrangement allowed the pereopods to maintain respiratory currents across the gills. The seawater in the chamber was temperature controlled by a Peltier cooling system, for mesopelagic species, the temperature of the water was maintained at 5°C, and for the shallow-water, coastal species the temperature of the water was maintained at 10°C. The Peltier cooling system operated by transferring heat from the seawater to a metal heat sink at one end of the chamber. A cold-water flow (pumped from a reservoir of iced freshwater) across the heat sink ensured that the heat sink remained effective. Because the ambient temperature was often above that of the seawater in the chamber, the chamber was also well insulated using expanded polystyrene tiles.

The recording electrode was an expoxylite insulated tungsten microelectrode (10μm tip, 2-4MΩ impedance; Fredrick Haer & Co.). Using a micromanipulator, and with the aid of a dissecting microscope (outputting dim-red illumination) mounted inside the Faraday cage, the microelectrode was placed just below the corneal surface of the eye. A red filter (see section *2.2.1.1*, Fig. 2.5) was placed in the light path of the light of the dissecting microscope to alter its spectral output. The reference electrode was identical to the recording electrode, and was placed into the seawater in the chamber, close to the animal, but far enough away to prevent the

animal disturbing the electrode with its appendages. Fig. 2.6 illustrates the preparation during experimentation.

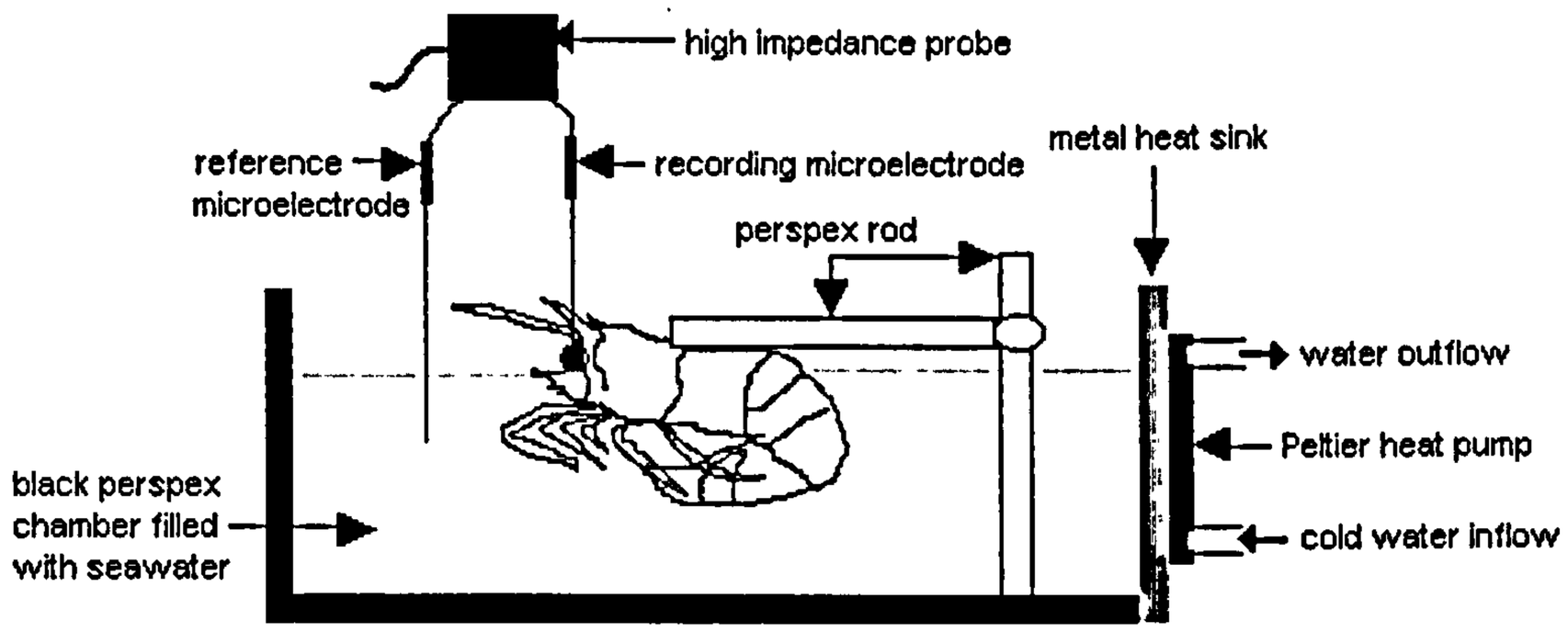

Figure 2.6. The seawater chamber used in experimentation. The position of the animal with respect to the microelectrodes is shown. The animal is submersed to allow respiratory currents over the gills to be maintained.

Signals from the eye were amplified using a DC amplifier (Neurolog, NL106; Digitimer Ltd) with a gain of 100, a 50Hz notch filter, and high and low pass filtering capability. The DC amplifier was used in conjunction with a high impedance (10MΩ) probe (Neurolog NL100AK; Digitimer Ltd) (amplification x1). The very high impedance of the probe was to eliminate any artefacts in the signal caused by electrode polarisation, and to ensure that the power across the electrodes was not attenuated (Armington, 1974). The ERG signals generated by the eye are of such small amplitude (μV – mV) that it was necessary to situate the probe inside the Faraday cage as close to the preparation as possible to ensure that the signal from the eye was not attenuated before it reached the probe. The low pass filter within the amplifier removed frequencies >100Hz from the signal. The amplified ERG signals were then captured on a digital oscilloscope (HAMEG, model no HM407). Data were transferred from the oscilloscope to a PC, using SP107 software via an RS232 interface, where they were stored for subsequent analysis.

2.2.2.2 Source of optical stimuli

The ERG signal was produced in response to light stimuli. The following properties of the light stimulus were controlled: a) intensity of light falling on the eye; b) the spectral output of the light; c) the duration of the light stimulus; d) the geometric shape of the stimulus; and e) the temporal-intensity 'shape' of the stimulus.

The source of the light stimulus was a blue ultra high bright light-emitting diode (LED), (Marl Optosource, λ_{max} 464nm). A LED was used for the following reasons: they are inexpensive; the light emitted by a LED has a narrow wavelength range, typically 20-50nm (as opposed to an incandescent lamp for example, which contains a wide range of wavelengths); they require relatively little power to drive them, generally LEDs draw currents between 10 and 40 mA; and they are durable and of small size and weight. LEDs convert electrical current directly into light, and as the intensity of the LED light output was to be varied during experimentation, it was necessary to determine the output properties of the LED in relation to the current input to the LED. A spectroradiometer was used to measure the output of the LED at 1nm intervals between 350–550nm, at a number of different current inputs to the LED between 0.5 and 30mA (30mA is the maximum forward current for this particular LED). The plots in Fig. 2.7 show the relationship between current input and light output for the ultra high bright blue LED.

It is apparent that there is an increase in LED output with current input (Fig. 2.7a), however, this increase in LED output is accompanied by a shift in peak spectral output (λ_{max}) of the LED, shown in Fig. 2.7b. At minimum current input to the LED the λ_{max} is 468nm, whereas at maximum current input to the LED the λ_{max} is 464nm, thus there is a 4nm shift in the peak spectral output of the LED between minimum and maximum current input. This non-linearity in the LED output is further emphasised in Fig. 2.7c, which shows the non-linear relationship between current input and light output of the LED.

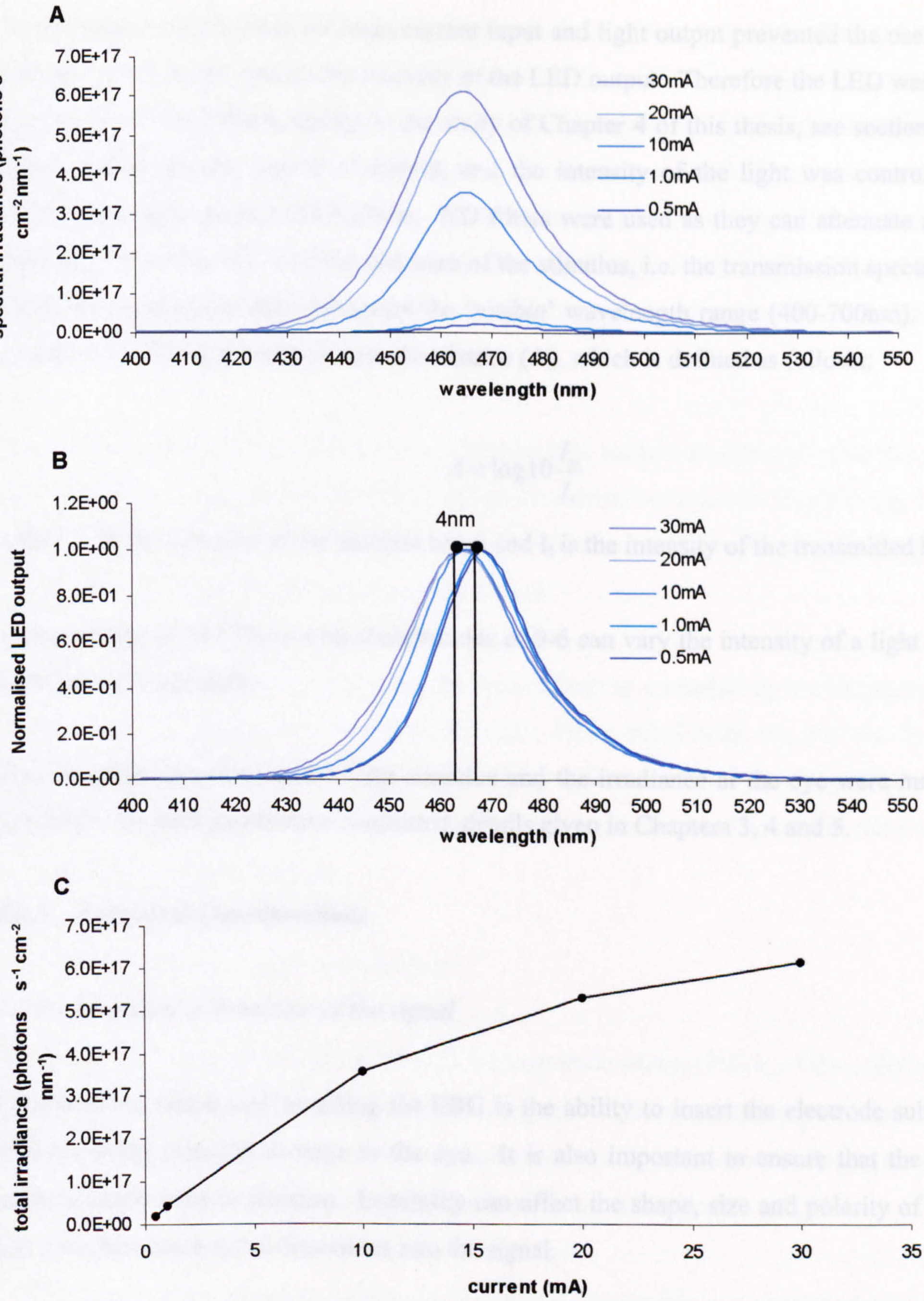

Figure 2.7. These plots show the results of measuring the output of the ultra high bright blue LED (λ_{max} 464nm) at different current outputs between 0.5 and 30mA, with a spectroradiometer. A) shows an increase in light output (displayed as photon irradiance on the cosine collector of the spectroradiometer) with an increase in current input to the LED. B) shows the irradiance normalised to the maximum, this reveals a shift of 4nm in peak spectral output; the peak spectral output at 30mA current input is shifted 4nm to shorter wavelengths relative to the peak spectral output of the LED at minimum (0.5mA) current input. C) shows the non-linearity in the relationship between LED output (integrated irradiance) and current input.

The non-linear relationship between current input and light output prevented the use of simple current control to manipulate the intensity of the LED output. Therefore the LED was driven at maximum current (30mA, except in the study of Chapter 4 of this thesis, see section *4.2*), and thus constant spectral output of 464nm, and the intensity of the light was controlled using calibrated neutral density (ND) filters. ND filters were used as they can attenuate a beam of light with very little effect on the spectrum of the stimulus, i.e. the transmission spectrum of the ND filter is approximately flat across the 'visible' wavelength range (400-700nm). They are normally described in terms of their absorbance (A), which is defined as follows:

$$A = \log 10 \frac{I_o}{I_t}$$

where: I_o is the intensity of the incident beam and I_t is the intensity of the transmitted beam.

Thus, a range of ND filters with absorbencies of 0-6 can vary the intensity of a light source by six orders of magnitude.

The temporal properties of the light stimulus and the irradiance at the eye were manipulated differently for each experiment conducted, details given in Chapters 3, 4 and 5.

2.2.3 Technical Considerations

2.2.3.1 Mechanical distortion of the signal

Crucial to the success of recording the ERG is the ability to insert the electrode subcorneally whilst causing minimal damage to the eye. It is also important to ensure that the electrode remains stable once in position. Instability can affect the shape, size and polarity of the ERG, and introduce mechanical distortions into the signal.

To reduce the possibility of mechanical distortion of the microelectrode, a stable mounting for the microelectrode was used. Each microelectrode was secured to a micromanipulator with a magnetic base, which in turn, was secured to the metal base plate of the Faraday cage. Positioning of the microelectrode was performed by operating the micromanipulator manually.

Another source of mechanical distortion can arise from animal movement during recording. It was necessary to ensure that once the microelectrode was in position for recording, that the animal would not dislodge it from the eye. Unless the animal was attached very securely by the length of its dorsal surface of the carapace/cephalothorax to the holder, it would attempt the 'caridoid escape reaction'. This is a rapid contraction of the ventral abdominal muscles, causing the animal to shoot quickly backward, and is common to those malacostracans with well-developed abdomens. This violent movement uses the whole body for leverage, and as such is to be avoided during recording.

The malacostracans used in this study all possessed stalked compound eyes; the eyes were borne on distinct movable stalks. Thus, before the microelectrode was inserted into the eye, the eyes had to be securely stabilised. This was achieved by using small amounts of superglue gel (Loctite) around the eyestalk to prevent movement.

The Faraday cage and preparation inside were vibration protected by mounting the cage on airfeet (Barry Controls Ltd, model SLM-1A). Once filled with the air, the airfeet were effective as anti-vibration devices, preventing vibrations from both general laboratory movement and ship movement from disrupting the preparation. The airfeet themselves were securely fixed to the bench top.

2.2.3.2 Electrical distortions of the signal

As previously mentioned (section *2.2.2.1*) the amplitude of the ERG is of the order of μV-mV, thus substantial amplification of the signal is required. This need for amplification means that the amplifier has a high gain and a consequence of this is that the recording system becomes responsive to extraneous, interfering signals that are not related to the ERG.

There are a number of stages within the recording system that are particularly susceptible to radiative electrical pick-up, or 'noise'. Examples of radiative pick-up include line frequency noise from lights and power sockets; this 'mains' noise (50Hz in the UK, 60Hz in the USA) is a particular problem as it is very common and once amplified can completely obliterate the ERG signal.

The most vulnerable stage of the recording system is the point at which the signal is transmitted from the eye to the high impedance probe via the microelectrode. This is a good reason for making the distance between the microelectrodes and the probe as short as possible. This stage in the recording system was protected from extraneous noise by placing the preparation inside the Faraday cage, which is electrically isolated from the surrounding environment (see section *2.2.2.1*). This was helped by the use of shielded cable to connect the microelectrode lead to the probe.

Once the signal has reached the probe it still has to be carried to the DC amplifier for amplification. This stage is again susceptible to extraneous noise pick-up, and this was prevented by using shielded BNC cable.

Another common cause of electrical distortion of the signal is ground loop noise. This arises when shielding is grounded to more than one place, there are two consequences of this: 1) magnetic fields may induce currents in the loop; 2) if the grounds are at different potentials a current may flow through the shielding, thus introducing extraneous noise. This was prevented by ensuring that there was a single common ground point for every shielding or piece of equipment.

2.2.3.3 Design for use at sea

Working in a laboratory on board a vessel at sea presents a number of problems to an electrophysiologist. This is an inherently noisy environment, both in terms of an abundance of extraneous electrical noise, and in terms of potential for mechanical distortion to ERG measurements.

It is very rare that a vessel at sea is stationary. Thus, one has to contend with a more or less constant movement, which varies in amplitude, so presenting difficulties to maintaining a stable preparation. All equipment for electrophysiology in this study was constructed so that it could be securely fastened down.

Not only is a vessel at sea a mechanically unstable environment, it is also inherently electrically noisy. Screening of mains electricity is poor on a ship and thus mains noise is a common

problem. This was anticipated and was dealt with by the use of a 50Hz notch filter, which was built into the DC amplifier in the recording system. The bandwidth of this notch filter was such that it operated equally effectively to cut out 60Hz mains noise, which was a problem on board American ships. In some instances, extra shielding of leads and cables was also required.

CHAPTER 3: MARINE MALACOSTRACAN VISUAL SENSITIVITY

3.1 INTRODUCTION

Many animals inhabit environments in which the ambient mean light intensity varies considerably; for terrestrial diurnal animals, ambient irradiances can vary by a factor of 10^{10} from day to night (Laughlin, 1981). In contrast to this, animals that inhabit the depths of the open ocean are exposed to less variable and low mean ambient light intensities (for more detail of the photic environment in the open ocean, see section *1.3*). The light intensity at a depth of 800-1000m in the open ocean (for the clearest tropical water) is reduced by approximately 12 orders of magnitude in comparison with light intensity at sea level during full midday sunlight on a cloudless day (Denton, 1990). Despite this paucity of light, animals found at all depths in the ocean, even at abyssal depths, possess well-developed eyes.

Many oceanic organisms are capable of generating their own light through bioluminescence, and this represents an increasing proportion of light as depth increases; in the mesopelagic zone, approximately 90% of all animals are bioluminescent (see section *1.3.1*). However, bioluminescent events are relatively rare in the ocean in the absence of mechanical stimulation. Nearest-neighbour values for many mesopelagic species (based upon theoretical calculations of abundance in the ocean) put individuals beyond the range at which bioluminescent signals are visually detectable (Herring, 2000a). It is proposed that bioluminescent signals are used for conspecific and sexual signalling at intermediate ranges once initial contact is made using another sensory modality, for example, olfaction (Herring, 2000a). The generation of bioluminescent signals in the absence of the intended receiver is both energetically wasteful and dangerous as it may attract predators. The visual systems of deep-sea animals are therefore required to both function effectively in a photon-limited environment (under the influence of downwelling light), and effectively detect both diffuse and point source bioluminescent emissions.

Photon-limited environments are not exclusive to the deep-sea; they are also experienced by a large number of terrestrial/shallow water animals, particularly those that occupy the temporal niche of night-time. For nocturnal animals, most ambient irradiance is caused by full moonlight, which is typically 6-7 orders of magnitude less bright than midday sunlight,

depending on cloud cover (Denton, 1990). This ambient irradiance is dependent on the phase of the moon however; starlight and airglow alone produce an ambient irradiance that is approximately 2 orders of magnitude less than full moonlight (Dusenbery, 1992). Although bioluminescence is rare in the terrestrial environment (in comparison with the oceanic environment), some terrestrial animals are also capable of generating bioluminescence; for example, fireflies (Lampyridae), and luminous beetles in the families Elateridae, Phengodidae, and some species of earthworm, centipedes and millipedes (Herring, 2000b).

Photon-limited environments are inherently 'noisy' with respect to visual imaging, i.e. under these conditions, a given signal has a low signal-to-noise ratio. To maximise the signal-to-noise ratio in such conditions a visual system must be highly sensitive and the visual systems of both deep-sea and shallow water nocturnal malacostracans could thus be expected to show adaptations conferring high sensitivity. When describing the sensitivity of a visual system, reference is made to a measurement of the ability of that system to capture and efficiently utilise photons. A visual system with a high sensitivity is one that: a) maximises photon capture and b) can efficiently transduce the information (e.g. spectral composition, spatial and temporal distribution, contrast) contained in the photon signal for subsequent neural processing.

Land (1981) warns that it is not possible to put an exact value to the absolute sensitivity of an eye, as different receptors within an eye may be involved in different visual tasks and thus have different sensitivities and resolving powers. However, for purposes of comparative study absolute sensitivity can be approximated by an equation that accurately describes, sensitivity in terms of the number of photons absorbed per receptor, per unit of luminance in the visual field being imaged (Land, 1981). This equation is as follows:

$$\text{Sensitivity } (S) = \left(\frac{\pi}{4}\right)^2 \cdot \left(\frac{A}{f}\right)^2 \cdot d^2 \cdot (1 - e^{-kx})$$

Where: A/f = relative aperture of the photoreceptor
d = photoreceptor diameter
x = photoreceptor length
k = absorption coefficient of visual pigment

The definition of S is the ratio of the number of photons absorbed per receptor to the number emitted per steradian by $1m^2$ of an extended source, and changes in A/f, d and x can produce substantial differences in receptor sensitivity.

Increased visual sensitivity is achieved both optically and neurally. Optical adaptations to increased sensitivity in mesopelagic malacostracans involve changes in the aperture, diameter and length of photoreceptors (e.g. Hiller-Adams and Case, 1985; Gaten *et al.* 1992, see section *1.6.1*). Superposition optics, tapeta and enlarged eyes also increase visual sensitivity (Hiller-Adams and Case, 1988; Land, 1990; Shelton *et al.* 1992; Gaten *et al.* 1992; Johnson *et al.* 2000b, see sections *1.5.3* and *1.6.1*). The shallow-water, nocturnal species of malacostracan, *Crangon crangon* and *Palaemon elegans*, also possess superposition optics and tapeta. At a neural level, high conductance gain of the photoreceptor cell membrane can increase visual sensitivity (see section *2.1.2.2* for a more detailed explanation). For example, the number of conductance channels opened in the photoreceptor cell membrane of *Limulus*, per absorbed photon, is increased when in dim light (cited in Laughlin, 1981). Photoreceptors are also required to register photons efficiently; under photon-limited conditions it is necessary that the optics and the sampling and processing in the retina and subsequent neural structures integrate over space and time to ensure that the maximum amount of information is extracted from the visual signal (Laughlin, 1990). Such sensitivity is inevitably obtained at the expense of spatial and temporal resolution; the resulting visual image is of low resolution as a result, but it is a necessary trade-off in visual systems operating in low luminances (Laughlin, 1990).

Evolutionary adaptations in optical and retinal morphology to maximise photon capture can be predicted through anatomical measurements and observations, and interspecific comparisons of sensitivity can be based on comparisons of optical structure. This has been a favoured method for investigating differences in sensitivity between deep-sea species (for example, Gaten *et al.* 1992; Shelton *et al.* 1992), as it does not require the capture of living, viable specimens, which is particularly difficult in the case of deep-sea animals. This approach predicts the sensitivity of the visual response on the efficiency with which the optical and retinal structures will capture and absorb photons but it does not allow for contribution of the temporal and spatial processing properties of the photoreceptor cells towards visual sensitivity. In order to study the sensitivity of the visual system as a whole, one of the following approaches must be adopted: a) studying an animals behavioural responses to changing light intensities (e.g. Frank and Widder

1994a; Frank and Widder, 1994b) (although defining sensitivity unambiguously in a behavioural context is difficult: other aspects of an animal's physiology, besides the response of the photoreceptor, may affect its behavioural response [Autrum, 1979]); b) recording the visual response from the eye electrophysiologically, *in vivo* (see Chapter 2 for a review of electrophysiology).

Electrophysiological techniques have been widely used to investigate many aspects (e.g. absolute sensitivity, spectral sensitivity, spatial and temporal resolution) of the visual response of the invertebrate compound eye in a large number of species: see section *2.1.3* for a review of electrophysiological studies of the invertebrate visual system.

Electrophysiological recordings from deep-sea animals are relatively rare due to the difficulties of obtaining living, robust animals with intact visual systems and keeping them alive during transport to shore-based laboratories. Consequently, in the few studies that have used electrophysiological recordings from deep-sea species (Frank and Case, 1988a; Frank and Case, 1988b; Frank 1999; Frank and Widder, 1999; Johnson *et al.* 2000a; Lindsay *et al.* 1999; Moeller and Case, 1994 and 1995) most electrophysiological recordings have been obtained on board ship. Under these conditions, only extracellular electrophysiological recording is possible due to the difficulties of maintaining stable preparations on board a moving vessel (see section *2.2.3.3* for details).

3.1.1 Aims of This Study

The purpose of this study is to use extracellular electrophysiological recordings to compare the visual sensitivities of the following: a) different species of mesopelagic decapod and euphausiid malacostracans (throughout this study, the alternative collective term, 'shrimp', may be used), which occupy different daytime depth distributions in the water column; b) mesopelagic decapod and euphausiid malacostracans with that of nocturnally active, coastal species of decapod malacostracans. The attenuation of downwelling light in the ocean is strongly predictable, therefore species of malacostracan inhabiting the greatest depths of the mesopelagic zone (200-1000m depth) will be exposed to less ambient illumination than those species inhabiting shallower depths in the mesopelagic zone. This study aims to identify differences in visual sensitivity based on daytime depth distribution in the ocean. Nocturnally

active, coastal malacostracan species are also active in a photon-limited environment; and one would expect that, if the visual sensitivity of an animal is adapted to the ambient light irradiances in its habitat, these coastal species would have similar visual sensitivities as species from the deep-sea. Therefore, extracellular electrophysiology is used to establish the sensitivity of photoreceptor response in species of malacostracans from different habitats; thus exploring the relationship between visual sensitivity and ecology.

The following hypotheses were tested:

1. That mesopelagic malacostracan species that inhabit deeper depths during the daytime will have a higher visual sensitivity than those mesopelagic species with a shallower daytime depth distribution.

   H_0 = there will be no difference in visual sensitivity between the mesopelagic species studied.

2. That shallower living mesopelagic species of malacostracan will have a more sensitive visual response than coastal, nocturnally active malacostracans.

   H_0 = there will be no difference in visual sensitivity between coastal and mesopelagic malacostracans.

3.2 ELECTRORETINGRAPHIC METHODS

3.2.1 Protocol for ERGs on Mesopelagic Malacostracans

Details of animal collection and maintenance are given in Chapter 2, section *2.2.1.* Five species of mesopelagic malacostracans from four locations (Northwest Providence Channel, Bahamas; Northeast Atlantic, region of the Cape Verde Islands; Oceanographers Canyon and Wilkinsons Basin, Gulf of Maine) were used in this study; see Table 3a for details of the animals from which the data presented in this study were obtained.

Order	Family	Species	*n*	Daytime Depth(m)	Bioluminescence	Water Type[4]
Euphausiacea	*Euphausiidae*	*Meganyctiphanes norvegica*	6	300-500[1]	photophores	IB
Decapoda	*Oplophoridae*	*Acanthephyra purpurea*	3	700-950[2]	spew	II
		Systellaspis debilis	7	650-950[2]	photophores spew	II, IA
	Sergestidae	*Sergestes arcticus*	5	450-600[1]	photophores	IB
	Pasiphaeidae	*Pasiphaea multidentata*	5	220-240[3]	—	IB

Table 3a. Details of adult mesopelagic malacostracans used in this study, information includes: taxonomy, *n* (number of individuals of a species used in the present study), approximate daytime depth distribution for each species, bioluminescent capability, water type inhabited. The term 'spew' describes a projectile evacuation of bioluminescent material from the stomach. [1]Sardou *et al.* 1996; [2]Foxton, 1970; [3]Frank and Widder, 1997; [4]Jerlov, 1976.

3.2.1.1 Animal handling and preparation

All animal handling and preparation were carried out under dim-red light to prevent photoisomerisation of the short wavelength sensitive visual pigment (see section *2.2.1.1* for details). All animals were prepared for electrophysiological recording as described in section *2.2.2.1.* Once the preparation was complete, the only light to which the animals were exposed was the optical stimulus described below.

3.2.1.2 Electrical recording

Electrophysiological recording of the electroretinogram is described in section *2.2.2.1*, and the same procedure was followed in all cases.

3.2.1.3 Optical apparatus

A blue LED (Marl Optosource, ultra high bright LED: λ_{max} 464nm, FWHM (Full Width Half Maximum) 28nm; see Fig. 3.1 and section *2.2.2.2*) was driven by square wave pulses to generate individual, brief (1.4ms), flashes. The wavelength of optical stimulus was chosen to approximate the spectral content of light in the mesopelagic environment (see Fig. 3.2). The wavelength of maximum transmission below 200m depth in clear oceanic water (Jerlov type I) is *ca.* 460nm (Jerlov, 1976); and studies of marine bioluminescence spectra (e.g. Herring, 1983; Widder *et al.* 1983) show that the peak wavelength of bioluminescent emissions of mesopelagic shrimps ranges from 440-490nm (see Fig. 3.2).

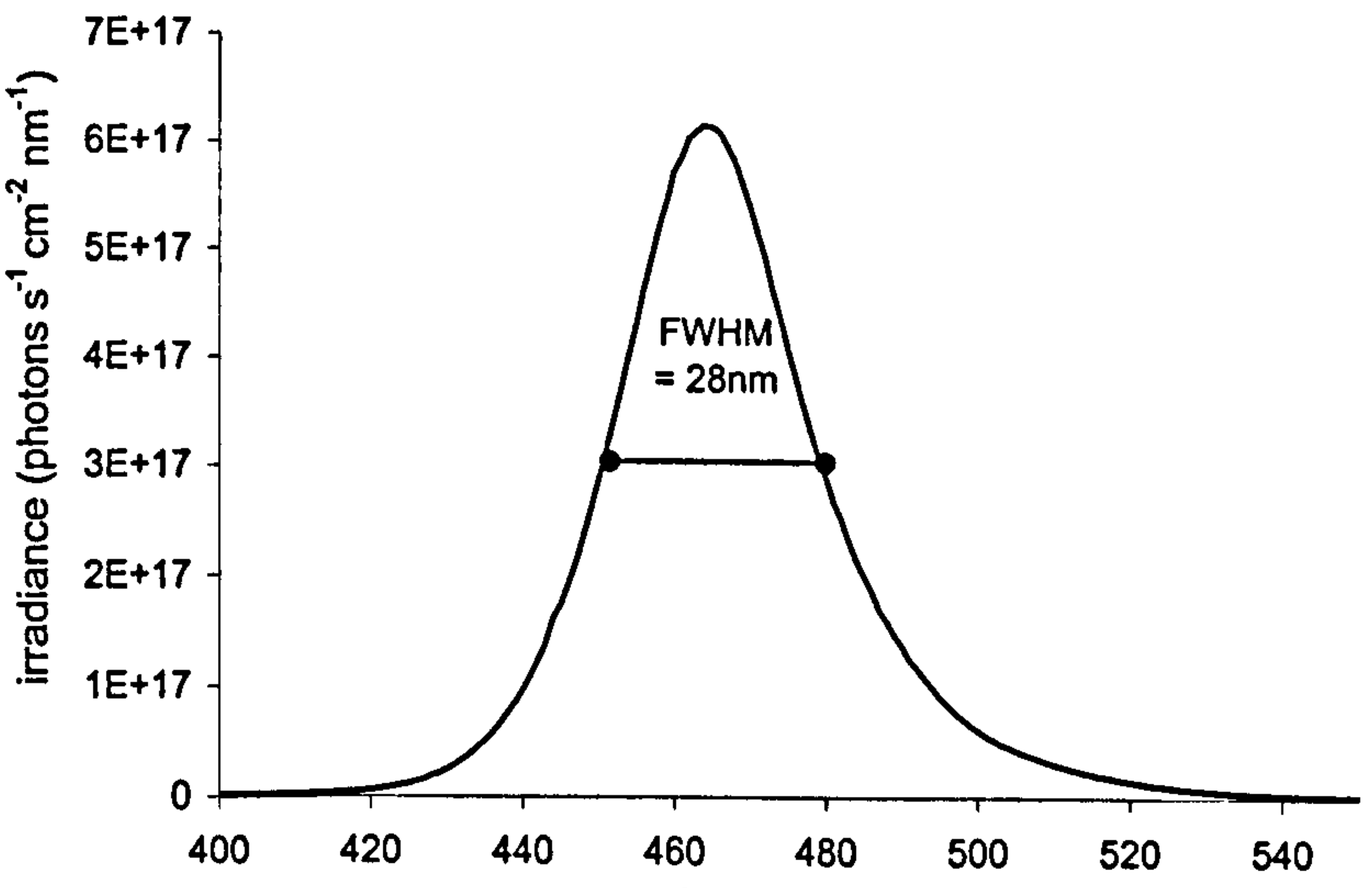

Figure 3.1. Spectral output of the blue LED with max input current, I=30mA (λ_{max} 464nm), FWHM 28nm, measured with a spectroradiometer (Macam, model SR9910-PC).

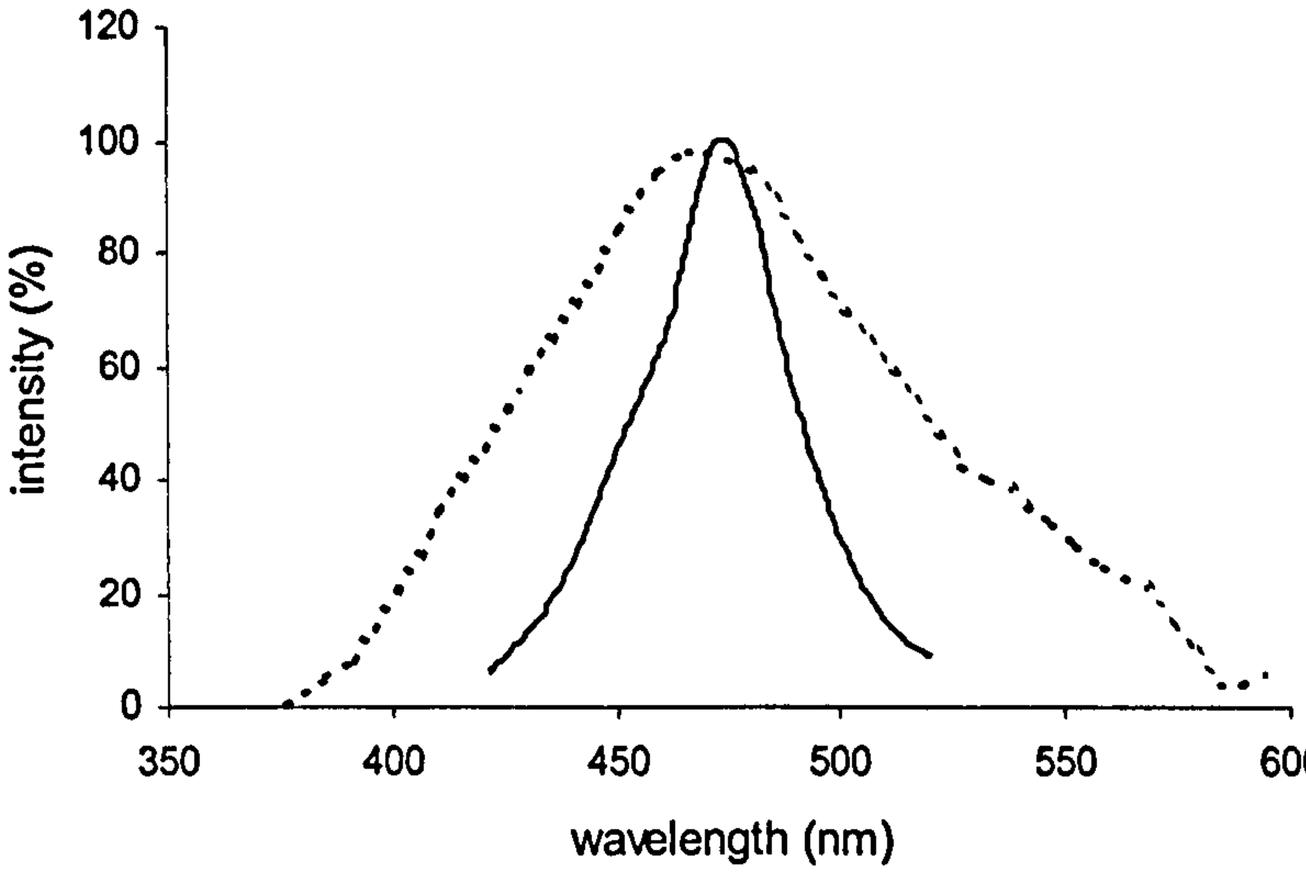

Figure 3.2. The spectral distribution of light intensity at 500m depth in clear ocean water (smooth line; redrawn from Denton, 1990), compared with the bioluminescence emission spectra from photophores of *Sergestes* spp. (dotted line; redrawn from Herring, 1983).

The output of the LED was transmitted to one eye via one branch of a bifurcated (randomised fibre) silica light guide (the other branch had no input and was light-protected). This created a broad light output close to the eye. The output of the silica light guide was placed at a fixed position from the eye (4mm) and this set position was constant in both axial alignment and distance from the eye for all preparations and ensured that the whole eye surface was illuminated, i.e. the circle of light at the output was larger than the eye. The reference electrode was not placed in the other eye (see section *2.2.2.1*) therefore no care was taken to prevent the light stimuli from falling on the second eye. Irradiance at the eye was calibrated with a research radiometer (International Light; model IL1700) and measured directly, over the wavelength range of 400-700nm, in photons s^{-1} cm^{-2}. Irradiance was controlled using calibrated absorptive neutral density filters (see section *2.2.2.2*). The neutral density filters were inserted into the light path between the LED and the silica light guide, this arrangement allowed irradiance at the eye to be changed without disturbing the preparation. The unattenuated light source gave a maximum irradiance at the eye of 2.0×10^{15} photons s^{-1} cm^{-2}.

3.2.1.4 Experimental procedure

Initially, the eye was stimulated with dim, 1.4ms test flashes, with a constant background of complete darkness. A low stimulus irradiance was used to avoid light adapting or damaging the eye and if no ERG signal was observed in response to these initial test flashes, the preparation was rejected. Such brief flashes were used to minimise light adaptation upon stimulation. These essentially instantaneous stimuli were of a duration considerably shorter than the integration time of the photoreceptor, therefore minimising light adaptation; evidence of this can be seen when studying the waveform of the electroretinogram.

As previously illustrated in section *2.1.2.2* (Fig. 2.4), when photoreceptors are illuminated with prolonged stimuli, an initial transient response reaches maximum amplitude and this is followed by decay in the response amplitude to a steady plateau level, which is maintained until the stimulus is switched off. In the transition between peak amplitude transient phase and maintained plateau phase, the conductance gain of the photoreceptor (transducer) changes. The ratio of activated depolarising conductances to effective photons falls, and sensitivity is reduced. By stimulating the eye with very brief (effectively instantaneous) light flashes, only the peak transient phase of the ERG is observed, indicating minimal change in the conductance gain of the photoreceptor (Fig. 3.3).

Dim-red light (>600nm) was the only light the animals in this study were exposed to during preparation. Although light of this wavelength does not isomerise a large proportion of the short wavelength sensitive visual pigment in these animals, it does light adapt the eye to some extent (Frank and Widder, 1999). Consequently, time was allowed for the eyes to dark-adapt before data were collected (see below).

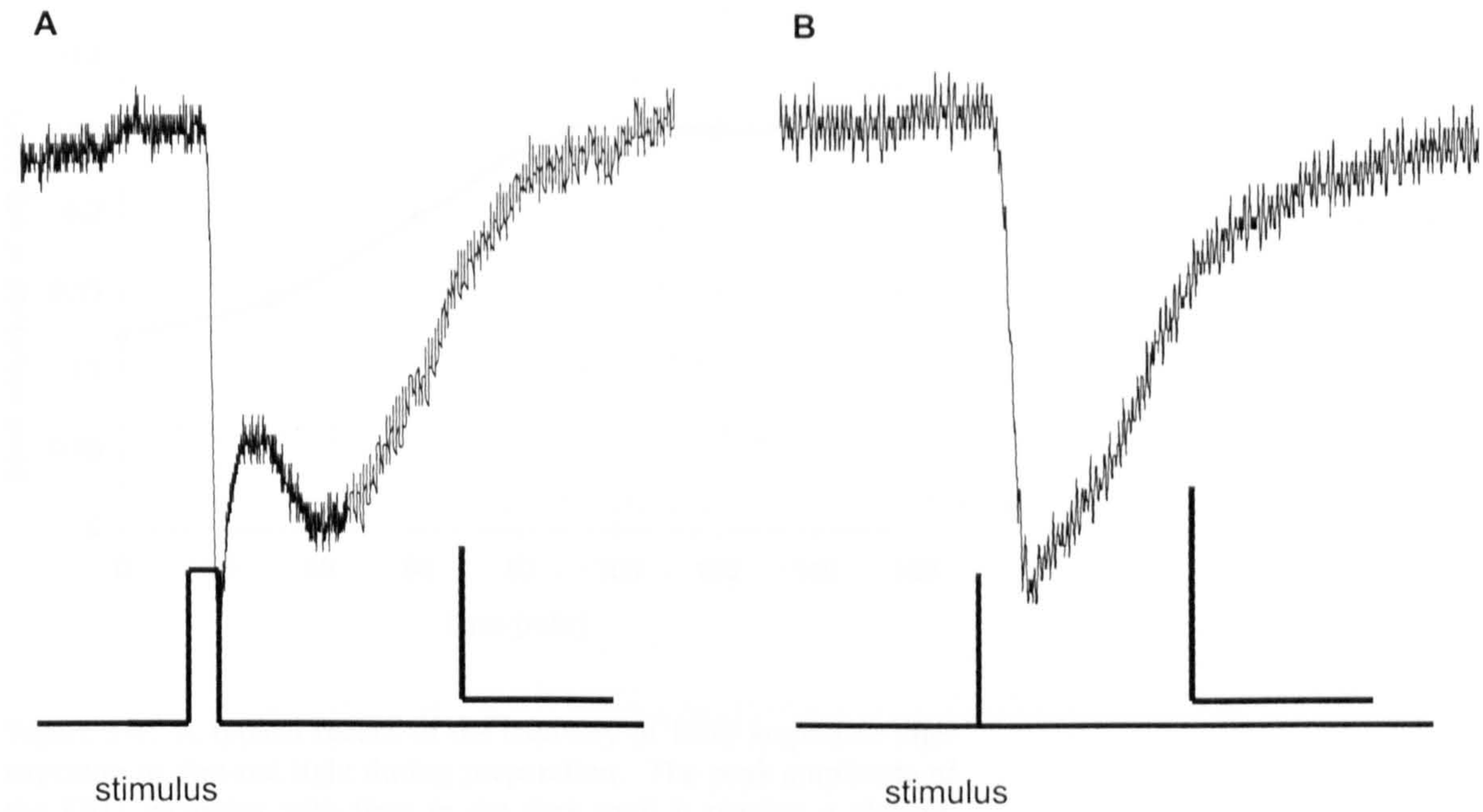

Figure 3.3. Unfiltered ERG signals from the eye of *Systellaspis debilis* in response to: A) 100ms light stimulus; B) 1.4ms light stimulus (both stimuli gave an irradiance at the eye generating a response in the linear region of the intensity response function). A) shows an initial peak transient followed by a decline to a lower amplitude prior to the return to pre-stimulus baseline. B) shows the initial peak transient followed by a decline to the pre-stimulus baseline. Scale bars represent 0.4 seconds along horizontal axis and 0.04 mV along vertical axis. Irradiance at eye was the same in both cases ($8x10^{11}$ photons s^{-1} cm^{-2}) so that the total number of photons delivered to the eye was: in A) $8x10^{10}$ photons cm^{-2} (per 100ms pulse); and in B) $1x10^{9}$ photons cm^{-2} (per 1.4ms pulse).

In order to determine when the eye had fully recovered from the light exposure during preparation, and was fully dark-adapted, dim, 1.4ms test flashes were used to stimulate the eye once every 30 minutes until the ERG had stopped increasing in peak amplitude (see Fig. 3.4). This indicated that the eye had reached a stable, dark-adapted state, and usually took 2-3h. Once fully dark-adapted, the preparation was only used providing that the eye produced a defined criterion response set as a response with a peak amplitude at least 20μV above background noise. Background noise was typically of the order of 20-30μV and therefore, if an eye had a peak response amplitude of less than 50μV to the test flash once dark-adapted, the preparation was rejected. This selection criterion rejects preparations which are producing signals with a low signal-to-noise ratio. A low signal-to-noise ratio is an indication of a severely damaged or unstable preparation.

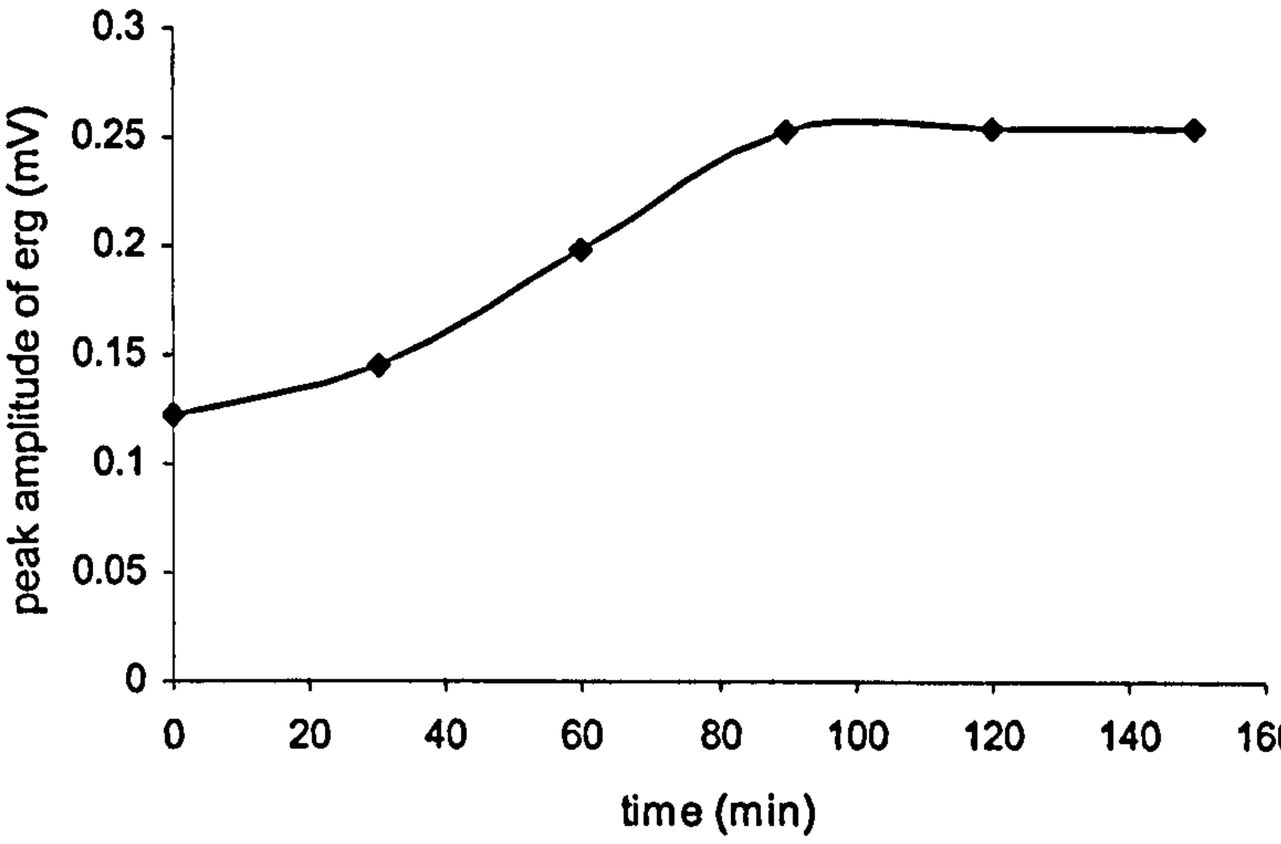

Figure 3.4. A typical record of the recovery of ERG amplitude after exposure to dim-red light during preparation. The peak amplitude of the ERG increases with time in the dark until it reaches a plateau. Data from one individual of the species *Systellaspis debilis*.

Sensitivity measurements were taken by stimulating the eye with 1.4ms flashes of light of varying irradiances; irradiances were not presented to the eye in ascending or descending order, they were presented in a variable order. A minimum period of 2 minutes was allowed between each light stimulus to avoid reducing the sensitivity of the eye. If the eye was stimulated a second time immediately after the first, the peak amplitude of the response was significantly reduced. Different inter-pulse periods were tested and two minutes was found to be adequate to ensure that the peak amplitude of the response to a constant irradiance remained unaltered (a selection criterion of a maximum of +/-5% difference in peak amplitude was employed, see section *3.3*). At the highest irradiances (those that produced responses from the eye that were approaching saturation), a two minute inter-pulse period was insufficient. Under these circumstances, a minimum of five minutes was allowed between stimuli.

The irradiance of the light stimulus was increased until the peak amplitude of the ERG signal approached saturation. Similarly, irradiance was decreased until a threshold response was observed. Throughout the experiment, the eye was periodically stimulated with the dim test flash, to check that the eye had retained its initial sensitivity. At the conclusion of the experiment, the dim test flash was used to check that the preparation had not deteriorated and that sensitivity had not changed during the experiment. If the response to the dim test flash did

not recover to it's original amplitude as determined at the beginning of the experiment (peak amplitude no different, within +/-5% error, to the original), the data were rejected.

In each experiment, a number of extrinsic factors could introduce distortions or artefacts into the ERG signal, for example, during rough weather, ship pitch and roll could have a significant effect on the shape of the ERG signal (see Fig. 3.5). Personal observation of ship-roll generally coincided with an observed distortion or artefact in the ERG signal similar to that displayed in Fig. 3.5. In the event of the ERG response failing to return to the pre-stimulus baseline as shown in Fig. 3.5b, the ERG response was rejected.

Acquisition of the ERG data, via a digital oscilloscope, is described in section *2.2.2.1*.

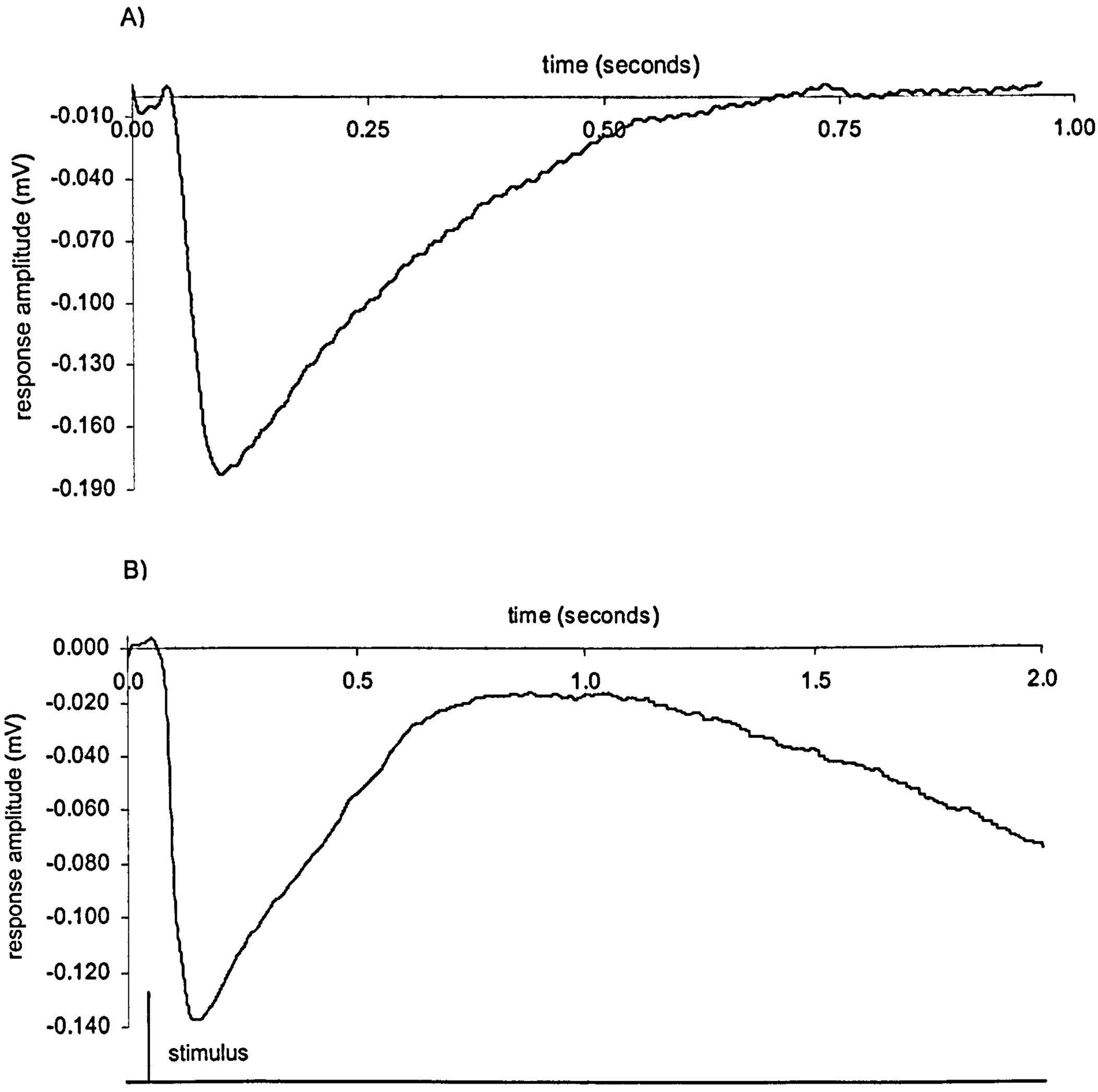

Figure 3.5. An example of the effect of ship-roll on recording an ERG signal. A) and B) are digitally filtered ERG signals (see section *3.3* for details of digital filter) in response to a 1.4ms stimulus (shown below plot B) with a photon flux at the eye of: A) 1.9×10^{12} photons cm^{-2} (per 1.4ms pulse); B) 2.7×10^{10} photons cm^{-2} (per 1.4ms pulse). In A) the trace returns to the pre-stimulus baseline immediately after the peak transient; in B) ship motion causes a distortion of the ERG signal and forces the signal to swing to negative voltages on its return to the pre-stimulus baseline. Data from *Sergestes arcticus*.

3.2.2 Protocol for ERGs on Shallow-water, Coastal Malacostracans

Details of animal collection and maintenance are given in Chapter 2, section *2.2.1.* Data were obtained from two species of coastal malacostracan from one location (University Marine Biological Station Millport [UMBSM] Millport, Isle of Cumbrae, Scotland), details of the species from which the data used in this study were obtained are given in Table 3b.

Order	Family	Species	*n*	Distribution[1]	Temporal activity
Decapoda	*Crangonidae*	*Crangon crangon*	8	Midshore –150m depth/lower reaches of estuaries	Nocturnal[2]
	Palaemonidae	*Palaeomon elegans*	8	Shore-dwelling, rockpools and mid-tide level	Increased activity at night[3]

Table 3b. Details of adult malacostracans used in this study. Details include: taxonomy; *n* (number of individual of each species used in the present study); habitat distribution; temporal activity; water type. [1]Smaldon (1993); [2]Tiews (1954); [3]Horton, A., British Marine Life Study Society, Sussex UK (pers. observation over 25 years).

3.2.2.1 Animal handling and preparation

The coastal malacostracans were maintained in aquaria as described in section *2.2.1.2*, and exposed to a 12h light: 12h dark light regime. All experiments were conducted during the 12h dark phase of the light regime. Consequently, all animal handling was performed under dim-red light to prevent photoisomerisation of the short wavelength sensitive visual pigment (see section *2.2.1.1* and *2.2.1.2* for details) and hence light adaptation. Animals were prepared for electrophysiological recordings (as described in section *2.2.2.1*). Once the preparation was complete, the only light to which the animals were exposed was the optical stimulus described below.

3.2.2.2 Electrical recording

Electrophysiological recording of the electroretinogram is described in section *2.2.2.1*, and the same procedure was followed in all cases.

3.2.2.3 Optical apparatus

A blue LED (Marl Optosource ultra high bright LED: λ_{max} 464nm, FWHM 28nm; see section *2.2.2.2*) was driven by square wave pulses to generate individual, brief (1.4ms) flashes. Species from coastal and estuarine waters generally have visual systems with spectral sensitivities that are shifted to longer wavelengths (greater than 500nm) relative to deep-sea species (Herring and Roe, 1988). The wavelength of maximum transmission in coastal (shallow) water is similarly shifted to longer wavelengths; see sections *1.2* and *1.4* for a detailed explanation. In preliminary experiments the eyes of the two coastal species (*C. crangon* and *P. elegans*) were stimulated with both blue (λ_{max} 464nm, FWHM 28nm) and green (λ_{max} 530nm, FWHM 44nm) light (calibrated such that the irradiance at the eye was equal for both wavelengths). This revealed no difference in the amplitude of the ERG whether stimulated with blue or green light. Consequently, blue light was used to stimulate the eyes of the coastal species, as it was possible to generate higher irradiances using the blue LED than the green.

Preliminary experiments revealed that the optical apparatus used for the deep-sea species (detailed in section *3.2.1.3*), was ineffective for use with the coastal species. The bifurcated fibre optic attenuated too much light and therefore it was impossible to generate responses close to saturation for the eye. To prevent this, the LED was positioned close to the eye. A filter holder was placed between the LED and the eye allowing the ND filters (see sections *3.2.1.3, 2.2.2.2*) to be placed into the light path to control irradiance at the eye. Filter changes therefore had to be performed under dim-red light. The LED was placed at a fixed position from the eye and this set position was constant in both axial alignment and distance from the eye for all preparations and ensured that the whole eye was illuminated, i.e. the circle of light at the output was larger than the eye, creating a broad light output close to the eye. As mentioned in section *3.2.1.3*, no effort was made to shield the second eye from the light stimulus. Irradiance at the eye was calibrated with a research radiometer (International Light; model

IL1700) and measured directly in photons s^{-1} cm^{-2}. The unattenuated light source gave a maximum irradiance (over the wavelength range of 400-700nm) at the eye of 7.0×10^{16} photons s^{-1} cm^{-2}.

3.2.2.4 Experimental procedure

The experimental procedure was the same as for the deep-sea species (see section *3.2.1.4*). However, when changing the irradiance of the stimulus, the preparation was exposed to dim-red light. Preliminary experiments tested the effect of red light exposure during a filter change and it was found that immediately after this exposure the sensitivity of the ERG response was depressed. Different time periods were tested, and it was found that a ten minute waiting period after the red light exposure allowed recovery of the ERG response to pre-red light exposure sensitivity.

3.3 DATA ANALYSIS

3.3.1 Determining Sensitivity of the Visual Response

Sensitivity measurements were taken by exposing the eye to a range of irradiances such that the highest and lowest stimulus irradiances generated saturating and threshold responses respectively (see *3.2.1.4* for detail). At each stimulus irradiance, four responses were obtained (figs 3.3, 3.5 & 3.6 show a typical ERG waveform response to a 1.4ms light pulse). The peak amplitude of each response was measured as the difference in voltage between the pre-stimulus DC baseline and the point of maximum deflection of the trace. The peak amplitude measurements were recorded instantaneously via a digital oscilloscope (HAMEG, model HM407), and stored for further analysis. Subsequently, the mean peak amplitude was calculated (the average of the peak amplitudes of four responses at each stimulus irradiance) for each stimulus irradiance, for each individual. During the recording of the ERG signals, a selection criterion was employed: responses to constant irradiances were rejected if peak amplitude measurements differed in agreement by more than +/- 5% (after Glantz, 1968). A change of more than +/- 5% could indicate that the sensitivity of the eye is changing (for example, the eye is light–adapting during the experiment).

As mentioned in section *3.2.1.4*, the background noise in the ERG signal typically had an amplitude of 20-30μV (variable between preparations). Consequently, the digitised data for each response were processed by a digital low pass (50Hz cut-off) linear phase filter using MatLab (version 6.0.0.88, release 12) software; Fig. 3.6 illustrates the effect of the digital filter.

The mean peak amplitude of response for each stimulus irradiance was normalised to V_{max} (V/V_{max}: where V = mean peak amplitude of signal; V_{max} = maximum response amplitude obtained), after Glantz (1968). The sensitivity of the ERG response can be affected by electrode placement, for example, if the eye is damaged during electrode insertion the sensitivity of the visual response may be depressed.

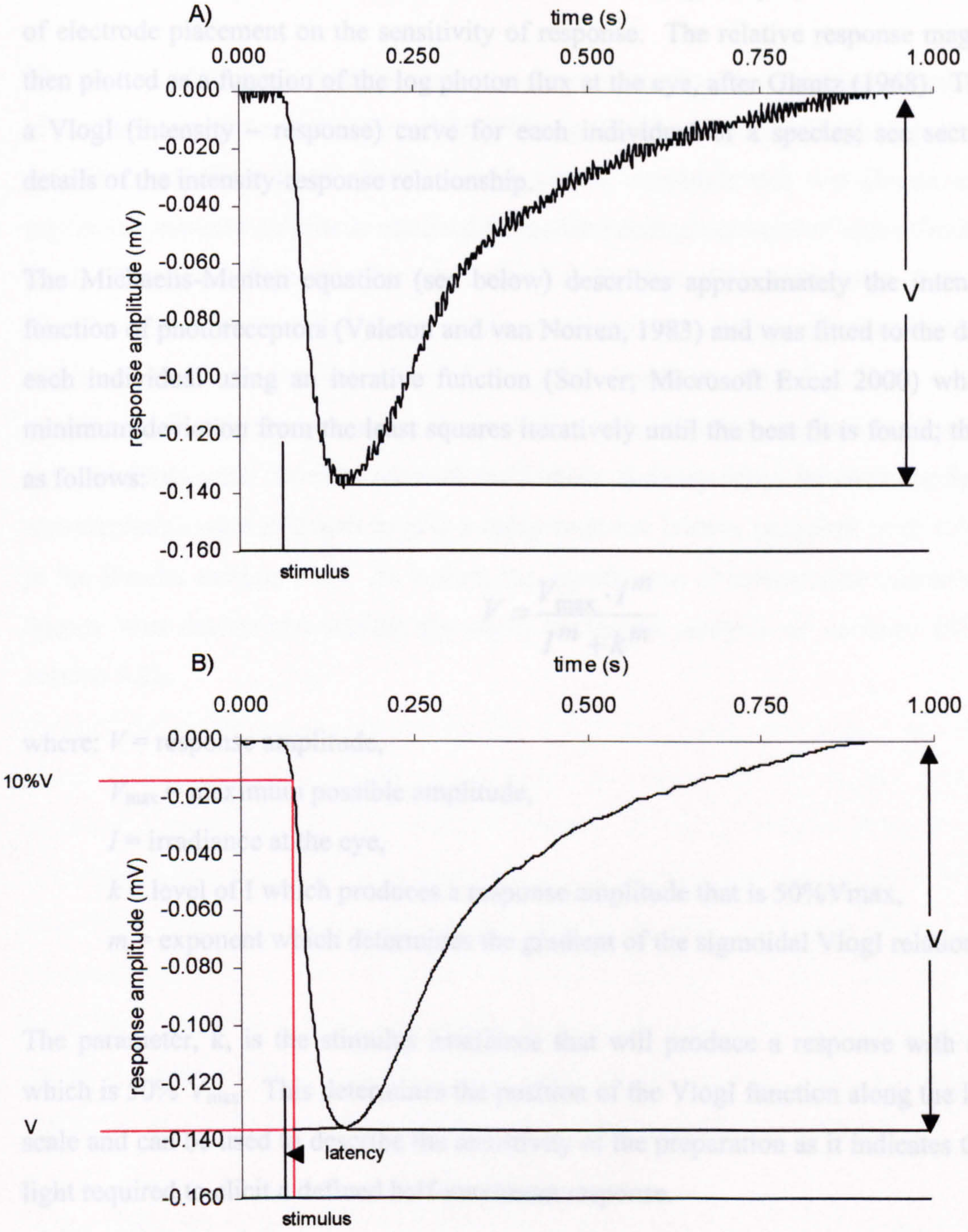

Figure 3.6. The effect of low pass digital filtering (cut-off frequency 50Hz) on an ERG signal; A) unfiltered signal, B) filtered signal. ERG signal generated in response to a 1.4ms stimulus with an irradiance at the eye of 1.5×10^9 photons s^{-1} cm^{-2} (shown as the vertical bar at the bottom of each trace). V = peak amplitude of response. Data from *Systellaspis debilis*. The horizontal red lines indicate both V and 10%V of the ERG response, the vertical red line and black arrow indicate the time difference between the light stimulus and the 10%V level: this is the method used to determine response latency of the eye (see section *3.3.2*).

Using the relative response magnitude (V/V_{max}) for any given preparation removes any effect of electrode placement on the sensitivity of response. The relative response magnitudes were then plotted as a function of the log photon flux at the eye, after Glantz (1968). This generated a VlogI (intensity – response) curve for each individual of a species; see section *2.1.2* for details of the intensity-response relationship.

The Michaelis-Menten equation (see below) describes approximately the intensity-response function of photoreceptors (Valeton and van Norren, 1983) and was fitted to the data points for each individual using an iterative function (Solver; Microsoft Excel 2000) which finds the minimum deviation from the least squares iteratively until the best fit is found; the equation is as follows:

$$V = \frac{V_{\max} \cdot I^m}{I^m + k^m}$$

where: V = response amplitude,

V_{max} = maximum possible amplitude,

I = irradiance at the eye,

k = level of I which produces a response amplitude that is 50%Vmax,

m = exponent which determines the gradient of the sigmoidal VlogI relationship.

The parameter, k, is the stimulus irradiance that will produce a response with an amplitude which is 50% V_{max}. This determines the position of the VlogI function along the log irradiance scale and can be used to describe the sensitivity of the preparation as it indicates the amount of light required to elicit a defined half-maximum response.

Both the values of mean V/V_{max}, k and *m* for all individuals were averaged to give a single VlogI function and values of k and *m* for the species (standard error values are given in the Results section, *3.4*). The significance of interspecies variation in the values of k and *m* was determined statistically using univariate analysis of variance (SPSS software version 9.0).

3.3.2 Determining Latency of the Visual Response

The latency of the photoreceptor response was measured as the time period between the onset of the light stimulus and the start of the ERG signal. For each individual, response latency was measured only from those responses with a peak amplitude that was closest to 50% of the maximum response amplitude obtained (response latency measured at approximately 50%V_{max} level). The onset of the stimulus was defined as the start of the rising edge of the square wave stimulus. The start of the photoreceptor response was defined as the point at which the response amplitude reached 10% of the peak amplitude (see Fig. 3.6). As previously mentioned, four responses were obtained for each stimulus irradiance; thus, four latency measurements were obtained for each individual. Subsequently, for each species, all latency measurements were averaged to give a mean response latency (standard error values are given in the Results section, *3.4*). As before, the significance of interspecies variation in response latency was determined statistically using univariate analysis of variance (SPSS software version 9.0).

3.4 RESULTS

Univariate analysis of variance revealed that interspecies variation in the mean value of k for all the species tested (both mesopelagic and coastal) was highly significant, $F_{6,35} = 90.6$, $p<0.0005$; interspecies variation in latency of response values for all the species tested was highly significant, $F_{6,33} = 44.6$, $p<0.0005$; interspecies variation in the value of *m* was significant, but not highly, $F_{6,35} = 4.0$, $p=0.004$. A post hoc Tukey test was used (SPSS software, version 9.0) to perform a pairwise comparison of the means for each species group, and the significance of difference for the values of k, response latency and *m* between species is given in appendices I, II and III respectively. The residuals for k, latency of response and *m* were tested for normality using the Kolmogorov-Smirnov test. The residuals did not significantly depart from normal distribution ($p>0.05$).

3.4.1 Visual Sensitivity of Mesopelagic Malacostracans

Plots of the VlogI relationship for the visual system of each mesopelagic species studied are given in Fig. 3.7. The VlogI relationships show that peak membrane depolarisation (V) increases sigmoidally with log stimulus intensity for all species; there is a clear threshold response plateau at low stimulus intensities and a saturating response plateau at high stimulus intensities, with an approximately linear relationship between the variables at intermediate stimulus intensities. The VlogI plots presented in Fig. 3.7 define the intensity-response functions of the dark-adapted eyes of the mesopelagic species tested in this study. Thus they reveal the range of light intensities over which the dark-adapted eyes will operate; i.e. they define the dynamic range of the visual response from threshold to saturation.

In this study, the value of k is determined for each species. This is the log photon flux (photons s^{-1} cm^{-2}) of light of λ_{max} 464nm (FWHM 28nm, see Fig. 3.1) at the eye that generates a response that is $50\%V_{max}$. The value of k is used to compare the relative sensitivities of the dark-adapted visual systems of five species of mesopelagic malacostracan to light with a wavelength of maximum transmission (λ_{max}) approximating that experienced in their natural environment. The dynamic range of the photoreceptors in the eye is determined from the VlogI relationship

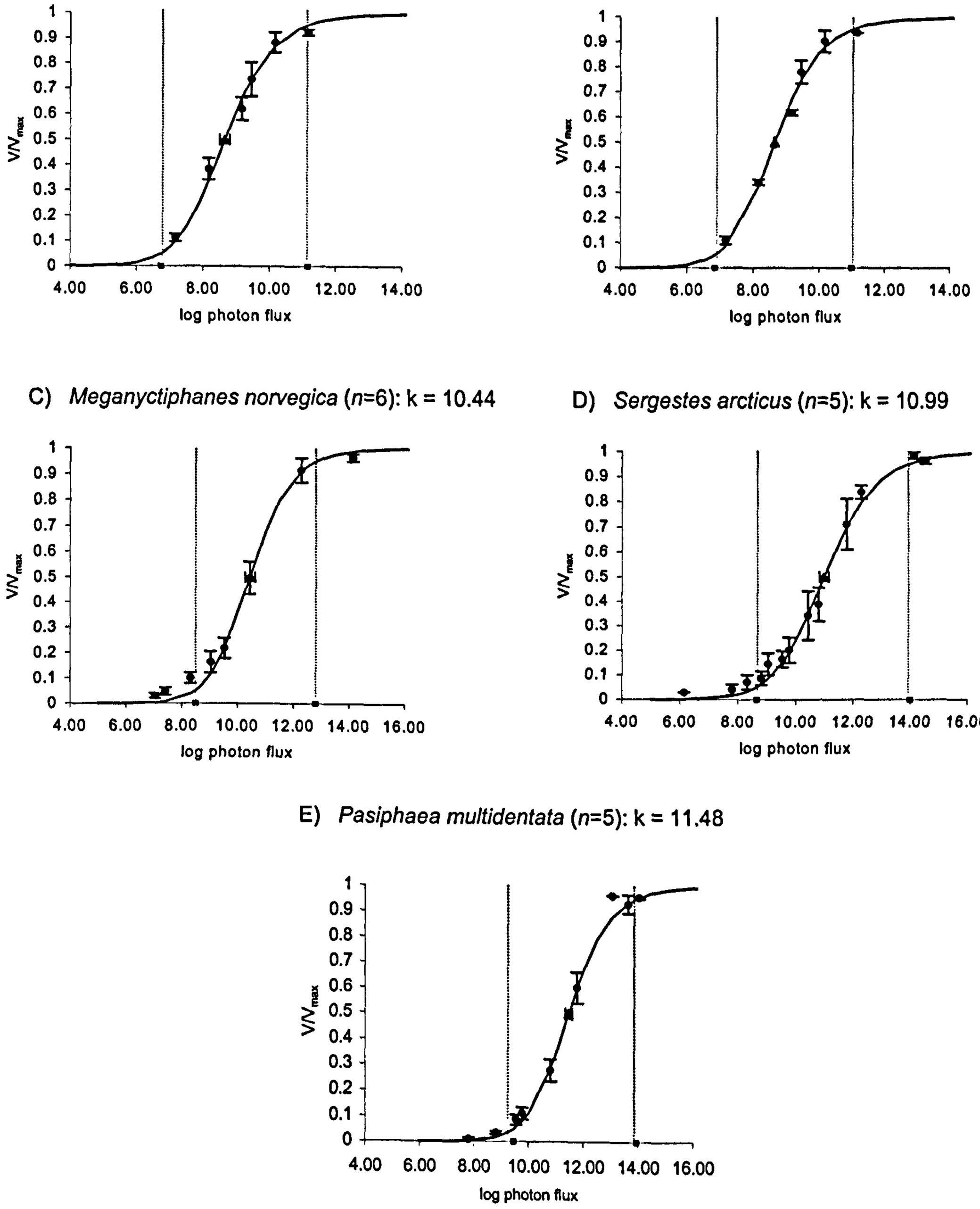

Fig 3.7. The VlogI relationships for each species of mesopelagic malacostracan studied. The circles indicate mean V/V_{max} values (standard errors shown); the triangular points on each plot indicate the mean value of k for each species (standard errors shown), which falls in the centre of the linear portion of the intensity-response function. The smooth line represents the fit of the Michaelis-Menten equation through the mean V/V_{max} points (using sum of least squares regression analysis). The vertical lines on each plot indicate the dynamic range of the photoreceptors (defined by the log units between the response limits of 5 and 95%V_{max}, after Laughlin and Hardie, 1978); the dynamic ranges plotted in figures A to E are, respectively, *ca.* 4.0, 4.5, 4.5, 5.0 and 4.5 log units.

for each species. The dynamic range is defined as the log unit range between the response limits of 5-95%V_{max} (after Laughlin and Hardie, 1978).

3.4.1.1 Visual sensitivity

Acanthephyra purpurea and *Systellaspis debilis* (decapod malacostracans)

The data included in this study for *Systellaspis debilis* come from two groups of animals caught in the region of the Cape Verde Islands (North East Atlantic) (n=3) and the region of the Northwest Providence Channel (Bahamas) (n=4). In the first instance, the results from animals from the different locations were treated independently. However, the resulting mean values of k for the two groups were very similar (North East Atlantic; k=8.41, Bahamas; k=8.85). An independent sample (2-tailed) t-test was carried out on the k values for the two groups and this revealed that the difference in k between the two groups was non-significant at the 95% level: $t_5 = 1.438$, p=0.210. Consequently, the data for both groups of individuals were subsequently averaged and treated as a single representation of the species.

The mean value of k for both *A. purpurea* and *S. debilis* is 8.66 (see Fig. 3.8 and appendix I), which suggests that both species have very similar visual sensitivity to blue light (λ_{max} 464nm) produced by the LED. This value of k, 8.66, is equivalent to an irradiance at the eye of $4.6x10^{8}$ photons s^{-1} cm^{-2}.

The sigmoidal VlogI relationship for the dark-adapted photoreceptors of *A. purpurea* covers a dynamic range of approximately 4.0 log units, for *S. debilis*, this dynamic range spans approximately 4.5 log units (see Fig. 3.7).

Pasiphaea multidentata and *Sergestes arcticus* (decapod malacostracans)

P. multidentata and *S. arcticus* have similar visual sensitivity to blue light (λ_{max} 464nm). The mean value of k for *P. multidentata* is 11.48; this is not significantly different to the mean value of k for *S. arcticus*, which is 10.99 (p=0.427, see appendix I, and Fig. 3.8). For *P. multidentata* the value of k of 11.48 is equivalent to an irradiance at the eye of $3.2x10^{11}$ photons s^{-1} cm^{-2},

similarly for *S. arcticus*, the value of k of 10.99 is equivalent to an irradiance at the eye of $9.77x10^{10}$ photons s^{-1} cm^{-2}.

The dynamic range of the dark-adapted VlogI relationship for *P. multidentata* photoreceptors spans approximately 4.5 logs units and compares with that of *S. arcticus* which spans approximately 5.0 log units (see Fig. 3.7).

Meganyctiphanes norvegica (euphausiid malacostracan)

There is no significant difference between the mean value of k for *M. norvegica* (k=10.44) and the mean value of k for *S. arcticus* (k=10.99) (p=0.235, see appendix I and Fig. 3.7), suggesting that these two species have a similar visual sensitivity to blue light. The value of k of 10.44 for *M. norvegica* is equivalent to an irradiance at the eye of $2.75x10^{10}$ photons s^{-1} cm^{-2}.

The dynamic ranges of the VlogI relationships of the dark-adapted photoreceptors for both species are also similar; for *M. norvegica* the VlogI relationship spans approximately 4.5 log units, and for *S. arcticus* the relationship spans approximately 5.0 log units (see Fig. 3.7).

3.4.1.2 A comparison of visual sensitivity between mesopelagic species

Fig. 3.8 illustrates the shift in placement along the log intensity axis of the dynamic ranges of the dark-adapted visual systems of each of the species studied. The shape of the VlogI relationship is very similar for all species. The variable *m* (the exponent in the Michaelis-Menten equation, see section *3.3.1*) determines the gradient of the VlogI relationship. Statistical analysis of the mean values of *m* for each mesopelagic species (see Table 3c for means and standard errors) reveals that there is no significant difference in the values of *m* between the mesopelagic species studied ($p>0.05$ for all pairs of mesopelagic species, see appendix III) and consequently no significant difference in the shapes of the VlogI curves. Species with similar sensitivities in terms of the variable k have been described above. However, it is clear from Fig. 3.8 that there are considerable differences in sensitivity between some of the species studied. The difference in sensitivity between species is indicated by a horizontal shift of the dynamic range of each species along the log intensity axis, which results in differences in the value of k.

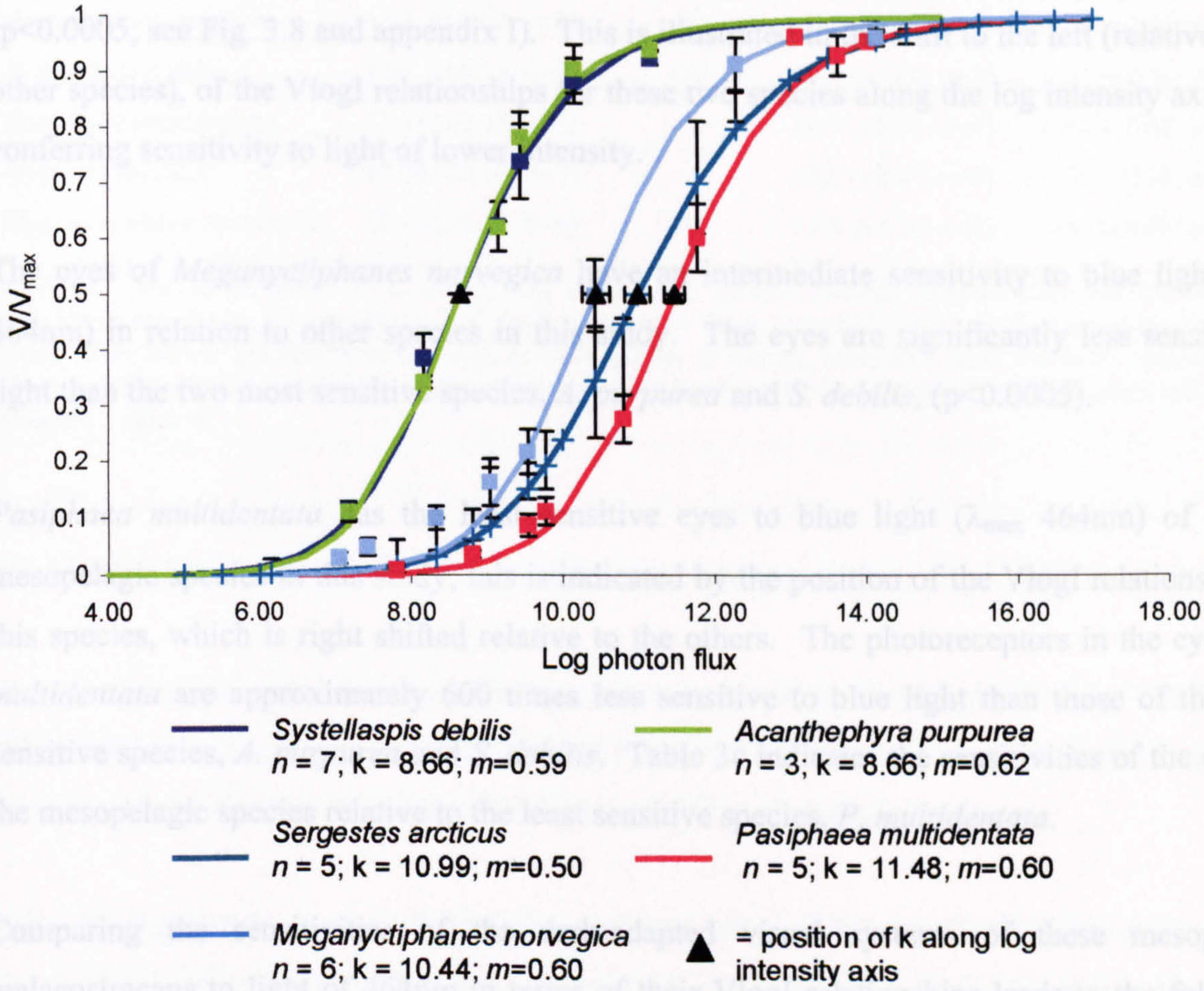

Figure 3.8. The VlogI relationships of the visual systems of all the mesopelagic species studied. The shape of the VlogI relationship is the same for all species; the relationships differ in their placement along the log intensity axis, resulting in different values of k for each species. The value of k for *A. purpurea* and *S. debilis* is the same, this value of k is significantly different to that for: *M. norvegica*, *S. arcticus* and *P. multidentata* ($p<0.0005$). There is also a significant difference between the values of k for *M. norvegica* and *P. multidentata* ($p=0.001$). *P. multidentata* and *S. arcticus* share similar visual sensitivity (difference in value of k is non-significant, $p=0.427$) as do *S. arcticus* and *M. norvegica*, ($p=0.235$, in comparison of k values). The variable *m* is an exponent in the Michaelis-Menten equation used to determine the VlogI relationship for each species, and this exponent determines the gradient of the VlogI relationship. Statistical analysis of the mean values of *m* for each species reveals that there is no significant difference ($p>0.05$) in the gradients of the VlogI relationships of the mesopelagic species studied.

The sensitivity of the dark-adapted visual systems of *A. purpurea* and *S. debilis*, as defined by the value of k, is significantly greater than that for the other three mesopelagic species ($p<0.0005$, see Fig. 3.8 and appendix I). This is illustrated in the shift to the left (relative to the other species), of the VlogI relationships for these two species along the log intensity axis, thus conferring sensitivity to light of lower intensity.

The eyes of *Meganyctiphanes norvegica* have an intermediate sensitivity to blue light (λ_{max} 464nm) in relation to other species in this study. The eyes are significantly less sensitive to light than the two most sensitive species, *A. purpurea* and *S. debilis*, ($p<0.0005$).

Pasiphaea multidentata has the least sensitive eyes to blue light (λ_{max} 464nm) of all the mesopelagic species in this study; this is indicated by the position of the VlogI relationship for this species, which is right shifted relative to the others. The photoreceptors in the eye of *P. multidentata* are approximately 600 times less sensitive to blue light than those of the most sensitive species, *A. purpurea* and *S. debilis*. Table 3c indicates the sensitivities of the eyes of the mesopelagic species relative to the least sensitive species, *P. multidentata*.

Comparing the sensitivities of the dark-adapted visual systems of these mesopelagic malacostracans to light of 464nm in terms of their VlogI relationships leads to the following conclusions:

a) Both *A. purpurea* and *S. debilis* have very similar sensitivities and these species possess the most sensitive visual systems of the five species studied.

b) *M. norvegica* has a visual system with an intermediate sensitivity when compared with the other four species studied.

c) *P. multidentata* has the least sensitive visual system of the five species studied (the sensitivity of the visual system of *S. arcticus* is neither significantly different to that of *M. norvegica* or *P. multidentata* thus, relatively, it has an intermediate to low sensitivity).

Species	k (log photons s^{-1} cm^{-2})	Relative sensitivity	Latency (ms)	*m*
Acanthephyra purpurea	8.66 (±0.02; *n*=3)	661	49.5 (±0.85; *n*=3)	0.62 (±0.06; *n*=3)
Systellaspis debilis	8.66 (±0.15; *n*=7)	661	48.2 (±1.04; *n*=7)	0.59 (±0.04; *n*=7)
Pasiphaea multidentata	11.48 (±0.13; *n*=5)	1	30.5 (±0.91; *n*=7)	0.60 (±0.05; *n*=5)
Sergestes arcticus	10.99 (±0.16; *n*=5)	3	33.0 (±2.47; *n*=4)	0.50 (±0.18; *n*=5)
Meganyctiphanes norvegica	10.44 (±0.18; *n*=6)	11	14.3 (±1.20; *n*=5)	0.60 (±0.08; *n*=6)

Table 3c. The mean values of k, latency and *m* for each species studied, standard error and number of individuals are shown in parentheses (all data is extracted from recorded ERG signals from dark-adapted eyes). The relative sensitivity of the eyes of each species is shown, calculated from the back transformed (from the logarithmic state) values of k, relative to the least sensitive species, *P. multidentata*, which is assigned a value of 1.

3.4.1.3 Significant differences in latency of response between mesopelagic species.

The latency of the visual response (the time between the onset of the light stimulus and the start of the ERG response), gives an indication of the speed of transduction of the photoreceptors of the eye (refer to Chapter 2, section *2.1.2.1* for details of phototransduction).

Table 3c displays the results of the latency analysis of the ERG signals from the dark-adapted eyes of the mesopelagic malacostracans. *A. purpurea* and *S. debilis* have mean response latencies of 49.5ms (s.e. ±0.85) and 48.2ms (s.e. ±1.04) respectively. These are very similar values (p=1.000, see appendix II), and are the longest response latencies of all the species studied, i.e. these species have the slowest visual response. This long response latency is accompanied by a relatively highly sensitive visual response.

P. multidentata and *S. arcticus* have mean response latencies of 30.5ms (s.e. ±0.91) and 33.0ms (s.e. ±2.47) respectively. These are similar values and do not significantly differ from each other (p=0.856, see appendix II). This shorter response latency is accompanied by a relatively less sensitive visual response.

The mean response latency for the euphausiid species *M. norvegica*, however, does not follow the trend between response latency and sensitivity as described for the other species. The response latency for *M. norvegica* is 14.3ms (s.e. ±1.2) and is significantly different to the

response latencies of all the other mesopelagic species ($p<0.0005$ in comparisons with all other mesopelagic species, see appendix II). Thus, the euphausiid *M. norvegica* has the shortest response latency of all the mesopelagic species despite having an intermediate visual sensitivity as described by its value of k. It is somewhat surprising that this species has the fastest dark-adapted visual response (in terms of response latency), considering it is more sensitive to light than the decapods *P. multidentata* and *S. arcticus*.

The software Minitab (release 12.22) was used to determine the Pearson's correlation coefficient of the relationship between the two variables k and response latency for the mesopelagic species studied. Pearson's correlation coefficient, *r*, measures the strength of the linear relationship between two variables; p-values are supplied and these indicate the statistical significance of *r* (i.e. if $p<0.05$ there is a statistically significant relationship between the two variables).

Fig. 3.9a displays plots of the correlation between the variables k and response latency for all the mesopelagic species studied. The *r* value for the plot in Fig.3.9a is –0.720, indicating that there is no correlation between the two variables ($p=0.170$, $df = 3$).

Fig. 3.9b displays plots of the correlation between the variables k and response latency for all the decapod mesopelagic species studied excluding the data for the euphausiid species *M. norvegica*. The variables for this species are omitted as the response latency for this species is unusually fast when one considers that this species has an eye with intermediate sensitivity and this species belongs to a different order compared with the other species (see Table 3a, section *3.2.1*). The *r* value for the plot in Fig.3.9b is –0.998 indicating a negative correlation between the two variables. This correlation is highly significant ($p=0.002$, $df = 2$).

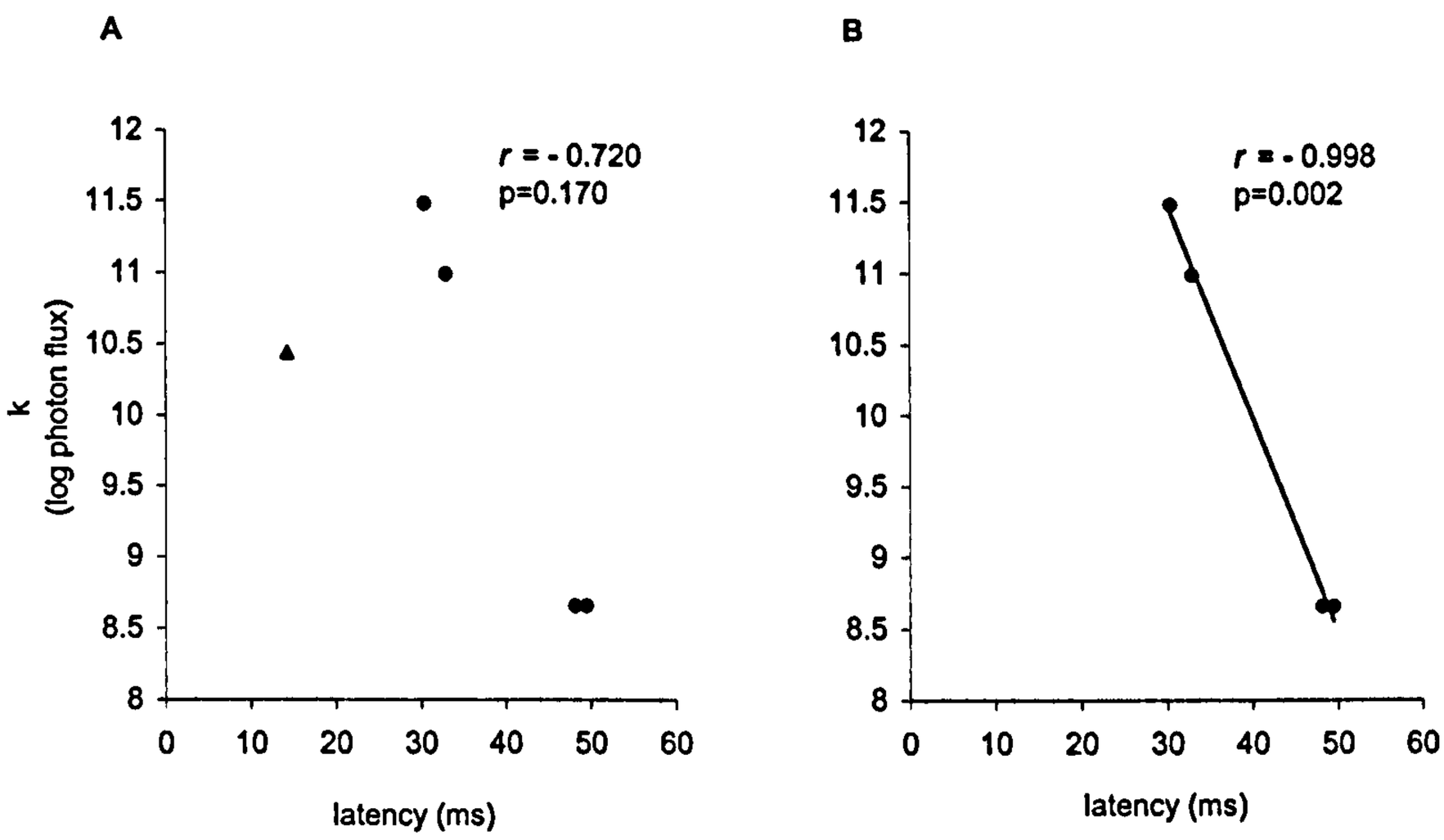

Figure 3.9. The correlation between the variables k and response latency for the mesopelagic species studied, the Pearson's correlation coefficient for each correlation is signified by the value of *r*. The p-values indicate the statistical significance of *r*, a value less than 0.05 indicates that there is a significant correlation between the two sets of variables. In A) the variables k and latency are plotted for all mesopelagic species studied (the triangular data point represents the datum point for the euphausiid species *M. norvegica*); Pearson's correlation coefficient, *r*, is - 0.720, indicating that there is no significant correlation between k and response latency, as shown by the p-value (p=0.170, df = 3). B) the variables k and latency are plotted for all decapod mesopelagic species only (excluding the datum point for the euphausiid mesopelagic species *M. norvegica*). When the values for the euphausiid *M. norvegica* are omitted there is a strong negative correlation between k and response latency (*r* = - 0.998, p=0.002, df = 2) for the visual response of the decapod mesopelagic species studied.

It may be tentatively concluded, therefore, that with the exception of the euphausiid species *M. norvegica*, there is a statistically significant negative correlation between sensitivity and latency of the visual response for the decapod mesopelagic species studied here. The decapod species with the most sensitive visual responses have the longest response latencies, and those decapod species with less sensitive visual responses have shorter response latencies.

3.4.2 Visual Sensitivity of Coastal, Shallow water Malacostracans

Plots of the dark-adapted VlogI relationship for the two species of coastal, shallow water malacostracan (*Crangon crangon* and *Palaemon elegans*) studied are given in Fig. 3.10. These plots have a sigmoidal shape as do those for the mesopelagic malacostracans, see Fig. 3.7 and section *3.4.1* for details.

The relative sensitivity of the visual response of these coastal, shallow water species is described by the value of k as for the mesopelagic species (see section *3.4.1*).

3.4.2.1 Visual sensitivity

Crangon crangon and *Palaemon elegans* have a similar sensitivity to blue light (λ_{max} 464nm, FWHM = 28nm). The value of k for *Crangon crangon* is 12.31, which is not significantly different to the value of k for *Palaemon elegans*, which is 12.02 (p=0.734, see appendix II and Fig. 3.10). For *C. crangon*, the value of k of 12.31 is equivalent to an irradiance at the eye of 2.04×10^{12} photons s^{-1} cm^{-2}. For *P. elegans*, the value of k of 12.02 is equivalent to an irradiance at the eye of 1.05×10^{12} photons s^{-1} cm^{-2}. *C. crangon* has a dark-adapted VlogI relationship with a dynamic response range (as defined by the log units between the response limits of 5 and 95%, after Laughlin and Hardie, 1978) that spans 5 log units, this is compared with *P. elegans* which has a dark-adapted VlogI relationship with a dynamic response range which spans 6.5 log units. The mean values of *m* for the VlogI relationships of *C. crangon* and *P. elegans* are 0.52 and 0.37 respectively (see Table 3d). Statistical analysis reveals that these values are not significantly different (p=0.172, see appendix III). Consequently the VlogI curves for *C. crangon* and *P. elegans* have similar gradients.

3.4.2.2 Response Latency

The mean response latency for *C. crangon* is 24.0ms, which is not significantly different to the mean response latency for *P. elegans* of 20.3ms (p=0.902, see appendix II and Table 3d).

Thus, *C. crangon* and *P. elegans* share similar visual sensitivity and have similar speeds of visual response, as reflected in the values for response latency for each species. *C. crangon* is a nocturnally active species and *P. elegans* shows increased activity at night (see Table 3b, section *3.2.2*), both inhabit shallow, coastal waters and so experience similar light environments.

A *Crangon crangon* (*n*=8): k = 12.31

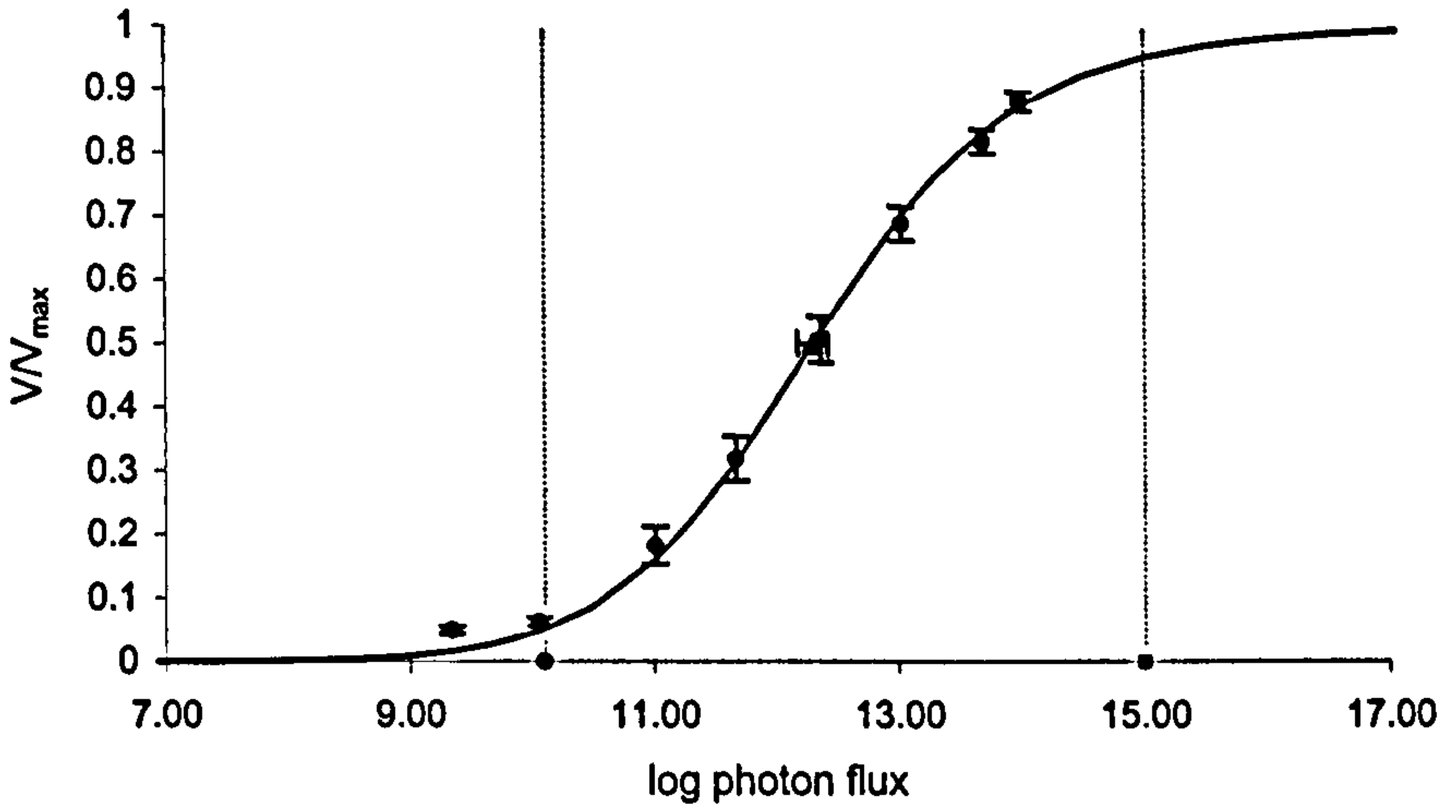

B *Palaemon elegans* (*n*=8): k = 12.02

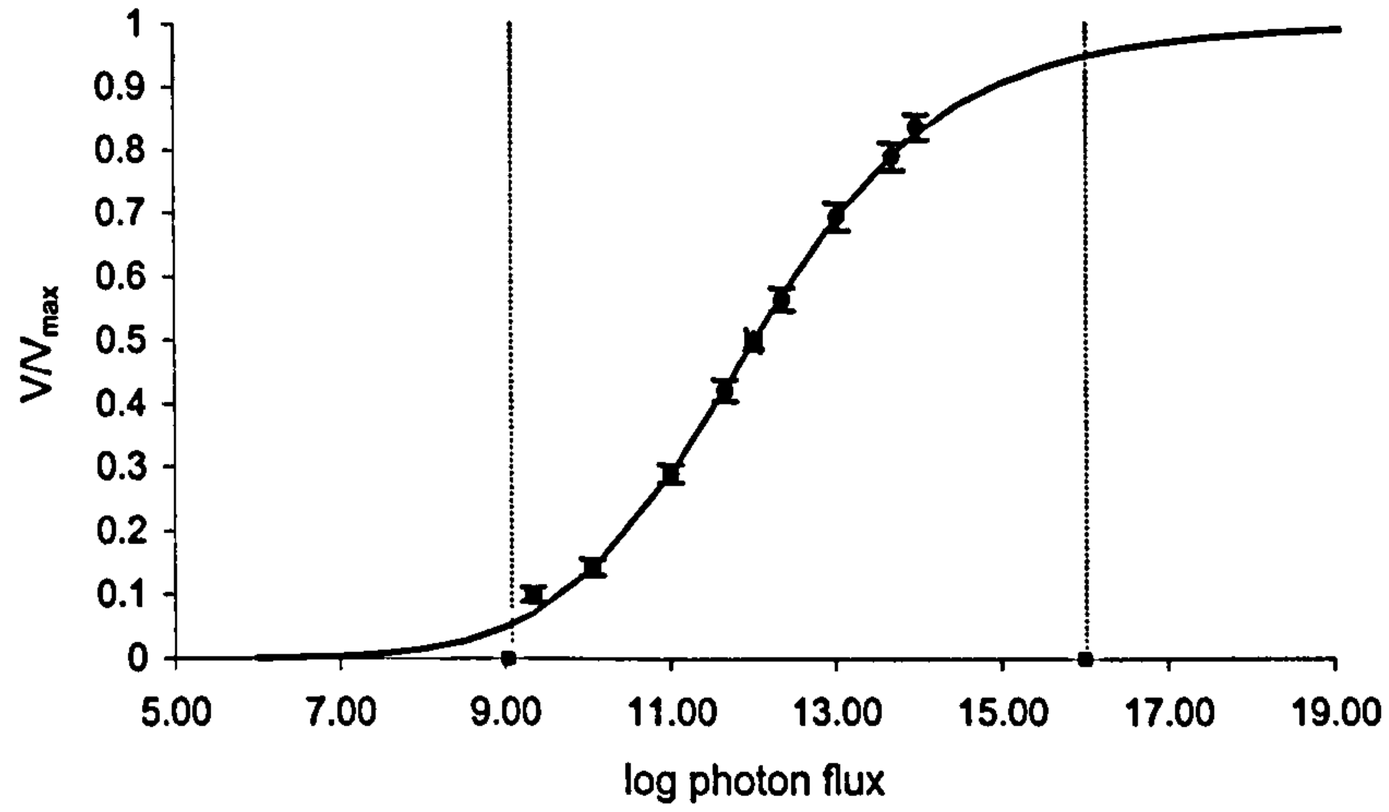

Figure 3.10. The VlogI relationships for the two species of shallow water malacostracan studied. The circles indicate mean V/V_{max} values (standard errors shown); the triangular points on each plot indicate the mean value of k for each species (standard errors shown), which fall in the centre of the linear portion of the intensity-response function. The smoothed line represents the fit of the Michaelis-Menten equation (Valeton and van Norren, 1983) through the mean V/V_{max} points (using sum of least squares regression analysis). The dashed lines on each plot indicate the dynamic range of the photoreceptors (defined by the log units between the response limits of 5 and 95%V_{max}, after Laughlin and Hardie, 1978), in both A) and B) this is *ca.* 5.0 and 6.5 log units respectively.

3.4.3 Visual Sensitivities of Coastal and Mesopelagic Malacostracans: A Comparison

Fig. 3.11 is a plot of the dark-adapted VlogI relationships of both the mesopelagic and coastal species of malacostracan. The shape of the VlogI relationships are similar for all the animals studied; between all of the mesopelagic species and the coastal species *C. crangon*, there is no significant difference in the value of *m* ($p>0.05$, see appendix III). However, the value of *m* for the VlogI relationship of the coastal species *P. elegans* is significantly different to that for all the species studied with the exception of *S. arcticus* ($p=0.398$) and *C. crangon* ($p=0.172$). *C. crangon*, *P.elegans* and *S. arcticus* have relatively small values of *m*, *P. elegans* having the lowest (see Table 3d). Consequently the VlogI curve for the eye of *P. elegans* is less steep than that for the other species studied and therefore covers a greater dynamic range (see section *3.4.1.1* and Table 3e). The VlogI curves also differ between species with respect to their placement along the log intensity axis. Table 3d displays the results of the analysis of visual sensitivity (in terms of k), relative sensitivity (RS), response latency, and shape of the VlogI curve, in terms of *m*, for all malacostracan species studied.

	Species	k (log photons s^{-1} cm^{-2})	RS	Latency (ms)	*m*
Meso-pelagic	*Acanthephyra purpurea*	8.66 (±0.02; *n*=3)	4467	49.5 (±0.85; *n*=3)	0.62 (±0.06; *n*=3)
	Systellaspis debilis	8.66 (±0.15; *n*=7)	4467	48.2 (±1.04; *n*=7)	0.59 (±0.04; *n*=7)
	Meganyctiphanes norvegica	10.44 (±0.18; *n*=6)	74	14.3 (±1.20; *n*=5)	0.60 (±0.08; *n*=6)
	Sergestes arcticus	10.99 (±0.16; *n*=5)	21	33.0 (±2.47; *n*=4)	0.50 (±0.18; *n*=5)
	Pasiphaea multidentata	11.48 (±0.13; *n*=5)	7	30.5 (±0.91; *n*=7)	0.60 (±0.05; *n*=5)
Coastal	*Crangon crangon*	12.31 (±0.12; *n*=8)	1	24.0 (±0.72; *n*=8)	0.52 (±0.03; *n*=8)
	Palaemon elegans	12.02 (±0.08; *n*=8)	2	20.3 (±0.67; *n*=7)	0.37 (±0.02; *n*=7)

Table 3d. The mean values of k, response latency and *m* for both mesopelagic and coastal species of malacostracan. Also included is the relative sensitivity (RS) of the visual response, calculated from the back transformed (from the logarithmic state) values of k relative to the least sensitive visual response, which is produced by the eye of *C. crangon* and is assigned a value of 1.

The results show that the dark-adapted visual responses of the two coastal species are significantly less sensitive to blue light (λ_{max} 464nm, FWHM = 28nm) than the following mesopelagic species: *A. purpurea, S. debilis, M. norvegica* and *S. arcticus* ($p<0.05$, in

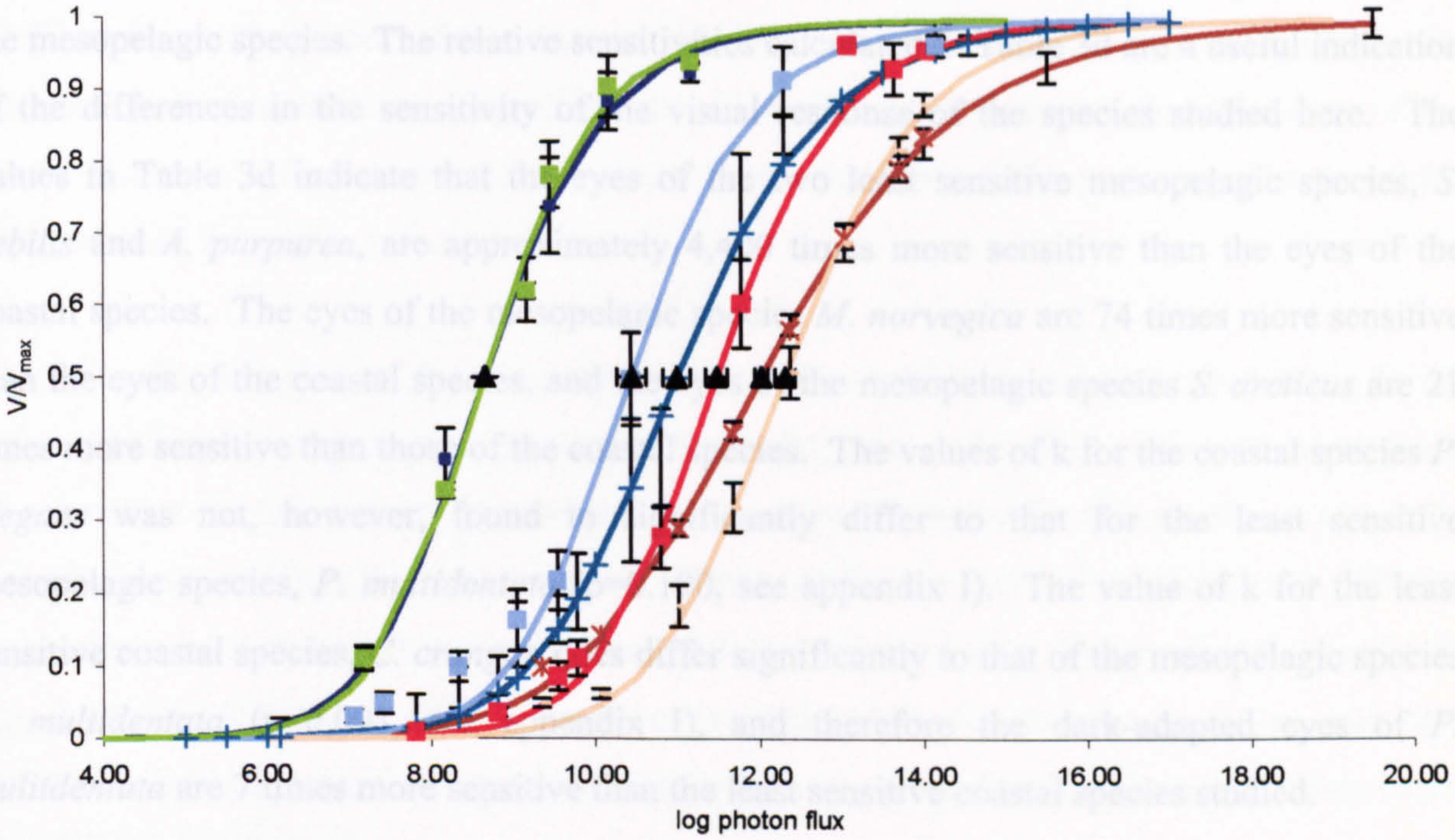

Figure 3.11. The VlogI relationships of the dark-adapted visual systems of all species (both coastal and mesopelagic) studied. The VlogI relationships for the eyes of all the mesopelagic species and the coastal species *C. crangon* are very similar in terms of their shape, i.e. there is no significant difference in the values of *m* ($p>0.05$) for these species. The value of *m* for the coastal species *P. elegans* is significantly different to that for all the species studied ($p<0.05$) with the exception of the coastal species *C. crangon* ($p=0.172$) and the mesopelagic species *S. arcticus* ($p=0.398$). This is reflected in the fact that the VlogI curve for this species is less steep than the curves for the other specie studied. The VlogI relationships for the coastal species are right-shifted along the log intensity axis relative to the mesopelagic species, resulting in a higher value of k. There is no significant difference between the values of k for *C. crangon* and *P. elegans* ($p=0.734$). The values of k for *C. crangon* and *P. elegans* are significantly greater than those for: *A. purpurea*; *S. debilis*; *M. norvegica* and *S. arcticus*. ($p<0.05$). The value of k for *P. multidentata* is not significantly different to the values of k for the coastal species ($p>0.05$), indicating similar visual sensitivity.

comparing k values, see appendix I). This is illustrated in Fig. 3.11 in the right shifted positioning of the VlogI relationships, and thus values of k, of the coastal species relative to the mesopelagic species. Table 3d shows higher mean values of k for the coastal species than for the mesopelagic species. The relative sensitivities calculated in Table 3d are a useful indication of the differences in the sensitivity of the visual response of the species studied here. The values in Table 3d indicate that the eyes of the two least sensitive mesopelagic species, *S. debilis* and *A. purpurea*, are approximately 4,400 times more sensitive than the eyes of the coastal species. The eyes of the mesopelagic species *M. norvegica* are 74 times more sensitive than the eyes of the coastal species, and the eyes of the mesopelagic species *S. arcticus* are 21 times more sensitive than those of the coastal species. The values of k for the coastal species *P. elegans* was not, however, found to significantly differ to that for the least sensitive mesopelagic species, *P. multidentata* ($p=0.190$, see appendix I). The value of k for the least sensitive coastal species, *C. crangon* does differ significantly to that of the mesopelagic species *P. multidentata* ($p=0.008$, see appendix I), and therefore the dark-adapted eyes of *P. mulitdentata* are 7 times more sensitive than the least sensitive coastal species studied.

Table 3d shows that, with the exception of the euphausiid species, *M. norvegica,* the response latencies of the dark-adapted photoreceptors of the decapod coastal species are shorter than the response latencies for the decapod mesopelagic species. This is another example of the relationship between visual sensitivity and speed of phototransduction for decapod species: the less sensitive the visual response, the shorter the response latency (see Fig. 3.12). Statistical analysis, using univariate analysis of variance, of the differences in response latency between species reveals that the response latency for *C. crangon* is not significantly shorter than that for the mesopelagic species *P. multidentata* ($p=0.064$ see appendix II). This is not surprising as both species share similar visual sensitivity. The value of response latency of *P. elegans* is not significantly different to that for the euphausiid *M. norvegica* ($p=0.417$, see appendix II). Therefore, although *M. norvegica* has a more sensitive dark-adapted eye than the decapod coastal species, it shares a similar length of response latency.

As before (see section *3.4.1.3*) the software Minitab (release 12.22) was used to determine the Pearson's correlation coefficient of the relationship between the two variables k and response latency for all the malacostracan species studied (both mesopelagic and coastal, and decapod and euphausiid).

Fig. 3.12a displays plots of the correlation between the variables k and response latency for all the malacostracan species studied. The *r* value for the plot in Fig. 3.12a is –0.776 indicating a negative correlation between the two variables, and this correlation is significant (p=0.040, df = 5). Therefore with the extra data points provided by the variables of k and response latency for the coastal species, there is a significant negative correlation between the sensitivity of the visual response and response latency even when the very short response latency of the euphausiid *M. norvegica* is included.

Fig. 3.12b displays plots of the correlation between the variables k and response latency for all the decapod malacostracan species studied (excluding the euphausiid species *M. norvegica*). The variables for this species are omitted as the response latency for this species is unusually fast when one considers the intermediate sensitivity of the eye and that it belongs to a different order compared with the other species (see Table 3a, section *3.2.1*). The *r* value for the plot in Fig. 3.12b is –0.982 indicating a negative correlation between the two variables, and, this correlation is highly significant (p<0.0005, df = 4), and a good fit of the linear trend line to the data points.

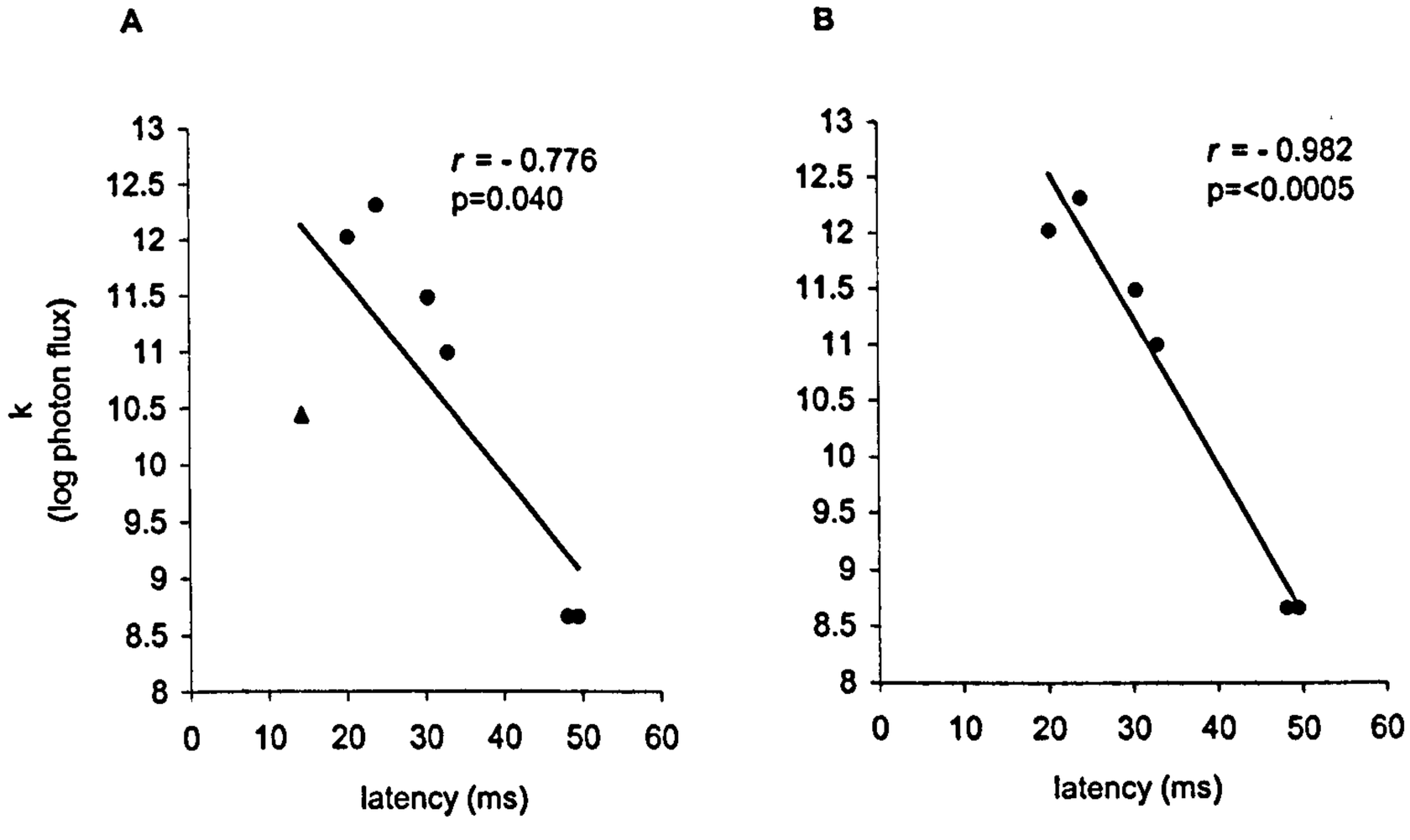

Figure 3.12. In A) the variables k and response latency are plotted for all malacostracan species studied (the triangular datum point represents the data for the euphausiid species *M. norvegica*) and a linear trend line is fitted to the data points; Pearson's correlation co-efficient, *r*, is - 0.776, and is significant (p=0.040, df = 5), i.e. there is a significant relationship between k and response latency. In B) the variables k and response latency are plotted for decapod malacostracan species only (the datum point for the euphausiid *M. norvegica* is excluded). When the values for the euphausiid *M. norvegica* are omitted there is a strong and highly significant negative correlation between k and response latency (*r* = - 0.982, p<0.0005, df = 4) for the visual response of the decapod malacostracan species (both mesopelagic and coastal) studied.

Table 3e presents a summary of the dark-adapted photoreceptor responses of all the malacostracan species in this study in terms of: k; the dynamic range; and the exponent *m* (see section *3.3.1* for the Michealis-Menten equation) that determines the gradient of the sigmoidal VlogI relationship.

	Species	k (log photons $s^{-1}cm^{-2}$)	*m* (exponent)	dynamic range (log units)
Mesopelagic	*Acanthephyra purpurea*	8.66	0.62	4.0
	Systellaspis debilis	8.66	0.59	4.5
	Meganyctiphanes norvegica	10.44	0.60	4.5
	Sergestes arcticus	10.99	0.50	5.0
	Pasiphaea multidentata	11.48	0.60	4.5
Coastal	*Crangon crangon*	12.31	0.52	5.0
	Palaemon elegans	12.02	0.37	6.5

Table 3e. The values of k, the exponent *m*, and the dynamic range of the VlogI relationship for each malacostracan species studied.

Comparing the sensitivities of the dark-adapted systems of all the coastal and mesopelagic species in this study leads to the following conclusions (see section *3.4.1.2* for conclusions regarding mesopelagic species alone):

a) The VlogI relationships of all the malacostracan species in this study (except for the coastal species *Palaemon elegans*) have similar sigmoidal shapes i.e. there are no significant differences between the values of *m* for these species ($p>0.05$, see appendix III). The value of *m* for *P. elegans* is significantly less ($p<0.05$) than the greatest values of *m* (e.g. *Meganyctiphanes norvegica* and *Pasiphaea multidentata*). The VlogI relationship for the eye of *P. elegans* therefore has a relatively lower gradient compared with the other species studied and the eyes of this species have the greatest dynamic response range of all the species studied.
b) Both *Crangon crangon* and *Palaemon elegans* have similar sensitivities to blue light and these species possess the least sensitive visual systems of all the species in this study.

c) The mesopelagic decapod, *Pasiphaea multidentata* shares a similar sensitivity with the coastal species *P. elegans*, and is the least sensitive mesopelagic species in this study.

d) For all the decapod malacostracan species studied, relative sensitivity as defined by the value of k is inversely related to response latency and this is a statistically significant negative correlation ($p<0.0005$). This is a strong correlation as it is still statistically significant if the data for the euphausiid species *M. norvegica* is included ($p=0.040$).

3.5 DISCUSSION

3.5.1 Comparisons with Previous Studies

3.5.1.1 Relative sensitivity

The plots of the VlogI relationships determined for each species in this study (see Figs 3.7; 3.8; 3.10; 3.11) are similar to those determined for many other invertebrate species, e.g. crayfish (Glantz, 1968); the honeybee drone (Bader *et al.* 1976); flies and dragonflies (Laughlin, 1976, Laughlin and Hardie 1978); and deep-sea and coastal decapods (Johnson, 1998). The dynamic range of the dark-adapted VlogI relationship for each species studied was defined as the log intensity range between the response limits of 5-95% V_{max}. The dynamic ranges were similar for all species in this study and covered 4.5-5.0 log units, although the species *P. elegans* has an eye with a dynamic response range covering 6.5 log units (see section *3.4.2.1*). These values are comparable with the dynamic ranges of both dragonfly photoreceptors (Laughlin, 1976), and crayfish photoreceptors (Glantz, 1968). The dynamic range of all the photoreceptors in the eye describes the response bandwidth of the eye in units of incident intensity. This response bandwidth is fixed, irrespective of the adaptation state of the photoreceptor, but is shifted horizontally along the intensity axis upon light or dark adaptation (Glantz, 1968; Bader *et al.* 1976; Laughlin and Hardie, 1978; Weckström *et al.* 1991) to keep the intensity signal within the linear region of the VlogI relationship for all stimulus intensities.

The present study considers the dark-adapted photoreceptor sensitivity of the eyes of mesopelagic and coastal malacostracans. The dark-adapted VlogI curve provides a direct reading of the relative sensitivity of the photoreceptors in the eye (the value of k), and by its gradient (*m*) also indicates the dynamic range of the photoreceptors in the eye. The purpose of this study is to compare the relative sensitivities of species of malacostracans inhabiting different light environments, and the dark-adapted VlogI curve allows this. The dark-adapted visual response may be more ecologically relevant to the species in this study as it may be assumed that animals inhabiting the mesopelagic environment spend a large proportion of their time in an essentially dark-adapted state, as they inhabit an environment in which background light is photon-limited and bioluminescent events may be rare (Herring, 2000a). Similarly, the coastal species in this study are essentially nocturnal and thus are active under photon-limited

conditions. Attempts at light-adapting the eyes of deep-sea species must be made with care, as this can result in irreversible damage to the eye (Loew, 1976; Shelton *et al.* 1985; Moeller and Case, 1995; Johnson *et al.* 2000a). Additionally, previous studies on the optical properties of the compound eyes of deep-sea decapod and euphausiid malacostracans indicate that there is a lack of mobile screening pigment present (Land, 1976; Hallberg and Elofsson, 1989; Gaten *et al.* 1992); the movement of screening pigments within compound eyes is an optical mechanism to alter quantum capture efficiency, and is a key mechanism in light adaptation (Land, 1981) (see section *1.5.4* for a review). However, obtaining measures of the VlogI relationship over the entire voltage and adaptation range of a group of photoreceptors provides a complete summary of visual function under different light regimes. Future studies of the visual sensitivity of mesopelagic malacostracans should include an examination of the extent to which the photoreceptors in the eyes light adapt and how this may be related to visually detecting bioluminescent events in the ocean.

Throughout this study, the sensitivity of the visual response to a wide field light source with peak emission (λ_{max}) of 464nm at the eye is compared between species. It is important that the values of sensitivity given for the eyes of each species should not be considered as the absolute sensitivity of the visual system for each species. Absolute sensitivity is difficult to determine for an eye as it is dependent on the individual sensitivities of the photoreceptors in the eye (Land, 1981) and these can be different in different regions of the eye (see Land, 1999, for a review and Gaten *et al.* 1992; Shelton *et al.* 1992). Consequently this study compares the relative sensitivity of the response of the eyes of mesopelagic and coastal species to a wide field light source with a λ_{max} of 464nm.

The wavelength of a light stimulus will affect the quantum capture efficiency of the photoreceptors in the eye. Consequently, a monochromatic light stimulus with a λ_{max} matched to the λ_{max} of the spectral sensitivity function of the photoreceptors is generally used in determining visual sensitivity, in order to remove any wavelength-dependent effect on the sensitivity of the visual response. In this study, an LED with a peak spectral output of 464nm and a narrow bandwidth (FWHM 28nm) was used instead (see sections *2.2.2.2* and *3.2.1.3* for detail). The results of this study therefore express the relative sensitivities of the species studied to light of 464nm. Justification for comparing relative visual sensitivity to light of 464nm between mesopelagic and coastal species is given in section *3.5.3*.

There are no published studies that report measures of the relative sensitivities of mesopelagic malacostracans in terms of k, and just one study which demonstrates the shift in the value of k upon light adaptation in the crayfish, *Procambarus clarkii* (Glantz, 1968). However, a study by Frank (1999) determines the dark-adapted visual sensitivity of mesopelagic crustaceans using a methodology which is comparable to that used here, and reports visual sensitivity for *Systellaspis debilis* in terms of $\log I_{10}$. This is the log of the irradiance at the eye required to produce a response with an amplitude that is 10% of the maximum. The $\log I_{10}$ value given is 8.9 ($\equiv 8x10^8$ photons cm^{-1} s^{-1}); this compares with a log 10% V_{max} value of 7.20 ($\equiv 1.6x10^7$ photons s^{-1} cm^{-2}) obtained in this study for the same species; thus Frank (1999) finds that *S. debilis* has a slightly less sensitive eye than the results of this study suggest. It is doubtful that the disagreement in results is due to the difference in λ_{max} of the stimulating light used. Frank (1999) used light with a λ_{max} of 490nm (the present study uses light with a λ_{max} of 464nm) and the spectral sensitivity function for *S. debilis* is sufficiently broad (Frank and Case, 1988a) that sensitivity to 490nm light should be approximately equal to sensitivity to 464nm light (see section *3.5.3*). The disagreement in results for *S. debilis* between the present study and that of Frank (1999) could be due to the differences in the optical apparatus used, as visual sensitivity as determined using the ERG is highly dependent on both the recording apparatus and light delivery system used (see section *3.5.2*). However, the values of $\log I_{10}$ from the study of Frank (1999) and log $10\%V_{max}$ from the present study for *S. debilis* differ by less than an order of magnitude, indicating that in terms of relative sensitivity, the results of this study are comparable with those of Frank (1999).

Frank (1999) also finds that *S. debilis* has both the deepest daytime depth distribution and the most sensitive eye of eight species of mesopelagic crustacean studied. This is in agreement with the results of this study, as *S. debilis* shares the most sensitive visual response with *Acanthephyra purpurea* (k=8.66 for this species) and these two species have the deepest daytime depth distributions of all the species studied. Interestingly, behavioural studies of the response of *S. debilis* to diffuse downwelling light of (λ_{max}) 500nm indicate that the average behavioural threshold is in response to irradiances of $3x10^6$ photons s^{-1} cm^{-2} (Frank and Widder, 1994a). Figs 3.7 a&b (section *3.4.1*) show that the threshold of the VlogI relationships, generated in response to (λ_{max}) 464nm light, for both *S. debilis* and *A. purpurea*, occurs at *circa* 6 log units of photon flux, which is equivalent to approximately $1x10^6$ photons s^{-1} cm^{-2}. Thus, there is agreement between the physiological measure of the threshold ERG

response to 464nm light, as determined by this study, and the behavioural threshold to 500nm light.

3.5.1.2 Response latency

The latency of the visual response is used to compare the speed of photoreceptor response between the species in this study. The latency of photoreceptor response is dependent on both the adaptation state of the photoreceptors in the eye and the intensity of the stimulating light (e.g. Howard, 1981; Laughlin and Weckström, 1993). Consequently, response latency was measured from only dark-adapted photoreceptors and only for ERG responses with a peak amplitude that was closest to 50%$V_{max.}$ As the response latencies measured for each species are measured from responses at the same point in the VlogI relationship they can be compared between species.

The latency of the visual response gives an indication of the speed of transduction of photoreceptors. A visual system with a high sensitivity is one that can efficiently transduce information contained in a visual signal with a low signal-to-noise ratio for subsequent neural processing. In a photon-limited environment, a highly sensitive visual system may be expected to have a slower response than a less sensitive visual system as the integration time of the photoreceptors is increased to maximise the time over which the few photons available are absorbed. The interspecies horizontal shift in the VlogI relationship for the mesopelagic malacostracans in this study (see section *3.4.1.2*; Fig. 3.8) is similar to that reported in Laughlin and Weckström's (1993) study on the speed of transduction of the photoreceptors of dipterans. The 'slow' eyes of three species of tipulid have dark-adapted VlogI relationships which are shifted to the left along the log intensity axis relative to the VlogI relationships of several other dipteran species which are found to have 'fast' eyes. Thus, for three dipteran species, a greater sensitivity to light is related to a slower photoreceptor response.

The values for response latency obtained for the seven species in this study fall in the range of 14.3-49.5ms (Table 3d, section *3.4.1.2*). These values of dark-adapted response latency are of a similar order of magnitude as those determined for both eight species of mesopelagic crustaceans (Frank, 1999), and for the orthopteran species *Locusta migratoria* (Howard, 1981).

In the present study, response latency is inversely related to relative sensitivity, in terms of k, bar one exception (the euphausiid *Meganyctiphanes norvegica*, see section *3.5.3* of this discussion for detail). This negative correlation is statistically significant when the variables k and response latency for all the species studied (including the euphausiid species) are tested for correlation ($p=0.040$). If the variables for response latency and k for the euphausiid meospelagic species *M. norvegica* are omitted from the correlation analysis, the negative correlation between sensitivity and response latency becomes highly significant ($p<0.0005$) for the decapod malacostracan species studied (see section *3.5.3* for a discussion of the response latency of the eyes of *M. norvegica*). The most sensitive eyes have the longest response latencies and conversely, the least sensitive eyes have the shortest response latencies (see Table 3d, section *3.4.3*). Frank (1999) reports the same relationship between response latency and sensitivity for other mesopelagic species, including five decapod and three euphausiid species. Thus, as Laughlin and Weckström (1993) determined for dipteran species, for decapod malacostracans (both mesopelagic and shallow-water) and some euphausiid malacosotracans, the most sensitive eyes may be considered as 'slow' and the least sensitive as 'fast'. This confirms that visual sensitivity is related to the speed of phototransduction for some decapod malacostracan species. At the extremes of low light intensity detection the latency and duration of quantum bumps (discrete depolarisations across the photoreceptor membrane in response to the absorption of single photons, see section *2.1.2.1*) is increased and this leads to an increase in the temporal summation and sensitivity of the photoreceptors (Laughlin, 1990; Laughlin and Weckström, 1993). An increase in the latency and duration of quantum bumps has been identified as a dark adaptation mechanism in compound eyes, which leads to a loss of temporal resolution (Laughlin, 1990; Weckström and Laughlin, 1995). As the animals in the present study are essentially permanently photon-limited, it is probable that the latency and duration of quantum bumps are permanently increased. Intracellular recording techniques could be used to monitor quantum bump generation in a dark-adapted eye, and subsequent attempts at light–adapting the eye would reveal whether or not the quantum bumps are of fixed duration and latency.

3.5.2 Considerations of Methodology Used

There are a number of points to consider with respect to the use of the ERG in determining visual sensitivity. The fact that only relative sensitivities can be compared between species in this study is addressed in section *3.5.1.1*. The sensitivity of the visual response when recorded using the ERG is dependent on the electrode position in the eye for a number of reasons. Firstly, excessive damage to the eye during electrode insertion can lead to depressed visual sensitivity. Secondly, some marine malacostracan species have dual pigment systems e.g. *Systellaspis debilis* (Frank and Case, 1988) and the shallow-water species, *Palaemonetes vulgaris* (Goldsmith and Fernandez, 1968), with a near-ultraviolet sensitive visual pigment, which is located in the eighth distal, retinular cell (R8 cell, see section *1.5.1* for more detail). Placement of the recording electrode close to the R8 cell, (if present) will lead to a less sensitive response from the eye when stimulated with (λ_{max}) 464nm light as the R8 cell contains visual pigment with maximum sensitivity to short wavelength light (*ca.* 400nm). Thirdly, there is regional morphological variation in sensitivity in many compound eyes (see Land, 1999, for a review), and this has been identified in some species of mesopelagic decapod malacostracan (Gaten *et al.* 1992; Shelton *et al.* 1992; Johnson *et al.* 2000b).

In this study however, no ERG responses have been included which indicated contribution from the near-ultraviolet sensitive photoreceptors; this can be identified by reversed polarity of the ERG response (see Frank and Case, 1988a). Any effect of regional differences in sensitivity across the eye is removed by using the relative response magnitudes (V/V_{max}) of the ERG responses. The lack of variation in the values of k obtained for each individual indicates that comparable measures of sensitivity were being obtained for individuals of a species and this is apparent in the small standard error values associated with the mean k value for each species (see Table 3d, section *3.4.3*).

The optical stimulus used in this study was constant in both axial alignment and distance from the eye (4mm) for all preparations and ensured that the whole eye was illuminated. The consequence of this, however, is that only those photoreceptors with ommatidia that have an appropriate acceptance angle would actually be stimulated by the light source (see Fig. 3.13)

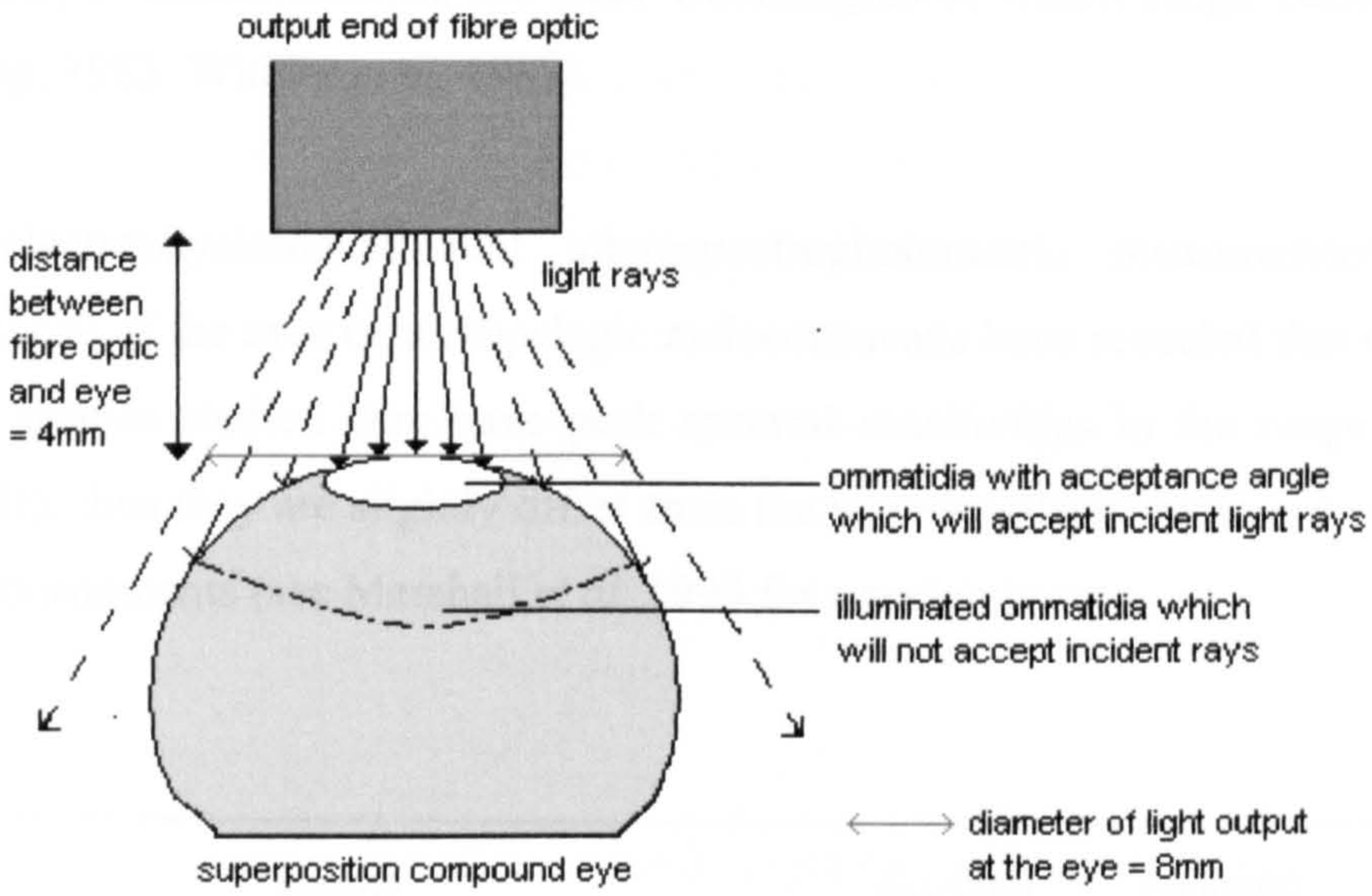

Figure 3.13. A diagrammatic representation of the effect of using a non-diffuse stimulus: only those ommatidia within a critical angle will accept light from the source. This critical angle is dependent upon the acceptance angle of the ommatidia in the eye. Continuous lines represent those incident light rays that will stimulate the photoreceptors in the eye. With the fibre optic at a distance of 4mm from the eye (constant for each preparation), the diameter of the light output at the eye is 8mm, which is a larger diameter than the diameter of any of the eyes stimulated (pers. obs.)

To ensure equal stimulation of all the photoreceptors in the eye a layer of diffuse material large enough to cover the entire surface of the eye may be placed close to the surface: this will act to distribute the light rays of the stimulus evenly over the surface of the eye. This was attempted in this study, but the diffuse material attenuated too much light and a maximum, saturating response from the eye could not be obtained. As this would prevent the full description of the dark-adapted VlogI curve, the diffuse material was not used.

3.5.3 The Light Environments in the Mesopelagic Zone and Coastal Habitats of the Species in this Study

3.5.3.1 Spectral distribution of light and spectral sensitivity

The λ_{max} of the light stimulus used in this study was 464nm. This wavelength was chosen as it is a component of both the spectral distribution of downwelling light at depths greater than 200m (see Fig. 3.2, section *3.2.1.3*), and the spectral content of bioluminescent emissions of

mesopelagic malacostracans; the peak wavelengths of which range between 440 and 490nm (Herring, 1983: Widder *et al.* 1983).

Both electrophysiological and microspectrophotometric measurements of the spectral sensitivities of the eyes of mesopelagic malacostracans have revealed that the visual systems of all the species studied here have peak spectral sensitivities in the range of 490-500nm (see Table 3f), thus they are slightly offset from the wavelengths of maximum transmission in their light environments (see Marshall *et al.* 1999 for a review).

	Species	S_{max} (nm)	Author(s)
Mesopelagic	*Meganyctiphanes norvegica*	490	Frank and Widder 1999
	Pasiphaea multidentata	497	Frank and Widder 1999
	Sergestes arcticus	495	Frank and Widder 1999
	Systellaspis debilis	500 & 400	Frank and Case 1988a
Shallow-water	*Crangon allmani*	526 & 400	Johnson 1998
	Pandalus montagui	520 & 397	Johnson 1998
	Palaemonetes paludosus	550 & 380	Goldsmith and Fernandez 1968
	Palaemonetes vulgaris	540 & 390	Wald and Seldin 1968

Table 3f. Displays the λ_{max} of the spectral sensitivity functions (S_{max}) of four of the mesopelagic species used in this study and four shallow-water decapod malacostracans (data unavailable for the shallow-water, coastal species used in this study). All spectral sensitivity functions were determined using electrophysiological techniques. No spectral sensitivity data available for *Acanthephyra purpurea*, but microspectrophotometric measurements show that the visual pigment, rhodopsin, for this species has a λ_{max} at 492nm (Kent, 1997).

Marshall *et al.* (1999), analysed the spectral sensitivity function of the eye of *Systellaspis debilis*, as determined by the consideration of the λ_{max} of the visual pigment (498nm for *S. debilis*), the length of the photoreceptors (150mm), and the specific absorbance of the photoreceptors (which is relatively high for *S. debilis*, 0.01μm^{-1}). This analysis reveals that the photoreceptors have a broadband photon capture efficiency in terms of wavelength sensitivity: within a 30-40nm wide spectral range centred around 475nm, the placement of λ_{max} of the visual pigment of *S. debilis* is not important. That is, as many photons would be absorbed if the λ_{max} was at 460nm as would be the case if the λ_{max} was positioned at 475nm. The study of Gaten *et al.* (1992) has shown that the eyes of other mesopelagic species (e.g. *Acanthephyra*

spp, Oplophorus spinosus) have similarly long photoreceptors as seen in *S. debilis*, and that this increase in photoreceptor length is a morphological adaptation to increasing sensitivity in a photon-limited environment. The spectral sensitivity functions of the eyes of the mesopelagic species in this study are broad, with FWHMs that span *ca.* 100nm (Frank and Case, 1988a; Frank and Widder, 1999). It is likely therefore, that the other mesopelagic species in this study also have similarly broadband spectral sensitivities. Consequently, interspecies comparisons of visual sensitivity in this study should not be significantly affected by the λ_{max} of the spectral output of the stimulus in relation to the position of λ_{max} of the spectral sensitivity function of each species.

The two coastal species tested in this study come from estuarine and littoral habitats. *Crangon crangon* is a nocturnally active animal, which usually inhabits the lower reaches of estuaries, although it is sometimes found on the midshore (Smaldon, 1993); *Palaemon elegans* is a littoral animal, which spends the majority of its time inhabiting rockpools (Smaldon, 1993) and shows increased activity at night (Horton, A. pers. comm.), presumably to reduce the risk of predation. During daylight, the wavelength of maximum quantal flux in coastal and estuarine waters is considerably longwave shifted relative to the λ_{max} of spectral transmission at midday in the mesopelagic environment (see sections *1.2.4* and *1.4*). At twilight, the wavelength of maximum quantal flux in coastal and estuarine waters is shifted towards shorter wavelengths and occurs around 480-520nm (Forward *et al.* 1988, see section *1.4*).

The eyes of the coastal species were also stimulated with blue (λ_{max} 464nm, FWHM = 28nm) light following preliminary experiments that showed no difference in peak response amplitude when stimulated with blue (λ_{max} 464nm) or green (λ_{max} 525nm) light adjusted to ensure equal irradiance at the eye for both wavelengths (see section *3.2.2*). It has been generally proved that animals inhabiting shallow coastal, and estuarine waters have eyes with spectral sensitivity maxima occurring at wavelengths greater than 500nm, which is consistent with the greener (longwave dominant) nature of the water (Herring and Roe, 1988) [see sections *1.2.4* and *1.4* and below]. Spectral sensitivity data are not available for the two species in this study, although there are data available for other species of shallow-water decapod malacostracans, which have dual pigment systems with maximum sensitivity in both the green and near-ultraviolet regions of the visible electromagnetic spectrum (see Table 3f). It is likely that the two shallow-water, coastal species studied here have similar spectral sensitivities to those for

the coastal species shown in Table 3f. The fact that there was no difference in response amplitude when the eyes were stimulated with blue *vs* green light suggests that the bandwidths of the spectral sensitivity functions for these animals are wide enough such that photons of 464nm and 525nm are equally effective at generating a visual response, or that the wavelength of peak sensitivity in these species is equidistant between these stimulating wavelengths. Consequently, the less sensitive visual response of *C. crangon* and *P. elegans,* as determined in this study (k= 12.31 and 12.02 respectively), cannot be attributed to the discrepancy in λ_{max} between the light stimulus used and the spectral sensitivity functions of these two species.

3.5.3.2 Downwelling irradiance

There is a lack of information on downwelling spectral irradiance at depth in the ocean due to the difficulties in accurately measuring irradiance at depth (Partridge and Cummings, 1999). Most of the data of downwelling irradiance that does exist is provided by irradiance measurements made in the euphotic zone (0-150m depth), where measuring the irradiance of PAR (Photosynthetically Active Region of the electromagnetic spectrum) is important in investigating the biology of phytoplankton. Below the euphotic zone, there is too little light for phytoplankton to exist, and consequently there are few measured data of downwelling irradiance below a depth of 200m. Because of this paucity of measurements, downwelling irradiance at depth has conventionally been determined through theoretical calculations using attenuation coefficients determined for surface waters. Downwelling light in the ocean decays exponentially with depth and thus attenuation coefficients may be used to extrapolate surface measures of irradiance to depth using Beer's Law. The problem with this, however, is that most measured attenuation coefficients have been determined for water within the euphotic zone, which contains phytoplankton and thus high levels of chlorophyll and particulate matter, which strongly affect the spectral attenuation of light (e.g. chlorophyll strongly absorbs blue light and reflects green). Below the euphotic zone phytoplankton is consumed and degraded, and thus the spectral attenuation properties of the water changes (Douglas *et al.* 1998). Consequently, extrapolation of downwelling irradiance to depth in the ocean using diffuse attenuation coefficients determined for surface waters will tend to underestimate the amount of light at depth.

Recent *in situ* measurements of downwelling irradiance at depths greater than 200m have been recorded using radiometers deployed on submersibles (Frank and Widder, 1996, 1997; Widder and Frank, 2001). This facilitates the measurement of attenuation coefficients below the euphotic zone and thus avoids the need for theoretical calculations of irradiance at depth. However, at present, these measurements have only been determined for three bodies of water (Northwest Providence Channel, Bahamas, Frank and Widder, 1996; Oceanographers Canyon, Gulf of Maine, Widder and Frank, 2001; Wilkinsons Basin, Gulf of Maine, Frank and Widder, 1997) which would be equivalent to water types IA and IB according to Jerlov's (1976) classification system (see section *1.2.4* for more detail).

Forward *et al.* (1988) have made spectral irradiance measurements for estuarine and coastal waters (see section *1.4*). These are shallow-water measurements (maximum depth in Newport River estuary [North Carolina, USA] is 3.7m), which differ by approximately an order of magnitude in comparison with surface measurements made under the same conditions (surface measures taken from Dusenbery, 1992). Consequently, measurements of irradiance at the water surface will be used as an indication of the irradiance in a rockpool, littoral or estuarine environment.

3.5.4 Visual Sensitivity and Response Latency of Mesopelagic Malacostracans in Relation to Daytime Depth Distribution

The mesopelagic animals used in this study come from three different water types, Jerlov types IA, IB and II (see Table 3g). Section *1.2.4* gives detail of Jerlov's classification system of water types based on their optical properties. The clearest oceanic water type (type I) has a peak transmission at about *ca.* 460nm, and the least attenuation of downwelling irradiance with depth. Type II water is less transparent, and although it has a similar spectral distribution with depth as type I (at 450m depth, λ_{max} 465nm [Jerlov, 1976]), a similar attenuation of downwelling irradiance is measured at 250m as is measured at 900m in type I water (Knowles and Dartnall, 1977). Consequently, the optical depth that the animals in this study inhabit is not simply defined by a comparison of their daytime depth distribution, and comparisons of relative sensitivity between the species in this study have to account for the optical properties of the water they were collected from.

Table 3g gives information on the visual sensitivity, in terms of k, and response latency along with habitat information for each species studied.

Species	Daytime depth (m)	Water type	k (log photons s^{-1} cm^{-2})	Latency (ms)
Acanthephyra purpurea	700-950	II	8.66 (±0.02; *n*=3)	49.5 (±0.85; *n*=3)
Systellaspis debilis	650-950	II,1A	8.66 (±0.15; *n*=7)	48.2 (±1.04; *n*=7)
Pasiphaea multidentata	220-240	1B	11.48 (±0.13; *n*=5)	30.5 (±0.91; *n*=7)
Sergestes arcticus	450-600	1B	10.99 (±0.16; *n*=5)	33.0 (±2.47; *n*=4)
Meganyctiphanes norvegica	300-500	1B	10.44 (±0.18; *n*=6)	14.3 (±1.20; *n*=5)

Table 3g. The mean values of k and latency of response for each species studied (all data is extracted from recorded ERG signals from dark-adapted eyes). The data are displayed along with the daytime depth distribution of each species, and water type inhabited: Table 3a (section *3.2.1*) gives references for information on daytime depth distribution and water type inhabited.

Systellaspis debilis and *Acanthephyra purpurea*

Individuals of the bioluminescent mesopelagic oplophorid malacostracan, *Systellaspis debilis*, were collected from two different locations for this study: Northwest Providence Channel, Bahamas, in which the water type is IA (*n*=4); the region of the Cape Verde Islands, Northeast Atlantic, in which the water is type II (*n*=3). The relative sensitivities of the animals from the two different locations were not significantly different and hence the data from the two groups were combined to produce a single mean value of k. The daytime depth distribution of this species at the two different locations is the same according to Foxton (1970) and Hopkins *et al.* (1989); although the study of Hopkins *et al.* (1989) maps the depth distribution of *S. debilis* in the Gulf of Mexico, which has type IA water. It may be assumed that individuals of *S. debilis* from the Gulf of Mexico will share a similar daytime depth distribution with individuals from Northwest Providence Channel as optical depth will be equal in the two locations.

Assuming equal daytime depth ranges, those individuals inhabiting Type II water in the Northeast Atlantic are at a greater optical depth than those individuals from the region of the Bahamas. Considering this, one might expect that individuals from the Northeast Atlantic would have a more sensitive visual response than those from the clearer water if daytime depth

distribution were correlated with visual sensitivity. However, both quantitative data on the depth distribution of *S. debilis* in the Northwest Providence Channel, Bahamas, and *in situ* downwelling irradiance measurements at depth for both the regions from which the animals were collected is required before inferences can be made about the similarity in the sensitivity of their visual responses.

Another bioluminescent mesopelagic oplophorid malacostracan, *Acanthephyra purpurea*, has a relative sensitivity equal to that of *S. debilis* (both species have k values of 8.66). Individuals of *A. purpurea* were collected from only the region of the Cape Verde islands, and share a similar daytime depth distribution with *S. debilis* in this location (Table 3g). These two species have both the most sensitive visual response, in terms of k, of all the species in this study (they are approximately 4,400 times more sensitive to light than the least sensitive malacostracan species, *Crangon crangon and Palaemon elegans*), and the longest response latencies of all the species studied. *A. purpurea* and *S. debilis* have the deepest daytime depth distribution of all the species studied and were taken from the least transparent water type (type II). Therefore, they occupy the greatest optical depth in the water column of all the species in this study, and they possess the slowest and most sensitive eyes.

Sergestes arcticus and *Pasiphaea multidentata*

Individuals of the bioluminescent mesopelagic sergestiid, *Sergestes arcticus*, were collected from Oceanographers Canyon (OC), Gulf of Maine (type IB water). These animals occupy a daytime depth range of 450-600m. This species has a visual response that is approximately 200 times less sensitive than that of both *A. purpurea* and *S. debilis*. The value of k for *S. arcticus* did not significantly differ to that for the non-luminescent mesopelagic pasiphaeid, *Pasiphaea multidentata*, and therefore they share a similar visual sensitivity to blue light (λ_{max} 464nm, FWHM 28nm). These two species also share similar response latencies that are intermediate relative to the other mesopelagic species in this study (see Table 3g). Individuals of *P. multidentata* were collected from Wilkinsons Basin (WB), Gulf of Maine (also type IB water), where this species has a statistically significant population maximum between depths of 220 and 240m (Frank and Widder, 1997). Although the water in the Gulf of Maine has been classified as type IB (Jerlov, 1976), *in situ* measurements of downwelling irradiance in both OC and WB using submersible-based technology (see Frank and Widder, 1997 for detail of

methodology) have revealed that the water in WB is optically murkier than that in OC. For WB water, downwelling irradiance measured at a depth of 200m, at midday and at λ_{max} 480nm (FWHM 10nm) is $3.1x10^{7}$ photons s^{-1} cm^{-2} (n=1) (pers comm. Widder, E. and Frank, T. M.). This compares with an equivalent value at λ_{max} 480nm (FWHM 10nm) of $1.5x10^{10}$ photons s^{-1} cm^{-2} (n=2) (pers. comm. Widder, E. and Frank, T. M.) for OC water at 200m depth measured under exactly the same conditions. There is, therefore, a difference of approximately three orders of magnitude in the downwelling irradiance levels at equal depths in the two water bodies. Consequently, although *P. multidentata* physically occupies the shallowest depth range of all the species in this study (Table 3g), optically, it shares a similar depth range as *S. arcticus*. The downwelling irradiance measured at midday at λ_{max} 480nm (FWHM 10nm) at the shallowest depths of the daytime depth ranges for each species is: 225m (the shallowest depth of the range for *P. multidentata*), $1.3x10^{7}$ photons s^{-1} cm^{-2} (n=2); and 450m (the shallowest depth range for *S. arcticus*) $1.5x10^{6}$ photons s^{-1} cm^{-2} (n=1) (irradiance measures from Widder, E. and Frank, T. M., pers. comm.).

Therefore, these two species share both similar visual sensitivity and response latency, which corresponds to both species occupying similar optical depths in the water column. Both *S. arcticus* and *P. multidentata* have a less sensitive visual response and 'faster' eyes than *A. purpurea* and *S. debilis* and this can be correlated with inhabiting a shallower optical depth.

Meganyctiphanes norvegica

Individuals of the bioluminescent mesopelagic euphausiid malacostracan, *Meganyctiphanes norvegica*, were collected from Oceanographers Canyon (OC), Gulf of Maine. This species occupies a daytime depth range of 300-500m, which is optically the shallowest depth of all the species in this study. At a depth of 300m in OC water at midday, at λ_{max} 480nm (FWHM), downwelling irradiance is measured as $3.11x10^{8}$ photons s^{-1} cm^{-2} (Widder, E. A., and Frank, T. M., pers. comm.). The visual sensitivity as determined for *M. norvegica* in terms of k, is not significantly different to that determined for *S. arcticus*. However, the value of k for *M. norvegica* is significantly less than that for *P. multidentata*, which corresponds to the eyes of *M. norvegica* being 12 times more sensitive to blue light than the eyes of *P. multidentata*. This is surprising, considering that *M. norvegica* inhabits a 'brighter' depth range, and does not agree with the correlation between visual sensitivity and daytime optical depth range seen for

the other mesopelagic species in this study. The response latency for this species however, is the shortest of all the species studied at 14.3ms, and this does agree with the relationship between speed of the eye and the optical depth range inhabited, as observed for the other mesopelagic species in this study.

Frank and Widder (1997) report that ERG measurements to determine photoreceptor sensitivity from the eyes of *M. norvegica* and *P. multidentata* revealed that individuals of *M. norvegica* were consistently 1-2 log units less sensitive to light than *P. multidentata*, whereas in this study it was found that *M. norvegica* was consistently 1 log unit more sensitive to blue light (λ_{max} 464nm) than *P. multidentata*. On consideration of the visual response of *M. norvegica* in relation to that of the coastal species studied here (see below), it is clear that the photoreceptors of *M. norvegica* have much shorter response latency than even those of the least sensitive, coastal species. The latency of response for *M. norvegica* (14.3ms) is also comparable to a latency of 16.0ms for the euphausiid species *N. sexspinosus* (Frank, 1999). However, *N. sexspinosus* has a $\log I_{10}$ value of 10.8 (Frank, 1999), which compares with a log $10\%V_{max}$ value of 9.05 for *M. norvegica* (present study) and therefore *M. norvegica* appears to be more sensitive to light than *N. sexspinosus*. A short response latency generally indicates a less sensitive eye (Laughlin and Weckström, 1993) and consequently one would expect *M. norvegica* to have a relative sensitivity comparable to that of the coastal species, or indeed a less sensitive visual response than the coastal species. Nevertheless, the results presented here, suggest that *M. norvegica* is approximately 70 times more sensitive than the coastal species.

M. norvegica, along with a number of other euphausiid species, are more commonly and collectively, known as krill. Krill are among the world's most abundant metazoan animals and are of great ecological importance as they form a key link in the food chain in the ocean and are preyed upon by animals ranging from fish, birds and marine mammals (Mangel and Nicol, 2000). They themselves are opportunistic feeders, although they particularly prey upon bioluminescent copepods (Beyer, 1992; Lass *et al.* 2001). *M. norvegica* is bioluminescent, and probably uses bioluminescent emissions from the ten photophores located on the ventral surface of their thorax, abdomen and eyes in counter-illumination, congener recognition, sexual signalling and predator-prey interactions (Herring, 1983; Herring 2000b). Considering this, it may be advantageous to this species to have a very sensitive eye for detecting faint bioluminescent signals in the ocean, and thus the intermediate sensitivity of the visual response

of this species, as determined here may be related to the behaviour of this animal. However, both *Systellaspis debilis* and *Sergestes arcticus* also possess photophores for use in counter-illumination and signaling and therefore presumably have the same requirements as *M. norvegica* for using and detecting bioluminescent emissions in the ocean. For both *S. debilis* and *S. arcticus* response latency is inversely related to sensitivity (see section *3.4.1.3*), which in turn is related to the optical daytime depth range inhabited by each species. See Chapter 6 for further discussion.

3.5.4.1 Sensitivity and irradiance in the natural habitat

The visual sensitivities of the mesopelagic species studied here can be related to the irradiance levels experienced in the natural habitats of these animals. Table 3h gives the irradiance measurements recorded at λ_{max} 480nm (FWHM 10nm) at the upper limit of the daytime depth range of each of the three mesopelagic species from the Gulf of Maine (see section *3.5.3.2*). Also given are the approximate irradiances at λ_{max} 464nm (FWHM 28nm), which produce responses from the eye that are 1% and 0.1% of the maximum ($1\%V_{max}$ and $0.1\%V_{max}$), i.e. threshold responses.

Species	Irradiance (photons s^{-1} cm^{-2}) at 464nm at $1\%V_{max}$	Irradiance (photons s^{-1} cm^{-2}) at 464nm at $0.1\%V_{max}$	Irradiance (photons s^{-1} cm^{-2}) at 480nm at upper limit of daytime depth range
Sergestes arcticus	$3.2x10^7$	$3.2x10^6$	$1.5x10^6$
Pasiphaea multidentata	$6.3x10^7$	$1.2x10^7$	$1.3x10^7$
Meganyctiphanes norvegica	$1.1x10^7$	$3.2x10^6$	$3.0x10^8$

Table 3h. The values of irradiance (measured at λ_{max} 464nm, FWHM 28nm) which generate a threshold response (defined as $1\%V_{max}$ and $0.1\%V_{max}$) from the eye (data from the present study), along with the approximate irradiance (measured at λ_{max} 480nm, FWHM 10nm) at the upper limit of the daytime depth range of each mesopelagic species from the Gulf of Maine (data from Widder, E., and Frank, T. M., pers comm.).

From the values in Table 3h it is apparent that the values of irradiance (at 480nm) for the upper limit of the daytime depth range for *S. arcticus* and *P. multidentata* are approximately 1 log unit less than the irradiances (at 464nm) which generate a threshold response from the eye that

is 1%V_{max}. For the euphausiid species *M. norvegica*, the irradiance at the upper limit of its daytime depth distribution at 480nm is approximately 1 log unit greater than the irradiance (at 464nm) that generates a threshold response from the eye that is 1%V_{max}. When one considers a threshold response from the eyes of these mesopelagic species that is 0.1%V_{max}, for the decapod species *S. arcticus* and *P. multidentata*, there is approximate agreement between the irradiance (at 464nm) that generates a threshold response and the irradiance (at 480nm) available in the environment. For *M. norvegica*, a threshold response of 0.1%V_{max} is produced in response to irradiances (at 464nm) that are 2 log units less than the irradiance available in the natural environment. A threshold response of 0.1%V_{max} is considered, as it is known that some photoreceptors can operate with high enough gain to detect individual photon hits (Dusenbery, 1992). The absolute photon resolution will depend upon the levels of photoreceptor noise in the eye, which can vary between species and within a single retina (Laughlin, 1981; Burton *et al.* 2001). A threshold response of 0.1%V_{max} will be elicited by the downwelling irradiance levels (at 480nm) in the environments of the species *S. arcticus*, *P. multidentata* and *M. norvegica*. It should be noted that the downwelling irradiance values quoted are for downwelling irradiance levels at λ_{max} 480nm and with a relatively narrow bandwidth (10nm). In reality there is likely to be more light available than this at depth, as there is a broader spectral distribution of light at depth in the ocean (see Fig. 3.2, section *3.2.1.3*). Therefore these irradiances are used as a guide and it is acknowledged that absolute downwelling irradiance levels will be higher than the values given in Table 3h. Consequently, it is highly likely that downwelling irradiance will stimulate the eyes of these mesopelagic malacostracans and produce more than a threshold response (0.1%V_{max}) from the eyes.

Bioluminescence must also be considered as a light source that will affect the sensitivity of the visual systems of mesopelagic animals, as there are so many mesopelagic animals capable of generating bioluminescence (see sections *1.3.1* and *3.1* for detail). It is much more difficult, however, to quantify the amount of bioluminescence likely to be observed in the ocean in terms of irradiance, than it is to determine the irradiance of downwelling light at depth. The irradiance of a bioluminescent source at the eye of the observer will be highly dependent on the distance and viewing angle between the bioluminescent source and the eye, and the transmission properties of the water. Herring (2000a) calculates that a bioluminescent signal when perceived from a distance of 10m, in the clearest ocean water, would provide an irradiance at the eye of $8x10^2 - 8x10^4$ photons s^{-1} cm^{-2} (assuming no scattering and absorption).

According to the results of the present study, another independent electrophysiological study (Frank, 1999), and a behavioural study (Frank and Widder, 1994a), an irradiance of $8x10^4$ photons s^{-1} cm^{-2} is below the threshold of vision for the very sensitive species, *S. debilis* (physiological and behavioural threshold is determined as approximately 10^6 photons s^{-1} cm^{-2}). This suggests that the mesopelagic species studied here will not be able to detect bioluminescent emissions at a distance greater than 10m. However, before reliable inferences can be made about the way in which visual sensitivity (as measured in the present study) may be related to irradiance levels in the mesopelagic environment, more information is required in the form of: a) more measurements of downwelling irradiance at depth (the values given in the present study are for just n=1 or 2); b) more estimates or direct measurements of the irradiance of bioluminescent emissions in sea water; and c) adequate modelling of the visual response to diffuse downwelling light and point source bioluminescent emissions.

3.5.5 Visual Sensitivity and Response Latency of Coastal Malacostracans in Relation to the Light Environment Inhabited.

The two nocturnally active, non-bioluminescent decapod shallow-water coastal species in this study, *Crangon crangon* and *Palaemon elegans*, have similar visual sensitivities, as estimated by their respective k values. The value of k for *C. crangon* (12.31) is not significantly different to that determined for *P. elegans*, which is 12.02 (see section *3.4.2.1* for results of statistical analysis). These species have significantly less sensitive visual responses than the mesopelagic species studied except for *P. multidentata* whose value of k is not significantly different to that for *P. elegans* (see section *3.4.3*). These coastal species also have shorter response latencies than all the mesopelagic species, except for the euphausiid *M. norvegica* (see above). There is no significant difference between the values of the exponent, *m*, describing the VlogI relationships for the two coastal species (p=0.172, see section *3.4.2.1*). These coastal species have eyes with a greater dynamic range in a given adaptation state than the mesopelagic species studied and this can be explained by the greater variety of light environments experienced by the coastal species relative to the mesopelagic species. of *C. crangon* but the purpose of this unclear as both species inhabit similar environments.

Twilight measurements of downwelling irradiance at 480nm at a depth of 0.5m in the lower reaches of an estuary give values of approximately $8x10^{10}$ photons s^{-1} cm^{-2} nm^{-1} (Forward *et al.* 1988). Irradiance measurements for the estuary bottom at night–time are not available, but surface measurements of irradiance at night can be used as a guide. On a moonlit night surface irradiance measured at 500nm is *ca.* 10^8 photons s^{-1} cm^{-2} nm^{-1} (Dusenbery, 1992). On a clear moonless night, with contribution from starlight and airglow, surface irradiance at 500nm is *ca.* 10^6 photons s^{-1} cm^{-2} nm^{-1}, compared with surface irradiance at 500nm on an overcast moonless night which is *ca.* 10^5 photons s^{-1} cm^{-2} nm^{-1} (Dusenbery, 1992). Consequently, irradiance at the surface can vary by up to three orders of magnitude depending on the weather conditions and lunar cycle. An irradiance of 10^6 or 10^5 photons s^{-1} cm^{-2} nm^{-1} at 500nm is comparable with the light regime (at 480nm) experienced by the mesopelagic species with an intermediate optical depth range, i.e. *S. arcticus* and *P. multidentata*, and this may explain the similarity in visual response between the coastal species *P. elegans* and the mesopelagic species *P. multidentata.* However, as coastal species can potentially be exposed to nocturnal irradiances of the order of 10^8 photons s^{-1} cm^{-2} nm^{-1}, it is not surprising to see that they are the least sensitive species with the fastest eyes (bar *M. norvegica*) of all those studied here. Although it could be expected, on the basis both of its daytime optical depth distribution and its very short response latency, that the euphausiid species, *M. norvegica* would share a similar visual sensitivity with these two coastal species.

A comparison of the irradiances over which the dark-adapted VlogI curve is generated with the irradiances in the environment as written above for the two shallow-water, coastal species reveals that under conditions of full moonlight the irradiance at the water surface at 500nm corresponds approximately with the threshold of the VlogI curve (defined here as $1\%V_{max}$) for both species. The irradiance at (λ_{max} 464nm) that produces a threshold response for *C. crangon* is approximately equal to $3x10^8$ photons s^{-1} cm^{-2} and for *P. elegans* this value is $1.5x10^8$ photons s^{-1} cm^{-2}. This corresponds with a value for irradiance at 500nm under conditions of full moonlight of approximately $1x10^8$ photons s^{-1} cm^{-2} nm^{-1} (Dusenbery, 1992). This suggests that the irradiance in the light environment generates only a threshold visual response when in the dark-adapted state. However, one must consider that the irradiance measures given are for 500nm only (FWHM not known), and that the spectral distribution of light in the natural environment of these animals will incorporate more wavelengths than 500nm; therefore the irradiance values given above are an underestimation of the true irradiance levels in the

environment. These animals show increased activity at night, but become active at around twilight (Horton, A., BMLSS [British Marine Life Study Society], pers. obsv. over 25 years; pers. obsv.). At twilight the irradiance at 480nm at the estuary bottom is measured as approximately $8x10^{10}$ photons s^{-1} cm^{-2} nm^{-1} (Forward *et al.* 1988), thus the dark-adapted visual response of the two coastal species appears to be adapted for vision under a range of irradiances experienced from twilight through to night.

3.5.6 Summary of Conclusions

This study has used extracellular electrophysiological recording techniques to determine the relative sensitivities of the eyes of seven species of marine malacostracans. These species include 4 decapod and 1 euphausiid mesopelagic species with differing daytime depth distributions in the ocean, and 2 shallow-water, coastal decapod species, which show nocturnal activity. There were two aims to this study, one of which was to compare the visual sensitivities of mesopelagic species with different daytime depth distributions, to establish whether or not there is a correlation between the visual sensitivity of an animal and the optical depth range it inhabits. The second aim was to determine the visual sensitivity of nocturnally active, shallow-water, coastal species, as these animals are active in a similarly photon-limited environment as shallower living mesopelagic species, and may therefore have a comparable visual sensitivity.

The following conclusions may be drawn from the results of this experiment:

a) The photoreceptors of both mesopelagic and coastal malacostracans have dark-adapted VlogI relationships that are comparable in sigmoidal shape to those determined for other arthropod species (i.e. flies and dragonflies [Laughlin, 1976]); the relationship between stimulus intensity and photoreceptor response (recorded as an ERG) is sigmoidal and shows both threshold and saturating responses in all species. The dynamic ranges of the VlogI relationships for the marine malacostracans in this study are also comparable to those determined for the photoreceptors of other arthropod species and typically cover 5 orders of magnitude.

b) The latency of the photoreceptor response for all the decapod malacostracans in this study is inversely related to the sensitivity of the visual response: the most sensitive eyes (*Systellaspis debilis* and *Acanthephyra purpurea*) have the longest response latencies, or 'slowest' eyes, and the least sensitive species (*Crangon crangon* and *Palaemon elegans*) have shorter response latencies or faster eyes. This indicates an adaptation to increased sensitivity at the level of the photoreceptor membrane, as a slow eye increases the integration time over which photons are absorbed. The euphausiid malacostracan *M. norvegica*, has an unusually short response latency considering it has intermediate visual sensitivity when compared with the other malacostracans.

c) The relative sensitivities of the four mesopelagic decapod species studied are related to the optical daytime depth range inhabited; those species at the greatest optical depth (*Systellaspis debilis* and *Acanthephyra purpurea*) have the most sensitive eyes and those species at brighter optical depths (*Sergestes arcticus* and *Pasiphaea multidentata*) have less sensitive eyes. The euphausiid species, *Meganyctiphanes norvegica*, has an intermediate visual sensitivity in comparison with the other species, despite inhabiting the shallowest optical depth and having the shortest response latency.

d) A comparison of the relative sensitivities of the eyes of nocturnally active shallow-water, coastal species with that of the mesopelagic species reveals that the coastal species, *Crangon crangon* and *Palaemon elegans* have the least sensitive eyes. This can be related to these species inhabiting an environment with equal or greater ambient irradiances in comparison with the natural habitats of the mesopelagic species with the lowest visual sensitivity.

3.5.7 Considerations for Future Work

To extend the conclusions of this study, it is suggested that the absolute sensitivities of the photoreceptors of these animals be determined, according to the equation given in section *3.1* (from Land, 1981). This would require the acquisition of data on the dimensions of rhabdoms and ommatidia, and the absorption coefficients of the visual pigment for each species. Absolute sensitivity would need to be determined for all the photoreceptors in the eye to give an indication of the absolute sensitivity of the entire eye (Land, 1981). There is a lack of

information regarding regional or spectral sensitivity of the eyes of the coastal species studied here and these should be determined for a complete description of the visual response of these animals.

Obtaining measurements of the VlogI relationship for both dark and light adapted states of the animals in this study would allow a complete description of visual function under different possible light regimes. It would be interesting to determine the extent to which the eyes of mesopelagic species light-adapt given that there is evidence which suggests a lack of mobile screening pigments in deep-sea decapod and euphausiid species (Land 1976; Hallberg and Elofsson. 1989; Gaten *et al.* 1992). The determination of the dark-adapted VlogI curve for the species in this study suggests that these animals may not depend upon light adaptation mechanisms, as bioluminescent signalling may be accommodated sufficiently by the dark-adapted dynamic range of the photoreceptors. It is likely that the eyes of the coastal species will significantly light adapt, however, as there will be circumstances under which these animals may require vision under conditions of daylight, for example on disturbance by a predator, or disturbance by wave action.

Behavioural studies to determine the visual threshold of *Systellaspis debilis* (Frank and Widder 1994a), *Acanthephyra curtirostris*, *A. smithi*, *Notostomus gibbosus*, *Janicella spinacauda* and *Oplophorus spinsosus* (Frank and Widder, 1994b) to blue (500nm) and near–ultraviolet (400nm) have already been conducted. The results of the behavioural threshold for *S. debilis* are comparable to the results of relative sensitivity as determined electrophysiologically in this study. It would be interesting to determine the behavioural sensitivity of the species to see if this agrees with the physiological relative sensitivity as determined in this study.

3.5.8 Hypotheses Tested

Hypothesis 1: Mesopelagic malacostracan species that inhabit deeper optical depths during the daytime will have a higher visual sensitivity than those species with a shallower daytime optical depth distribution.
H_0 = there will be no difference in visual sensitivity between the mesopelagic species studied.

The results of this study lead to the rejection of the null hypothesis above. The mesopelagic species inhabiting the greatest optical depths had a significantly more sensitive visual response ($p<0.05$, see section *3.4.1.2*) than those inhabiting shallower optical depths.

Hypothesis 2: That shallower living mesopelagic species of malacostracan will have a more sensitive visual response than coastal, nocturnally active malacostracans.
H_0 = there will be no difference in visual sensitivity between coastal and mesopelagic malacostracans.

The results of this study lead to the rejection of the null hypothesis. The coastal species, *Crangon crangon* had a visual response that was significantly less sensitive than that of the other species in this study, although the visual response of *Palaemon elegans* was not significantly less sensitive than that of the mesopelagic species, *Pasiphaea multidentata* ($p=0.190$, see section *3.4.2.1*).

CHAPTER 4: TEMPORAL RESOLUTION OF THE VISUAL SYSTEMS OF MALACOSTRACANS – THE FREQUENCY RESPONSE

4.1 INTRODUCTION

In order to extract detailed information from the environment the visual system of an animal is required to code both the spatial distribution of objects and the time-course of events within the visual field. The efficiency with which any visual system extracts spatial and temporal information can be a balance between the competing interests of maintaining maximum resolution and maximising sensitivity (Fuortes and Hodgkin, 1964), and, in these respects photoreceptor response dynamics determine the quality of the neural image formed (Laughlin, 1981).

Visual stimuli are very rarely stationary with respect to the eye. Thus, as an image passes across the retina, spatial detail of the image is lost if the response speed of the receptors is not matched to the speed of the movement of the image; a slow temporal resolving power of the photoreceptors in the eye will necessarily lead to loss of visual information as it is sampled in the time domain. Glantz (1991) showed that, for the crayfish (*Procambarus clarkii*), sensitivity to variations in stimulus velocity is dependent on the ratio of ommatidial acceptance angle to the time constant of the photoreceptor. The acceptance angles of the photoreceptors within an eye ultimately determine the spatial resolving power of the eye as a whole (Land, 1981). There is information available on the spatial resolving power of the compound eyes of a number of marine malacostracans, including: *Nephrops norvegicus* (the Norway lobster) and *Munida rugosa* (a squat lobster), (Shelton and Gaten, 1996); *Funchalia villosa* (a mesopelagic penaeid shrimp), (Herring and Roe, 1988); various species of mesopelagic decapods and euphausiids (Hiller-Adams and Case, 1984, 1988); *Palaemon serratus* (the common prawn), (Fincham, 1984) and *Phronima* (a mesopelagic hyperiid amphipod), (Land, 1981).

There is a relative paucity of information on the temporal resolving power of the eyes of marine malacostracans, particularly mesopelagic species (see section *4.1.2*). These animals are often moribund on retrieval from their natural habitat, and those that are active can be difficult to

maintain in good condition for experimentation. Consequently, obtaining electrophysiological recordings of the temporal response dynamics of the photoreceptors of mesopelagic malacostracans can be problematic. Conversely, there is comprehensive knowledge of the temporal resolving power of the eyes of terrestrial arthropod species as they are more readily accessible.

4.1.1 Photoreceptor Response Dynamics in Relation to the Light Environment

For a number of arthropod species the evolutionary resolution of the balance between maximum sensitivity and maintaining temporal resolution has been shown to depend on the light environment inhabited and the animals' physical needs and biological niche (Frank, 1999, 2000; Howard *et al.* 1984; Laughlin and Weckström, 1993; Moeller and Case, 1995; deSouza and Ventura, 1989; Weckström and Laughlin, 1995; Burton *et al.* 2001).

Temporal resolving power is highly dependent on the adaptational state of photoreceptors as it is intrinsically linked to the sensitivity of the visual response. Studies on arthropod photoreceptors by Fuortes and Hodgkin (1964), Pinter (1972), Glantz (1991), Laughlin and Weckström (1993) and Moeller and Case (1995), reveal that temporal resolving power is highly dependent on adaptation state: temporal resolution generally improving with light adaptation, this being accompanied by a less sensitive visual response.

The temporal resolution of photoreceptors is determined by the regulation of the time course of both the phototransduction cascade and the repolarising mechanisms of the photoreceptor membrane (Weckström and Laughlin, 1995). Fundamentally, temporal resolution is determined by the duration and latency of quantum bumps which are generated by the absorption of individual photons by the visual pigment (see section *2.1.3.1*). In dark-adapted eyes the duration and latency of quantum bumps is increased (Laughlin, 1990; Weckström and Laughlin, 1995). This results in an increase in the integration time of the photoreceptor membrane to maximise register of incident photons per time period. The consequence of this is a higher signal-to-noise ratio but a slower visual response. A slower visual response can lead to a loss of detail within the visual image, which is particularly relevant to moving visual stimuli, as spatial detail will be 'smeared' across the retina if the photoreceptor response is

slow. The result is a retinal image with low spatial detail, but this is traded for high gain at the photoreceptor membrane, allowing an eye to function under photon-limited circumstances.

As mesopelagic malacostracan species inhabit a photon-limited environment due to the exponential attenuation of downwelling sunlight with depth in the ocean (see section *1.3*), it may be expected that they will have highly sensitive eyes with slow response dynamics, i.e. a low temporal resolution. The spatial and temporal 'quality' of the retinal image is thus traded for the ability to be able to detect objects in the environment. Conversely, these animals may prioritise the detection of bioluminescence, as it may indicate the presence of prey or equally a predator. In excess of 70% of fish and shrimp species inhabiting the open oceans are bioluminescent (Widder, 1999) and in the deep-sea environment bioluminescent signals are relatively very bright visual stimuli against a dim background. Under these conditions, sacrificing visual sensitivity for a higher temporal resolving power may be a necessarily adaptive strategy allowing temporal analysis of bioluminescent signals. Generally, visual sensitivity is kept high under photon-limited conditions to allow the detection of the dimmest visual stimuli and to maximise contrast sensitivity between the object of interest and the background (see Laughlin, 1981). Both of these factors become less important when one considers a bright flash against a dark background, and consequently it may be advantageous for a mesopelagic animal to trade sensitivity for greater temporal resolution in order that the maximum amount of information may be extracted from a bioluminescent signal, or so, for instance, that a bioluminescent object may be tracked efficiently as it moves across the visual field.

4.1.2 Previous Studies of Temporal Resolution of Mesopelagic Malacostracans

Only a small amount of research has been conducted with respect to the temporal resolving powers of species of mesopelagic and benthic malacostracans (Moeller and Case 1995; Frank 1999, 2000; Johnson *et al.* 2000a). This is largely due to the inaccessibility of these animals and to the difficulties in keeping these animals alive during transport to shore-based laboratories. Consequently, electrophysiological recordings from these animals are generally obtained on board ship. Shipboard laboratories are inherently difficult environments in which to work and therefore only extracellular recording techniques are possible due to the difficulties of maintaining stable preparations on board a moving vessel (see section *2.2.3.3* for details) e.g.

Frank, (1999, 2000) and Johnson *et al.* (2000). Electroretinograms (ERGs) provide information on the combined temporal response dynamics of all the photoreceptors in the eye. The studies listed above report some correlation between temporal resolving power and the light environment inhabited. Frank (1999, 2000) showed that temporal resolving power declines with daytime depth distribution (and hence ambient light levels) for seven species of mesopelagic decapod malacostracans. Similarly, Moeller and Case (1995) report that for juvenile *Gnathophausia ingens* (a mesopelagic mysid) and adult *Oplophorus spinosus* (a mesopelagic decapod), faster response dynamics are related to a shallower daytime depth distribution in comparison with the slower response dynamics of the deeper living adult *G. ingens*. Johnson *et al.* (2000a) measured the temporal resolving power of the eyes of four species of decapod, from both deep-sea, benthic, and coastal habitats, and it is suggested that there is a correlation between higher temporal resolution and shallower habitat for the species studied.

4.1.3 Measuring the Temporal Response of Invertebrate Photoreceptors – Measuring the Frequency Response

The intensity-response function (or VlogI function) of invertebrate photoreceptors is a sigmoidal relationship in which photoreceptor response amplitude is plotted as a function of the log of stimulus intensity. The highest light intensities saturate the photoreceptor response and the lowest produce threshold responses from the photoreceptor (see section *2.1.2* and *3.4.1* for further detail) indistinguishable from inherent noise. Between saturation and threshold there exists an approximately linear relationship between response and log stimulus intensity. When stimulating within a relatively small fraction of this range the photoreceptors operate as linear systems. The consequence of this is that a sinusoidally modulated stimulus of a given frequency at the eye or photoreceptor (if recording intracellularly) leads to a sinusoidally modulated response from the eye/photoreceptor at the same frequency as the stimulus, but with a different amplitude and phase (Knight *et al.* 1970). Obtaining the responses of the eye to sinusoidal stimuli at a range of frequencies facilitates the determination of the frequency response of the photoreceptors of the eye which, along with the impulse response function and flicker fusion frequency, is a commonly used measure of the temporal response of photoreceptors (see Laughlin, 1981 for a review).

It is well established that the amplitude of the sinusoidal response is highly dependent on the frequency of sinusoidal stimulation, (e.g. Knight *et al.* 1970; Pinter, 1972; Howard, 1981; Glantz, 1991). The frequency response range of a visual system includes the frequency to which an eye is maximally sensitive and also the maximum and minimum frequencies of stimulus that the eye can resolve. One can also extract information about the lag in the visual response by comparing the phase difference between the sinusoidal response and the stimulating sinusoid.

Eyes are not perfect optical or light detection systems, and inevitably the information contained in visual stimuli is degraded to a certain extent as it is processed by the eye. The extent of this degradation is dependent on certain properties of components of the visual system. The frequency response of a physical system describes the temporal properties of that system; it provides information on the gain, bandwidth and time lag of an input-output system. Conventionally the temporal properties of a system are represented in a Bode plot, in which the magnitude and phase angle of the transfer function (magnitude and phase of the visual response relative to the input signal) is plotted as a function of frequency. This method of determining the transfer function of a system within the frequency domain is important in the analysis of analogue filters and feedback control systems, and thus, it is a commonly used tool in engineering. Obtaining the frequency response of a time-invariant linear system allows one to infer the response of the system to any given input. However, as photoreceptors are essentially non-linear in their response, in determining their frequency response one can only determine the temporal resolving power of the photoreceptors to a defined irradiance level/contrast. It is, nevertheless, a useful tool in visual science as, information on the gain, bandwidth and time lag of the photoreceptor response is highly relevant in terms of visual processing; if one can determine these properties of an animals visual response, one can begin to understand the quality of neural images being perceived. In a comparative study this can be used to relate the visual ecology of an animal with its visual capability.

The frequency response has been the adopted method of investigating temporal resolution of invertebrate photoreceptors in a large number of studies, these include: Knight *et al.* (1970), *Limulus*; Pinter (1972), *Acheta domsesticus* (house cricket) and *Schistocerca gregaria* (desert locust); Glantz (1991), *Procambarus clarkii* (crayfish); Laughlin and Weckström (1993), various dipteran species; Johnson *et al.* (2000), four species of marine decapod.

4.1.4 Aims of This Study

This study examines the use of the frequency response method in determining the temporal resolutions of the dark-adapted eyes of mesopelagic malacostracans. Extracellular electrophysiology is the adopted technique for recording electroretinograms in response to sinusoidal stimuli of differing frequencies. In this study the frequency response range of the eye is determined from ERG responses to sinusoidally modulated light for four species of mesopelagic malacostracan. The temporal resolutions of the dark-adapted eyes of malacostracans that inhabit differing daytime depth distributions in the mesopelagic zone are investigated in order to determine whether the light environment inhabited determines the temporal resolution of the photoreceptors in the eye. If this were the case, one would expect to find that the photoreceptors of shallower living mesopelagic species, which inhabit a less photon-limited environment than deeper living species, to have a higher temporal resolving power than the photoreceptors of deeper living species. However, obtaining frequency response data from these animals using the frequency response method proved impractical for reasons that will be explained. This study therefore also includes details of: a) technical problems encountered in delivering a sinusoidal stimulus to the eye using an LED; b) the inherent difficulties of obtaining stable sinusoidal responses from these animals on board a moving vessel; and c) the problems encountered with the frequency response method when dealing with the highly sensitive dark-adapted visual systems of mesopelagic malacostracans.

4.2 OPTICAL STIMULATION

The light stimuli used in this experiment were generated using a blue LED (Marl Optosource, ultra high bright LED: λ_{max} 464nm (at maximum current input), FWHM 28nm; see Fig. 3.1 section *3.2.1.3*, and section *2.2.2.2*). Section *2.2.2.2* gives details of the output properties of the LED.

4.2.1 Pulse Stimuli

Prior to investigating the frequency response of the eyes of the animals in this study, pulse stimuli (of 1.4ms duration) were used to determine the intensity-response functions (VlogI relationships) of the eyes in order to identify the linear response region for each eye. These pulse stimuli were generated in the same manner described in sections *2.2.2.2* and *3.2.1.3*.

4.2.2 Sinusoidal Stimuli

To follow the frequency response methodology using an LED as the optical source, it is necessary to generate a sinusoidally modulating light output from the LED. Preliminary experiments revealed that the intensity of light output from the ultra high bright blue LED did not vary linearly with voltage or current input. It was also found that the wavelength of maximum transmission (λ_{max}) of the LED output varied with current input. There was found to be a 4nm shift in λ_{max} between maximum current input and minimum current input. Refer to section *2.2.2.2* and Fig. 2.7 for full details of the non-linear properties of the LED.

4.2.3 Non-linearity of the LED

The non-linear properties of the LED as described in section *2.2.2.2*, eliminated the possibility of using sinusoidally modulating voltage or current input to the LED to produce an equivalent light output. The non-linear optical power response of the LED would cause the light output sinusoid of the LED to be distorted relative to the current input, and, as the λ_{max} of spectral output shifts 4nm between minimum and maximum current inputs, emission wavelength would modulate during the sinusoidal stimulus.

4.2.3.1 Standardising optical wavelength

To prevent modulation of emission wavelength a bandpass interference filter (CWL 488nm, FWHM *ca.* 10nm, peak transmission 49%, Coherent-Ealing) was placed in the light path between the LED and the eye. Fig. 4.1 illustrates the effect of the bandpass interference filter on the shift in λ_{max} of the LED output when driven with current inputs of 1 and 30mA.

Fig. 4.1 shows that insertion of the interference filter into the light path of the LED forces the optical wavelength of the LED output to a λ_{max} of 488nm. At this wavelength, the spectral output of the LED does not vary with current input and therefore the interference filter prevents a shift in λ_{max} of the LED output with varying current input between 0 and 30mA. A consequence of inserting the interference filter into the light path is a large reduction in total intensity output of the LED. The peak transmission of the filter is 49% and this reduces the total output of the LED, when driven with a current of 1mA, to 3.1% of the original. When the LED is driven with a current input of 30mA the integrated output is attenuated to 2.9% of the unfiltered output. The attenuated light output resulting from the combination of blue LED and interference filter was still sufficient, however, to produce responses within the centre of the VlogI relationships of the eyes of mesopelagic malacostracans. Another obvious consequence of using the interference filter is a shift in the stimulus λ_{max} at the eye to 488nm from 464nm, the inherent wavelength of maximum emission of the LED.

4.2.3.2 Preventing non-linear distortion of the LED output

Sinusoidal signals can be generated using a function generator, but direct coupling of the function generator output to the LED was not possible, as the non-linear input-output properties of the LED would lead to a distorted (non-sinusoidal) output. Consequently, the LED was operated using a 1kHz square wave signal (pulse train), which alternated over the widest range of current input possible, and the duty cycle was manipulated to vary the quantity of light output (see below and Fig. 4.2b). Use of the full current range of the LED was necessary in order to maximise light output. To attain maximum output from the LED it would be alternated between 0-30mA, i.e. 100% modulation (15mA represents the mean current input, and is equivalent to the mean light output, $\bar{I}_I$). However, a 100% modulation of current input

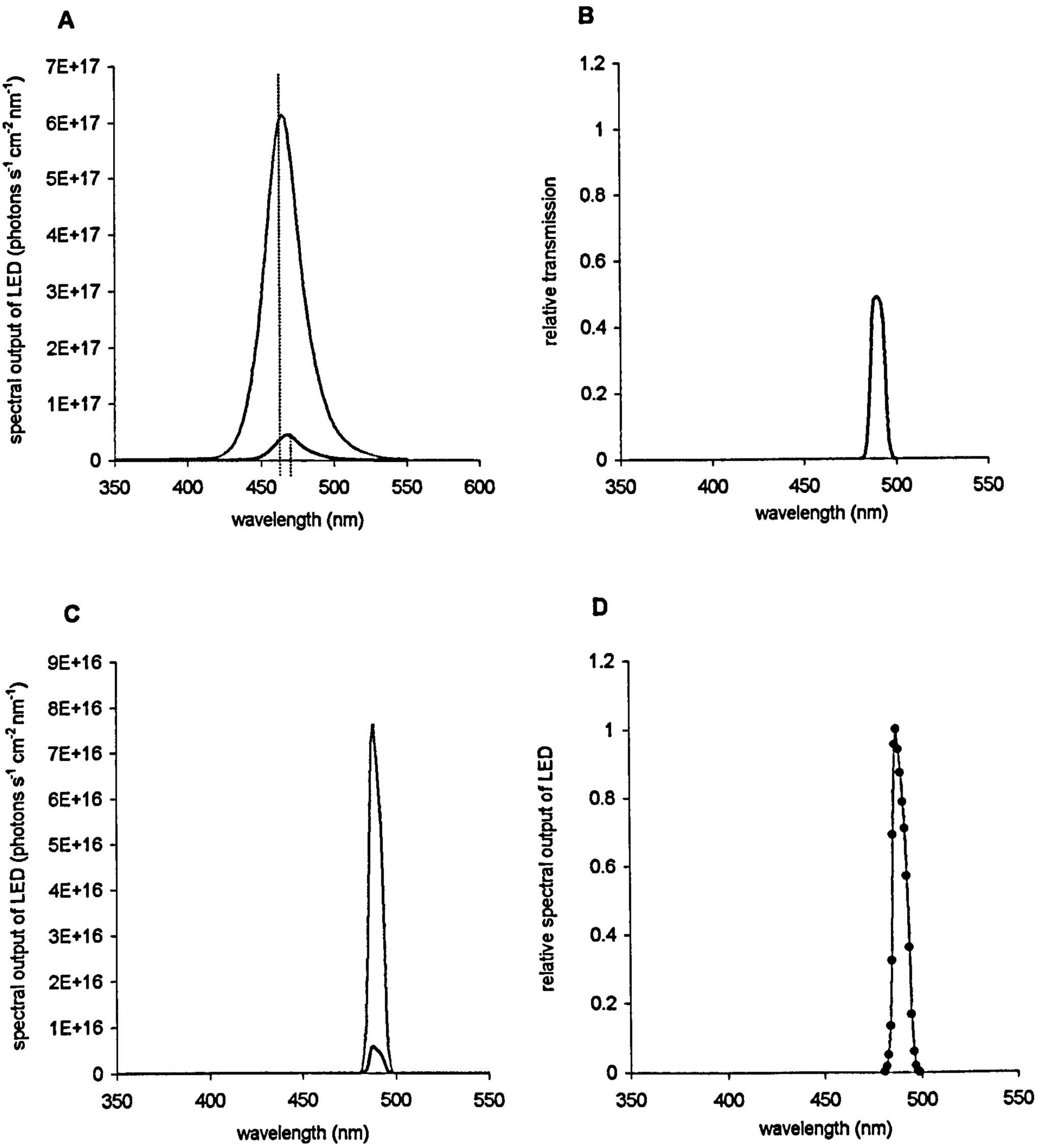

Figure 4.1. Plots to illustrate the use of a bandpass interference filter (CWL 488nm) to standardise the optical wavelength of the LED output. A) shows the spectral outputs of the blue LED when driven with input currents of 1mA and 30mA. The dashed lines show the shift in λ_{max} of 4nm from 468nm (at 1mA input) to 464nm (at 30mA input). B) shows the transmission of the interference filter (CWL = 488nm, FWHM = *ca.* 10nm, peak transmission = 49%). C) shows the effect on the spectral output of the LED at both 1mA and 30mA when it is passed through the interference filter. The total light output of the LED when driven at 1mA current input and passed through the interference filter, is 3.1% of the unattenuated output (shown in A). The total output of the LED when driven at 30mA current input and passed through the interference filter is 2.9% of the unattenuated output (shown in A). The effect of the interference filter is to align the optical wavelengths of the LED spectral outputs and this is clearly shown in D), the dark blue data points are the relative spectral output of the LED when driven with a 1mA current input overlayed on the relative spectral output of the LED when driven with a 30mA current input.

would necessarily lead to a termination of the light output at 0mA. Therefore, the 1kHz pulse train was modulated at ±90% of the mean, i.e. the current input to the LED was alternated between 1.5 and 28.5mA (see Fig. 4.2a). This ensured that there was no distortion in the output signal from the LED that could be caused by a termination of the light output.

The duty cycle of a pulse train is the ratio of pulse duration to pulse period, and is independent of the frequency of the pulse train. Thus, if, for example, a pulse train modulating at 1kHz had a duty cycle of 0.99 (99%), the pulse duration would equal 0.99ms, and the pulse period would equal 0.01ms. When this is related to LED output the result is an overall increase in light intensity as a greater proportion of time is spent at the highest current input. Conversely, a duty cycle of 0.01 (1%) would cause an increase in pulse period relative to pulse duration and hence overall light output would be lowered. For this study, sinusoidal signals from a function generator (TG215, 2MHz Function Generator, Thurlby Thandar Instruments) were input to an electronic circuit that varied the duty cycle of the 1kHz pulse train driving the LED, between 0.01 and 0.99. The result was a sinusoidal modulation of the LED output without a sinusoidal modulation of current input, thus avoiding any problems of distorted optical output due to the non-linear response of the LED. Fig. 4.2 illustrates both the 90% modulation depth of the 1kHz pulse train and how varying duty cycle can effect a sinusoidal modulation of light output.

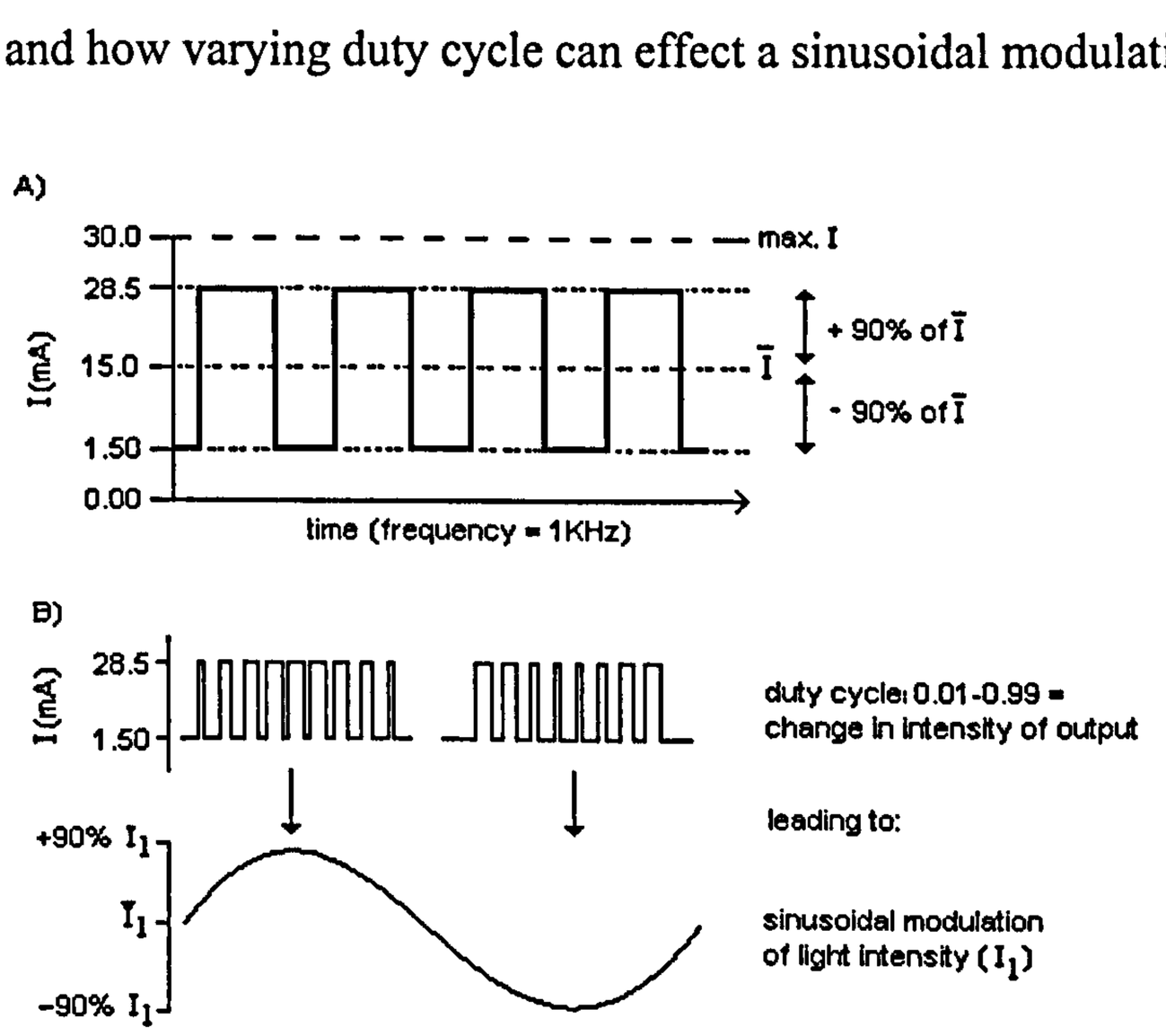

Figure 4.2. A representation of the mechanism used to operate the LED. A) shows the ±90% modulation of the 1kHz pulse train about the mean current, $\bar{I}$, to maximise light output of the LED (whilst avoiding pushing the LED between minimum and maximum currents [0-30mA]). B) is a schematic representation of the effect of varying the duty cycle of the pulse train between 0.01 and 0.99 on the intensity output (I_1) of the LED. This leads to a sinusoidal modulation of the intensity of light output about the mean ($\bar{I}_1$).

4.2.4 Testing the Optical Response of the LED

The function generator was used to supply a sinusoidal signal modulating at 30Hz to the electronic circuit powering the LED. The light output of the LED was subsequently measured using a high frequency resolution photodiode (see Fig. 4.3). The response of the photodiode was captured on a digital oscilloscope (HAMEG, model no. HM407), and downloaded to a PC using SP107 software, via a RS232 serial interface. The photodiode measured the 1KHz square wave modulation of the LED output and this is shown in Fig. 4.3a. Subsequent processing of the photodiode signal with a digital low pass (50Hz cut-off) linear phase filter using Matlab software (version 6.0.0.88, release 12), revealed that the LED light output modulates sinusoidally at the same frequency as that supplied to the electronics. (Fig. 4.3b)

There is no evidence to suggest that any marine malacostracan species has a visual system capable of resolving frequencies of 1kHz. Currently, the fastest photoreceptors known are found in blowflies and flesh flies, these photoreceptors can resolve flicker at over 250Hz (Laughlin and Weckström, 1993), which is substantially lower than 1kHz (humans have a flicker fusion frequency of *ca.* 60Hz). Additionally, the few previous studies that have investigated the temporal resolving powers of marine malacostracans, have indicated that these animals have relatively slow eyes compared with terrestrial arthropods (Frank, 1999, 2000; Johnson *et al.* 2000a; Moeller and Case, 1995). Thus, the 1kHz modulation of light output from the LED, will not be visually detectable and thus will not contaminate the visual response to the much lower sinusoidal frequencies used to stimulate the eye.

4.2.5 Control of Stimulus Irradiance

Previous studies of the frequency response of invertebrate photoreceptors have shown that the peak-to-peak amplitude of the sinusoidal response from the photoreceptors is dependent on the modulation depth of the sinusoidal stimulus. Response amplitude is linearly related to stimulus modulation depth (contrast within the stimulus) for stimuli of relatively low contrast (Pinter, 1972; Glantz, 1991). In the present study, the modulation depth of the stimulating sinusoid was constant (i.e. constant modulation depth of current input to the LED which was ±90% of the mean, see section *4.2.3.2* and Fig. 4.2) throughout all experiments in order to isolate the effect of the frequency of the stimulus on response amplitude (see section *4.3.4.2* for detail of the

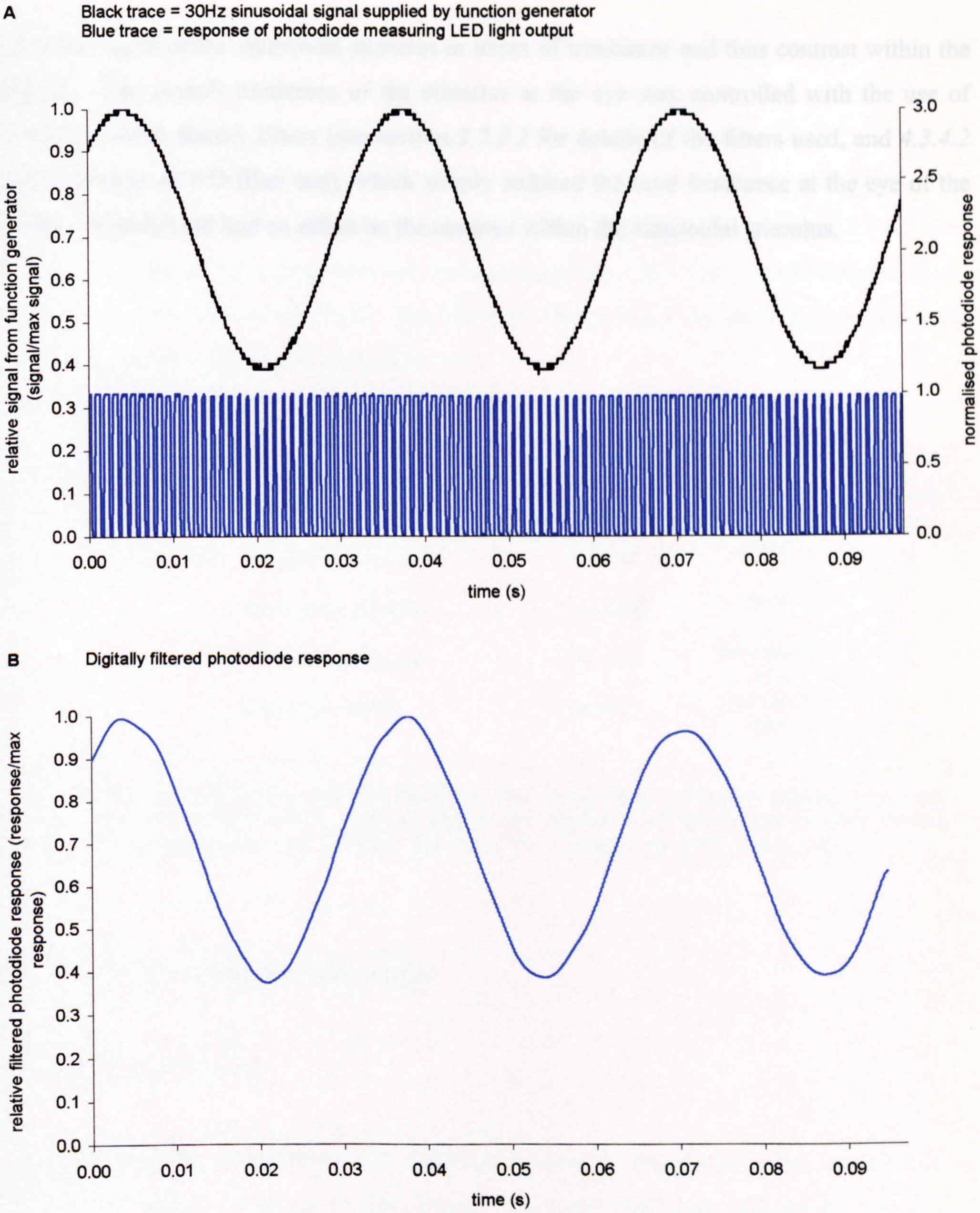

Figure 4.3. The light output of the LED when driven with a 1kHz pulse train with a variable duty cycle. A) the black trace shows the sinusoidal signal (modulating at a frequency of 30Hz) input to the electronic circuit responsible for varying the frequency dependant duty cycle of the 1kHz pulse train. The blue trace shows the response of the high frequency resolution photodiode used to measure the light output of the LED; the photodiode detects the 1kHz modulation and a variation in duty cycle can be seen which corresponds to the peaks and troughs of the 30Hz sinusoidal signal. B) shows the photodiode response once it has been digitally filtered using a low-pass linear phase filter (50Hz cut-off). It is evident that the sinusoidal LED output is modulating at the same frequency as the original signal from the function generator. The slight distortion seen in both the 1kHz pulse train in fig. A and the filtered 1kHz signal in fig. B is due to digitization limitations inherent in the oscilloscope used to record high frequency modulated output.

modulation depth of the sinusoidal stimulus in terms of irradiance and thus contrast within the stimulus). The overall irradiance of the stimulus at the eye was controlled with the use of absorptive neutral density filters (see section *2.2.2.2* for details of the filters used, and *4.3.4.2* for methodology of ND filter use), which simply reduced the total irradiance at the eye of the sinusoidal stimulus but had no effect on the contrast within the sinusoidal stimulus.

4.3 MATERIALS AND METHODS

4.3.1 Species Studied

Details of animal collection and maintenance are given in Chapter 2 section *2.2.1.1.* Four species of mesopelagic decapod from one location (region of the Cape Verde Islands, North-East Atlantic) were used in this study. See Table 4a for details of the animals from which the data presented in this study were obtained.

Order	Family	Species	*n*	Daytime Depth (m)	Bioluminescence	Water Type[3]
Decapoda	Oplophoridae	*Acanthephyra purpurea*	1	700-950[1]	spew	II
		Notostomus gibbosus	2	800-1000[2]	spew	II
		Oplophorus spinosus	1	300-500[1]	photophores spew	II
		Systellaspis debilis	3	650-950[1]	photophores spew	II

Table 4a. Details of the adult mesopelagic malacostracans used in this study, information includes: taxonomy; number of individuals of each species used (*n*); approximate daytime depth distribution for each species; bioluminescent capability; water type inhabited. [1]Foxton, 1970; [2]Hopkins *et al.* 1989; [3]Jerlov, 1976.

4.3.2 Animal Handling and Preparation

See Chapter 3 section *3.2.1.1*

All animal handling, preparation and electrophysiological recordings were carried out in shipboard laboratories out at sea on RRS Discovery, cruise D243 (see sections *2.2.1* and *2.2.2* for detail).

4.3.3 Electrical Recording

Electrophysiological recording of the electroretinogram is described in section *2.2.2.1*, and the same procedure was followed in all cases.

4.3.4 Optical Apparatus

Details of the LED and the bandpass interference filter used, (CWL 488nm, FWHM *ca.* 10nm), are given in section *4.2*.

The optical apparatus used in this study is the same as that used in the study of Chapter 3 (see section *3.2.1.3*); see section *4.3.4.1* and *4.3.4.2* for details of delivery to the eye of pulse and sinusoidal stimuli.

4.3.4.1 Pulse stimuli

When pulse stimuli were used, no interference filter was placed in the light path of the LED, therefore the λ_{max} of the stimulus was 464nm (FWHM, 28nm). The pulse stimuli were used to determine the VlogI relationship of the eye and so maximum possible light output was required to saturate the response of the eye and use of the interference filter attenuated too much light for this purpose. Irradiance of the pulse stimuli at the eye was controlled with the use of calibrated absorptive neutral density filters (see section *2.2.2.2*). The neutral density filters were inserted into the light path between the LED and the silica light guide, this arrangement allowed the irradiance at the eye to be changed without disturbing the preparation. Irradiance at the eye was calibrated with a research radiometer (International Light, IL1700). The unattenuated light source gave an irradiance at the eye of $2x10^{15}$ photons s^{-1} cm^{-2}.

4.3.4.2 Sinusoidal stimuli

For sinusoidal stimuli, the bandpass interference filter was placed in the light path between the LED and the silicon light guide such that the light was restricted in bandwidth before being transmitted to the eye. This arrangement allowed the interference filter to be inserted after the pulse stimuli experiment without disturbing the preparation. Total irradiance at the eye was

again controlled with the use of calibrated absorptive neutral density filters. The neutral density filters were inserted into the light path between the bandpass interference filter and the silicon light guide. Again, irradiance at the eye was calibrated using a research radiometer and the unattenuated light source (driven at maximum light output and with the interference filter in the light path) gave an irradiance at the eye of 9.31×10^{13} photons s^{-1} cm^{-2}.

Using the VlogI curve constructed according to section *4.3.4.1*, and knowing the irradiance contrast of the sinusoidal stimulus (see below) it was possible to calculate the maximum and minimum irradiance outputs required to ensure that the sinusoidal stimulus (both peak and trough irradiances) fell within a small (approximately linear) range of the central region (close to $50\%V_{max}$) of the VlogI relationship of the eye. Having established the maximum irradiance that would correspond to the peak irradiance of the sinusoid and fall close to the $50\%V_{max}$ point (ensuring that the minimum irradiance of the sinusoidal stimulus also falls close to the $50\%V_{max}$ point), one could determine from the VlogI curve for the eye the amplitude of response one would expect from this defined irradiance. The LED was subsequently driven with pulse stimuli of 1.4ms duration (see section *4.3.4.1*) but the light was delivered to the eye via the format described above (i.e. through the interference filter and fibre optic). ND filters were then used to manipulate the irradiance output until a response was generated from the eye of the required amplitude. As the pulse stimuli are driven at maximum current input to the LED, and the peak of the sinusoidal stimulus is driven at 90% of the maximum current input, one can safely assume that the response generated using the pulse stimuli will be of a similar amplitude as that that would be generated by the maximum irradiance of the sinusoidal stimulus. Consequently, one can ensure that the irradiance of the sinusoidal stimulus is controlled such that the maximum and minimum irradiances (the irradiance at the peak and trough of the sinusoidal stimulus respectively) fall close to the $50\%V_{max}$ point of the VlogI relationship for each individual.

The individuals used in this study all had eyes with VlogI relationships with $50\%V_{max}$ responses generated in response to similar log units of irradiance (see results, section *4.5.1*). Therefore, irradiance at the eye was the same for all individuals: the intensity modulation of the stimulus gave a maximum output range of 9.38×10^{8} to 4.65×10^{9} photons s^{-1} cm^{-2}, with a mean irradiance of 2.89×10^{8} photons $s^{-1}cm^{-2}$. Fig. 4.4 shows the modulation of light output and the

subsequent maximum and minimum irradiances at the eye. Section *4.5.1*, Fig. 4.8 indicates how this irradiance modulation relates to the VlogI relationships of each individual studied.

The contrast within the stimulus can be calculated using the formula below (taken from Laughlin, 1981):

$$C = \frac{I_{max} - I_{min}}{I_{max} + I_{min}}$$

where: C = contrast and I_{max} and I_{min} are maximum and minimum irradiances respectively.

The contrast within the sinusoidal stimulus used in this study was therefore 0.66 (66%) and was constant throughout the experiment.

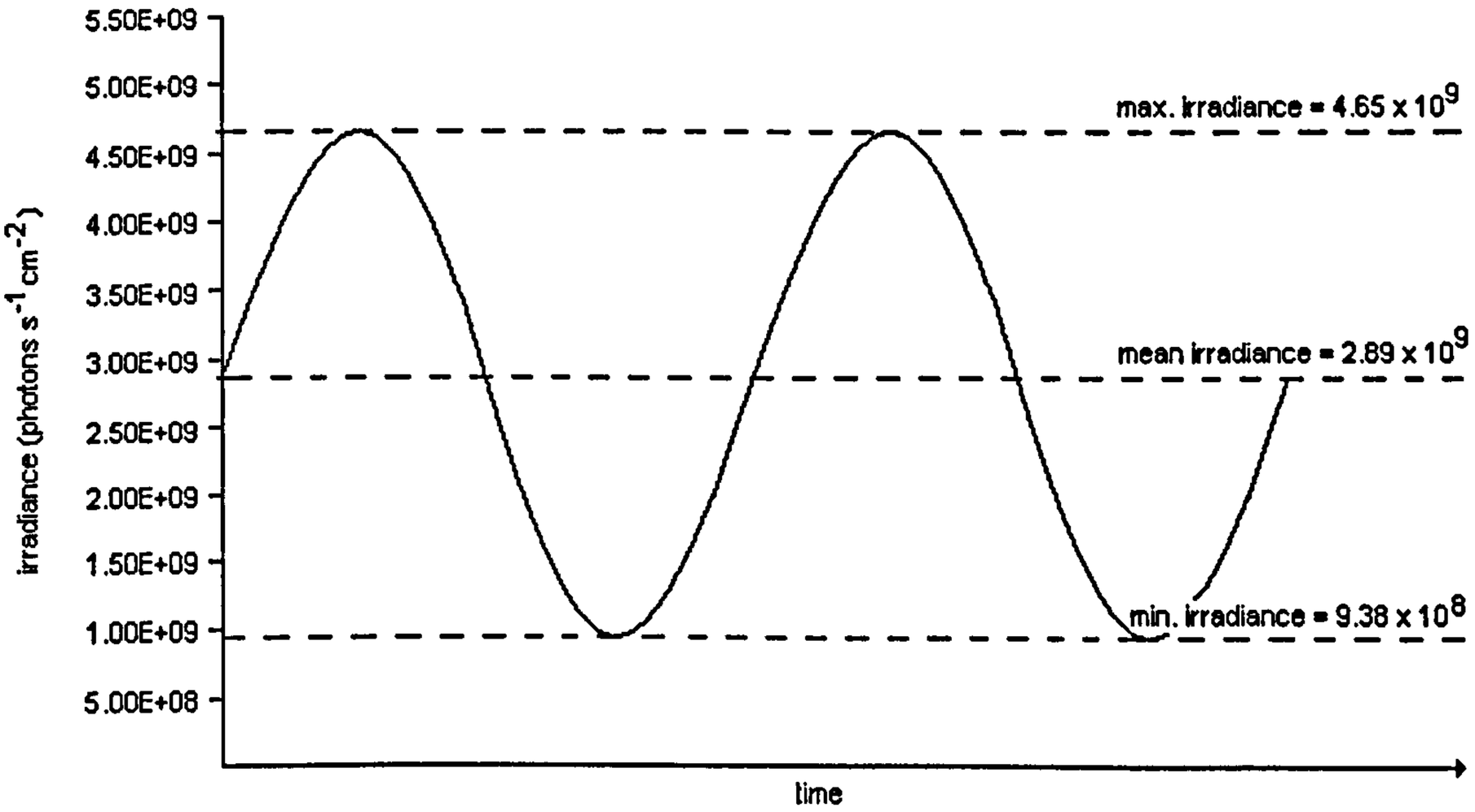

Figure 4.4. The maximum and minimum irradiances at the eye of the sinusoidal stimuli. Modulation contrast of the sinusoidal stimulus was 66%.

4.3.4.3 Wavelength of stimulation

The λ_{max} of the pulse stimulus was 464nm, compared with a λ_{max} of 488nm for the sinusoidal stimulus. This 25nm shift in stimulus wavelength was unavoidable for the reasons described above. However, both values of 464nm and 488nm fall within the range of peak

bioluminescent emissions of mesopelagic shrimps (440-490nm, Herring, 1983; Widder *et al.* 1983), and at a depth of 500m in the clearest ocean water both wavelengths are present (see Fig. 4.5). Justification for this shift in λ_{max} between pulse and sinusoidal stimuli is given in section *4.6.3.1*.

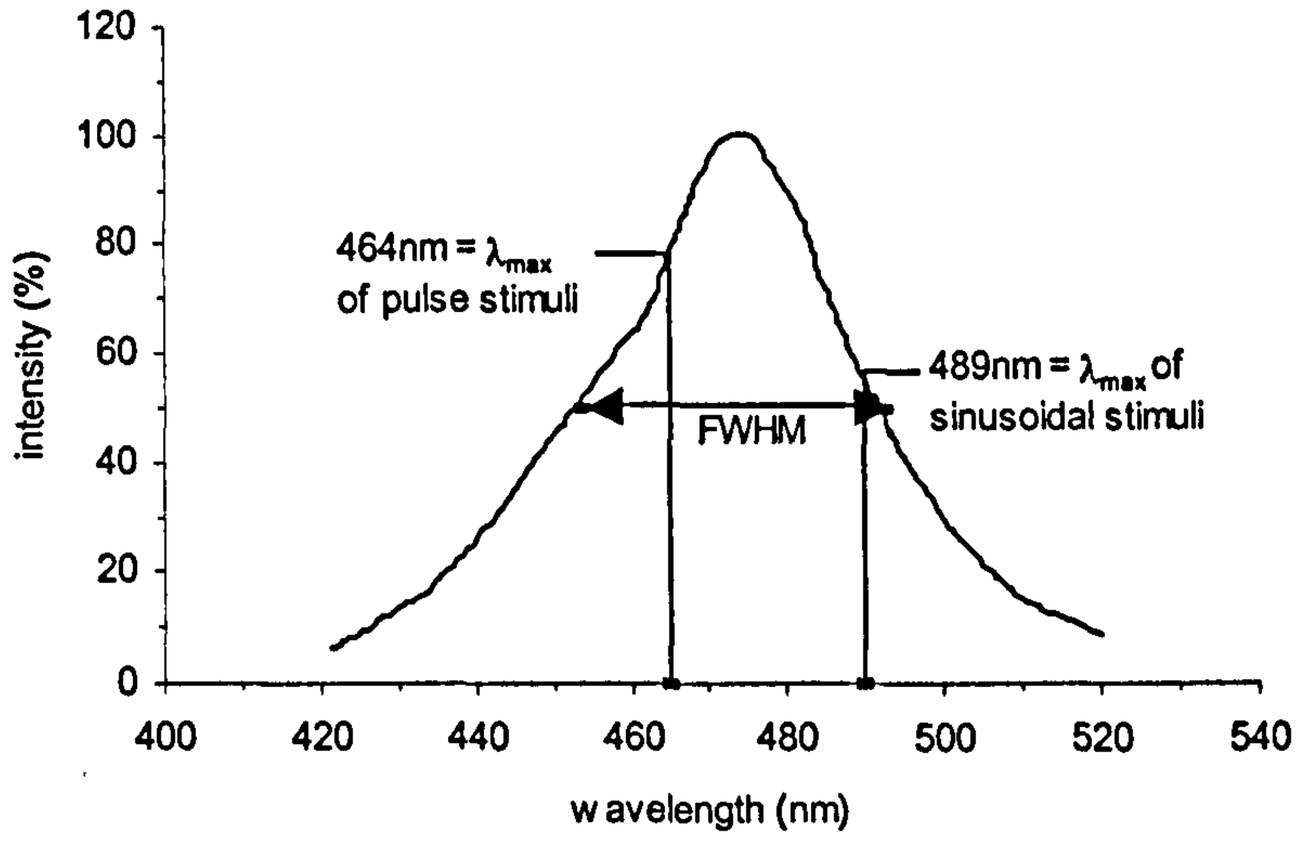

Figure 4.5. The spectral distribution of intensity of downwelling light at 500m depth in clear ocean water (re-drawn from Denton, 1990). Also shown are the spectral positions of the λ_{max} of the pulse and sinusoidal stimuli used in this study. Both fall above the FWHM level of the spectral distribution of downwelling light at 500m.

4.3.5 Experimental Procedure

4.3.5.1 Determining the VlogI relationship

Initially, pulse stimuli (of 1.4ms duration) were used to determine the dark-adapted VlogI relationship of the photoreceptors of one eye of each individual animal used in this study, (see section *4.4.1* for details of data analysis). The protocol followed for this purpose is exactly as that described in Chapter 3, section *3.2.1.4*.

4.3.5.2 Determining the frequency response

All recordings were taken from dark-adapted eyes. For each animal, a 1.4ms test flash, with an irradiance calibrated to produce a response occurring near threshold of the intensity-response

function, was used initially to ensure that the sensitivity of the visual response was comparable to that during the pulse stimuli experiment. To fulfil this criterion, the peak amplitude of the response could not have changed by more than ±5%. Subsequently, this test flash was used periodically throughout the experiment and at the end to ensure that the magnitude of the visual response (i.e. the sensitivity of the eye) was not changing. If the peak amplitude of response to this test flash had altered by more than ±5% during the experiment or by the end and would not recover to pre-stimulus sensitivity, the data were rejected.

Sinusoidal stimuli (irradiance of stimulus described in section *4.3.4.2*) of a range of frequencies between 0.5 and 20Hz were used to stimulate the eye and differing frequencies of stimulus were presented to the eye in a random order.

In most cases, ten cycles of each frequency were used to stimulate the eye to allow averaging of the response. This necessarily meant that the total duration of each stimulus varied as the time taken to stimulate the eye with 10 cycles of sinusoid is dependent on the frequency of the sinusoid. Table 4b indicates the duration of each stimulus.

Frequency of sinusoidal stimulus (Hz)	No. of cycles	Duration of stimulus (s)
20	10	0.5
15	10	0.7
10	10	1.0
7	10	1.4
5	10	2.0
2	10	5.0
1	10	10.0
0.5	10	20.0

Table 4b. Information on the number of cycles delivered at each frequency of stimulation and the consequent duration of each stimulus frequency.

The duration of the sinusoidal stimulus determined the duration of the period between stimuli. A time period between stimuli is necessary to allow the eye to regain its pre-stimulus sensitivity to light (see also section *3.2.1.4*). Between each sinusoidal stimulus delivered to the eye, the test flash described above was used to check the sensitivity of response. Only once the

response had recovered in amplitude to differ by no more than ±5% of the pre-stimulus amplitude, was the next sinusoidal stimulus delivered to the eye. For stimulation frequencies of 20, 15 and 10Hz, a ten minute period between stimuli was required for the eye to regain sensitivity. For frequencies of 7 and 5Hz, a twenty minute period between stimuli was required, this increased to 30 minutes for stimulation at 2Hz and increased further to 60 minutes for frequencies of 1 and 0.5Hz. Consequently, to collect data on responses to all the frequencies and perform repeated measures took considerable time. Mesopelagic species are not very robust animals once they are removed from their natural habitat and in some cases the preparation deteriorated before a full data set could be obtained.

The frequency of sinusoidal stimulus was increased until the eye no longer produced a resolvable sinusoidal response. As measured noise in the preparations was typically of the order of 20μV peak-to-peak, responses with a peak-to-peak (peak to trough of sinusoid) amplitude of less than approximately 40μV were not resolvable against the background noise. In most cases, no resolvable response was seen at stimulus frequencies above 10Hz. However, as the response data would be digitally filtered during analysis, and thus background noise removed, the eyes were stimulated with frequencies up to 20Hz, in case low amplitude responses were occurring at the highest stimulus frequencies, and being masked by the noise in the signal.

During these experiments, a number of extrinsic factors introduced distortion into the ERG signal. Ship pitch and roll on the ocean could have a significant effect on the shape of the ERG response to sinusoidal stimuli. Fig. 4.6 shows an example of the effect of ship movement on a sinusoidal ERG response.

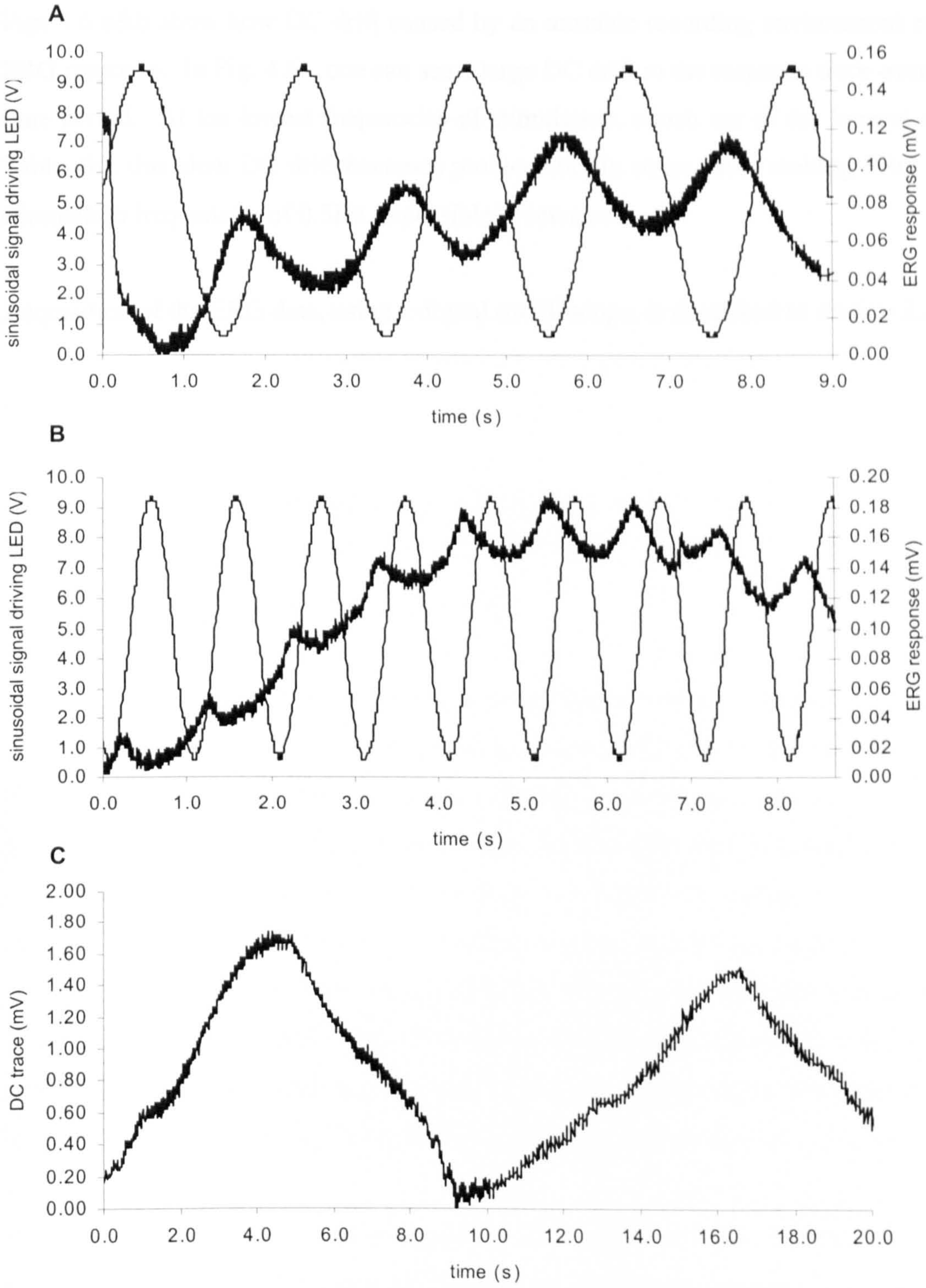

Figure 4.6. A and B show unfiltered ERG responses (the thick black traces) to sinusoidal stimuli of 0.5 and 1Hz respectively. In A) there is a small amount of DC drift in the ERG response, but the cycles of sinusoidal response are well defined. In B) there is a large DC drift, which distorts the sinusoidal ERG response. C) is an example of the DC drift caused by ship movement, in this case the electrode is in the eye but the animal is in darkness. Data from *Systellaspis debilis*.

Figs 4.6 a&b show how DC drift caused by an unstable recording environment can effect the ERG response. In Fig. 4.6c, one can see a large DC drift in the response trace over a 20 second time period. At the lowest frequencies of stimulation, which are of the longest duration (see Table 4b), this slow DC drift becomes problematic, in some cases making ERG responses to stimulation frequencies of 0.5Hz impossible to interpret.

Acquisition of the ERG data, using a digital oscilloscope, is described in section *2.2.2.1*.

4.4 DATA ANALYSIS

4.4.1 Determining the VlogI Relationship of the Eye

The VlogI relationship for the eye of each individual studied was determined (in terms of analysis of the data) in the same manner as that described in section *3.3.1*. However, as the purpose of this was to identify the $50\%V_{max}$ region of the intensity-response function, no statistical analysis was conducted to identify interspecies variation in the value of k, as is described in section *3.3.1*.

4.4.2 Determining the Frequency Response of the Eye

4.4.2.1 Measuring the amplitude of response

In most cases the eye of each individual was stimulated with ten cycles of a sinusoidal stimulus (the stimulus sinusoid was of constant amplitude/modulation depth, but varied in frequency between 0.5 and 20Hz), thus, ten cycles of ERG response were obtained for each stimulus frequency. Each stimulus frequency was used to stimulate the eye twice. However, the long duration of the 0.5Hz stimulus (20 seconds, see Table 4b, section *4.3.5.2*), increased the likelihood of the DC drift distorting the response (see section *4.3.5.2* and Fig. 4.6), and also necessitated a long recovery period between stimuli (60 minutes, see section *4.3.5.2*). Therefore, often only 5 cycles of 0.5Hz were used to stimulate the eye in order to: a) reduce the risk of DC distortion in the response and b) to reduce experimental time and thus reduce the risk of the preparation deteriorating before completing the experiment.

Background noise in the signal was typically of the order of 20μV, so to ensure that resolvable sinusoidal ERG responses were not hidden in the noise, the response data were digitally filtered. Digital filtering was performed using Matlab software (version 6.0.0.88, version 12), with a digital low pass (50Hz cut-off) linear phase filter.

For each individual studied, the peak-to-peak amplitude, ΔV (the difference between maximum and minimum amplitude within a cycle), of each of the ten cycles of the response to a given frequency was measured. These ten values were then averaged to give a value of mean peak-

to-peak amplitude (ΔV) for each frequency of stimulus. Each stimulus frequency was repeated twice, and therefore the two mean amplitude values from each stimulus run were averaged to give a single mean peak-to-peak amplitude for each frequency of stimulus. For each individual, there was a maximum response amplitude (ΔV_{max}) obtained in response to a particular frequency, within the range of 0.5-20Hz. Subsequently, the other values of response amplitude for the individual were scaled relative to the maximum response amplitude, $\Delta V/\Delta V_{max}$, (after Howard, 1981). This was necessary to facilitate a comparison of response amplitude between individuals, as the amplitude of response is dependent on the position of the electrode in the eye (as mentioned in section *3.3.1* and discussed in section *3.5.2*). In cases where data were obtained from more than one individual of a species, the relative response magnitudes for each individual of the species were averaged to obtain a mean (with associated standard error) for the species.

The relative response magnitudes for each species were then plotted as a function of stimulus frequency on a logarithmic scale to display the magnitude of the response of the eye to varying frequencies (after Knight *et al.* 1970).

4.4.2.2 Measuring the phase lag in the response

Information about the phase lag in the response can be measured by comparing the phase of the sinusoidal response with the phase of the sinusoidal stimulus. Phase information is interesting as it describes the lag in the photoreceptor response and so gives an indication of the speed of the photoreceptor response in a given adaptation state. The phase information can be displayed with amplitude information ($\Delta V/\Delta V_{max}$) as a function of frequency in a Bode plot (Pinter, 1972, and see section *4.1.3*).

For each individual studied, the phase difference between the sinusoidal stimulus and response was determined by measuring the time period (Δt) between the first peak of the sinusoidal stimulus and the first trough (minimum amplitude) of the sinusoidal ERG response (see Fig. 4.7; because responses were recorded extracellularly, the ERG response is inverted, and therefore a hyperpolarising response in the ERG record represents a depolarisation of the photoreceptor membrane). Experiments were conducted on dark-adapted eyes, and consequently the lack of a background light source at the onset of the first peak of the

sinusoidal stimulus resulted in an initial large, transient depolarising response from the eye (see Fig. 4.7). The peak of this 'on' response was taken as the first depolarising peak of the sinusoidal response. The time periods (Δt) between the subsequent peaks of the sinusoidal stimulus and troughs of the ERG responses were then measured for all the cycles in each trace (usually ten). These values of time period (Δt) were then converted to difference in phase in degrees (°), for each stimulus frequency as follows:

$$\Delta p = \frac{\Delta t \cdot 360}{f}$$

where:
Δp = the difference in phase in degrees between the stimulus and response
Δt = the time period (s) between stimulus peak and ERG trough
f = frequency of sinusoidal stimulus

The values of Δp (or the phase angles) were then averaged to give a single value of Δp for each stimulus frequency. Where more than one individual of a species was used, the mean Δp values for each frequency of stimulus were averaged to produce a mean value of Δp (with associated standard error) for the species.

The mean values of phase angle between the sinusoidal response and stimulus were then plotted as a function of log stimulus frequency to display the phase of the response of the eye to varying frequencies (after Knight *et al.* 1970)

Bode plots were also constructed which display both the relative magnitude (as determined in section *4.4.2.1*) and the phase angle of the ERG response as a function of frequency. The Bode plot describes the temporal properties of the eye and indicates the extent to which optical information is degraded by the eyes of the species studied here (see section *4.1.3*)

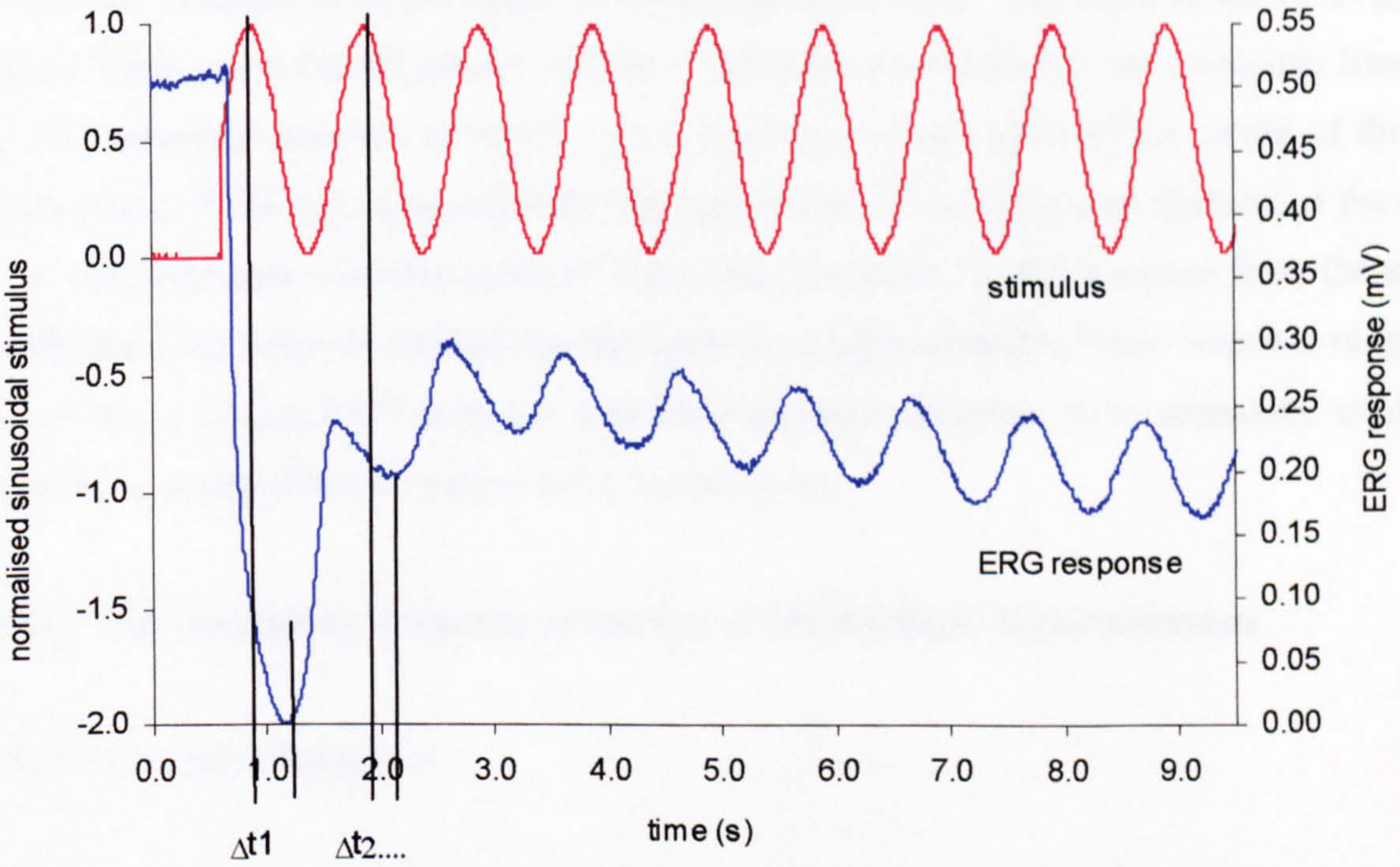

Figure 4.7. ERG data from the dark-adapted eye of *Oplophorus spinosus*, showing a typical dark-adapted ERG signal in response to a sinusoidal stimulus. The blue trace is the low pass filtered (cut-off 50Hz) ERG response signal; the red trace is the sinusoidal stimulus (at a frequency of 1Hz). At the onset of the sinusoidal light stimulus, the fully dark-adapted eye responds with a large 'on' response before following the sinusoidally modulating stimulus. This 'on' response was taken as the first depolarizing peak of the sinusoidal response, and the first time difference (Δt) was measured between this and the first peak of the sinusoidal stimulus. Values of Δt were then determined for all subsequent sinusoidal cycles of stimulus and response, converted to phase difference in degrees, and averaged.

4.5 RESULTS

4.5.1 VlogI Relationships

The VlogI relationships of the visual response for each of the species studied are shown in Fig. 4.8. The plots for all species show a sigmoidal relationship between relative response amplitude (V/V_{max}) and the log of stimulus irradiance at the eye. The figure shows that the maximum (irradiance) output range of the sinusoidal stimulus falls close to the $50\%V_{max}$ point on the VlogI curve for all species studied. Therefore, the maximum and minimum irradiances of the sinusoidal stimulus used fell over a relatively small region of the centre of the VlogI relationship of the eye. Consequently, the application of the sinusoidal stimulus at the eye led to a sinusoidal response that suffered from little distortion, as the response from the eye was generated in response to irradiances that covered an approximately linear response range. Fig. 4.9 shows a typical ERG response with little apparent distortion from sinusoidal modulation (distortion as described in section *4.3.5.2* and Fig. 4.6).

4.5.2 The Frequency Response of the Eye of Mesopelagic Malacostracans

4.5.2.1 Response magnitude

The relative response magnitudes ($\Delta V/\Delta V_{max}$) of the visual response to sinusoidal stimuli of fixed irradiance but differing frequencies are shown for each species in Fig. 4.10. The low values of *n* were inevitable with the technique employed (these plots represent recordings taken over a period in excess of 24 hours) and the limited access to study animals. The plots in Fig. 4.10 are a similar shape to those determined for other arthropod species (e.g. Knight *et al.* 1970; Pinter, 1972). The decrease in response magnitude of the visual response with increasing frequency for each species is analogous to the 'roll-off' properties of a low-pass filter.

For all species studied, the frequency to which the eye responds maximally is 0.5Hz (using stimuli at frequencies lower than 0.5Hz was not possible due to extrinsic factors; see section *4.6.3.3b*).

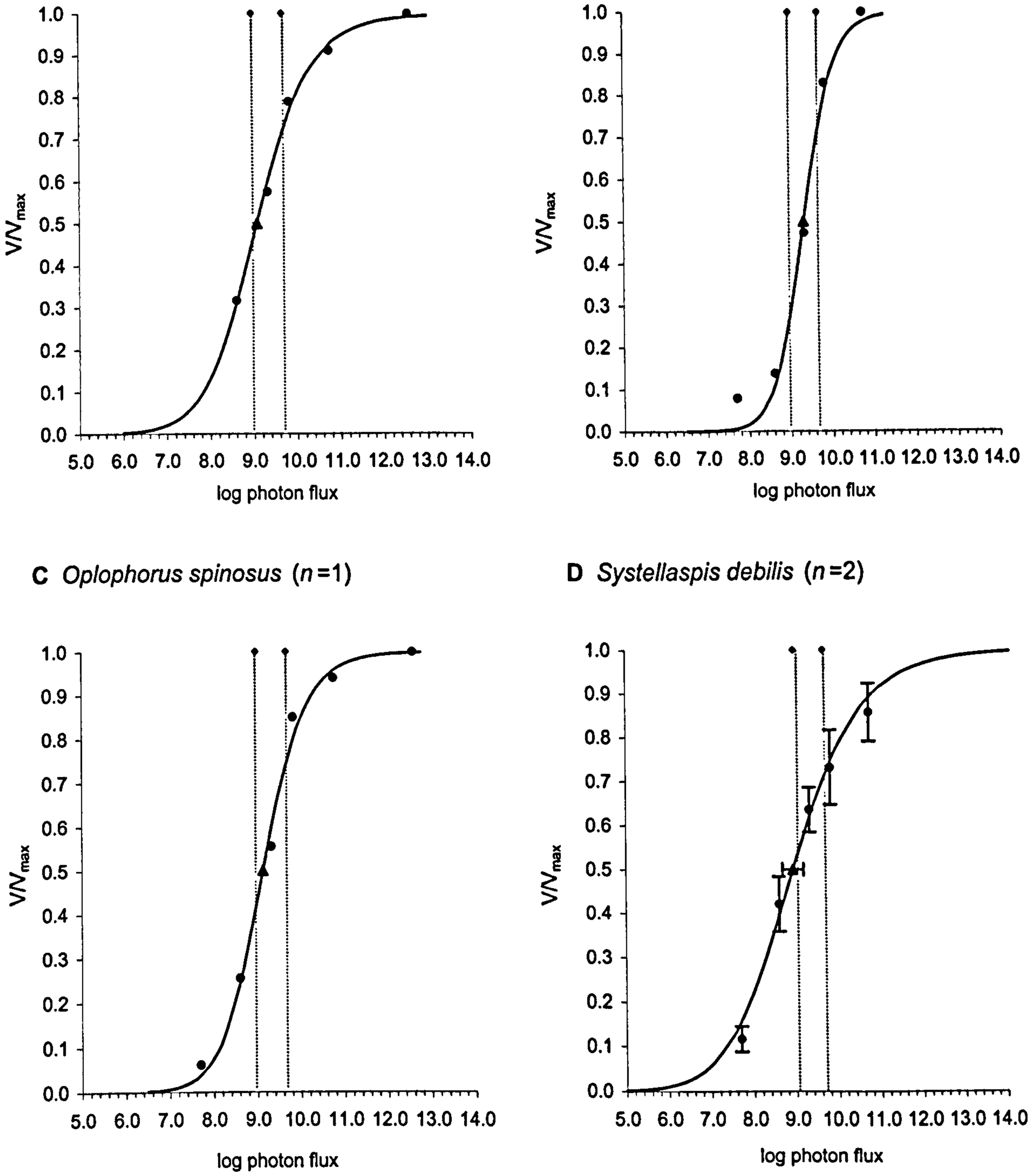

Figure 4.8. The VlogI relationships of the eyes of each species studied. The shapes of the VlogI curves are similar for all species. Differences in the gradient of the relationships may be attributed to the low numbers of individuals tested (*n*), and the low number of data points. For each plot, the circular data points represent V/V_{max} values and the triangular data points represent the value of k (irradiance generating a $50\%V_{max}$ response): k for *A. purpurea* = 9.08; k for *N. gibbosus* = 9.31; k for *O. spinosus* = 9.13; k for *S. debilis* = 8.94. The dotteed vertical lines on each plot represent the maximum and minimum irradiances of the sinusoidal stimulus used (modulation contrast = 0.66). For all species these values fall within the linear portion of the VlogI relationship.

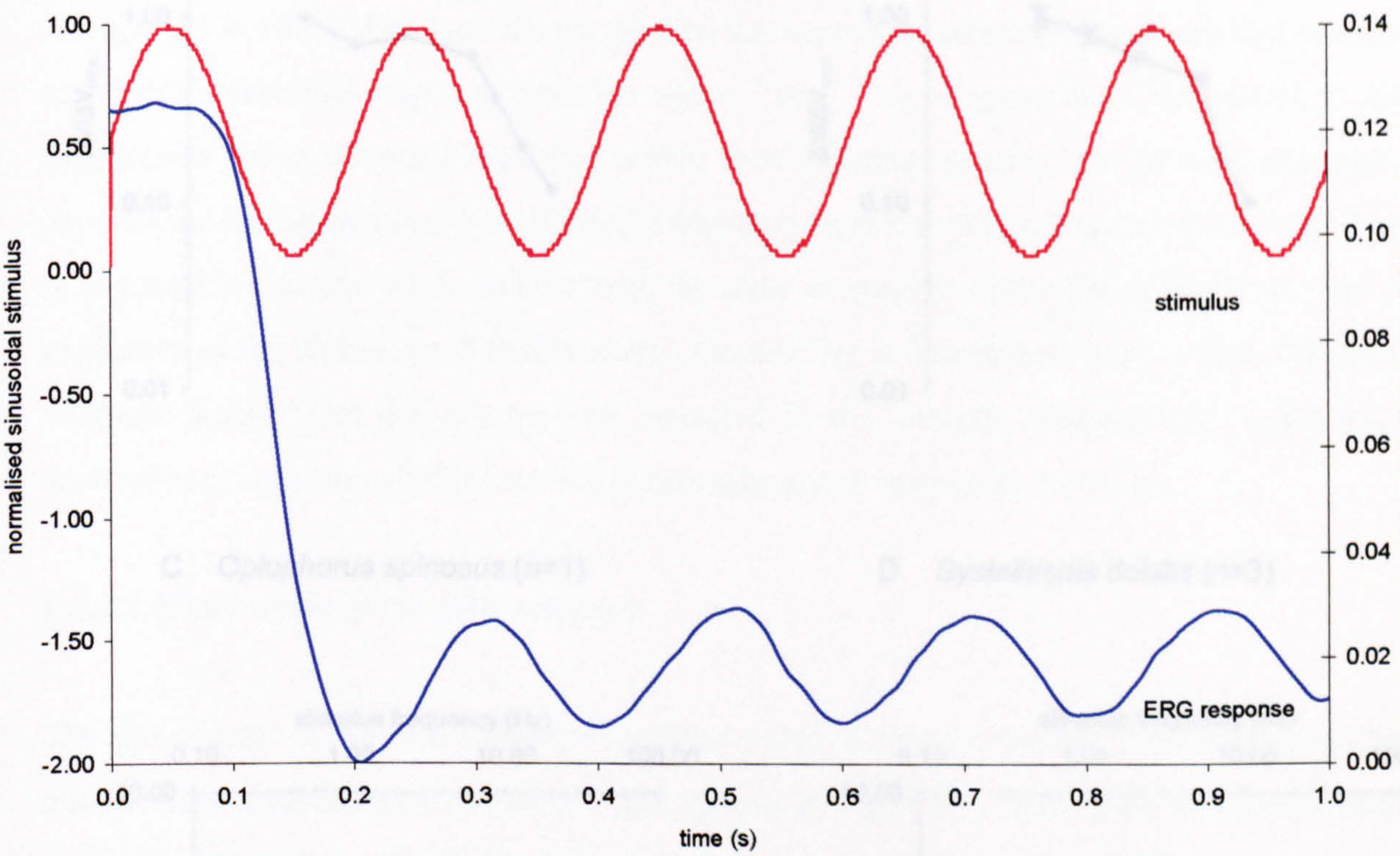

Figure 4.9. Typical ERG response from the eye of *Notostomus gibbosus* in response to a sinusoidal stimulus (5Hz). The maximum and minimum irradiances of the stimulus fall either side of the 50%V_{max} point of the VlogI relationship of the photoreceptors of this individual. Consequently, the photoreceptors respond as approximately linear systems, and produce a sinusoidal response with little distortion, which although different in amplitude and phase, modulates at the same frequency as the stimulus.

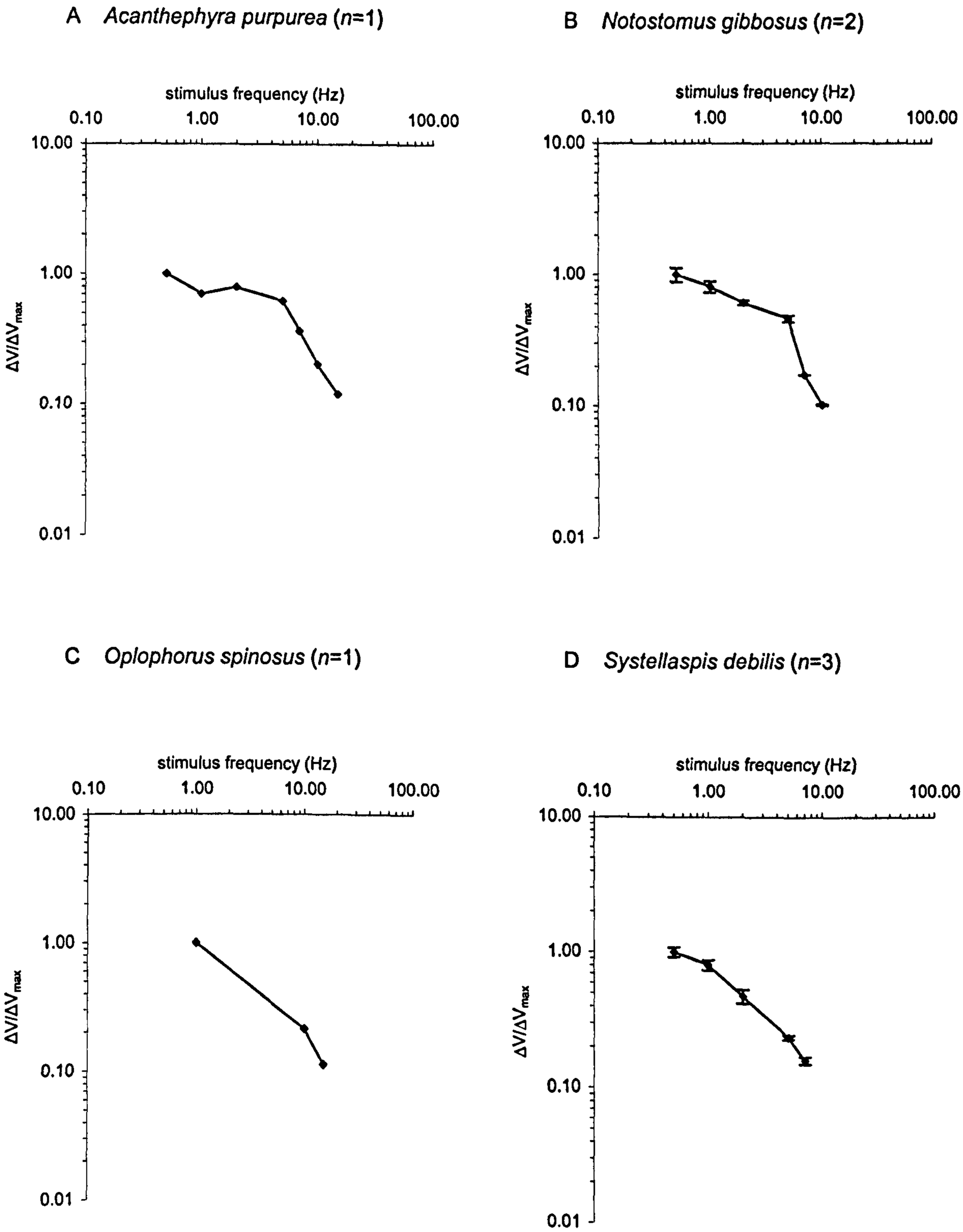

Figure 4.10. The frequency response range of the photoreceptors in the eyes of four mesopelagic species with differing depth distributions. Relative response magnitude ($\Delta V/\Delta V_{max}$) is plotted against sinusoidal stimulus frequency, with standard errors included for those species where $n>1$. There is a decrease in response magnitude with increasing stimulus frequency for all species. The maximum resolvable frequencies of the eyes of each species are as follows: *A. purpurea* = 15Hz; *O. spinosus* = 15Hz; *N. gibbosus* = 10Hz; *S. debilis* = 7Hz.

The frequency response ranges displayed in Fig. 4.10 do differ between species, however, in terms of the highest stimulus frequency resolvable by the eye, i.e. the maximum stimulus frequency that produces a response from the eye that is discernible from the intrinsic photoreceptor noise. For both *Acanthephyra purpurea* and *Oplophorus spinsosus* the maximum frequency of stimulus that produces a resolvable sinusoidal response from the eye is 15Hz (see Table 4c, section *4.5.2.3*). This is in comparison with *Notostomus gibbosus*; the maximum frequency of stimulus that produces a resolvable sinusoidal response from the eye of this species is 10Hz. For *Systellaspis debilis*, the maximum stimulus frequency that produces a resolvable sinusoidal response from the eye is 7Hz. This suggests that the eyes of *S. debilis* may have a lower temporal resolving power than the other species studied here, although this depends on the signal-to-noise ratio of the response from the photoreceptors in the eye. That is, it is possible the eye of *S. debilis* may be able to resolve sinusoidal stimuli (of the same irradiance as the stimuli used in this study) modulating at frequencies greater than 7Hz, but the response signal from the eye may be obscured in the intrinsic photoreceptor noise and not detectable using extracellular recordings (see discussion in section *4.6.3.3a*)

4.5.2.2 Phase angle of the ERG response

The phase angle of the visual response relative to the sinusoidal stimuli (Δp) of fixed irradiance but differing frequencies is shown for each species in Fig. 4.11. These plots are similar to those determined for other arthropod species (e.g. Knight *et al.* 1970; Pinter, 1972).

The plots in Fig. 4.11 show that for all the mesopelagic species studied, the visual response always lags behind the sinusoidal stimulus over the frequency range of 0.5Hz to the maximum resolvable frequency of the eye. It is also apparent from Fig. 4.11 that the least amount of phase lag in the visual response occurs at the lowest stimulus frequencies (i.e. 0.5Hz for *A. purpurea*, *N. gibbosus* and *S. debilis* and 1Hz for *O. spinsosus*), and that the phase lag in the visual response increases with increasing stimulus frequency for all the species studied. Such phase lags are typical of near dark-adapted arthropod eyes (e.g. Pinter, 1972; Howard, 1981; Johnson *et al.* 2000a, see section *4.6.2* for a discussion of 'near' dark-adapted eyes); phase advances only being seen in some cases in light-adapted eyes in response to a low frequency stimulus

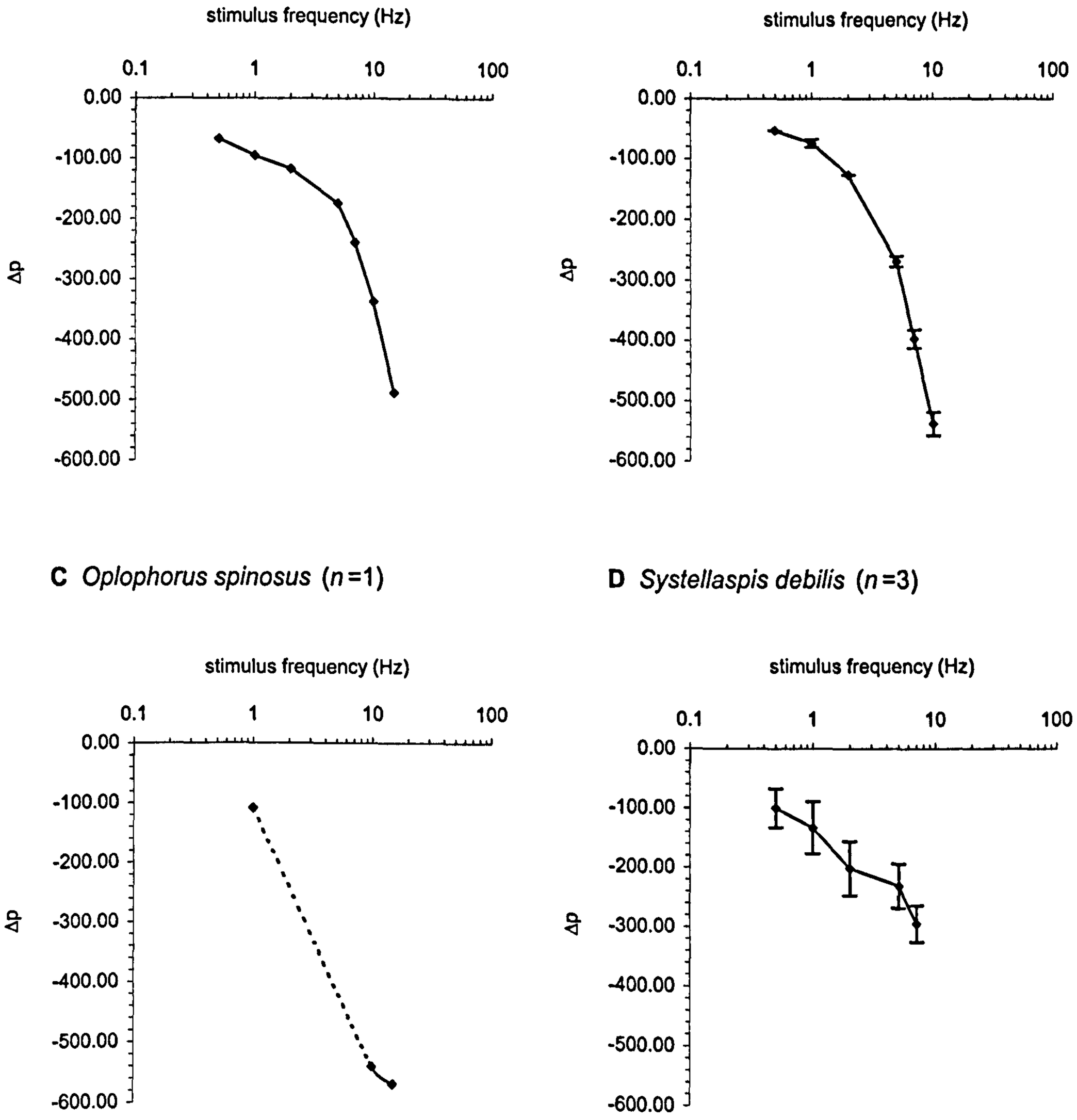

Figure 4.11. The phase characteristics of the response of the eyes of four mesopelagic species with differing depth distributions. The difference in phase angle between the sinusoidal response and the sinusoidal stimulus (Δp) is plotted as a function of the stimulus frequency, with standard errors included for those species where $n>1$. There is an increase in the phase lag of the response relative to the stimulus with increasing stimulus frequency for all species. The phase lag in the response from the eye relative to the stimulus, at a frequency of 1Hz, for each species is: *A. purpurea* = 96°; *N. gibbosus* = 75°; *O. spinosus* = 110°; *S. debilis* = 133°. The dotted line in C) represents the uncertainty of the relationship between phase delay and frequency between 1 and 10Hz in the response of the eye of *O. spinosus*, due to a lack of data points.

(e.g. *Limulus polyphemus*, Knight *et al.* 1970; *Schistocerca gregaria*, Pinter, 1972; *Pandalus montagui*, Johnson *et al.* 2000a)

In order to compare the phase characteristics of the visual responses between species, the phase angle of the response relative to the stimulus at a frequency of 1Hz (Δp1) can be compared, and these values are given in Table 4c (section *4.5.2.3*). The visual responses of *A. purpurea* and *N. gibbosus*, in response to a 1Hz sinusoidal stimulus, show phase lags of 96° and 75° respectively. Thus the visual responses of both species lag behind a 1Hz stimulus by approximately one quarter of a cycle. When the eyes of these two species are stimulated with sinusoidal stimuli at a frequency of 10Hz, the visual response shows a phase lag of 337° for *A. purpurea* and 539° for *N. gibbosus*. Thus there is a greater increase in phase lag in the visual response with increasing frequency for *N. gibbosus* than for *A. purpurea*. This is apparent in the plots in Fig. 4.11. The phase lag in the visual response for *A. purpurea* declines at a steady and relatively low level with increasing frequency up to a stimulus frequency of 5Hz, but beyond this frequency there is a rapid increase in phase lag as stimulus frequency increases. For *N. gibbosus* a similar relationship is seen between phase and stimulus frequency except that the phase lag in the visual response shows a more rapid increase at frequencies beyond 1Hz as opposed to 5Hz as for *A. purpurea*. Thus these species have eyes with similar phase lags at 1Hz, yet the rate of increase in phase lag for the visual response of *N. gibbosus* is higher than that for *A. purpurea*.

The visual responses of the two species *O. spinosus* and *S. debilis* in response to a 1Hz stimulus have phase lags of 110° and 133° respectively. Thus the visual response of *O. spinosus* lags behind a 1Hz stimulus by approximately one quarter of a cycle, and in the case of *S. debilis*, the visual response lags behind the 1Hz stimulus by approximately one third of a cycle. At a stimulus frequency of 7Hz, the visual response of *O. spinosus* has a phase lag of *ca.* 480° and for *S. debilis*, at a stimulus frequency of 7Hz; the visual response has a phase lag of 295°. Therefore, despite the visual response of *S. debilis* showing a greater lag in response to a stimulus frequency of 1Hz than that of *O. spinosus*, the rate of increase in lag with increasing stimulus frequency up to 7Hz for *S. debilis* is less than that for *O. spinosus*. This is apparent from the plots in Fig. 4.11 that show a relatively small increase in phase lag with increasing

stimulus frequency for *S. debilis* compared with the other three species. For *S. debilis*, the phase lag in the visual response increases steadily up to a frequency of 5Hz after which it appears to begin to increase more rapidly. However, as the maximum resolvable frequency of the eye of this species was 7Hz, no data are available on the phase lag in the response to stimuli beyond this frequency.

The plot in Fig. 4.11c shows that the phase lag (Δp) in the visual response of *O. spinosus* increases with increasing stimulus frequency up to 10Hz. The lack of data points between 1 and 10Hz prevents one from describing the phase in the response when stimulated with frequencies between 1 and 10Hz.

These results would suggest that the eyes of *A. purpurea* and *N. gibbosus* have faster response dynamics than those of *O. spinsosus* and *S. debilis* at low stimulus frequencies as there is less lag in the visual response relative to a stimulus of 1Hz. The eyes of *O. spinsosus* have intermediate response dynamics in response to 1Hz sinusoidal stimuli, and the eyes of *S. debilis* have the slowest response dynamics (i.e. greatest lag) in response to 1Hz sinusoidal stimuli.

4.5.2.3 Bode plots

Plots of the relative response magnitude ($\Delta V/\Delta Vmax$) and phase (Δp) characteristics of the visual response as a function of frequency are given in Fig. 4.12. These plots are known as Bode plots and are conventionally used to describe the temporal response of the input-output properties of a (linear) physical system (see section *4.1.3*). These Bode plots are similar to those plotted for the visual response of other arthropod species (e.g. Knight *et al.* 1970; Pinter, 1972).

The Bode plots in Fig. 4.12 illustrate that for the three species *A. purpurea, N. gibbosus* and *S. debilis*, there is a close relationship between response magnitude and the phase delay of the visual response with respect to stimulus frequency, as both curves have a similar shape. As the phase lag in the response increases, the magnitude of the response decreases, presumably because as the response signal falls further out of phase with the stimulus, the power of the response signal declines. The Bode plot for *O. spinosus* (Fig. 4.12c) shows slightly different shapes for the magnitude and phase curves, but this is almost certainly due to the lack of data

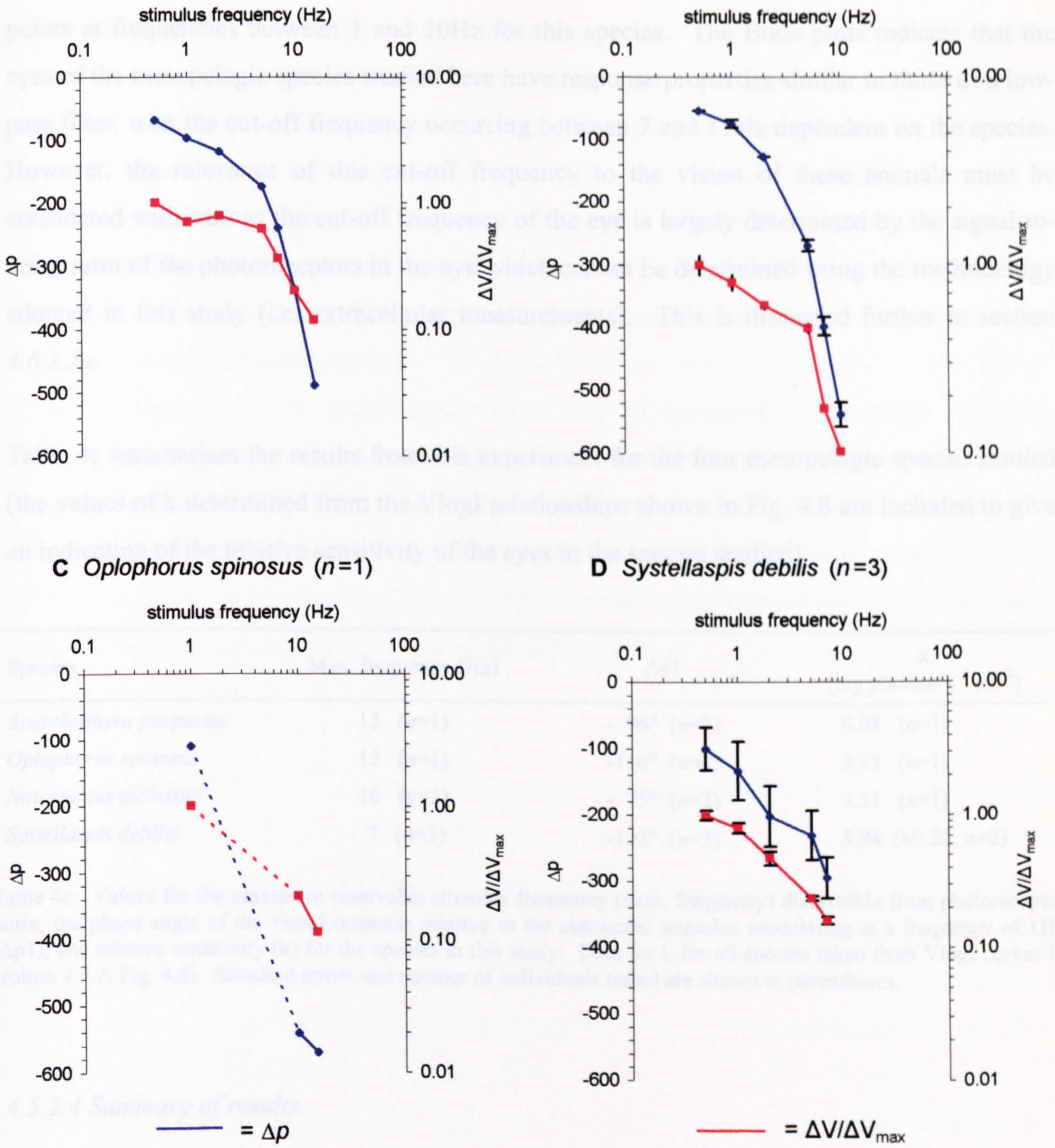

Figure 4.12. The relative response magnitude ($\Delta V/\Delta V_{max}$) and phase (Δp) characteristics of the visual response as a function of frequency for four mesopelagic species with differing daytime depth distributions. These plots are Bode plots which are conventionally used to describe the temporal properties of the transfer function of a physical system. The Bode plot for each species describes the gain, bandwidth and lag of the ERG visual response within it's linear response range. The plots show that for each species both the relative response magnitude and the phase characteristics of the visual response decline with increasing stimulus frequency in an approximately identical manner, thus indicating that these two properties of the visual response are closely related. The dotted lines in C) represent the uncertainty of the relationship between both response magnitude and phase delay and frequency between 1 and 10Hz in the response of the eye of *O. spinosus*, due to a lack of data points.

points at frequencies between 1 and 10Hz for this species. The Bode plots indicate that the eyes of the mesopelagic species studied here have response properties similar to those of a low-pass filter, with the cut-off frequency occurring between 7 and 15Hz dependent on the species. However, the relevance of this cut-off frequency to the vision of these animals must be considered with care as the cut-off frequency of the eye is largely determined by the signal-to-noise ratio of the photoreceptors in the eye which cannot be determined using the methodology adopted in this study (i.e. extracellular measurements). This is discussed further in section *4.6.3.3a*.

Table 4c summarises the results from this experiment for the four mesopelagic species studied (the values of k determined from the VlogI relationships shown in Fig. 4.8 are included to give an indication of the relative sensitivity of the eyes in the species studied).

Species	Max. frequency (Hz)	Δp1	k (log photons s^{-1} cm^{-2})
Acanthephyra purpurea	15 (*n*=1)	- 96° (*n*=1)	9.08 (*n*=1)
Oplophorus spinosus	15 (*n*=1)	-110° (*n*=1)	9.13 (*n*=1)
Notostomus gibbosus	10 (*n*=2)	- 75° (*n*=2)	9.31 (*n*=1)
Systellaspis debilis	7 (*n*=3)	-133° (*n*=3)	8.94 (±0.25; *n*=2)

Table 4c. Values for the maximum resolvable stimulus frequency (max. frequency) discernible from photoreceptor noise, the phase angle of the visual response relative to the sinusoidal stimulus modulating at a frequency of 1Hz (Δp1), and relative sensitivity (k) for the species in this study. Data for k for all species taken from VlogI curves in section *4.5.1*, Fig. 4.8). Standard errors and number of individuals tested are shown in parentheses.

4.5.2.4 Summary of results

a) The eyes of the species *S. debilis* have both the lowest frequency response of all the species studied, as defined by the maximum resolvable frequency of the eye (7Hz), and the greatest sensitivity, as defined by the value of k in Table 4c. The visual response of this species also has the greatest amount of lag in response to a stimulus frequency of 1Hz.

b) The eye of the species *A. purpurea* and *O. spinosus* have maximum resolvable frequency values of 15Hz, and thus, have the highest frequency responses of all the species studied. The visual response of *O. spinosus* however, has a relatively

greater amount of lag in response to frequencies of 1Hz than that of *A. purpurea*, which could indicate slower response dynamics. The eye of *O. spinosus* appears to have a less sensitive response than that of *A. purpurea* (as indicated by the value of k) although recordings from more individuals would be required in order to determine whether this difference is significant or not. The sensitivity of the visual response of *A. purpurea* (k=9.08) is comparable to that for *S. debilis* (k=8.94) despite there being a large difference in the maximum resolvable frequencies of the eyes of these two species.

c) The species *N. gibbosus* has eyes with an apparently intermediate frequency response (max frequency 10Hz), and the least amount of lag in the visual response to frequencies of 1Hz. This species also has the least sensitive eye as defined by the value of k for this species (9.31). However, recordings from more individuals would be required to determine whether the relative sensitivity of this species is significantly different to that of the other species.

4.6 DISCUSSION

4.6.1 VlogI Relationships

The plots of the dark-adapted VlogI relationships obtained for each species in this study (section *4.5.1*, Fig. 4.8) are comparable in shape to those obtained for mesopelagic and shallow-water, coastal malacostracans in Chapter 3 of this study (section *3.4*, Figs 3.7; 3.8; 3.10; 3.11), and are also comparable in shape to those determined for many other invertebrate species (see section *3.5.1.1* for examples). The relative sensitivities of the two species, *Acanthephyra purpurea* and *Systellaspis debilis* were also studied in Chapter 3 and the VlogI relationships resulting from this study are plotted in section *3.4*, Figs 3.7 & 3.8. There is a slight difference in the values of k for *A. purpurea* and *S. debilis* between the present study and that of Chapter 3. This is because the plots in section *3.4* are calculated for a greater number of individuals of each species (*A. purpurea*, n=3; *S. debilis*, n=7), than the VlogI plots in this study (*A. purpurea*, n=1, *S. debilis*, n=2).

The VlogI relationships determined in this study are used to identify the irradiances that produce a response in the middle of the response range of the eye, i.e. the irradiances that produce responses close to the $50\%V_{max}$ point. The k values determined from these VlogI relationships are used, along with the irradiance that produces a response that is 1% of V_{max} (threshold response, see Table 4e, section *4.6.5*), to give an indication of the relative sensitivity of the eye, although conclusions about visual sensitivity drawn from such small sample sizes should be treated with care.

4.6.2 The Dark-adapted Visual Response

This study considers the frequency response of only dark-adapted photoreceptors of mesopelagic oplophorid malacostracans. The temporal response properties of a visual system are highly dependent on the state of adaptation of the eye and the intensity of the stimulating light (Fuortes and Hodgkin, 1964; Pinter 1972; Howard, 1981; Laughlin and Weckström, 1993; Laughlin, 1996). Consequently these factors were controlled during this study, all eyes were tested in the dark-adapted state, and the same irradiance of stimulus was used for all individuals; the irradiance of the stimulus was controlled such that it generated a response

within the linear region of the intensity-response relationship, close to 50%V_{max} (see section *4.5.1*, Fig. 4.8). The dark-adapted visual response is also likely to be more ecologically relevant to the species in this study for the same reasons as discussed in section *3.5.1.1*, Chapter 3.

Measuring the frequency response of fully dark-adapted photoreceptors has an effect on the beginning of the sinusoidal response from the eye (see Fig. 4.7, section *4.4.2.2*). The fully dark-adapted visual response to the initial onset of light is a transient, large depolarisation before the response from the eye begins to modulate sinusoidally at the same frequency as the stimulus. Consequently, the peak amplitude of this initial, relatively large depolarisation was taken as the first 'peak' (this depolarisation is actually apparent as a trough in the response but this corresponds to the peak response of the eye as extracellular records show the inverted response of the photoreceptors) of the sinusoidal response from the eye, although it was not used in calculation of phase delay or response amplitude (see section *4.4.2.2* for details of phase analysis).

Other studies which examine the frequency response of 'dark-adapted' photoreceptors (Knight *et al.* 1970; Pinter, 1972; Howard, 1981; Johnson *et al.* 2000a) do not use fully dark-adapted eyes, but eyes which are adapted to a background light of low irradiance, presumably in order to avoid the initial large depolarising response due to the onset of the light from complete darkness. As mesopelagic species spend the majority of their time in a dark-adapted state it is inappropriate to light-adapt the eye and make inferences about the temporal response properties of the eyes of animals as they function in their natural habitat. The phase information, which is extracted from the frequency response of the dark-adapted eyes of mesopelagic oplophorid malacostracans in this study, reports the lag in the visual response with increasing stimulus frequency. Data on the phase properties of the eyes of the mesopelagic species used in this study are given in Table 4c, section *4.5.2*, and Table 4e, section *4.6.5.1* of this discussion.

4.6.3 Methodological Considerations

4.6.3.1 Wavelength of light stimuli

The λ_{max} of the pulse stimuli used to determine the VlogI relationship for the eye of each animal was 464nm (FWHM 28nm). The VlogI relationship was determined so that the irradiance of the sinusoidal stimuli could be controlled such that they generated a response close to the 50%V_{max} response of the eye (see section *4.3.4.2* for detail). When delivering sinusoidal stimuli to determine the frequency response of the eye, an interference filter was placed in the light path to alter the spectral output of the LED to a λ_{max} of 488nm (FWHM *ca.* 10nm, see section *4.2.3*). As the VlogI relationship was determined using a stimulus with a λ_{max} at 464nm and the sinusoidal stimulus had a λ_{max} of 488nm, it may be argued that the 50%V_{max} response of the eye as determined using λ_{max} 464nm light maybe different to that determined with λ_{max} 488nm because the sensitivity of the visual response is wavelength dependent.

Table 4d displays the λ_{max} and the approximate FWHM of the spectral sensitivity function for each species in this study as determined electrophysiologically, although only microspectrophotometric data are available for the visual pigment of *Acanthephyra purpurea*.

Species	S_{max} or λ_{max} of rhodopsin (nm)	FWHM (nm)	Author(s)
*Acanthephyra purpurea**	492	—	Kent (1997)
Notostomus gibbosus	490	≈110	Frank and Case (1988a)
Oplophorus spinosus	400 and 500	≈100	Frank and Case (1988a)
Systellaspis debilis	400 and 500	≈110	Frank and Case (1988a)

Table 4d. The λ_{max} of the spectral sensitivity functions (S_{max}) of three of the mesopelagic species used in this study. All spectral sensitivity functions were determined using electrophysiological techniques. *O. spinosus* and *S. debilis* have spectral sensitivity functions with bimodal peaks. Also displayed are the approximate full width half maximum (FWHM) of each spectral sensitivity function (in the case of *O. spinosus* and *S. debilis*, the FWHM is given for the spectral sensitivity function with a λ_{max} of 500nm). *No spectral sensitivity data available for *Acanthephyra purpurea*, but microspectrophotometric measurements show that the visual pigment, rhodopsin, for this species has a λ_{max} at 492nm.

Table 4d shows that the λ_{max} of both the spectral sensitivity functions, and the absorbance spectrum of rhodopsin from the eye of *A. purpurea* fall within the range of 490-500nm and that the spectral sensitivity functions of the eyes of the mesopelagic species in this study are broad, with values for FWHM which span *ca.* 100nm (Frank and Case, 1988a). For the same reasons discussed in section *3.5.3.1*, Chapter 3, it is probable that all the mesopelagic species in this study will have broadband spectral sensitivities and, consequently, a shift in stimulus λ_{max} from 464 to 488nm will not have a great effect on the amplitude of the ERG response. Therefore it is safe to assume that a sine wave modulated stimulus with a λ_{max} of 488nm and irradiance adjusted to generate a response close to the $50\%V_{max}$ point of the VlogI curve as determined using λ_{max} 464nm light, will produce a response close to $50\%V_{max}$.

4.6.3.2 Optical stimulation

There are a number of points to consider with respect to the use of the ERG in determining the visual response to a given stimulus. These are described in section *3.5.2* Chapter 3, and the description given is equally applicable to the present study.

4.6.3.3 Problems with the frequency response method in determining the temporal resolution of the photoreceptors of mesopelagic malacostracans

4.6.3.3a Photoreceptor noise

The results of the present study give an indication of the extent to which the photoreceptors in the eyes of mesopelagic species degrade temporal information within a visual signal as it is transduced to the nervous system. As mentioned in section *4.1.3*, eyes are not perfect optical or light-transducing systems and, as in the case of almost any physical system, information is degraded as it is processed. The extracellular recording techniques used in this study therefore give an indication of the combined temporal resolving powers of all the photoreceptors in the eye, or at least all those stimulated by the light delivery system.

The results of the present study provide useful data for interspecies comparisons. They do not, however, exactly determine the maximum temporal resolution limit of the eyes of mesopelagic species as the eye is stimulated with a fixed irradiance. The temporal resolving power of eyes

is highly dependent on the intensity of stimulating light (e.g. Frank, 1999) and thus if the light used to stimulate the eye produces a saturating response from the eye (as in the case of determining the maximum critical flicker fusion frequency (CFFF) of the eye, see section *4.6.4*), the temporal resolving power would be much higher than that determined here. However, by assessing the frequency response of the eyes using stimuli that produce responses within the mid-range of the VlogI relationship of the eye, one is obtaining an estimate of the temporal resolving power of the eye in response to stimuli of 'natural' contrast, i.e. one is stimulating the eye with stimuli of contrast that may be encountered in the natural light environment of the animal.

The intensity of the light stimuli used is not the only factor that determines the absolute frequency response of the photoreceptors in the eye. Intrinsic photoreceptor noise and transducer noise must also be considered. Intrinsic photoreceptor noise originates from the random arrival of photons at the eye (and in complete darkness spontaneous isomerisation of the visual pigment causes intrinsic photoreceptor noise) and transducer noise is present as the process of phototransduction itself is noisy (see Laughlin, 1981, for a comprehensive review). These noise levels will determine the absolute resolving power of a photoreceptor in the eye as, for example, high frequency signals may produce responses from the photoreceptors of such low amplitude that they are not resolvable from the intrinsic noise of the photoreceptor. Intracellular recording techniques can be used to determine both intrinsic photoreceptor noise and transducer noise but this is well beyond the scope of the present study and may be impossible at sea.

It has been shown that there is variation in photoreceptor noise level between species (Smola and Gemperlein, 1973; Smola, 1976, cited in Laughlin, 1981) and even between different cells within a single retina (Laughlin 1976a, cited in Laughlin, 1981). As the ERG records the combined response of all the photoreceptors within the eye it is possible in the cases of those species that have more than one cell type in their retina, e.g. *S. debilis* and *O. spinosus* (both have blue and near-UV sensitive receptors in the retina, see Table 4d, section *4.6.3.1*) that different intrinsic noise levels, and indeed different temporal properties of receptors (e.g. Burton *et al.* 2001 found regional variation in the temporal resolving power of photoreceptors across the eye of the blowfly [*Calliphora vicina*]), contribute to the overall temporal resolution of the visual response. Also, without direct measurements of the photoreceptor noise

amplitude, it is impossible to allow for the effect of species-specific noise levels when making interspecies comparisons. Laughlin (1981) indicates that it is possible that the optic lobes may filter out a large amount of photoreceptor noise during neural processing of the visual signal, and that behavioural studies to determine the temporal thresholds of animals may compliment physiological measures by indicating to what extent the nervous processing of the visual signal differs, interspecifically, to that of the phototransduction mechanism.

4.6.3.3b Experimental difficulties

Determining the frequency response of the photoreceptors of the species in this study involved stimulating the eye with a stimulus of ten cycles of sinusoidally modulated light with frequencies ranging from 0.5-20Hz (see section *4.3.5.2*). The duration of the 0.5Hz stimulus therefore, was 20 seconds. After a 20 second exposure to light the highly sensitive eyes of the mesopelagic species took at least 60 minutes to recover to pre-stimulus sensitivity. Consequently, each frequency response experiment took a minimum of 7.5 hours (and generally took longer than this), and often the preparation would deteriorate before the end of the experiment or the animal would die (most mesopelagic animals are not very robust once removed from their natural habitat). This problem leads to the small sample size of the results of this study.

Working in a laboratory at sea means experiments are susceptible to extrinsic factors such as ship pitch and roll which can distort electrophysiological measurements, an example of the effect of ship movement on an ERG response and the DC trace is shown in Fig. 4.6, section *4.3.5.2*. The DC drift caused by ship movement often made long duration responses impossible to interpret and consequently, there are no responses to stimuli of 0.1Hz included in this study. This is unfortunate as other studies using the frequency response methodology have shown that 'dark-adapted' eyes can be maximally sensitive to very low frequencies, e.g. Johnson *et al.* (2000a) found the estuarine species *Pandalus montagui* was maximally sensitive to 0.48Hz, and Howard (1981) obtained responses of maximum amplitude from the 'dark-adapted' photoreceptors of the locust (*Locusta migratoria*) in response to frequencies well below 0.5Hz. On the basis of the near dark-adapted eye of a locust (which is a diurnal animal and thus would be expected to have photoreceptors with a less sensitive response and faster response dynamics) being maximally sensitive to frequencies below 0.5Hz, it is probable that

mesopelagic species would show maximal sensitivity to frequencies below 0.5Hz, but under the experimental circumstances, this was impossible to determine.

4.6.4 Comparisons with Previous Studies on Species of Deep-sea Malacostracans

There are relatively few studies that have examined the temporal response properties of mesopelagic and deep-sea benthic malacostracans, for reasons explained in section *4.1.2*. These studies have identified that for certain species of mesopelagic malacostracans there is a correlation between temporal resolving power and the light environment inhabited (see section *4.1.2*). However, the studies of Frank (1999, 2000) also conclude that for two species of mesopelagic euphausiid malacostracan, temporal resolving power is not correlated with daytime depth distribution, but a higher than expected temporal resolving power may be explained by the requirement of these animals to hunt bioluminescent prey (higher than expected temporal resolving power relative to the temporal resolving powers of other mesopelagic species in the study, which are associated with daytime depth distribution and thus ambient light levels in the environment).

Comparisons of the results of this study with those of other studies of the temporal resolving power of mesopelagic species are difficult as the methodologies employed in other studies are quite different. The studies of Frank (1999, 2000) provide the most comprehensive description of the dark-adapted temporal resolving power of mesopelagic species, and use the maximum critical flicker fusion frequency (max CFFF) of the eye, determined *via* the electroretinogram, to compare temporal resolving power between species. In the studies of Frank (1999, 2000) the critical flicker fusion frequency (CFFF) of an eye is determined by increasing the frequency of a square wave stimulus until the eye no longer produces an electrical signal that is in phase with the stimulus (it should be noted that in using the frequency response methodology in the present study, the visual response was never exactly in phase with the stimulus, it was always slightly behind or lagging considerably behind the stimulus). The CFFF is dependent on the irradiance of stimulating light used and will increase with increasing irradiance of the stimulus at the eye (Frank, 1999). Therefore, increasing the irradiance of the stimulus until no further increases in CFFF are observed, determines the maximum CFFF for an eye. This method allows for comparisons of temporal resolving power between species as it removes any irradiance dependent effect on the flicker response of the eye. It does not, however, allow

direct comparisons with the results of this study, as the stimulus irradiances used in this study fall within the centre of the VlogI relationship for each animal and are well below those irradiances that would saturate the photoreceptor response. In the study of Frank (1999) an example given (in measuring the FFF of the eyes of *Oplophorus gracilirostris*) shows that the irradiance of stimulus is increased to approximately $1x10^{11}$- $1x10^{12}$ photons s^{-1} cm^{-2}, which is 2-3 orders of magnitude greater than the maximum irradiance used in this study. Laughlin (1981) reviews a number of methods used in determining the temporal response properties of photoreceptors, and warns that flicker fusion frequency values should be interpreted with care as this method involves the use of stimuli of maximum contrast and therefore does not provide information on the temporal response characteristics of the photoreceptors at lower, more natural and visually relevant contrasts.

The study of Moeller and Case (1995) uses intracellular recording and the CFFF method to determine the temporal resolutions of two species of mesopelagic malacostracans (see section *4.1.2*), the CFFF is determined in response to stimulus irradiances that are one order of magnitude above the irradiance that produces a threshold response from the eye. The CFFF reported for the dark-adapted eye of *Oplophorus spinsosus* by Moeller and Case (1995) is 12Hz, and for the dark-adapted eye of *Gnathophausia ingens*, the CFFF is 6Hz. These CFFF values are comparable to the maximum resolvable frequencies determined in this study for the mesopelagic species *Acanthephyra purpurea*, *Notostomus gibbosus*, *Oplophorus spinosus* and *Systellaspis debilis*. However, the extent to which these maximum resolvable frequency values determine the temporal resolving power of the eye depends on the signal-to-noise ratio of the photoreceptors in the eye as discussed in section *4.6.3.3*.

The study of Johnson *et al.* (2000a) uses the frequency response method to determine the temporal resolving power of two deep-sea benthic and two coastal decapod species of malacostracan (see section *4.1.2*). However, the 'dark-adapted' frequency response is actually the frequency response determined for eyes that are adapted to a low level of irradiance. Although it is stated that the intensity range of the stimulus output was shifted to obtain a linear relationship between stimulus intensity and response, no indication is given as to where these irradiances fall within the VlogI relationship of the eye. The maximum resolvable frequency of the 'dark-adapted' eyes of the benthic crabs studied (*Chaceon affinis* and *Paromola cuvieri*, living at depths of approximately 800m) was approximately 20Hz (Johnson *et al.* 2000a),

which indicates that these animals have a higher frequency response than the mesopelagic species in this study. However, as the eye was not fully dark-adapted and no information is given regarding the irradiance of the stimuli in relation to the VlogI relationship of this species, comparisons should be made with care.

An intracellular electrophysiological study of the temporal resolution of the eyes of the locust (*Schistocerca gregaria*) and the house cricket (*Acheta domesticus*) by Pinter (1972), employs the frequency response method, although again, the 'dark-adapted' responses are obtained from eyes that have been adapted to a background light of low irradiance. The irradiance of the stimulus is controlled so that a response is obtained within the linear response range of the eye, although no indication of the position of the stimulus irradiances relative to the VlogI relationship is given. The 'dark-adapted' frequency response of the locust gives a maximum resolvable frequency of 25Hz, in comparison with the 'dark-adapted' response of the cricket that gives a maximum resolvable frequency of 15Hz. It is difficult to draw comparisons between these results and those of the current study, as the eyes were not fully dark-adapted during stimulation. Also, the results of the current study report the combined temporal response dynamics of all the photoreceptors in the eye, *via* the ERG, as opposed to using intracellular recording techniques to determine the temporal resolving power of individual photoreceptors.

4.6.5 The Frequency Response in Relation to the Light Environment Inhabited and Behaviour

4.6.5.1 The light environment

The mesopelagic, oplophorid malacostracan decapods in this study were all collected from the Northeast Atlantic, in the region of the Cape Verde Islands, where the open ocean water is type II (Jerlov, 1976). There are no irradiance measurements available for Jerlov type II water at depths similar to those inhabited by the species in this study. However, as all species were obtained from the same location, the optical properties of the water inhabited will be the same for all species (see section *1.3*) and consequently, the daytime depth distribution of each species will give a good indication of the relative optical depth inhabited.

The daytime depth distribution given for *Notostomus gibbosus* (Tables 4a&4d), however, is determined for the distribution of this species in the Gulf of Mexico (Hopkins *et al.* 1989) which has open ocean water of type IA (Jerlov, 1976). The results of Chapter 3 of this study indicate that visual sensitivity is related to the optical depth inhabited for four mesopelagic species. Consequently it is possible that, as Jerlov type II water is less transparent than type IA (see section *1.3* for more detail), *Notostomus gibbosus* may have a shallower depth distribution in the waters in the region of the Cape Verde Islands compared with that in the Gulf of Mexico, because the optical depth at 800m in type IA water will be reached at shallower depths in type II water due to greater attenuation of downwelling sunlight (see section *1.3*).

Table 4e shows for each species, the maximum frequency of stimulus that produces a sinusoidal response from the eye that is resolvable above intrinsic photoreceptor noise using ERG recordings. These values are used to compare the frequency responses of the four mesopelagic species but they should not be considered as a definitive measure of the maximum temporal resolving power of the eye for reasons discussed in section *4.6.3.3.* This is presented along with the phase angle of the sinusoidal response relative to a 1Hz sinusoidal stimulus ($\Delta p1$) and the relative sensitivity of the visual response of each species, in terms of both the log relative irradiance that generates a response from the eye that is 50% of the maximum, k ($50\%V_{max}$), and the irradiance that generates a threshold response from the eye (threshold response is defined as 1% of V_{max}). This information on the visual capabilities of four mesopelagic species is considered along with the daytime depth range and bioluminescent capabilities of each species.

Species	k (log photons s^{-1} cm^{-2})	$1\%V_{max}$ (photons s^{-1} cm^{-2})	Max resolvable frequency (Hz)	Δp1	Daytime depth range (m)	Biolumine-scence
Acanthephyra purpurea	9.08 (*n* =1)	$5.01x10^6$ (*n*=1)	15 (*n*=1)	- 96° (*n*=1)	700-950[1]	spew
Oplophorus spinosus	9.13 (*n* =1)	$1.58x10^7$ (*n*=1)	15 (*n*=1)	-110° (*n*=1)	300-500[1]	photophores spew
Notostomus gibbosus	9.31 (*n* =1)	$7.08x10^7$ (*n*=1)	10 (*n*=2)	- 75° (*n*=2)	800-1000[2]	spew
Systellaspis debilis	8.94 (*n* =2)	$1.00x10^6$ (*n*=2)	7 (*n*=3)	-133° (*n*=3)	650-950[1]	photophores spew

Table 4e. Details of the visual sensitivity of each species in this study in terms of both the value of k ($50\%V_{max}$) and the threshold response (defined as the irradiance which produces a response that is 1% of V_{max}); these values are determined from the VlogI relationships for each species (as plotted in fig 4.8, section *4.5.1*), which is generated in response to blue (λ_{max} 464nm, FWHM 28nm) light. Data for all species obtained from present study. Also given is the maximum frequency the eyes of each species were capable of responding to with a sinusoidal ERG response of the same frequency (max. resolvable frequency, stimulating light has λ_{max} of 488nm), the phase angle of the visual response relative to the sinusoidal stimulus modulating at a frequency of 1Hz (Δp1) and information on the daytime depth range and bioluminescent capability of each species ([1]Foxton, 1970; [2]Hopkins *et al.* 1989)

Oplophorus spinosus

The maximum frequency of sinusoidal stimulus (blue light, λ_{max} 488nm, FWHM *ca.* 10nm) to which the eye of *Oplophorus spinsosus* will respond with a resolvable sinusoidal ERG response, is 15Hz. This is the fastest stimulus frequency an eye responds to in this study, and only the eyes of *O. spinosus* and *Acanthephyra purpurea* were capable of resolving a frequency this high.

Table 4e indicates that *Oplophorus spinosus* is the shallowest living species of the four in this study, and consequently it will inhabit the brightest optical environment. This can be related to this species also having a relatively high value of k (9.13, *n*=1), and the fact that the threshold response of the eye of this species occurs at relatively high irradiance ($1.58x10^7$ photons s^{-1} cm^{-2}, see Table 4e). Therefore this species has a relatively insensitive eye when compared with the other species in this study and this is accompanied by the ability to resolve the fastest sinusoidal frequencies. This relationship may be expected on the basis of the results of Chapter 3, which determined that for both mesopelagic and shallow-water, coastal decapod species, the least sensitive eyes have the shortest response latencies, and therefore are the 'faster' eyes. This agrees with the findings that diurnal insect species have a better temporal resolving power than arrhythmic or nocturnal species (Howard *et al.* 1984; deSouza and Ventura, 1989;

Laughlin and Weckström, 1993), and a better temporal resolving power in diurnal insects is correlated with a less sensitive visual response due to the abundance of light available during the daytime in a terrestrial habitat.

On the basis of the relationship between visual sensitivity, response latency and optical depth as determined in Chapter 3 for five species of mesopelagic malacostracan, one would expect the photoreceptors in the eye of *O. spinosus* to have a relatively short latency of response. However, the values in Table 4e indicate that the eye of *O. spinosus* has one of the higher phase lags in response to stimuli modulating at 1Hz of the four species. This indicates that the eye of this species may have a slower response latency than *A. purpurea* and *N. gibbosus*. In order to determine if there is a significant difference in the phase relationships between these species, however, one would require recordings from more individuals.

O. spinosus therefore has a relatively insensitive visual response, which is accompanied by a relatively fast frequency response. Both of these properties of the visual response of this species can be related to its shallow daytime depth distribution in the mesopelagic zone and thus the relatively 'bright' environment inhabited.

Systellaspis debilis and *Acanthephyra purpurea*

Systellaspis debilis is one of the deepest living species in this study and shares a similar daytime depth distribution with *Acanthephyra purpurea* (see Table 4e). These two species also have relatively very sensitive eyes, as determined both in this study and in Chapter 3. Table 4e shows that the values of k for *S. debilis* and *A. purpurea* are the lowest of the values for all four species. Similarly, the irradiances that generate a threshold response ($1\%V_{max}$) from the eyes of these two species are comparable and lower than the $1\%V_{max}$ values of the other two species in this study. The physiologically determined value for response threshold for *S. debilis* ($1x10^6$ photons s^{-1} cm^{-2}) is comparable with the average behavioural threshold as determined by Frank and Widder (1994a); this study found that the behavioural response threshold of *S. debilis* (to light of λ_{max} 500nm) occurred at an irradiance of $3x10^6$ photons s^{-1} cm^{-2}.

In the present study, *S. debilis* has the lowest temporal response. For *S. debilis*, the maximum frequency to which the eye will respond to is 7Hz, and the phase lag in the visual response at a

stimulus frequency of 1Hz is 133°, which is the greatest lag of all the species studied. The relationship between a highly sensitive eye and a slow temporal response may be expected on the basis of the results of Chapter 3, which showed that a relatively sensitive visual response is significantly correlated with a relatively long response latency for four mesopelagic decapod species. This indicates that a highly sensitive eye has a 'slow' response, and the results of the present study confirm this for the species *S. debilis*.

S. debilis therefore has a relatively sensitive visual response, which is accompanied by a relatively slow frequency response. These properties of the visual response can be related to the deep daytime depth distribution of *S. debilis* and thus the relatively 'dim' environment inhabited.

For the species *A. purpurea*, despite having both a relatively sensitive visual response and a daytime depth distribution similar to that of *S. debilis*, the maximum frequency of stimulus that the eye will resolve is 15Hz. Thus this species has one of the highest temporal resolving powers of the species in this study and this is accompanied by a relatively small amount of lag in the visual response to stimuli modulating at 1Hz. The results of Chapter 3 indicate that these two species have response latencies that are not significantly different, and the same may be true of the phase lag in the visual responses at 1Hz, but recordings from more individuals would be required to determine this.

For *A. purpurea* there is no apparent relationship between visual sensitivity, daytime depth distribution and frequency response of the eye. Although visual sensitivity is intrinsically linked to temporal resolving power (Laughlin, 1981; Laughlin, 1990; Weckström *et al.* 1991; Laughlin and Weckström, 1993; Weckström and Laughlin, 1995), the temporal resolving power of an eye can be related to the behavioural requirements of an animal. The study of Laughlin and Weckström (1993) shows a difference in the frequency response of the 'slow' photoreceptors of tipulids (crane flies) and the 'fast' photoreceptors of blowflies, despite these terrestrial arthropod species inhabiting similar photic environments. The difference in photoreceptor speed between these animals is attributed to the difference in their visual requirements: tipulids are slow moving with long legs that prevent rapid turning during flight, and blowflies are small, fast animals with the ability to perform elaborate aerobatics. Laughlin and Weckström (1993) also describe the sexually dimorphic temporal resolving power of the

photoreceptors of bibionids (march flies). The males have an enlarged dorsal eye adapted to detect and track females (Zeil 1983, cited in Laughlin and Weckström, 1993) and these enlarged eyes have photoreceptors with a higher temporal resolving power than those of the females to aid the resolution required to efficiently track females as they move across the visual field (Laughlin and Weckström, 1993). The differences in the temporal resolving power of the photoreceptors of these terrestrial arthropod species are attributed to differences in the distribution of voltage-gated conductances in the photoreceptor membranes (Laughlin and Weckström, 1993; Weckström and Laughlin, 1995). The faster photoreceptors are commonly found to possess delayed-rectifier potassium channels that enable rapid response dynamics by reducing the membrane time constant of the photoreceptor. This is a metabolically expensive strategy however, and consequently the advantages of a high frequency response must justify the need for a fast eye (Laughlin and Weckström, 1993; Weckström and Laughlin, 1995).

It is possible therefore, that some aspect of the behaviour of *A. purpurea* requires that the eyes have a faster temporal resolving power than those of its oplophorid 'neighbour' *S. debilis*. Table 4e indicates that the oplophorids *S. debilis* and *O. spinosus* possess photophores and these may be used in congener recognition, conspecific mating and camouflage through counterillumination (described in section *1.3.1*). The species *A. purpurea* produces a defensive bioluminescent secretion ('spew') to startle predators but does not possess photophores, and therefore will not be involved in conspecific signaling and thus require a better resolution of vision for that purpose. Both *O. spinosus* and *S. debilis* possess photophores and are thus concerned with conspecific signaling, and yet have temporal resolutions that are correlated with the visual requirements imposed by their daytime depth distribution.

It is possible that an eye with a relatively high temporal resolving power combined with a high spatial resolution would have the resolution required to visualise individual photophore emissions from the ventral surface of an animal attempting to use counter-illumination to camouflage its presence in the water. This could provide an explanation for the relatively high temporal resolving power of *A. purpurea* if it had a preference for a prey species that used counter-illumination to avoid predators from beneath. However, it is unlikely that the eye of *A. purpurea* has a high spatial resolution as measurements from the eyes of the deepest living mesopelagic species show spatial resolution is low to allow a wider effective aperture for the collection of photons (see Herring and Roe, 1988 for a review).

A. purpurea is a strong vertical migrator (Shelton *et al.* 1992) and thus ascends to shallower depths after sunset to feed. The higher temporal resolution of the eyes of *A. purpurea* may allow this animal to track silhouettes of prey items near the water surface at night, or equally silhouettes of prey items which occur higher in the water column during the day. A higher temporal resolution will prevent smearing of spatial detail within the visual image as it moves across the visual field. Land (1992) showed in behavioural studies, that both mesopelagic hyperiid amphipod species and euphausiid species actively track dark objects above them in the water. Similarly, the higher temporal resolution of the eye of *A. purpurea* may enable it to track bioluminescent prey items more efficiently in the water. A relatively sensitive eye will provide high contrast sensitivity between an object and its background (Laughlin, 1981), and high sensitivity accompanied by a relatively high temporal resolving power, will optimise the visualization of moving objects in the environment. If this is the case it is possible that the photoreceptors of *A. purpurea* may have voltage-gated conductances similar to those found in terrestrial arthropod species, which allow a reduction in the membrane time constant in order to increase the speed of their response. However, as this is likely to be a metabolically expensive strategy, the benefits of a faster temporal resolution would need to outweigh the disadvantages of the high-energy expenditure required.

Notostomus gibbosus

Table 4e shows that *Notostomus gibbosus* has a daytime depth distribution that extends to the greatest depth of all the species in this study.

The value of k determined for *N. gibbosus* is the highest in this study (k = 9.31, see Table 4e), as is the irradiance that generates a threshold response ($1\%V_{max}$) from the eye (7.08×10^{7} photons s^{-1} cm^{-2}) of this species. Consequently, *N. gibbosus* has a relatively insensitive eye in comparison with the other species studied. This is supported by the behavioural study of Frank and Widder, (1994b) which determined that the average behavioural threshold of *N. gibbsosus* to 500nm light was in response to irradiance levels of 3.8×10^{7} photons s^{-1} cm^{-2}. Frank and Widder (1994b) indicate that, despite *N. gibbosus* having the deepest reaching daytime depth distribution of all the five mesopelagic species in their study, it had the least sensitive behavioural response to 500nm light. Consequently Frank and Widder (1994) conclude that *N.*

gibbosus has a relatively insensitive visual response; and the results of the present study confirm this.

The results of the present study show that the maximum frequency of sinusoidal stimulus that will generate a resolvable response from the eye of *N. gibbosus* is 10Hz. This puts the frequency response of *N. gibbosus* at intermediate levels in comparison with the frequency responses of the other species in this study. The phase lag in the visual response of this species to stimuli modulating at 1Hz is the least of all the species in this study. Therefore it seems that the faster eye of *N. gibbosus* is related to a less sensitive visual response and these results agree with those of Chapter 3, which indicate that a less sensitive visual response in mesopelagic species is accompanied by a shorter response latency. There does not appear to be a relationship between daytime depth distribution and visual sensitivity for *N. gibbosus*, but the depth distribution of this species given in table 4e was determined for Jerlov type IA water and the animals used in this study were obtained from Jerlov type II water, which is less transparent. Therefore, the depth distribution of *N. gibbosus* in the region of the Cape Verde Islands needs to be determined before visual sensitivity and depth distribution can be accurately related.

Although this may be the case, the results of this study will be considered in relation to the depth distribution given for *N. gibbosus* in Table 4e. Using these ecological data it would seem that whilst relative sensitivity, temporal resolution and phase lag in the visual response are related for this species, these factors are not related to its daytime depth distribution. The depth distribution of this animal indicates that it inhabits the most photon-limited environment with respect to downwelling light of all the species studied.

N. gibbosus does not possess photophores and therefore, as described for *A. purpurea*, its relatively insensitive eye with a relatively fast frequency response cannot be adapted for resolving conspecific bioluminescent signals. Similarly, as for *A. purpurea*, it is unlikely that the eye of *N. gibbosus* will have the spatial resolving power that would be required to resolve individual photophore emissions from the ventral surface of an animal using counterillumination to camouflage its presence in the water column.

Interestingly, Frank (1999) found that the critical flicker fusion frequency (CFFF, see section *4.6.4* for details of this methodology) of two euphausiid species, *Nematobranchion flexipes* and *N. sexspinosus* were unusually high, and higher than that of another shallower living euphausiid species, *Stylocheiron maximum*. This high CFFF was accompanied by a relatively insensitive visual response in comparison with *S. maximum* despite both *N. flexipes* and *N. sexspinosus* having a deeper depth range than *S. maximum*. The author attributes this to the difference in prey items between the three species, *S. maximum* preys on nonbioluminescent prey in the waters from which it was collected, whereas both *N. flexipes* and *N. sexspinosus* feed on bioluminescent prey, and so it is concluded that the advantages of a higher temporal resolution may outweigh the advantages of a highly sensitive eye for animals which prey on bioluminescent animals. This is a plausible conclusion when one considers that viewing bioluminescent emissions against a dim background provides a high level of contrast between the object of interest and the background. Thus, reducing visual sensitivity and therefore contrast sensitivity (Laughlin, 1981), is less important for an animal that is primarily 'interested' in viewing bioluminescence. It is possible, therefore that despite the photon-limited depths inhabited, the intermediate frequency response and relative insensitivity of the eye of *N. gibbosus* as determined here and in Frank and Widder (1994b) (quantified behavioural response threshold to downwelling light) are an adaptation to hunting bioluminescent prey. Unfortunately there is no information on the prey preferences of *N. gibbosus* at present.

Consequently, the light environment that *N. gibbosus* inhabits does not provide an explanation for the relatively high frequency response and low visual sensitivity determined for this species. It is probable, therefore, that the relatively higher frequency response of *N. gibbosus* is an adaptation to hunting bioluminescent prey.

4.6.6 The Temporal Resolving Power of Mesopelagic Oplophorid Malacostracans

The eyes of all the mesopelagic species in this study have response properties that are analogous to a low-pass filter in that the eyes will not process high frequency information (i.e. high frequency components are filtered out). Autrums' work in the 1950s indicated that slow compound eyes are generally associated with a high sensitivity and this was compared with analogue measuring devices which are generally used in conjunction with a low pass filter at

high sensitivity settings to provide a workable signal-to-noise ratio (cited in Laughlin, 1981). The temporal properties of bioluminescent emissions have not been studied in terms of their frequency components, but it is unlikely that bioluminescent signals are emitted at a repetition frequency greater than 10-12Hz (Herring, P. J. pers. comm.). Therefore an eye with photoreceptors that have low pass temporal response properties is well adapted to following the flash rate of a bioluminescent signal. However, the rate of rise of a bioluminescent flash is likely to contain high frequency components that may be beyond the 'cut—off frequency' of the eye. Consequently, bioluminescent signals that consist of pulse trains of light for example, are probably not perceived as discrete, rapid pulses of light, but as a constant light signal that modulates in intensity.

A low temporal response is not comparable to a decrease in spatial resolution, which increases photon catch at the expense of resolution (see section *1.5.6* for detail). A slower temporal resolution does not increase photon catch; it simply allows sampling of the photon signal over a longer time interval, which improves the signal-to-noise ratio of an image under photon-limited conditions. Therefore, as Laughlin (1981) indicates, a poor temporal resolution is not an advantage, but a by-product of improving sensitivity in low light conditions. For mesopelagic animals a high visual sensitivity is important and this is accompanied by a low temporal response for the species *Systellaspis debilis*. The species *O. spinosus* and *N. gibbosus* have relatively high frequency responses and these are accompanied by relatively insensitive visual responses (relative to the other mesopelagic species in this study). The species *A. purpurea* may require the advantage of a relatively higher temporal resolving power and relatively high visual sensitivity for optimising vision with respect to moving objects in its environment.

In order to ultimately determine the efficiency with which eyes of mesopelagic species will detect visual targets moving across the visual field information on both the temporal resolving power of the eye and the spatial resolution of the eye is required (Glantz, 1991). In compound eyes, spatial resolution is determined by interommatidial angle (the angle between the ommatidia in the eye), the smaller the interommatidial angle the greater the resolution of fine detail within a visual image (Snyder, 1979). For the superposition eyes of photon-limited mesopelagic malacostracans, which are adapted to high sensitivity, a trend is seen towards large eyes with large effective apertures to increase photon catch. Measurements of the interommatidial angles of the eyes of certain mesopelagic species have revealed that these

angles are large relative to shallow water species (e.g. Land, 1984, Shelton and Gaten, 1996). Consequently mesopelagic species have generally poor spatial resolving power, and this is accompanied by a low temporal resolving power. Thus, it seems probable that the eyes of mesopelagic species have overall low resolution.

4.6.7 Summary of Conclusions

a) The results of this study reveal that the frequency response of the eyes of both *Systellaspis debilis* and *Oplophorus spinosus* is related to the relative sensitivity of the visual response and the daytime depth distribution of each species. This could be expected on the basis of the results of electrophysiological studies of other invertebrate species in which the photoreceptor response dynamics have been found to be tuned to the light environment inhabited.

b) The results of this study indicate that neither the frequency response nor the relative sensitivity of the eyes of *Notostomus gibbosus* is related to the daytime depth distribution of this species (although daytime depth distribution for the region of the Cape Verde Islands needs to be confirmed). It is possible, therefore, that the eyes of *N. gibbosus*, which have a relatively insensitive response and an intermediate frequency response, are adapted for the detection of bioluminescent prey.

c) The frequency response of *Acanthephyra purpurea* is not related to either the relative sensitivity of the eye or the daytime depth distribution of this species. The eyes of *A. purpurea* have one of the highest relative sensitivities in this study, and yet the frequency response of the eye suggests that this species has a similar temporal resolving capability as the relatively insensitive eye of *O. spinosus*. It is possible that this species has eyes adapted to detecting bioluminescent prey and that this is very important in terms of this animal's visual ecology, as it is likely to involve a metabolically expensive strategy.

d) The photoreceptors of the mesopelagic oplophorid species studied here appear to have low temporal resolving power when compared with terrestrial arthropods and may be described as low pass filters.

e) The frequency response methodology used in this study is unsuitable for determining the dark-adapted temporal properties of the highly sensitive eyes of mesopelagic malcostracans in ship-board laboratories, as it does not allow one to

obtain responses over the entire frequency range desired, and the length of the experiments prevent one from obtaining data from a sufficient sample size.

4.6.8 Considerations for Future Work

The use of a more suitable method for determining the temporal resolution of the photoreceptors of mesopelagic species, given that they are likely to deteriorate once in an electrophysiogical preparation, and that the eyes are highly sensitive to prolonged exposure to light. An alternative method must enable the recordings to be made quickly and in a manner suitable for a moving vessel. Chapter 5 presents the results of an alternative method in determining temporal resolution and compares the resolving power of the photoreceptors of mesopelagic species with that of coastal species.

Electrophysiological determination of the spatial resolving power of the photoreceptors of the same mesopelagic species would enable a complete description of the response of the eye to moving stimuli. Glantz's (1991) study of the photoreceptors of the crayfish (*Procambarus clarkii*) indicates that the ratio of the time constant of the photoreceptor to the acceptance angle of the ommatidium will determine the sensitivity of the eye to variations in stimulus velocity (see section *6.4.2*).

Intracellular investigation of the photoreceptor response will enable the determination of the photoreceptor signal-to-noise ratio and consequently the absolute frequency response capabilities of the photoreceptors of these mesopelagic species. These investigations would also allow one to determine whether there are differences in the voltage-gated membrane conductances of these mesopelagic species, which could further explain the differences in temporal resolution between these species.

CHAPTER 5: TEMPORAL RESOLUTION OF THE VISUAL SYSTEMS OF MARINE MALACOSTRACANS – THE IMPULSE RESPONSE METHOD

5.1 INTRODUCTION

Chapter 5 of this thesis investigates the temporal resolving powers of the eyes of four mesopelagic malacostracan species and two shallow-water, coastal malacostracan species. The temporal resolving powers of the eyes of these species are determined using the impulse response method (see section *5.1.1* of this introduction). The results of this study are considered in relation to the visual ecology of the animals studied.

Section *4.1* describes the effect that photoreceptor response dynamics have on vision and the reader is referred to section *4.1.1* for a review of photoreceptor response dynamics in relation to the light environment.

5.1.1 Measuring the Temporal Response of Invertebrate Photoreceptors using the Impulse Response Method

In order to physically characterise the input-output properties (or transfer function) of a system, one is required to take measurements of the responses of that system to a potentially infinite number of inputs and this is not a practical approach when dealing with biological systems. It is possible, however, to reduce the time taken to collect measurements by using impulse stimuli to excite impulse responses from the given system. A unit impulse is defined as an impulse of infinite amplitude and zero width, and is also referred to as the Dirac Delta function which is given by:

$$\int_{-\infty}^{\infty} f(t)\delta(t)dt = f(0)$$

$\delta(t)$ is defined as the unit impulse and always has infinite amplitude but finite or unit area, so it must have zero duration in time:

$$\int_{-\infty}^{\infty} \delta(t)dt = f(1)$$

A unit impulse contains all frequencies and this can be confirmed *via* the Fourier transformation (see below) of a unit impulse. Obviously such a stimulus is not physically realisable, and consequently, in practice, nearly instantaneous impulses are used to obtain impulse responses from systems. An 'essentially instantaneous' impulse will contain a broadband frequency signal, the frequency components of which may be determined through Fourier analysis.

The Fourier theory states that any periodically repeating signal, no matter how irregular, may be decomposed to reveal that the original signal is a composite of pure sines and cosines (see Fig. 5.1). All waveforms are made up exclusively of specific sines and cosines with varying amplitude and phase relations.

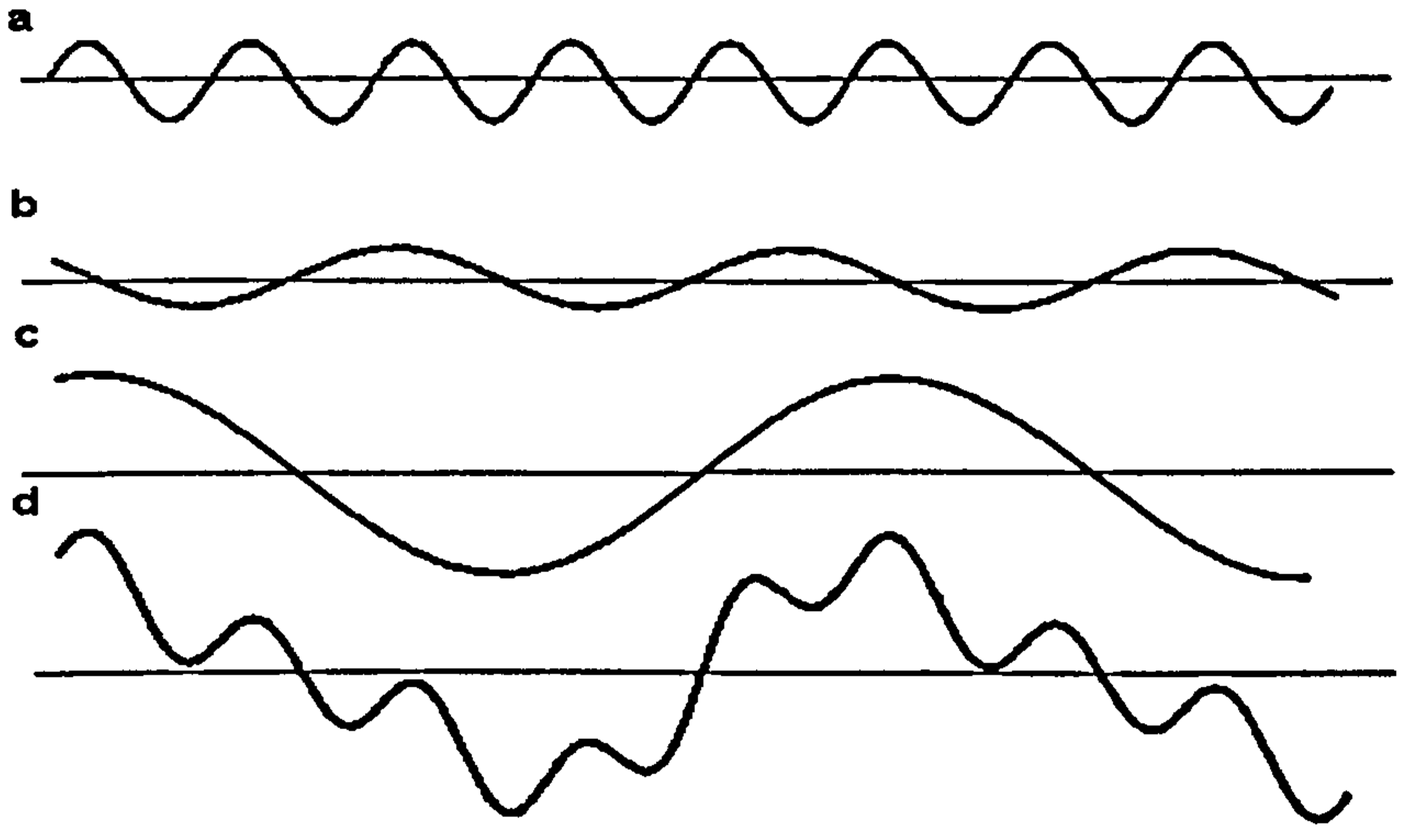

Figure 5.1. A diagrammatic representation of the decomposition of a waveform into its constituent frequency components. The function shown at the bottom (d) is composed of the three above it. Fourier transform analysis expresses a given function in the frequency domain and thus reveals the frequency components (a, b and c) of the function (redrawn from Hubbard, 1996)

A function that is expressed in the time domain contains information on the time of occurrence and duration of an event, but no information regarding the frequency components within the function. At the simplest level, Fourier analysis transforms a function expressed in the time domain to express it in the frequency domain, thus revealing the frequency components of the

function. This is a commonly used tool in digital signal processing and can be used to extract a signal from background noise in circumstances of a low signal-to-noise ratio. The Fourier transform may also be used to extract frequency information from non-periodic functions such as impulse responses. A non-periodic function, i.e. a function that decreases sufficiently rapidly at infinity such that the area under its graph is finite, may also be described in terms of a superposition of sines and cosines (Hubbard, 1996).

The application of a unit impulse stimulus to a system provides a stimulus containing broadband frequency information (transient stimuli contain all frequencies); the Fourier transform of a unit impulse (as given by the Dirac Delta function) equals 1 for all frequencies. Consequently, an 'essentially instantaneous' pulse will also contain broadband frequency information (although there will be some restriction in bandwidth) in which the frequency components are of equal amplitude. The impulse response generated from such a stimulus in the time domain may be Fourier transformed and presented in the frequency domain, the Fourier transform yielding the magnitude of the response of a system as a function of frequency. As the impulse stimulus contains broadband frequency information, the Fourier transform of the impulse response will report the response of the system to a range of given frequency inputs.

The impulse response functions of the photoreceptors in an eye can be determined electrophysiologically to provide information on the temporal resolving powers of individual photoreceptors (via intracellular electrophysiology), or equally it can be used to provide information on the temporal response of all the photoreceptors in the eye (extracellular recording of the ERG). This methodology has been applied to the visual systems of animals e.g., the locust (*Schistocerca gregaria)* and the cricket (*Acheta domesticus*; Pinter, 1972); the locust (*Locusta migratoria*; Howard, 1981); various species of insect (Howard *et al.* 1984); the crayfish (*Procambarus clarkii*; Glantz, 1991); various dipteran species (Laughlin and Weckström, 1993).

The impulse response of a time-invariant linear system can provide information on the response of the system to any given input when subjected to linear systems analysis. A time-invariant linear system must obey the principles of superposition i.e. if the input to the system is a linear combination of signals, then the output is the linear combination of the responses to each

signal. However, photoreceptors are only linear over very small input ranges (Laughlin, 1981; Glantz, 1991) and consequently it is difficult to make inferences about their output over their entire response range on the basis of a response to a stimulus of a given light intensity. The impulse response of a photoreceptor/eye, however, generated in response to an impulse stimulus of a given irradiance is useful in determining the temporal properties of the photoreceptor/eye in response to the given stimulus irradiance.

Using the impulse response functions of the eyes of marine malacostracans to determine temporal resolving power has distinct advantages over using the frequency response methodology as described in Chapter 4. The impulse stimulus is easy to produce (a simple pulse of light of short duration), easy to average and responses from the eye may be obtained quickly (which is particularly important when dealing with mesopelagic animals which are rarely robust), see Laughlin (1981) for a review. Providing one is operating within a similar intensity-response range of the visual response (i.e. stimulating the eye with a similar level of irradiance), the impulse response from the eye will contain the same frequency information as can be obtained using the frequency response method. Pinter (1972), Howard (1981) and Glantz (1991) all demonstrate (using both the frequency response technique and the impulse response technique on a single preparation) that the Fourier transform of the impulse response from the eye agrees with the frequency response of the eye which is obtained by measuring the responses of the eye to sinusoids of varying frequencies (see section *4.1.3*).

5.1.2 Aims of This Study

The purpose of this study is to obtain comparative information of the temporal resolution of the eyes of species of mesopelagic and shallow water (coastal), nocturnally active, malacostracans through the use of the impulse response method. This study uses extracellular electrophysiology and thus measures the ERG impulse response to brief pulses of light. Previous studies of the temporal resolving powers of the eyes of mesopelagic malacostracans are few, (see section *4.1.2*) and no previous study of the visual response of these animals has used the impulse response function to describe temporal resolving power.

The species used in this study are the same as those used in the study of visual sensitivity reported in Chapter 3. Therefore this study aims to: a) determine the temporal resolution of the

eyes of mesopelagic species with differing depth distributions and compare them; and b) determine the temporal resolutions of the eyes of shallow water, nocturnally active, species in order that they can be compared with those of the mesopelagic species, and to determine the extent to which temporal resolution is correlated with the visual ecology of these animals. The results of Chapter 3 indicate that the deepest living mesopelagic species studied have the most sensitive visual response, it could be expected therefore, that these species will also have the lowest temporal resolution.

The following hypotheses were tested:

1 That the temporal resolutions of all species will be related to visual sensitivity, i.e. visual sensitivity is the primary factor in determining temporal resolution.
H_0 = temporal resolution will not be related to visual sensitivity.

2 That mesopelagic malacostracan species which inhabit greater depths during the daytime will have a lower temporal resolution than those species with a shallower daytime depth distribution.
H_0 = there will be no difference in temporal resolution between the mesopelagic species studied regardless of their daytime depth distribution.

3 That shallower living mesopelagic malacostracans will have a temporal resolution different to that of shallow water, coastal nocturnally active, malacostracans.
H_0 = there will be no difference in temporal resolution between shallow water, nocturnally active and mesopelagic malacostracans.

5.2 MATERIALS AND METHODS

5.2.1 Protocol for ERGs on Mesopelagic Malacostracans

Details of animal collection and maintenance are given in Chapter 2 section *2.2.1.1*. Four species of mesopelagic malacostracan from three locations (Northwest Providence Channel, Bahamas; Oceanographers Canyon, Gulf of Maine; and Wilkinsons Basin, Gulf of Maine) were used in this study. Table 5a presents details of the animals from which the data in this study were obtained.

Order	Family	Species	*n*	Daytime Depth (m)	Bioluminescence	Water Type[4]
Euphausiacea	Euphausiidae	*Meganyctiphanes norvegica*	5	300-500[1]	photophores	IB
Decapoda	Oplophoridae	*Systellaspis debilis*	4	650-950[2]	photophores spew	IA
	Sergestidae	*Sergestes arcticus*	6	450-600[1]	photophores	IB
	Pasiphaeidae	*Pasiphaea multidentata*	3	220-240[3]	—	IB

Table 5a. Details of adult mesopelagic malacostracans used in this study, information includes: taxonomy; *n*, number of individuals of each species studied; approximate daytime depth distribution for each species; bioluminescent capability; water type inhabited. [1]Sardou *et. al.* 1996; [2]Foxton, 1970; [3]Frank and Widder, 1997; [4]Jerlov, 1976.

5.2.1.1 Animal handling and preparation

See Chapter 3 section *3.2.1.1*

5.2.1.2 Electrical recording

Electrophysiological recording of the electroretinogram is described in section *2.2.2.1*, and the same procedure was followed in all cases.

5.2.1.3 Optical apparatus

The optical apparatus used in this study does not differ to that used in the study of Chapter 3 (see section *3.2.1.3*)

5.2.1.4 Experimental Procedure

In Chapter 3 of this study, the relative sensitivities of the eyes of *Meganyctiphanes norvegica*, *Systellaspis debilis*, *Sergestes arcticus* and *Pasiphaea multidentata* were determined. This involved measuring ERGs from the eyes in response to light stimuli of varying irradiances and led to the construction of a VlogI curve for each species (see section *3.2.1.4* for details of methodology).

Determination of the VlogI relationship of the dark-adapted eye allows the identification of the 50%V_{max} point (the irradiance at the eye that generates a response from the eye which is 50% of the maximum response possible, also referred to as k, see Chapter 3 for detail), which falls within the centre of the sigmoidal relationship between log irradiance and response amplitude (section *3.4.1*, figs 3.7 & 3.8, indicate the location of k within the VlogI relationship of the dark-adapted eyes of the mesopelagic malacostracan species studied here). Consequently, for the purpose of obtaining impulse response ERGs from the eye, the irradiance of the optical stimulus at the eye was controlled such that it generated a response from the eye that was close to the 50%V_{max} response, as determined in Chapter 3. This ensured that the impulse responses for each species were obtained from the mid-range of the visual response and were comparable between species.

Once fully dark-adapted (see section *3.2.1.4* for detail of procedure), the preparation was only used providing that the eye produced a defined criterion response; i.e. set as a response with a peak amplitude at least 20μV above the background noise (see Fig. 5.2, section *5.4.1* for examples of impulse response waveforms).

Impulse responses were obtained from the dark-adapted eye in response to 1.4ms pulses of light with a constant irradiance that generated a response that was 50% of the maximum (50%V_{max}, see above). Individual 1.4ms pulses were used to stimulate the eye at two minute intervals. The two minute interval ensured that the eye remained in a stable adaptation state, and thus retained its

sensitivity to the light stimuli of constant irradiance (see section *3.2.1.4* for detail). Only ERG responses that returned to the pre-stimulus DC level were accepted as impulse responses (see below for detail of circumstances under which the response would not return to the pre-stimulus level). A total of 30 impulse responses were obtained from one eye of each animal studied, to allow for averaging of the response.

In each experiment, a number of extrinsic factors could introduce distortions or artefacts into the ERG signal. For example, during rough weather, ship pitch and roll could have a significant effect on the shape of the ERG signal. Personal observation of ship-roll generally coincided with an observed distortion or artefact in the ERG signal similar to that displayed in section *3.2.1.4*, Fig. 3.5. In the event of the ERG response failing to return to the pre-stimulus baseline as shown in section *3.2.1.4*, Fig. 3.5b, the ERG response was rejected.

Acquisition of the ERG data, via a digital oscilloscope, is described in section *2.2.2.1*.

5.2.2 Protocol for ERGs on Shallow-water, Coastal Malacostracans

Details of animal collection and maintenance are given in Chapter 2, section *2.2.1.2*. Data were obtained from two species of coastal malacostracan from one location (University Marine Biological Station Millport [UMBSM] Millport, Isle of Cumbrae, Scotland), details of the species from which the data used in this study were obtained are given in Table 3b section *3.2.2* with the exception that in the present study there were ten individuals of *Crangon crangon* used.

5.2.2.1 Animal handling and preparation

See Chapter 3 section *3.2.2.1* for detail.

5.2.2.2 Electrical recording

Electrophysiological recording of the electroretinogram is described in section *2.2.2.1*, and the same procedure was followed in all cases.

5.2.2.3 Optical apparatus

The optical apparatus used in this study does not differ to that used in the study of Chapter 3 for (see section *3.2.2.3*)

5.2.2.4 Experimental procedure

In Chapter 3 of this study, the relative sensitivities of the eyes of *Crangon crangon* and *Palaemon elegans* were determined, and consequently the VlogI relationships (see figs 3.11 & 3.12, sections *3.4.2 & 3.4.3*), were used to identify the irradiance required to generate a response from the eyes that was close to 50%V_{max}. The experimental procedure adopted to obtain impulse responses from the dark-adapted eyes of shallow-water, coastal malacostracans is the same as that described for the mesopelagic species in section *5.2.1.4.*

5.3 DATA ANALYSIS

5.3.1 Time Domain Analysis

A total of 30 impulse response waveforms were obtained from each individual. The analysis was identical for each waveform measured and was performed on the unfiltered waveform data. For each unfiltered impulse response waveform, the mean pre-stimulus voltage level was calculated. The DC level of the trace prior to the application of the stimulus to the eye was averaged, this generally being a mean of 25-30 data points. The mean pre-stimulus level was then set to zero (in order to remove the DC offset in the signal) and the waveform was normalized to its peak amplitude such that the depolarising ERG response ranged between 0 and 1. Each waveform was then fitted with a two parameter lognormal model from Howard *et al.* (1984):

$$v(t) = K \exp[-\{\ln(t/t_p)\}^2 / 2\sigma^2]$$

where $v(t)$ is the voltage impulse response, K is the relative amplitude of the peak of the response (K=1), t is the time after the start of the response (determined using the parameter, d, see below), t_p is the time-to-peak of the response (from the start of the response) and σ is the width, or skew factor of the impulse response, which indicates the ratio between the duration of the impulse response and the time-to-peak (Laughlin, 1996). In order to provide the best fit of the model to the data, it was necessary to determine the time period between the onset of the stimulus and the start of the response, (and this is termed d) in order that t_p would represent the time between the start of the response and the peak of the response. The model was fitted to the data points for each waveform, using Solver (Microsoft Excel 2000), which finds the minimum least squares deviation iteratively until the best fit is found. The best fit was found by varying the parameters t_p, σ and d. The two parameter lognormal model from Payne and Howard (1981) provides an empirical fit to the impulse response of invertebrate photoreceptors (e.g. Payne and Howard, 1981; Howard, 1981; Howard *et al.* 1984; Laughlin, 1996), and in the present study the best fit of this equation to the impulse response functions was found by using the parameter d to force t=0 until the start of the response. The result is a convenient and precise three parameter description of the impulse response which can be used for quantitative interspecies comparison of photoreceptor response dynamics in the time domain.

This method of analysis generated values for the parameters t_p, σ and d for all 30 impulse response waveforms measured from one individual. These values were then averaged to produce mean values of t_p, σ and d for each individual of a species and subsequent averaging of these parameters for each individual produced a set of mean parameters for each species (standard errors are given in section *5.4*). This allowed the construction of a mean lognormal curve of the impulse response function for each species (see sections *5.4.1* and *5.4.2*)

Statistical analysis of the significance of interspecies variation in the values of t_p, d and σ was conducted using univariate analysis of variance (SPSS software version 9.0).

5.3.2 Frequency Domain Analysis

The digital oscilloscope used (HAMEG, model no HM407) captured the impulse responses obtained from the eyes over a maximum period of 2 seconds, and as the digital oscilloscope has a resolution of 2048 data points, the impulse responses were obtained at a maximum sampling rate of 1kHz, i.e:

$$\frac{2048}{2s} = 1024s^{-1} \approx 1kHz$$

The 'three' parameter lognormal model was then fitted to the data points obtained, and mean values for the parameters were used to generate a lognormal curve for each species as described in *5.3.1*. For the purpose of the Fourier transform, the mean parameters were used to generate a lognormal curve at 1ms intervals and the data record was extended to 16384 points by adding zeroes to the end (zero-padding). Consequently each data record had a sampling rate of 1kHz irrespective of the sampling rate at which the signal was digitally stored.

The data record was fast Fourier transformed (FFT) using Matlab software (version 6.0.0.88, release 12) to produce a power spectrum of the frequency components contained in the lognormal fit to the impulse response. The FFT is a faster version of the discrete Fourier transform (DFT) which takes a discrete signal in the time domain and transforms that signal into its discrete frequency domain representation. The formula for the FFT performed by Matlab software is as follows:

$$X(k+1)=\sum_{n=0}^{N-1}x(n+1)e^{-j(2\pi/N)kn}$$

where:

$x(n)$ = point in the input time domain data array

$X(k)$ = point in the output frequency domain data array

N = length of the FFT input data block

k = index to the current output data point

n = index to the imput data array

j = square root of -1

By extending the data record to 16834 data points one is both providing the FFT with a data set that is a power of two, which minimizes the execution time of the FFT, and improving the frequency resolution of the FFT. The frequency resolution (FR) of the FFT is determined as:

$$\mathrm{FR}=\frac{\text{sample rate}}{\text{FFT size}}$$

where, in the present study, the sample rate is 1kHz and the FFT size is 16834, therefore the frequency resolution (FR) is equal to 0.06Hz. This describes the minimum difference in frequency between frequency components that still allows the resolution of two distinct frequency components in the power spectrum of the FFT. In this case the frequency resolution of the FFT power spectrum will be high (at 0.06Hz).

A sampling rate of 1kHz was used as this sets the Nyquist frequency of the signal to 500Hz. The maximum bandwidth of a sampled waveform is determined by its sampling rate and the maximum frequency that can be accurately represented in a sampled waveform is termed the Nyquist frequency. The Nyquist frequency is equal to half the sampling frequency of the signal, and is derived from the Nyquist theorem, which states that the sampling rate must be equal to, or greater than, twice the highest frequency component in the signal. If the frequency component of interest in a signal is more than half the sampling rate at which the signal was obtained, performing an FFT on the data leads to aliasing i.e. the production of artefacts above the Nyquist frequency.

Generally, if the sampling interval is too great, high frequency components are replicated as low frequency components, and this leads to a distortion of the components. Consequently any frequency components above 500Hz in the impulse response signals in this study may be represented as 'extra' frequency components below 500Hz once the signal is analysed using the FFT.

There is no evidence to suggest that any marine malacostracan species has photoreceptors capable of resolving frequencies greater than 500Hz (see Chapter 4, section *4.2.4*). Therefore by using a sampling rate of 1kHz, and consequently a Nyquist frequency of 500Hz, there should be no distortion of the frequency domain representation of the components of the impulse response.

Section *5.1.1* discusses the use of instantaneous impulse stimuli as defined by the Dirac Delta function. Such stimuli are not physically realisable, and consequently in the present study, the impulse stimuli were individual square waves of 1.4ms duration. A stimulus that is not a unit impulse, as defined by the Dirac Delta function, does not contain all possible frequencies at equal amplitude and consequently the impulse stimulus used in the present study was subjected to FFT analysis to reveal the frequency components of equal amplitude within the impulse stimulus used to stimulate the eye (see Fig. 5.5, section *5.4.3* for plot of the power spectrum of the impulse stimulus). The FFT of the impulse response function obtained for each species was divided by the FFT of the stimulus (Boonman, A., pers. comm.) to allow for the fact that the stimulus does not contain infinite frequency information.

5.4 RESULTS

5.4.1 The Three parameter Lognormal Model

The three parameter lognormal model described in section *5.3.1* provides a good fit to the impulse response ERG signals obtained from the eyes of all the species in this study. Fig. 5.2 shows the fit of the model to raw, unfiltered ERG data for each species used in this study, along with the values of the parameters t_p and σ used for each fit of the model. In order to fit the lognormal model to the data it was necessary to determine the time between onset of the light stimulus and the start of the response. This is given as the parameter d for each species.

5.4.1.1 Statistical analysis of parameters

Univariate analysis of variance was performed (SPSS software, version 9.0) to determine interspecies variation in the mean values of the parameters t_p (time-to-peak from start of response), σ (width factor of the impulse response) and d (response latency) for all the species tested (both mesopelagic and coastal). Interspecies variation in the parameter t_p was highly significant, $F_{5,30}=17.9$, $p<0.0005$, as was interspecies variation in the parameter d, $F_{5,30}=27.7$, $p<0.0005$. Interspecies variation in the parameter σ, however, was found to be non-significant, $F_{5,30}=2.4$, $p=0.059$. Post hoc Tukey tests were also used to perform pairwise comparisons of the means for each species group, and the significance of difference for values of t_p, σ and d between species is given in appendices IV, V and VI respectively. The residuals for t_p, σ and d were tested for normality using the Kolmogorov-Smirnov test. In all cases the residuals did not significantly depart from normal distribution ($p>0.05$).

5.4.2 Comparison of the Impulse Responses of Malacostracan Species in the Time Domain

Fig 5.3a shows the plots of the lognormal curves, or impulse response functions, of the eyes of all the species used in this study. These impulse response functions are generated from the means of the parameters t_p, σ and d (see section *5.3.1* for detail of how the means were obtained). The mean values of the parameters t_p, σ and d are given in Table 5b.

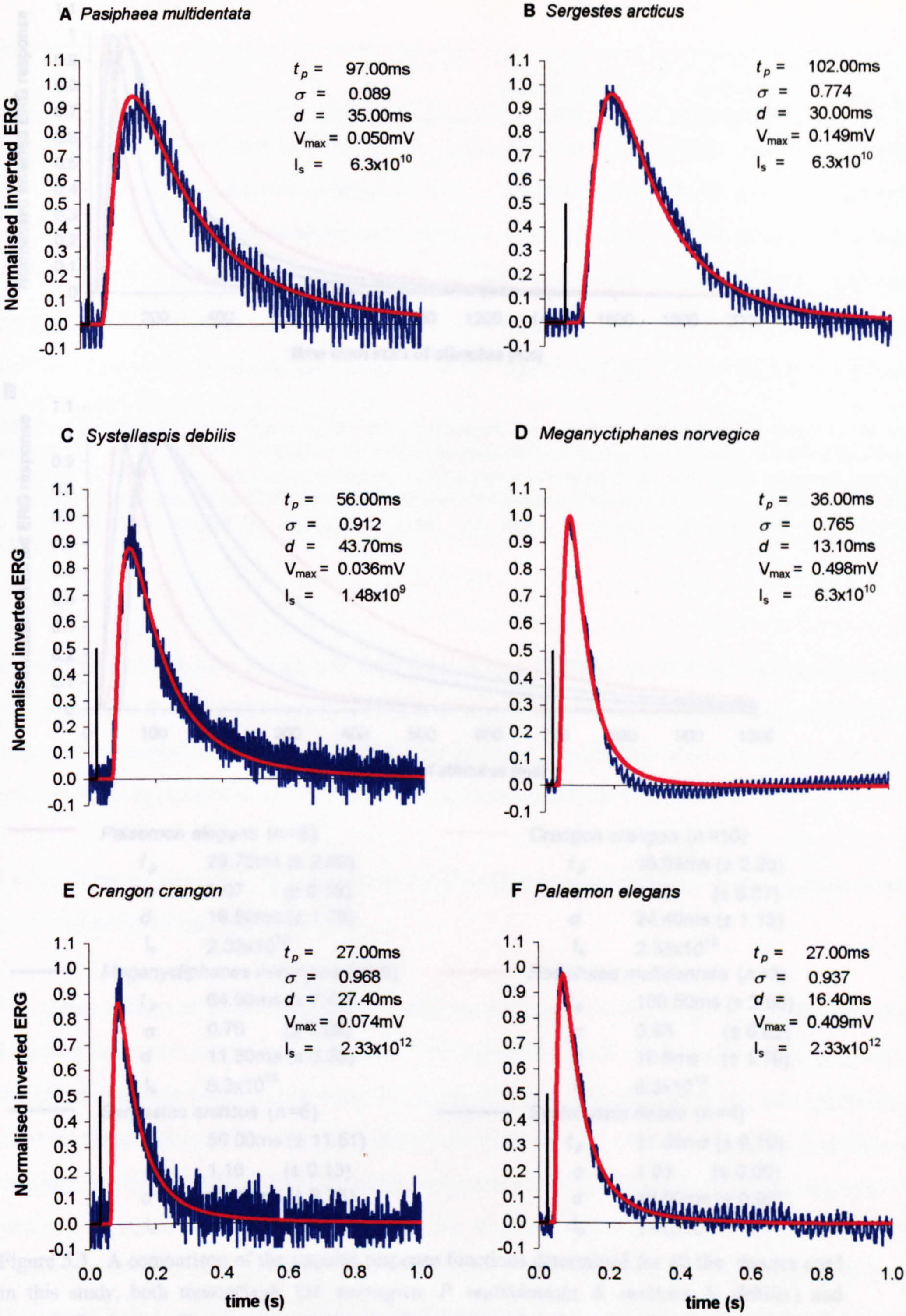

Figure 5.2. Typical, inverted and unfiltered impulse response ERGs (blue trace) from each species used in this study. Impulse responses were obtained in response to a 1.4ms pulse of light (λ_{max} 464nm) and this is represented by the vertical black line at the left-hand side of each plot. The red line overlaying each impulse response is the fit of the two parameter lognormal model shown in section *5.3.1*. The inset for each plot displays the values of the three parameters t_p, σ and d used to fit the lognormal curve shown; V_{max} is the voltage amplitude of the ERG response; I_s is the irradiance at the eye of the 1.4ms pulse used.

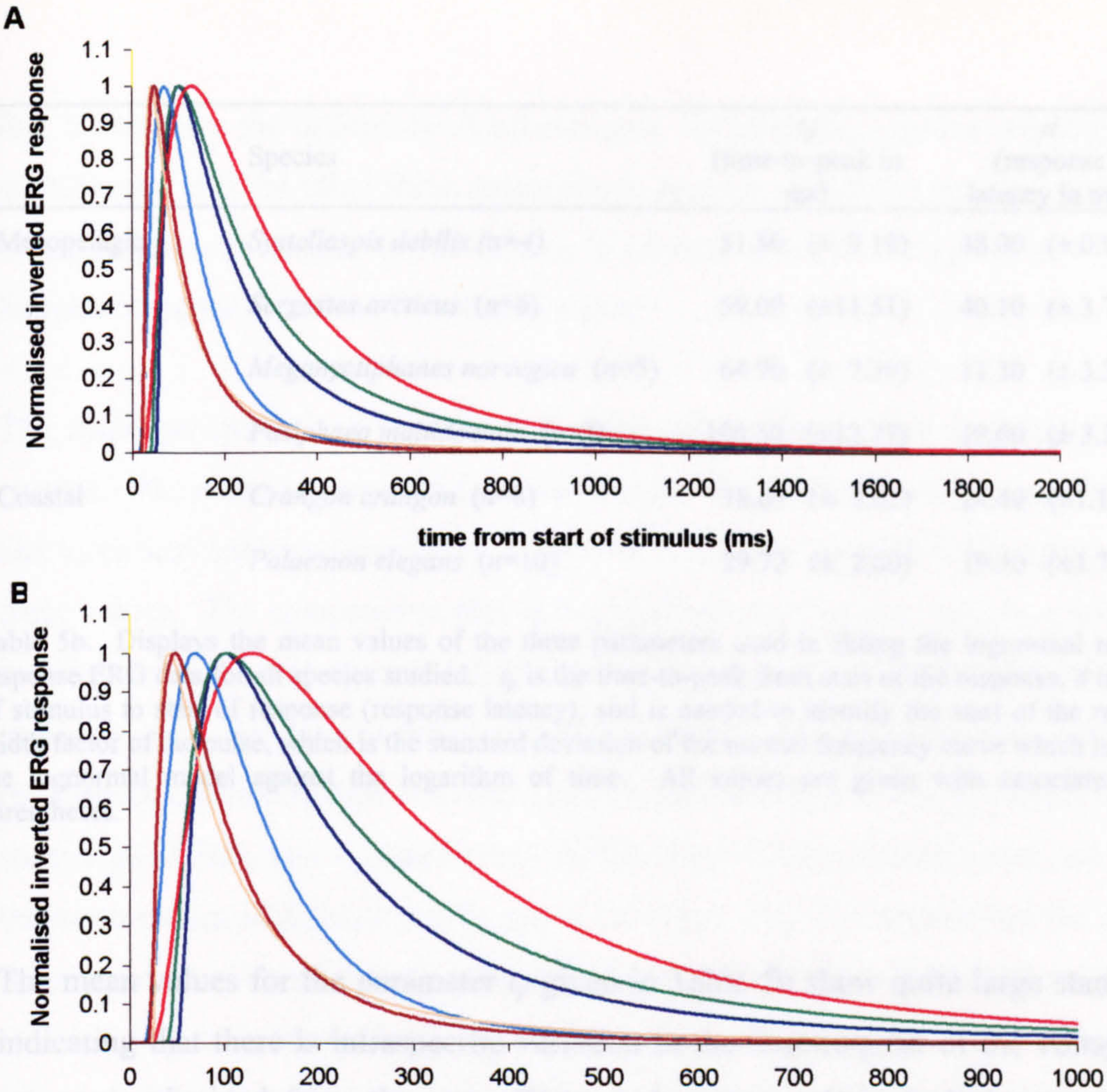

Palaemon elegans (n=8)

t_p	29.72ms (± 2.60)
σ	1.07 (± 0.13)
d	19.50ms (± 1.79)
I_s	2.33×10^{12}

Crangon crangon (n=10)

t_p	18.69ms (± 2.20)
σ	1.23 (± 0.07)
d	24.40ms (± 1.13)
I_s	2.33×10^{12}

Meganyctiphanes norvegica (n=5)

t_p	64.90ms (± 7.40)
σ	0.76 (± 0.09)
d	11.30ms (± 3.33)
I_s	6.3×10^{10}

Pasiphaea multidentata (n=3)

t_p	106.50ms (± 2.60)
σ	0.93 (± 0.02)
d	19.6ms (± 1.79)
I_s	6.3×10^{10}

Sergestes arcticus (n=6)

t_p	59.00ms (± 11.51)
σ	1.16 (± 0.13)
d	40.10ms (± 3.75)
I_s	6.3×10^{10}

Systellaspis debilis (n=4)

t_p	51.80ms (± 9.19)
σ	1.03 (± 0.09)
d	48.00ms (± 0.96)
I_s	1.48×10^{9}

Figure 5.3. A comparison of the impulse response functions determined for all the species used in this study, both mesopelagic (*M. norvegica, P. multidentata, S. arcticus, S. debilis*) and coastal (*P. elegans, C. crangon*). A) the impulse response functions are plotted over a timescale of 2s to display the full function; B) the impulse response functions are plotted over a timescale of 1s to allow examination of the timescale of the events at the beginning of the functions. The impulse response functions were determined as according to section *5.3.1*. The plots are accompanied with details of both the mean values of t_p, σ and d and the value of I_s, which is the irradiance at the eye of the 1.4ms light pulse (λ_{max} 464nm) used to generate the original ERG impulse responses from the eyes. The light pulse stimulus occurs at time 0.

	Species	t_p (time-to-peak in ms)	d (response latency in ms)	σ (width factor)
Mesopelagic	*Systellaspis debilis* (n=*4)*	51.80 (± 9.19)	48.00 (± 0.96)	1.03 (±0.09)
	Sergestes arcticus (*n*=6)	59.00 (±11.51)	40.10 (± 3.75)	1.16 (±0.13)
	Meganyctiphanes norvegica (*n*=5)	64.90 (± 7.39)	11.30 (± 3.33)	0.76 (±0.09)
	Pasiphaea multidentata (*n*=3)	106.50 (±12.77)	19.60 (± 3.25)	0.93 (±0.09)
Coastal	*Crangon crangon* (*n*=8)	18.69 (± 2.02)	24.40 (±1.13)	1.23 (±0.06)
	Palaemon elegans (*n*=10)	29.72 (± 2.60)	19.50 (±1.79)	1.07 (±0.13)

Table 5b. Displays the mean values of the three parameters used in fitting the lognormal model to the impulse response ERG data for all species studied. t_p is the time-to-peak from start of the response, d is the time from onset of stimulus to start of response (response latency), and is needed to identify the start of the response, and σ is the width factor of the pulse, which is the standard deviation of the normal frequency curve which is obtained by plotting the lognormal model against the logarithm of time. All values are given with associated standard errors in parentheses.

The mean values for the parameter t_p given in Table 5b show quite large standard errors, thus indicating that there is intraspecific variation in the time-to-peak of the voltage ERG impulse responses obtained from the eye. There is however, relatively little variation in the mean values for the parameter σ, as indicated by small standard error values.

5.4.2.1 Time–to–peak (t_p), response latency (d), and response width (σ) of the impulse response of mesopelagic species

The mean values of t_p of the impulse response functions of the eyes of *Systellaspis debilis*, *Sergestes arcticus* and *Meganyctiphanes norvegica* are 51.8, 59.0 and 64.9ms respectively. Statistical analysis reveals that there is no significant difference ($p>0.05$, see appendix IV) between these values. This suggests that these species have impulse response functions with comparable rise times from the start of the response to the peak amplitude of the response. The species *Pasiphaea multidentata* has an impulse response function with a comparatively greater mean value of t_p of 106.5ms and this is significantly different ($p<0.05$, see appendix IV) to the mean values of t_p of the impulse response functions of the other mesopelagic species studied. This indicates that the impulse response function of the eye of *P. multidentata* has a significantly slower rise time, from the start of the response to the peak amplitude of the response, in comparison with the impulse response functions of the other mesopelagic species.

Fig. 5.3b shows the difference in time-to-peak between the impulse response functions of *P. multidentata* and the other three mesopelagic species; whilst the gradient of the rising portion of the response is similar for *S. debilis*, *S. arcticus* and *M. norvegica*, it is less steep for the impulse response function of *P. multidentata*.

The response latency, or parameter *d*, also shapes the impulse response function for each species. The mean values of *d* for *S. debilis* and *S. arcticus* are 48.0 and 40.1ms respectively and statistical analysis reveals no significant difference ($p=0.304$, see appendix VI) between these values. The comparative plot in Fig. 5.3b shows that the impulse response functions of the eyes of these two species initiate at similar times and that the rise time of the impulse response is similar (as described above). Although *M. norvegica* has a mean rise time of response (t_p), which is similar to that for *S. debilis* and *S. arcticus*, the mean value of *d* for this species is 11.3ms, and is significantly different ($p<0.0005$ in both cases, see appendix VI) to the mean values of *d* for *S. debilis* and *S. arcticus*. Fig. 5.3b shows that the impulse response function of *M. norvegica*, despite having a similar rise time to the functions of *S. debilis* and *S. arcticus*, begins in advance of the impulse response functions of these two species. The mean value of *d* for *P. multidentata* is 19.6ms, which is not significantly different ($p=0.392$, see appendix VI) to the mean value of *d* for *M. norvegica* (11.3ms). Fig. 5.3b shows that a relatively small value of *d* and a large value of t_p for the impulse response function of *P. multidentata* results in a response that is more spread out over time than the responses from the eyes of the other species.

The parameter σ determines the width or 'skew' factor of the impulse response function. The value of this parameter determines how symmetrical the response function is as it indicates the relationship between the rise time and the fall time, i.e. the decay of the response. A small value of σ indicates a more symmetrical response and thus a response that has rise and decay times of similar duration. Conversely, a large value of σ leads to an asymmetrical response in which the decay of the response occurs over a longer time scale than the rise time of the response. Statistical analysis of the mean values of σ for the impulse response functions of each mesopelagic species reveals that there is no significant difference between these values ($p>0.05$, see appendix V). Therefore suggesting that the impulse response functions of the eyes of the mesopelagic species have comparable relationships between rise and decay times.

5.4.2.2 Time–to–peak (t_p), response latency (d), and response width (σ) of the impulse response of coastal, shallow-water species

The mean values of t_p for the impulse response functions of *Crangon crangon* and *Palaemon elegans* are 18.69 and 29.72 respectively. Statistical analysis reveals that there is no significant difference (p=0.707, see appendix IV) between these values. Fig. 5.3b illustrates that the rise times of the impulse response functions from the eyes of these two coastal species are very similar.

Similarly, there is no significant difference (p=0.507, see appendix VI) between the mean values of *d* of the impulse response functions of these two species. The values of *d* are 24.4 and 19.5ms for *C. crangon* and *P. elegans* respectively. Consequently, these species have comparable response latencies, i.e. the time between stimulus onset and the start of the response are similar for these two species (see Fig. 5.3b).

The parameter σ determines the symmetry of the relationship between the rise time and the decay time of the impulse response function. The mean values of the parameter σ for the impulse response functions of the eyes of the two coastal species are similar, and again statistical analysis reveals that there is no significant difference between these values (p=0.799, see appendix V). Consequently, the impulse responses of the eyes of the two coastal species have a similar shape and this is again apparent from the plot in Fig. 5.3b.

5.4.2.3 Comparison of the parameters of the impulse responses of the eyes of mesopelagic species and coastal, shallow-water species

Figs 5.3a & b show comparative plots of the impulse response functions determined for all the species used in this study, both mesopelagic and coastal. Table 5b displays the values of the mean parameters (with associated standard errors) used in defining the impulse response functions for all the species in this study.

The mean value of t_p of the impulse response functions of the coastal species *C. crangon* is 18.69ms and this is significantly different ($p<0.05$, see appendix IV) to the mean values of t_p of the impulse response functions of all the mesopelagic species. Similarly, the mean value of t_p

of the impulse response function of *P. elegans* (29.72ms) is significantly different ($p<0.05$, see appendix IV) to the mean values of t_p for all the mesopelagic species except for *S. debilis* (t_p = 51.8ms). Therefore, the rise time of the impulse response function from the eye of the coastal species *C. crangon* is faster than that of the impulse response functions of the mesopelagic species, and the same is true of the rise time of the impulse response function of *P. elegans*, except in comparison with the mesopelagic species *S. debilis*. In Fig. 5.3b it is clear that the rise times (t_p) of the impulse response functions of the coastal species *C. crangon* and *P. elegans* have steeper gradients compared with those of the mesopelagic species.

Fig. 5.3b indicates that the response latencies (given by the parameter d) of the impulse response functions of the coastal species *P. elegans* and *C. crangon*, and the mesopelagic species *M. norvegica* and *P. multidentata* are similar. Statistical analysis of the differences in the mean values of d between these species however, reveals that whilst the mean value of d for *C. crangon* (24.4ms) is not significantly different ($p>0.05$, see appendix VI) from the mean values of d for *P. elegans* (19.5ms) and *P. multidentata* (19.6ms), it is significantly different ($p=0.004$, see appendix VI) from the mean value of d for *M. norvegica* (11.3ms). Therefore response latency is very similar for the impulse response functions from the eyes of *Palaemon elegans*, *Pasiphaea multidentata* and *M. norvegica* ($p>0.05$ for comparison of the parameter d for these three species, see appendix VI) and whilst the same is true between the species *C. crangon*, *P. elegans* and *P. multidentata*, the impulse response function of the mesopelagic species *M. norvegica* has a significantly faster response latency than that of the coastal species *C. crangon*.

The parameter σ is of a similar value for the impulse response functions of all species, both mesopelagic and coastal, in this study (see Table 5b). Statistical analysis reveals that there is no significant difference ($p>0.05$, see appendix V) between the mean values of σ for the impulse response functions for all species except *M. norvegica* and *C. crangon*. The mean value of σ for the impulse response of *M. norvegica* is 0.76, and this is significantly different ($p=0.033$, see appendix V) to the mean value of σ for *C. crangon*, which is 1.23. Consequently, the impulse response function of the eye of *M. norvegica* has a slightly more symmetrical relationship between the rise time and the decay time than that of *C. crangon*. The other species in this study have eyes with impulse response functions with comparable symmetry, and thus the relationships between the rise times and decay times of these functions are alike.

5.4.2.4 *Summary of the time domain properties of the impulse response functions of malacostracan species*

a) Both mesopelagic and coastal species have impulse response functions with similar symmetry. That is the relationship between the rise time and the decay of the impulse response functions is similar among all the species studied.
b) The impulse response function of *M. norvegica* has the shortest duration of all the mesopelagic species studied; the impulse response function of *P. multidentata* has the longest duration, and the species *S. arcticus* and *S. debilis* have impulse response functions of intermediate duration.
c) The impulse response functions of the coastal species, *P. elegans* and *C. crangon* have similar mean values of the three parameters t_p, σ and d. These response functions have a short duration (from response start to return to 0), which is comparable to the duration of the impulse response function of *M. norvegica*, although the response function of *M. norvegica* has a slower rise time.

5.4.3 Comparison of the Impulse Responses of Malacostracan Species in the Frequency Domain

The FFT (Fast Fourier Transform) was used to transform the impulse response functions obtained for each species from the time domain into the frequency domain. This reveals the frequency response of the eye in terms of the power of the frequency components contained within the impulse response function (see sections *5.1.1* and *5.3.2* for detail of analysis).

Fig. 5.4 shows the power spectrum of the impulse stimulus used to produce impulse response ERG's from the eyes of the species in this study. The plot in Fig. 5.5 shows that the 1.4ms light pulse contains all frequencies up to *ca.* 200Hz at equal power. The 1.4ms light pulse actually contains frequencies of up to 700Hz, but beyond *ca.* 200Hz, the power of the frequency components decreases rapidly. Therefore, in using the 1.4ms light pulse to stimulate the eye, it is clear that one is stimulating the eye with a broadband frequency signal and dividing the FFT of the response by that of the stimulus compensates for the high frequency roll-off of the stimulus.

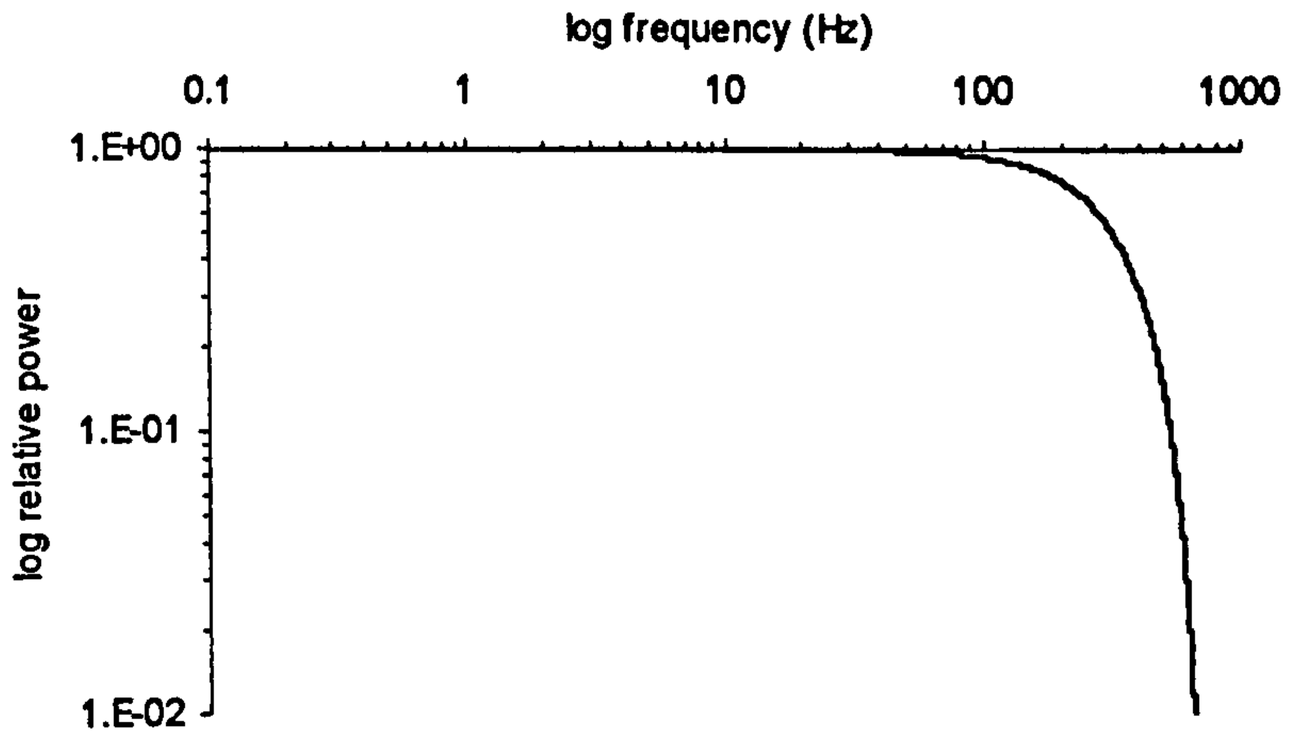

Figure 5.4. The frequency power spectrum derived from the FFT of a 1.4ms square pulse. This indicates the frequency components within the 1.4ms light pulse used to stimulate the eyes of the malacostracan species. It is clear that all frequencies up to *ca.* 100Hz are present at equal power in the light stimulus used.

Fig. 5.5 displays the frequency power spectrum obtained for each species from the FFT of the impulse response functions. Each plot shows an exponential decrease in response signal power with increasing frequency, which is analogous to the 'roll-off' response of a low-pass filter. In order to draw comparisons between the frequency responses of the eyes of the malacostracan species studied, both the corner frequency and the F_{10} value are identified on each plot.

The corner frequency (CF) is the frequency at which the signal power in the response from the eye falls to half maximum and this has previously been used as a measure to compare the frequency responses of terrestrial arthropod species (Laughlin and Weckström, 1993; Laughlin, 1996). The F_{10} value represents the frequency at which the signal power in the response from the eye falls to 10% of the maximum. This measure gives a more accurate indication of the maximum frequency resolvable by the eye than the corner frequency and this is discussed further in section *5.5.3.4.*

The parameters CF and F_{10} for each species studied are presented in Table 5c.

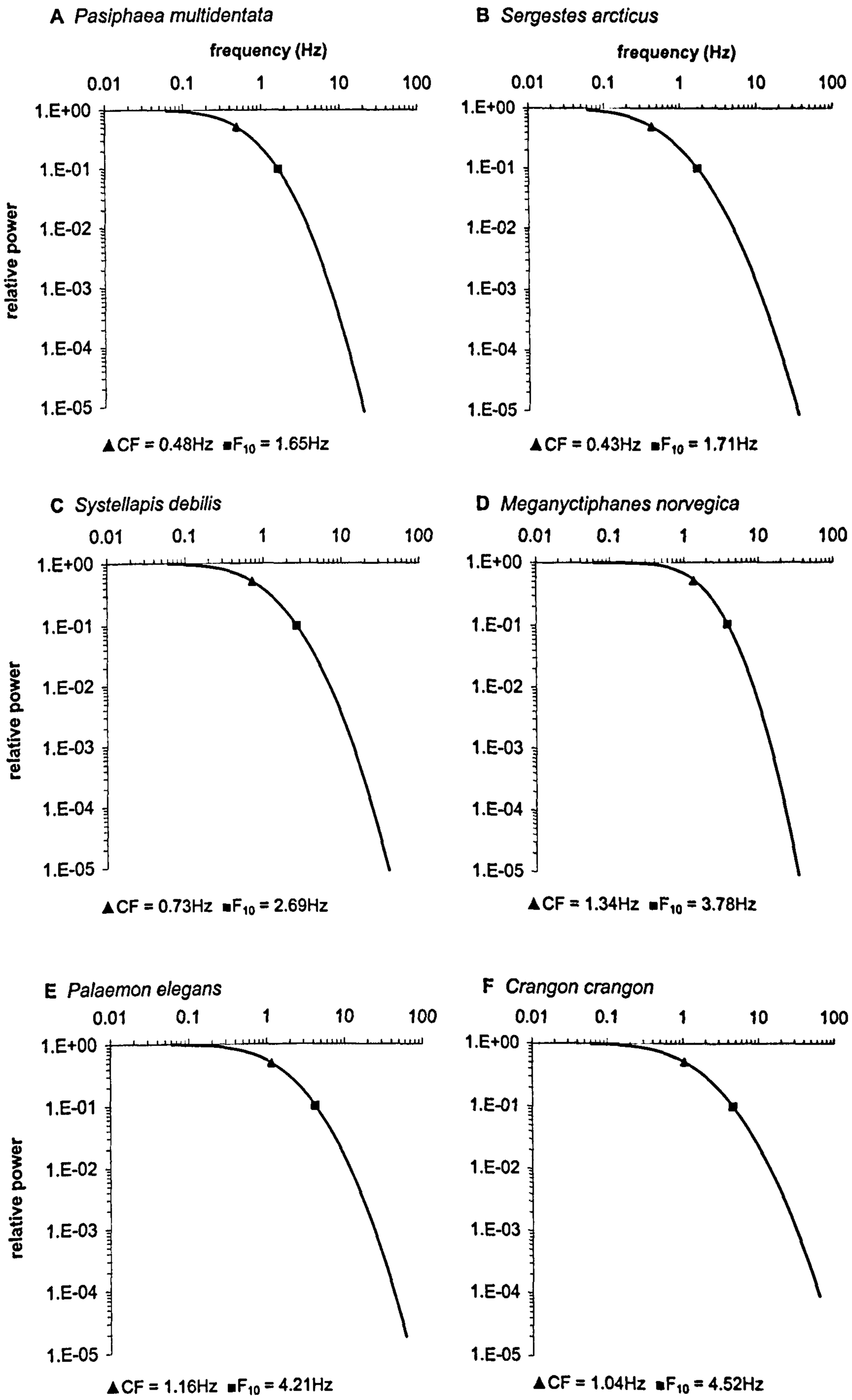

Figure 5.5. Frequency power spectra of the impulse response for each malacostracan species studied. Data is obtained through the FFT of the impulse response function for each species (as described in section *5.3.2*). Each plot shows the position of the corner frequency (CF, the frequency at which signal power falls to half maximum) and the value of F_{10} (the frequency at which the signal power falls to 10% of the maximum) along the frequency power spectrum.

	Species	CF (Hz)	F_{10} (Hz)
Mesopelagic	*Sergestes arcticus*	0.43	1.71
	Pasiphaea multidentata	0.48	1.65
	Systellaspis debilis	0.78	2.69
	Meganyctiphanes norvegica	1.34	3.78
Coastal	*Crangon crangon*	1.04	4.21
	Palaemon elegans	1.16	4.52

Table 5c. Displays the values of CF (corner frequency, i.e. the frequency at which the signal power in the response from the eye falls to half maximum) and F_{10} (the frequency at which the signal power in the response from the eye falls to 10% of the maximum). All values are extracted from the curves presented in Fig. 5.5.

5.4.3.1 A comparison of the parameters CF and F_{10} extracted from the FFT of the impulse response functions of the mesopelagic species studied

Frequency response

FFT analysis of the impulse response function generates an output with real and imaginary components, which can be re-expressed as a frequency power spectrum. This can be considered as a representation of the frequency response properties of the eye.

The frequency power spectra of the eyes of the species *P. multidentata* and *S. arcticus* have the lowest corner frequencies (0.48 and 0.43Hz respectively) indicating that these two species have the lowest frequency responses of the mesopelagic studied. The frequency power spectrum of the eye of *S. debilis* has an intermediate CF, with a value of 0.78Hz, and the frequency power spectrum the eye of *M. norvegica* has the highest CF with a value of 1.34Hz. Thus, based on the measure of corner frequency, the species *M. norvegica* has an eye with a comparatively high frequency response, the eye of *S. debilis* has a comparatively intermediate frequency response, and the eyes of both *P. multidentata* and *S. arcticus* have the lowest frequency response.

The same relationship between species and frequency resolving power of the eye is followed when the parameter F_{10} is considered. The only difference being that in using this parameter, it is apparent that the eye of *P. multidentata* now has the lowest frequency response, as indicated

by having the lowest value of F_{10} at 1.65Hz, compared with a value for F_{10} of 1.71Hz for *S. arcticus*. However, this change is small enough to be considered inconsequential in defining the frequency response of the eyes of these two species.

Fig. 5.6a is a comparative plot of the frequency power spectra of the impulse response functions for each mesopelagic species. From this plot it is apparent that the signal power of the frequency responses of *P. multidentata* and *S. arcticus* falls off more rapidly over the frequency range of 0.1-2Hz than the signal power of the frequency responses of *S. debilis* and *M. norvegica*. This explains the lower frequency responses of the eye for these two species.

What is also apparent from Fig. 5.6a is that although the frequency responses of *S. arcticus* and *P. multidentata* are similar over the range of 0-2Hz, beyond 2Hz, the signal power of the frequency response of the eye of *P. multidentata* decreases more rapidly than that of *S. arcticus*. The plot in Fig. 5.6a also shows that the frequency response of the eye of *M. norvegica* exhibits a relatively rapid decrease in power at frequencies above approximately 8Hz compared with the other mesopelagic species.

The plots of frequency power spectra of the visual responses of all the species studied (figs 5.5 and 5.6a) show that there are frequency components within the visual response at frequencies well above 20Hz. However, the signal power at a frequency of 20Hz falls by approximately 5 orders of magnitude for the species *P. multidentata* and by approximately 4 orders of magnitude for the species *S. arcticus*. Similarly, the signal power in the visual response of both *S. debilis* and *M. norvegica* falls by more than 3 orders of magnitude at this frequency. Thus, one must consider that such high frequency components may not be relevant in terms of vision for these animals as the response generated by such frequencies will be of such a low amplitude that it will probably be 'lost' in the photoreceptor noise of the eye. This is discussed further in section *5.5.3.4.*

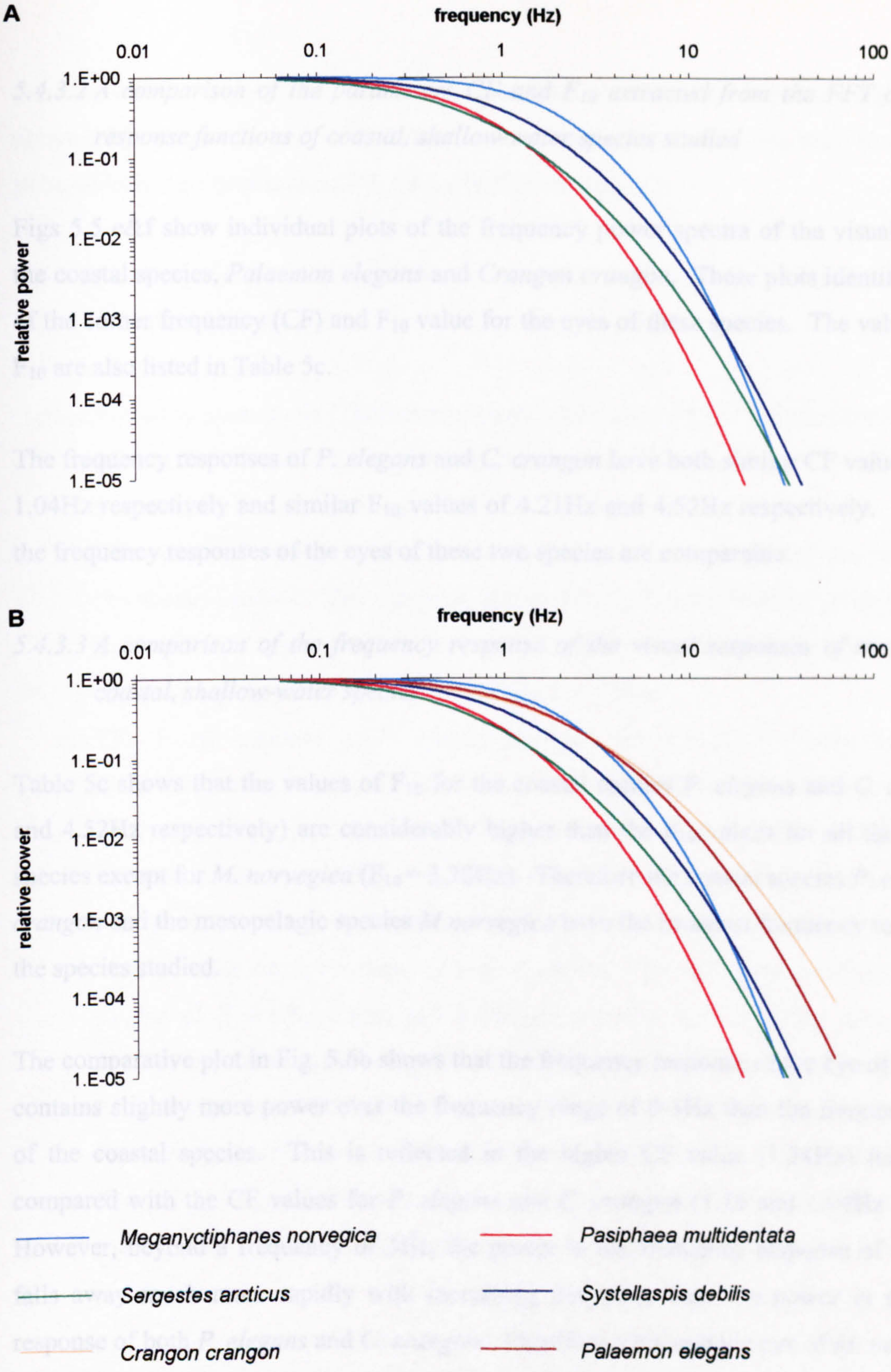

Figure 5.6. Comparative plots of the frequency power spectra of the visual response for A) the mesopelagic species studied and B) both mesopelagic and coastal, shallow-water species studied. Data are obtained from the FFT of the impulse response function for each species (as described in section *5.3.2*). The plots show the differences in the rate of roll-off of the signal power in the visual response with an increase in frequency of stimulus. In all cases the eyes operate as low pass filters.

5.4.3.2 A comparison of the parameters CF and F_{10} extracted from the FFT of the impulse response functions of coastal, shallow-water species studied

Figs 5.5 e&f show individual plots of the frequency power spectra of the visual responses of the coastal species, *Palaemon elegans* and *Crangon crangon*. These plots identify the position of the corner frequency (CF) and F_{10} value for the eyes of these species. The values of CF and F_{10} are also listed in Table 5c.

The frequency responses of *P. elegans* and *C. crangon* have both similar CF values of 1.16 and 1.04Hz respectively and similar F_{10} values of 4.21Hz and 4.52Hz respectively. Consequently the frequency responses of the eyes of these two species are comparable.

5.4.3.3 A comparison of the frequency response of the visual responses of mesopelagic and coastal, shallow-water species

Table 5c shows that the values of F_{10} for the coastal species *P. elegans* and *C. crangon* (4.21 and 4.52Hz respectively) are considerably higher than the F_{10} values for all the mesopelagic species except for *M. norvegica* (F_{10} = 3.78Hz). Therefore the coastal species *P. elegans* and *C. crangon* and the mesopelagic species *M norvegica* have the broadest frequency responses of all the species studied.

The comparative plot in Fig. 5.6b shows that the frequency response of the eye of *M. norvegica* contains slightly more power over the frequency range of 0-3Hz than the frequency responses of the coastal species. This is reflected in the higher CF value (1.34Hz) for this species compared with the CF values for *P. elegans* and *C. crangon* (1.16 and 1.04Hz respectively). However, beyond a frequency of 3Hz, the power in the frequency response of *M. norvegica* falls away much more rapidly with increasing frequency than the power in the frequency response of both *P. elegans* and *C. crangon*. Therefore, although the eye of *M. norvegica* has a slightly better frequency response than the coastal species at the lowest stimulus frequencies (0-3Hz), both *P. elegans* and *C. crangon* have a better frequency response than *M. norvegica* beyond a frequency of 3Hz. The extent to which this is relevant to the vision of these animals is dependent upon the photoreceptor noise in the eyes of these species. As signal power has fallen by more than 2 orders of magnitude at a stimulus frequency of 20Hz for all species, it is

possible that the eyes of these animals will not resolve visual stimuli modulating at frequencies above 20Hz as such stimuli will suffer from too low a signal-to-noise ratio in the process of phototransduction (see section *5.5.3.4* for further discussion).

5.4.3.4 Summary of the frequency domain properties of the impulse response functions of malacostracan species

a) For all species studied (both mesopelagic and coastal) there is an exponential decline in the signal power of the frequency response with increasing frequency of stimulus. This is analogous to the response properties of a low-pass filter.
b) The eyes of *P. multidentata* and *S. arcticus* have the lowest frequency responses of all the species studied. The eye of *S. debilis* has an intermediate frequency response and the eyes of *M. norvegica* and the coastal species *P. elegans* and *C. crangon* have the highest frequency responses of all the species studied.
c) The visual response of *P. multidentata* has the lowest frequency response and a frequency power spectrum that shows a relatively large decrease in signal power with increasing frequency. The visual response of *M. norvegica* has the highest frequency response of the mesopelagic species studied and the frequency power spectrum of this species shows the greatest rate of decrease with increasing frequency of all species studied. The visual response of *S. arcticus* has a low frequency response (comparable to that of *P. multidentata*) and a frequency power spectrum that shows a relatively gradual decrease in power with increasing frequency of stimulus. The visual response of *S. debilis* has an intermediate frequency response and a frequency power spectrum that shows a gradual decrease in power with increasing frequency of stimulus.
d) The visual responses of the coastal species *P. elegans* and *C. crangon* have both the highest frequency responses and the broadest frequency power spectra of all the species studied.

5.5 DISCUSSION

5.5.1 The Impulse Response

The ERG data obtained from the eyes of the malacostracan species in this study in response to an impulse light stimulus are comparable in shape to impulse responses obtained from other arthropod species including: *Schistocerca gregaria* (desert locust) and *Acheta domesticus* (house cricket), Pinter, (1972); *Locusta migratoria* (locust), Howard, (1981), Payne and Howard, (1981); various insect species, Howard *et al.* (1984); *Procambarus clarkii* (crayfish) Glantz, (1991); various dipteran species, Laughlin and Weckström, (1993); *Tipula paludosa* (crane fly), Laughlin, (1996); *Calliphora vicina* (blowfly), Burton *et al.* (2001). The two parameter lognormal model taken from Howard *et al.* (1984) is derived from the study of Payne and Howard (1981) and was modified slightly (see below) to provide an excellent fit to the ERG impulse responses obtained in this study.

Payne and Howard (1981) developed a simple two parameter model of phototransduction based on the assumption that photoreceptor membrane Na^+ channels open only once a threshold concentration of internal transmitter is reached (the release of internal transmitter signals the absorption of a photon by visual pigment molecules in the photoreceptor). The thresholds of the membrane channels are assumed to have a normal distribution about their means and the transmitter concentration is assumed to rise logarithmically (Payne and Howard, 1981). Consequently, it follows that the temporal frequency of the opening of the photoreceptor channels follows a lognormal distribution, and thus the voltage generated within the photoreceptor follows a lognormal equation (Payne and Howard, 1981). This model has been used to successfully describe the impulse responses obtained from the photoreceptors of a wide variety of terrestrial arthropods.

The studies of Payne and Howard (1981) and Howard (1981) investigated the impulse responses of the photoreceptors of the locust (*Locusta migratoria*) using the two parameter lognormal model. The results of both studies indicate that only the parameter t_p changes upon light adapting the photoreceptors; the parameter σ remains unchanged. Consequently it is suggested that the parameter t_p represents the rate constant of a signal transduction process (Payne and Howard, 1981). It is suggested that this signal transduction process is the rate of

rise of the concentration of the internal transmitter which links photon absorption to channel opening in the photoreceptor membrane and thus leads to the generation of a voltage signal (Payne and Howard, 1981). In the present study impulse responses are obtained from dark-adapted eyes only, and therefore the effect of light adaptation on the two parameters t_p and σ is not explored (reasons for studying only dark-adapted eyes are given in section *3.5.1.1*).

The present study incorporates a third parameter, d (time from onset of stimulus to the start of response, i.e. response latency). The parameter, d, is not directly used in the lognormal equation, it simply determines the time at which the response starts relative to the onset of the stimulus. Therefore t in the lognormal equation (see below) is forced to 0 until the time at which the response starts, and t_p represents the time period between the start of the response to the peak of the response. This is opposed to t_p representing the time period between the onset of the stimulus and the peak of the response as in previous studies (e.g. Howard *et al.* 1984).

$$v(t) = K \exp[-\{\ln(t/t_p)\}^2 / 2\sigma^2]$$

Using this method to fit the lognormal equation to the impulse response function provided a more exact fit than using just t_p to represent the time-to-peak from the onset of the stimulus. This method separates the beginning of the impulse response into two stages: the latency of the response (i.e. the time taken for internal transmitter to reach threshold concentration and trigger Na^+ conductance into the photoreceptor cell causing depolarisation) is represented by d; and the rising portion of the response (the increase in voltage generated as more photoreceptor membrane Na^+ channels open in response to rising transmitter concentration) is represented by t_p. Section *5.5.4* discusses the relationship between the three parameters used to describe the impulse response function in the time domain and shows that the sum of $t_p + d$ is related to the temporal resolving power of the eye. Therefore, despite these two parameters being separated in order to provide the best fit of the equation to the impulse response, they are intrinsically related in terms of their effect on the temporal resolving power of the eye, and the value of the sum of these two parameters can be compared with the values of the parameter t_p obtained in previous studies.

Interspecific comparisons of the parameters t_p and σ reveal that there is no significant difference in the parameter σ between the species studied (both mesopelagic and coastal) but there is a significant difference in the parameters t_p and d between the species studied (both mesopelagic and coastal). The lack of a difference in the parameter σ between species, which represents the ratio between the duration of the impulse response and the time-to-peak, suggests that similar transduction mechanisms are active in the photoreceptors of marine malacostracans (Howard, 1981). The significant difference in the parameters t_p and d between species suggests that, whilst the phototransduction mechanisms may be similar for the species in this study, a species specific rate-limiting factor in the response dynamics of the photoreceptors in the eye is the rate of rise of the concentration of the internal transmitter (see above). Intracellular studies of the response dynamics of arthropod photoreceptors have indicated that the regulation of the temporal dynamics of the phototransduction cascade is responsible for changing the sensitivity and the response dynamics of the photoreceptor response (Weckström and Laughlin, 1995). The relationships between the time domain and frequency domain properties of the impulse response functions of the species in this study are discussed in section *5.5.4*. The values of $t_p + d$ obtained in the present study (see section *5.5.4*, Table 5d) for the dark-adapted impulse response functions of marine malacostracan species (ranging from 43.09-126.10 ms) are higher than those determined for terrestrial insect species (ranging from 38 to 55ms) in the study of Howard *et al.* (1984). This suggests that the photoreceptor response dynamics of marine malacostracans are slower than those of some terrestrial insect species. The values of σ obtained for marine malacostracans in the present study (ranging from 0.76-1.23) are also greater than those determined for terrestrial arthropod species (ranging from 0.340-0.44, Howard *et al.* 1984). This indicates that the impulse response functions of terrestrial arthropod species are more symmetrical than those for marine malacostracans and different transduction mechanisms may be responsible for this.

The FFT of the impulse response function for each species generates frequency power spectra that are comparable in shape to those determined for several other arthropod species including: *Locusta migratoria*, Howard (1981) & Howard *et al.* (1984); *Procambarus clarkii*, Glantz (1991); various dipteran species, Laughlin and Weckström (1993); *Tipula paludosa*, (crane fly), Laughlin, (1996). The frequency power spectra of the dark-adapted eyes of species of marine malacostracan show that the eyes of these species have response properties that are similar to the response properties of a low-pass filter. The frequency responses of the eyes of these

animals show high sensitivity to the lowest stimulus frequencies. As stimulus frequency increases, the response signal from the eye loses power and, beyond a given frequency that is specific to the species studied, begins to decline rapidly. Although low-pass filters may be described in terms of their 'cut-off' frequency, it is generally the case that filters do not have a sharp cut-off point, but the response of the filter shows 'roll-off' near the cut-off frequency, i.e. power begins to decline rapidly at the 'cut-off' frequency, but does not fall immediately to zero.

The corner frequencies (CFs), defined as the frequency at which power in the response has declined to half maximum (extracted from the frequency power spectra generated for the dark-adapted visual response of the species in this study), may be compared with CF values determined for some terrestrial arthropod species. In comparing the CF values obtained for marine malacostracan species in the present study with CF values reported for terrestrial arthropod species by Laughlin and Weckström (1993) it is apparent that marine malacostracan species have relatively very slow temporal resolving powers. The highest CF value determined in the present study is 1.34Hz and this is for the dark-adapted eye of the mesopelagic euphausiid species, *Meganyctiphanes norvegica*. This may be compared with a CF value of 7Hz for the dark-adapted 'slow' photoreceptors of the crane fly *Tipula paludosa*, which has the lowest CF value of 20 dipteran species studied (Laughlin and Weckström, 1993). From such a comparison it can be concluded that the eyes of the marine malacostracan species investigated in the present study have very slow temporal dynamics in comparison with terrestrial arthropod species. The dark-adapted CF values for dipteran species determined in the study of Laughlin and Weckström (1993), however, were obtained from the Fourier transformation of impulse responses that were in turn obtained using intracellular recordings from the "linear response range" of the eye. In the dark-adapted state this linear response range would be very close to threshold as photoreceptors are only linear over small ranges and thus a light pulse stimulus beginning from zero light will provide large contrast and would have to be very dim in peak irradiance at the eye to ensure the response was even approximately linear. Such threshold responses are very difficult to record reliably using the ERG as they are lost in the noise of the recording set-up. Photoreceptor response dynamics are dependent on the intensity of stimulating light and decrease with a fall in stimulus intensity (Frank, 1999). Therefore the frequency responses of the species investigated in the present study may be expected to be even slower if determined in response to irradiances that generate threshold responses as opposed to

irradiances that generate 50%V_{max} responses. Consequently, if an absolute comparison were made between the CF values obtained for the species in the present study with those obtained for terrestrial arthropods (i.e. CF values obtained for threshold responses), it may be expected that the CF values for marine malacostracans would be even lower than the values stated in the present study.

5.5.2 Comparisons with Previous Studies of the Temporal Resolution of Deep-sea Malacostracan Species

The present study is the first to attempt to define the temporal resolving powers of the eyes of mesopelagic malacostracans by studying the impulse responses of the eyes, and consequently direct comparisons of temporal resolving power in terms of CF values for example, is not possible. Comparisons of the temporal resolving powers of the mesopelagic species investigated in the present study with that of species investigated in other studies is difficult for the reasons discussed in the discussion of Chapter 4 (section *4.6.4*). Different methodologies employed in other studies prevent direct comparisons of the results with those obtained in the present study. However, one is able to compare the relationships between temporal resolving power and visual ecology determined in other studies with those determined here. Previous studies do report some correlation between temporal resolving power and the light environment inhabited for certain species, in terms of the deepest living species having eyes with the lowest temporal resolving powers and conversely the shallowest living species having eyes with the highest temporal resolving powers (Moeller and Case, 1995; Frank, 1999 & 2000; Johnson *et al.* 2000a; see section *4.1.2* for detail). However, the study of Frank (1999) also reports that for two species of mesopelagic euphausiid malacostracan (*Nematobranchion flexipes* and *N. sexspinosus*), temporal resolving power is not correlated with daytime depth distribution but can be explained as an adaptation for the purpose of hunting bioluminescent prey (see sections *4.6.4* and *4.6.5*). The results of the present study indicate that for the mesopelagic species studied, there is a significant positive correlation ($p=0.017$) between temporal resolving power (as defined by F_{10}) and the ambient light level in the environment inhabited for each species (see section *5.5.5.1*, Fig. 5.9b), this is discussed further in section *5.5.5.*

5.5.3 Methodological Considerations

5.5.3.1 The dark-adapted impulse response

This study investigates the impulse response functions of only the dark-adapted eyes of marine malacostracan species. In section *5.5.1* it is reported that the parameter t_p is dependent upon the adaptation state of the photoreceptors in the eye, and in fact the value of t_p decreases upon light adaptation for terrestrial arthropod photoreceptors (Payne and Howard, 1981; Howard 1981; Howard *et al.* 1984). Similarly, the frequency response of photoreceptors is dependent upon adaptation state and photoreceptor temporal response dynamics improve (i.e. the photoreceptors become more sensitive to higher stimulus frequencies) upon light adaptation (Pinter, 1972; Howard, 1981; Laughlin and Weckström, 1993; Laughlin, 1996). Consequently, during the experiments conducted in the present study it was ensured that the eyes of the animals tested were maintained in a dark-adapted state (see section *5.2.1.4* for detail of the experimental procedure).

Justification for studying the temporal resolving power of only dark-adapted eyes of marine malacostracans is given in sections *3.5.1.1* and *4.6.2*

5.5.3.2 Wavelength of impulse light stimuli

The λ_{max} of the impulse stimuli used to generate impulse responses from the eyes of all the species in this study (both mesopelagic and coastal) was 464nm (FWHM 28nm). A comprehensive explanation for using light stimuli of this wavelength to generate impulse responses from the eyes of all the species in this study is given in section *3.5.2.1*.

5.5.3.3 Optical stimulation

There are a number of considerations with respect to the use of the ERG in determining the visual response to a given stimulus. These are described in section *3.5.1.3* Chapter 3, and these considerations are equally applicable to the present study.

5.5.3.4 Photoreceptor noise

Section *4.6.3.3a* briefly describes the origins of intrinsic photoreceptor noise. Photoreceptor noise ultimately determines the temporal resolving power of an individual photoreceptor, or indeed the combined response of the photoreceptors in an eye. The frequency response method used in Chapter 4 of this thesis clearly demonstrates that as stimulus frequency is increased the amplitude of the response to such stimuli decreases to the point at which a resolvable sinusoidal response is no longer generated by the eye. This is also the case in using the impulse response method to determine temporal resolving power. An impulse stimulus that contains broadband frequency information (see Fig. 5.4 section *5.4.3* for the frequency power spectrum of the impulse light stimulus used in the present study) is used to stimulate the eye and the FFT of the impulse response from the eye reveals which of the frequencies in the broadband stimulus stimulated the eye most effectively. The frequency power spectra generated from the FFT of the impulse response functions of the species in this study (Fig. 5.5 section *5.4.3*) show that the eye responds with less power to the higher frequency components within the impulse stimulus. In fact the frequency power spectra in Fig. 5.5 (section *5.4.3*) show the frequency response of the eye extends to high frequencies, but that at these high frequencies the response signal power has fallen by five orders of magnitude. Interpretation of such frequency responses must be made with care as it is unlikely that a response signal that has fallen in power by five orders of magnitude relative to the maximum will be resolvable above photoreceptor noise. Recording a signal of such small amplitude is beyond the scope of extracellular recording and this is where the Fourier analysis of the impulse response methodology has a distinct advantage over the frequency response methodology used in Chapter 4 of this study. One is able to generate a brief, relatively high amplitude response from the eye and transform this to reveal all frequency components within it. However, without recordings of the amplitude of intrinsic photoreceptor noise, one is unable to determine the signal-to-noise ratio of the photoreceptors. Consequently it is not possible to accurately determine the minimum response amplitude resolvable from photoreceptor noise and therefore the absolute maximum frequency to which the eye will respond. Intracellular recording techniques can be used to determine the amplitude of photoreceptor noise in the eye but this is well beyond the scope of the present study and, at present, impossible at sea.

The corner frequency (CF) of the frequency response has been used in previous studies on the photoreceptors of terrestrial arthropod species (Laughlin and Weckström, 1993; Laughlin, 1996) to provide a comparative figure with which to compare temporal resolving power, and this value is equivalent to the stimulus frequency that generates a response that is reduced in signal power by 50%. This does not provide a reasonable indication of the upper limits of the temporal resolving power of an eye/photoreceptor, as a response signal from the eye that is reduced in power by 50% is equivalent to a decrease in absolute response amplitude of just 30%. This is because the power in the response signal is equal to the square of absolute amplitude. The square root of 0.5 is 0.7 and thus half maximum power is equal to a reduction of 30% in response amplitude. A response amplitude that is 70% of the maximum will be well resolvable above the signal-to-noise ratio of the photoreceptors in the eye. Consequently in the present study, the parameter F_{10} has been extracted from the frequency power spectrum for each species studied. F_{10} corresponds to the frequency at which signal power has fallen to 10% of the maximum; this is equivalent to a decrease in response amplitude of 70% ($\sqrt{0.1} = 0.3$). In using this parameter to describe the temporal resolving power of the eyes of the species in this study one is able to infer that the F_{10} frequency is approaching the maximum frequency resolvable by the eye whilst being confident in assuming that the response amplitude generated by the F_{10} frequency will be resolvable above photoreceptor noise.

The impulse responses obtained in the present study were recorded extracellularly and consequently the temporal properties of the impulse responses reported are the properties of the combined response of all the photoreceptors in the eye. A recent study of the response dynamics across the retina of the blowfly *Calliphora vicina* by Burton *et al.* (2001) has revealed that there is variation in the temporal properties of a given class of photoreceptor within a single retina. Specifically it was found that there is a trend towards greater temporal resolution of the photoreceptors at the front of the eye and that these photoreceptors have a relatively higher signal-to-noise ratio. This is attributed to the need for greater tracking power in the anterior visual field for the purpose of mate pursuit. Gaten *et al.* (1992) indicate that there are regional morphological variations in the eyes of certain mesopelagic malacostracans which could be an adaptation concerned with both greater sensitivity to dim upwelling irradiance and greater resolution for viewing both objects against the relatively bright background of downwelling irradiance and bioluminescence. It is possible therefore, especially when one considers the possibility that mesopelagic animals have the requirement of tracking

bioluminescent prey or conspecifics (Land, 1992), that temporal resolving power may vary across the photoreceptors in the retina. Intracellular recordings of the impulse responses of the photoreceptors of mesopelagic species would allow one to determine whether there is regional variation in temporal resolving power across the retina. Intracellular recordings would also allow the determination of the signal-to-noise ratios of the photoreceptors in the eye. However, the constraints of working in a laboratory on board a moving vessel at sea make such recordings impossible at present.

5.5.4 The Properties of the Impulse Response Functions of Marine Malacostracans in both the Time Domain and the Frequency Domain

In section *5.4.2.4* a summary of the time domain properties of the impulse response functions of marine malacostracans is given. Similarly, in section *5.4.3.4* a summary of the frequency domain properties of the impulse response functions of the same animals is given. At this point the two representations of the impulse response function will be considered together. Table 5d reports both the time domain properties in terms of the three parameters t_p, σ and d and the frequency domain properties in terms of the value of F_{10} for the impulse response function of each species studied.

	Species	t_p (ms)	d (ms)	σ	$t_p + d$ (ms)	F_{10} (Hz)
Mesopelagic	*Sergestes arcticus*	59.00	40.10	1.16	99.10	1.71
	Pasiphaea multidentata	106.50	19.60	0.93	126.10	1.65
	Systellaspis debilis	51.80	48.00	1.03	99.80	2.69
	Meganyctiphanes norvegica	64.90	11.30	0.76	76.20	3.78
Coastal	*Crangon crangon*	18.69	24.40	1.23	43.09	4.21
	Palaemon elegans	29.72	19.50	1.07	49.22	4.52

Table 5d. Displays both the time domain and frequency domain properties of the impulse response functions of the marine malacostracans in this study. Time domain properties are represented by the parameters t_p (time-to-peak from start of response), d (time period between onset of light stimulus and start of response) and σ (width factor of pulse, i.e. the standard deviation of the normal frequency curve which is obtained by plotting the lognormal model against the logarithm of time). t_p and d are summed (t_p+d) as this represents the total time-to-peak of the response from the onset of the stimulus. The frequency domain properties of the impulse response functions are represented by the value F_{10} (the frequency of stimulus at which response signal power falls to 10% of the maximum).

Table 5d shows all the parameters measured from the impulse response functions of the marine malacostracan species in this study. As the time domain and frequency domain information is derived from the same function one would expect there to be some relationship between the properties of the two domains.

The software Minitab (release 12.22) was used to determine the Pearson's correlation co-efficient of the relationships between the time domain and frequency domain variables given in Table 5d for all the species studied (see section *3.4.1.3* for details of the Pearson's correlation co-efficient). There is no significant correlation between the values of σ and the values of F_{10} for each species ($r = 0.056$; p=0.916, df = 4, see Fig. 5.7a) and consequently the symmetry of the impulse response cannot be related to the frequency response of the eye. This is not surprising when one considers that there is no significant difference (p>0.05 see appendix V) between the values of σ for all the species studied here (see section *5.4.2.3*) and yet there is variation in F_{10}. In section *5.5.1* it is mentioned that the rise time of the response will determine the speed of phototransduction as this represents the rate of rise of internal transmitter (Payne and Howard, 1981). Consequently one must consider the parameter t_p as a determinant of the photoreceptor response dynamics. However, in considering this parameter alone it is clear that there is no significant correlation ($r = -0.767$; p=0.075; df = 3, see Fig. 5.7b) between the time-to-peak and the frequency response of the eye as defined by the value of F_{10}. This is not surprising when one considers that the parameter d is equally important in determining the speed of phototransduction as this parameter represents the time taken for the response to initiate after the onset of the stimulus at the eye (i.e. the time taken for the concentration of internal transmitter to reach threshold). The sum of these two parameters ($t_p + d$, see Table 5d) therefore represents the total time taken for the response to peak from the onset of the impulse stimulus. One can see from Fig. 5.7c that there is a significant negative correlation ($r = -0.932$; p = 0.007; df = 4) between the sum of $t_p + d$ and the value of F_{10} for each species: the greater the value of $t_p + d$ the smaller the value of F_{10} and conversely, the smaller the value of $t_p + d$ the greater the value of F_{10}. The total time taken to reach the peak of the impulse response after the onset of the impulse stimulus is therefore related to the frequency resolving power of the eye.

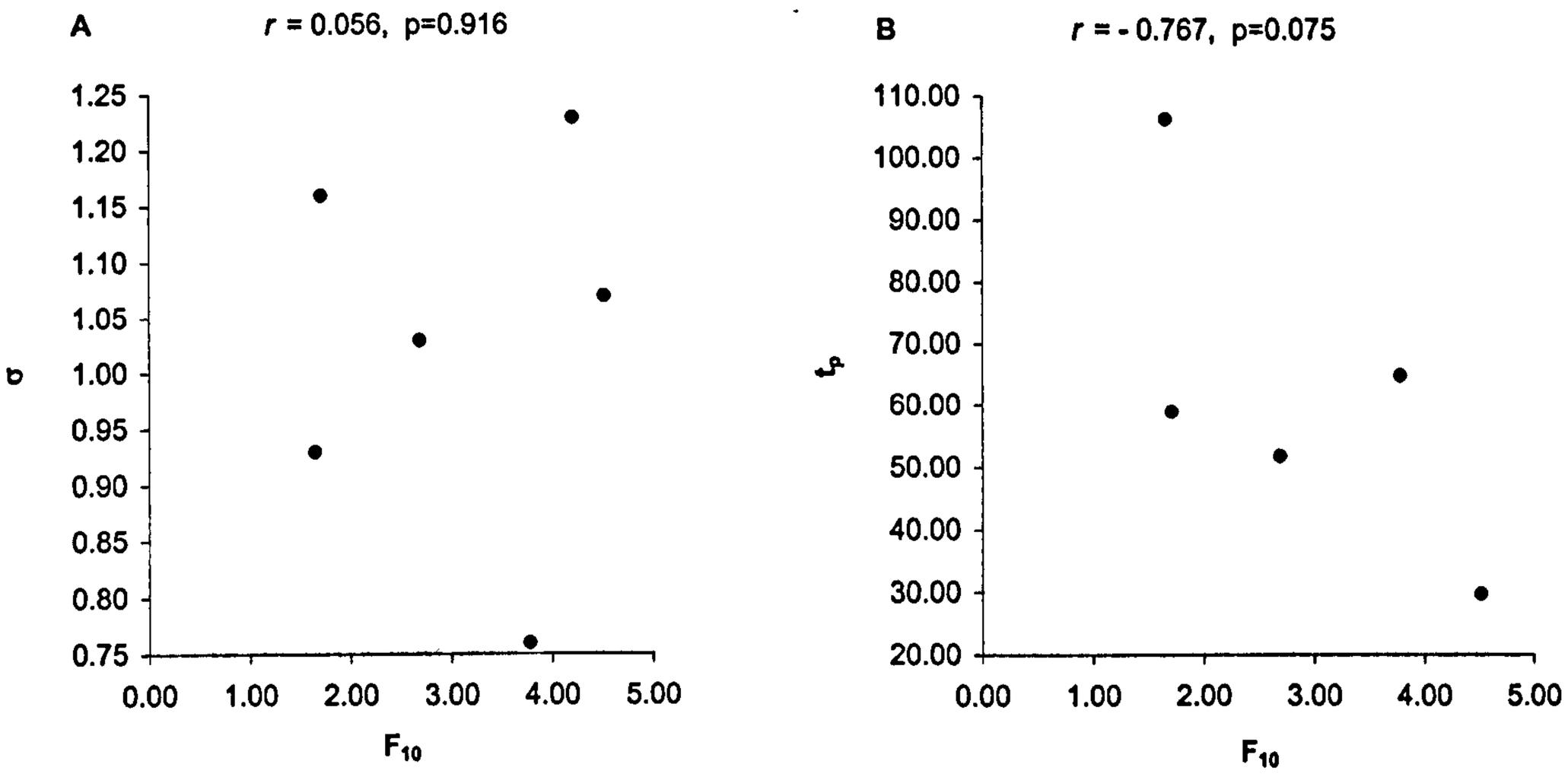

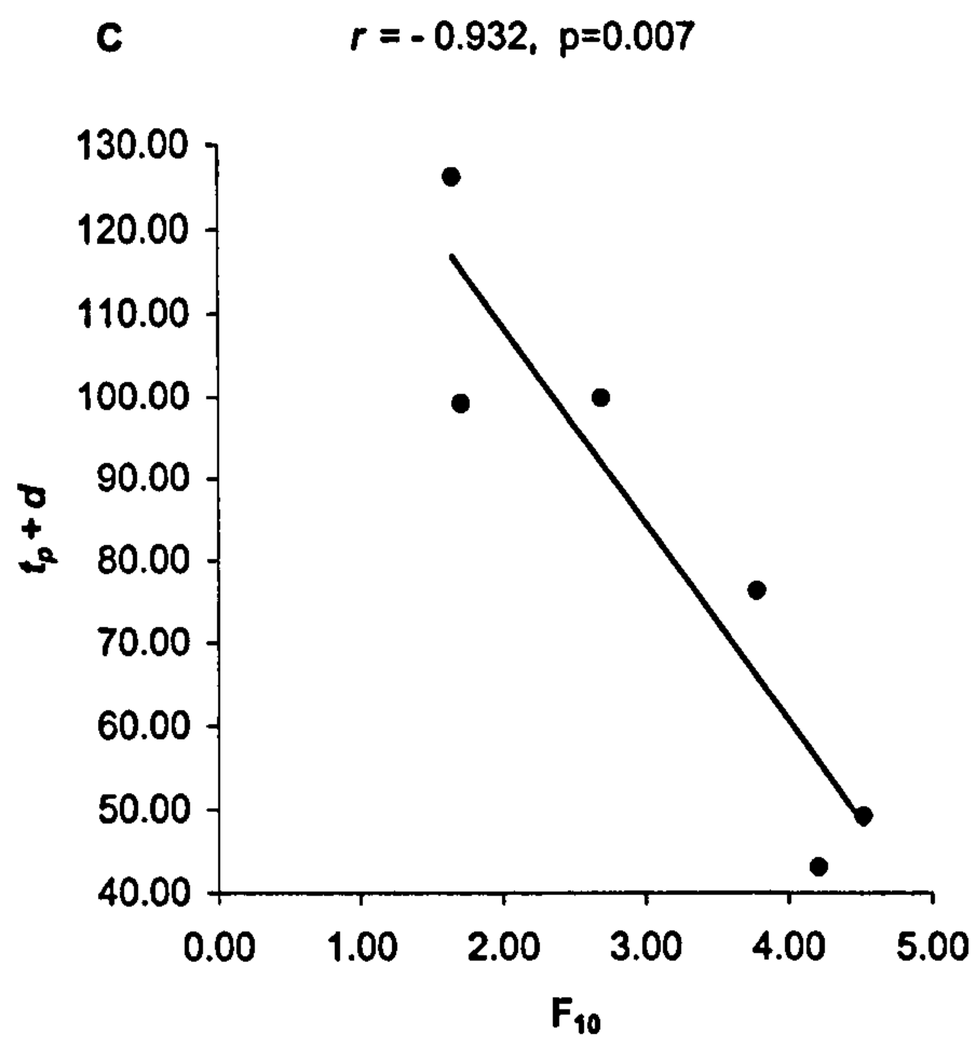

Figure 5.7. The correlation between the variables: A) σ and F_{10}; B) t_p and F_{10}; C) $t_p + d$ and F_{10}; for all the malacostracan species studied. The Pearson's correlation co-efficient for each correlation is signified by the value of r. The p-values indicate the statistical significance of r, a value of less than 0.05 indicates that there is a significant linear relationship between two sets of variables. In A) the relationship between the variables σ and F_{10} is highly non-significant ($r = 0.056$; $p = 0.916$; $df = 4$). In B) there is no significant correlation between the variables t_p and F_{10} ($r = -0.767$; $p = 0.075$; $df = 3$). In C) there is a highly significant negative correlation between the variables $t_p + d$ and F_{10} ($r = -0.932$; $p = 0.007$; $df = 4$) and the data points are well-fitted by a linear trendline. There is therefore an inverse relationship between the speed of the photoreceptor response, as defined by $t_p + d$ (time taken for impulse response to reach maximum amplitude after on set of impulse light stimulus), and the frequency response of the photoreceptors as defined by F_{10} (the frequency at which signal power in the response falls to 10% of the maximum).

The study of Weckström *et al.* (1991) investigates the membrane properties of blowfly (*Calliphora vicina*) photoreceptors using intracellular recording techniques. The results of this study indicate that the direct regulation of the 2nd messenger system (internal transmitter) that links photon absorption to a change in membrane conductance is a prominent adaptation mechanism in blowfly photoreceptors. This form of regulation trades gain for frequency response by speeding up the intermediate processes so as to reduce the duration of events triggered by light, i.e. the phototransduction cascade. This therefore suggests that the temporal dynamics of the phototransduction cascade have a significant effect on the temporal resolving power of the photoreceptors and this may be inferred from the results of the present study. The results presented here indicate that for both coastal, shallow-water and mesopelagic malacostracans, the time taken for the impulse response to reach its peak from stimulus onset may to some extent determine the frequency response of the eye.

The values displayed in Table 5d allow the following conclusions to be drawn:

a) The mesopelagic decapod species *P. multidentata* has eyes that produce impulse responses of the longest timescale in terms of the sum of t_p and d ($t_p + d$). This is related to this species having the lowest F_{10} value and thus eyes with the lowest temporal resolving power of all the species studied.
b) The mesopelagic euphausiid species *M. norvegica* has eyes that produce impulse responses of the shortest timescale ($t_p + d$) of the mesopelagic species studied. This is related to this species having the highest value of F_{10} of the mesopelagic species studied and thus eyes with the greatest temporal resolving power when compared with the other mesopelagic species studied.
c) Both mesopelagic decapod species *S. arcticus* and *S. debilis* have eyes that produce impulse response functions of an intermediate timescale ($t_p + d$) in comparison with the other two mesopelagic species studied. Whilst *S. debilis* has an accompanying intermediate value of F_{10} in comparison with the other mesopelagic species, *S. arcticus* has a low value of F_{10} comparable to that of *P. multidentata*. Therefore the eye of *S. debilis* has an intermediate temporal resolving power and generates impulse responses of an intermediate timescale (in comparison with the other mesopelagic species studied). The eye of *S. arcticus* generates impulse responses of an intermediate

timescale and yet has a low temporal resolving power comparable to that of *P. multidentata*

d) The two coastal species *C. crangon* and *P. elegans* have eyes that generate impulse responses of the shortest timescale ($t_p + d$) of all the species studied. This is related to both of these species having the highest values of F_{10} and consequently eyes with the greatest temporal resolving power of all the species studied.

e) The sum of $t_p + d$ for each species is inversely related to the value of F_{10} for each species. There is a significant negative correlation between these two variables (r = -0.932; $p<0.05$; df = 4, see Fig. 5.7c)

5.5.5 Temporal Resolving Power of the Eyes of Mesopelagic Malacostracans in Relation to Relative Sensitivity, Daytime Depth Distribution and Behaviour

The mesopelagic animals used in this study come from two different water types, Jerlov types IA and IB (see Table 5a). Section *1.2.4* gives detail of Jerlov's classification system of water types based on their optical properties. The clearest oceanic water type (type I) has a peak transmission at *ca.* 465nm, and the least attenuation of downwelling irradiance with depth (Jerlov, 1976). Type IA water is less transparent and at a depth of 100m only 0.28% of total irradiance from the sun and sky is present compared with 0.53% for type I water (Jerlov, 1976). Type IB water is less transparent than type IA water and at a depth of 100m only 0.10% of the total irradiance from the sun and sky is present (Jerlov, 1976). Consequently, the optical depth that the animals in this study inhabit is not simply defined by a comparison of their daytime depth distribution, and comparisons of temporal resolution and daytime depth distribution between the species in this study have to account for the optical properties of the water they were collected from.

Section *3.5.2.2* in Chapter 3 of this study gives details of the problems associated with determining downwelling irradiance at depth in the ocean. However, recent *in situ* measurements of downwelling irradiance at depths greater than 200m have been recorded using radiometers deployed on submersibles (Frank and Widder, 1996, 1997; Widder and Frank, 2001). Fortunately these measurements have been made in regions where the water types are IA (Northwest Providence Channel, Bahamas, Frank and Widder, 1996) and IB (Gulf of Maine, Oceanographers Canyon, Widder and Frank, 2001 and pers. comm., Wilkinsons Basin,

Frank and Widder, 1997 and pers. comm.). Therefore the results of this study, i.e. the temporal resolutions of the mesopelagic malaostracans studied, can be directly related to the optical depth inhabited.

Table 5e displays for each mesopelagic species studied, information on the water type inhabited, the downwelling irradiance at the upper limit of the daytime depth range (daytime depth distributions for each species are given in Table 5a section *5.2.1*), the relative sensitivity of each species in terms of k (the irradiance that generates a response from the eye that is 50% of the maximum), the value of F_{10} for each species, and the bioluminescent capabilities of each species. This information is compiled in order to provide some information on the visual ecology of each species and thus indicate whether or not the physiology of the visual response in terms of both sensitivity and temporal resolving power is adapted to the visual requirements of each species.

Species	Water Type	Irradiance (photons s^{-1} cm^{-2} nm^{-1}) at 480nm at upper limit of daytime depth range	10^k (photons s^{-1} cm^{-2} at 464nm)	F_{10} (Hz)	Bioluminescence
Meganyctiphanes norvegica	IB	$3.0x10^7$	$2.8x10^{10}$	3.78	photophores
Pasiphaea multidentata	IB	$1.3x10^6$	$3.0x10^{11}$	1.65	—
Sergestes arcticus	IB	$1.5x10^5$	$9.8x10^{10}$	1.71	photophores
Systellaspis debilis	IA	*$1.0x10^7$	$4.57x10^8$	2.69	photophores spew

Table 5e. For each mesopelagic species there are details of the optical properties of the environment inhabited along with physiological measures of the visual response and bioluminescent capabilities. The water type inhabited is given (according to Jerlov's [1976] classification system) along with the downwelling irradiance at 480nm at the upper limit of the daytime depth range of each species; all data except * are from Widder, E. A., and Frank, T. M., pers. comm. Irradiance data marked* are taken from Frank and Widder (1996). The values of 10^k for each species are determined through the back transformation of the value of k (irradiance that generates a response that is 50%Vmax) from the logarithmic state; these values of k are determined in Chapter 3 of this thesis. The values of F_{10} are determined in the present study.

Meganyctiphanes norvegica

The information in Table 5e indicates that the euphausiid species *M. norvegica* inhabits the brightest optical environment with respect to the irradiance of downwelling light at 480nm. This is accompanied by a relatively high value of F_{10} that suggests that the eyes of this species have the greatest temporal resolving power of all the mesopelagic species studied here. The relative sensitivity of the visual response is intermediate in comparison with the other mesopelagic species and, in fact, is not significantly different to that of *S. arcticus* (see Chapter section *3.4.1.1* for detail). One may expect that the eyes of *M. norvegica* would have the least sensitive visual response as this animal occupies the brightest light environment and has a relatively fast temporal resolving power. Additionally, the results of both the present study and that of Chapter 3 show that the response latency of the eye is relatively very fast. Chapter 3 reports a response latency of 14.3ms (see Table 3c, and section *3.4.1.3*) and the results of the present study report a response latency (*d*) of 11.3ms (see Table 5d, section *5.5.4*). Therefore the physiological measures of temporal resolution and response latency are related to the relatively bright optical environment inhabited by this species, i.e. a brighter environment is associated with faster response dynamics (e.g. Laughlin and Weckström, 1993; see section *5.5.5.1* for statistical correlations).

Frank and Widder (1997) found the eyes of *M. norvegica* to be consistently 1-2 log units less sensitive than the eyes of *P. multidentata* (see section *3.5.4*), whereas in Chapter 3 of this thesis it was found that *M. norvegica* was 1 log unit more sensitive to blue light (λ_{max} 464nm) than *P. multidentata*. The photoreceptors of *M. norvegica* have much shorter response latency than even those of the least sensitive, coastal species (information from section *3.4.2.2* and Table 3c. A short response latency indicates a less sensitive eye (Laughlin and Weckström, 1993) and consequently one may expect *M. norvegica* to have a relative sensitivity comparable to that of the coastal species, or indeed a less sensitive visual response than the coastal species (see section *6.2* for further discussion).

Pasiphaea multidentata and *Sergestes arcticus*

These two species share similar values of F_{10}, which indicates that, comparatively, these species have the lowest temporal resolving power of all the mesopelagic species studied here.

These two species also share similar relative sensitivities, as the values of k shown in Table 5e for these species are not significantly different ($p>0.05$, see Chapter section *3.4.1.1* for detail, and appendix I). The results of Chapter 3 indicate that these species have intermediate response latencies (*P. multidentata* = 30.5ms; *S. arcticus* = 33.0ms) in comparison with *M. norvegica* and *S. debilis*. The same is true of the findings of the present study for *S. arcticus* (d = 40.1ms), although the value of d for *P. multidentata* is much faster at 19.6ms.

The values in Table 5e indicate that these two species inhabit environments with similar optical depths and this can be related to these species having eyes with similar temporal resolving powers, relative sensitivities and response latencies.

The results of the study of Frank (2000) indicate that both *P. multidentata* and *S. arcticus* also have the lowest temporal resolving powers of twelve mesopelagic species studied and this is related to these species inhabiting (comparatively) the greatest optical depths in the water column.

Systellaspis debilis

Systellaspis debilis inhabits a light environment which is similar to that inhabited by *M. norvegica* as indicated by the values of irradiance of downwelling light at the upper limit of their respective daytime depth distributions (see Table 5e). However, the eyes of *S. debilis* have a relatively very sensitive visual response, and a relatively long response latency as determined here (48.0ms see Table 5e) and in Chapter 3 (48.2ms, see Table 3c section *3.4.1.3*). This may indicate that the eyes of this species would have the lowest temporal resolving power as both relatively high sensitivity and long response latency have previously been associated with low temporal resolving power (Laughlin and Weckström, 1993; Frank, 1999). However, the temporal resolving power of the eyes of *S. debilis* is intermediate in comparison with the other mesopelagic species studied here, as determined by the intermediate value of F_{10} given in Table 5e (2.69Hz). Consequently, the temporal resolving power of this animal can be related to the light environment inhabited (in terms of downwelling irradiance), i.e. this animal has a relatively fast frequency response and inhabits a relatively bright environment. However, this species has an eye that is relatively highly sensitive. A similar situation is explained for the

oplphorid decapod, *Acanthephyra purpurea* in Chapter 4 of this study and also for the euphausiid species *M. norvegica*, in the present study (see above).

S. debilis is a vertical migrator and possesses photophores, which are probably used in congener recognition, conspecific mating and camouflage through counterillumination (see Chapter 4 section *4.6.5* for detail). This species also produces a bioluminescent secretion ('spew') to startle predators. It is possible therefore that the higher than expected temporal resolving power of the eyes of this species is an adaptation to tracking bioluminescent signals across the visual field for the purpose of predation or mate identification. As mentioned in section *4.6.5* for the species *A. purpurea*, it is also possible that a higher temporal resolution of the eyes of *S. debilis* may allow this animal to track silhouettes of prey items near the water surface at night (as it vertically migrates), or equally silhouettes of prey items occurring higher in the water column during the day. A greater temporal resolving power reduces the degree of 'smearing' of spatial information in a visual image as it moves across the visual field. A relatively high temporal resolving power combined with a relatively high sensitivity will optimise visualisation of moving objects in the water (high sensitivity will maintain contrast sensitivity), but as previously mentioned this is a metabolically expensive strategy and therefore must confer some significant advantage to the animal.

The temporal resolving power of the eyes of *S. debilis* was also investigated in Chapter 4 of this thesis using the frequency response method (see Chapter 4 for detail). The maximum resolvable response frequency obtained from the eye of *S. debilis* was 7Hz in Chapter 4 and this was the lowest maximum response of four mesopelagic species studied. This value is considerably greater than the F_{10} value reported in the results of the present study. However, this is not surprising as the F_{10} value actually reports the frequency of stimulus that produces a response with power that is 10% of the maximum (absolute amplitude is 30% of the maximum, see section *5.5.3.4*) and it is possible that the eye is capable of producing responses that are resolvable from intrinsic photoreceptor noise and have absolute amplitudes that are less than 30% of the maximum. Fig. 5.8 shows the results of Chapter 4 plotted along with the frequency power spectrum derived for *S. debilis* in the present study. The relative response magnitudes for *S. debilis* from Chapter 4 were squared in order to derive the power of the visual response (see section *5.5.3.4*) and plotted as log signal power against log frequency along with the squared standard deviation of the mean values. In order to align the data sets, the results of

Chapter 4 were normalised to the relative signal power at 0.5Hz in the frequency power spectrum obtained from the impulse response data (the lowest frequency measurement taken in Chapter 4 was 0.5Hz, whilst the FFT power spectrum covers frequencies down to 0Hz).

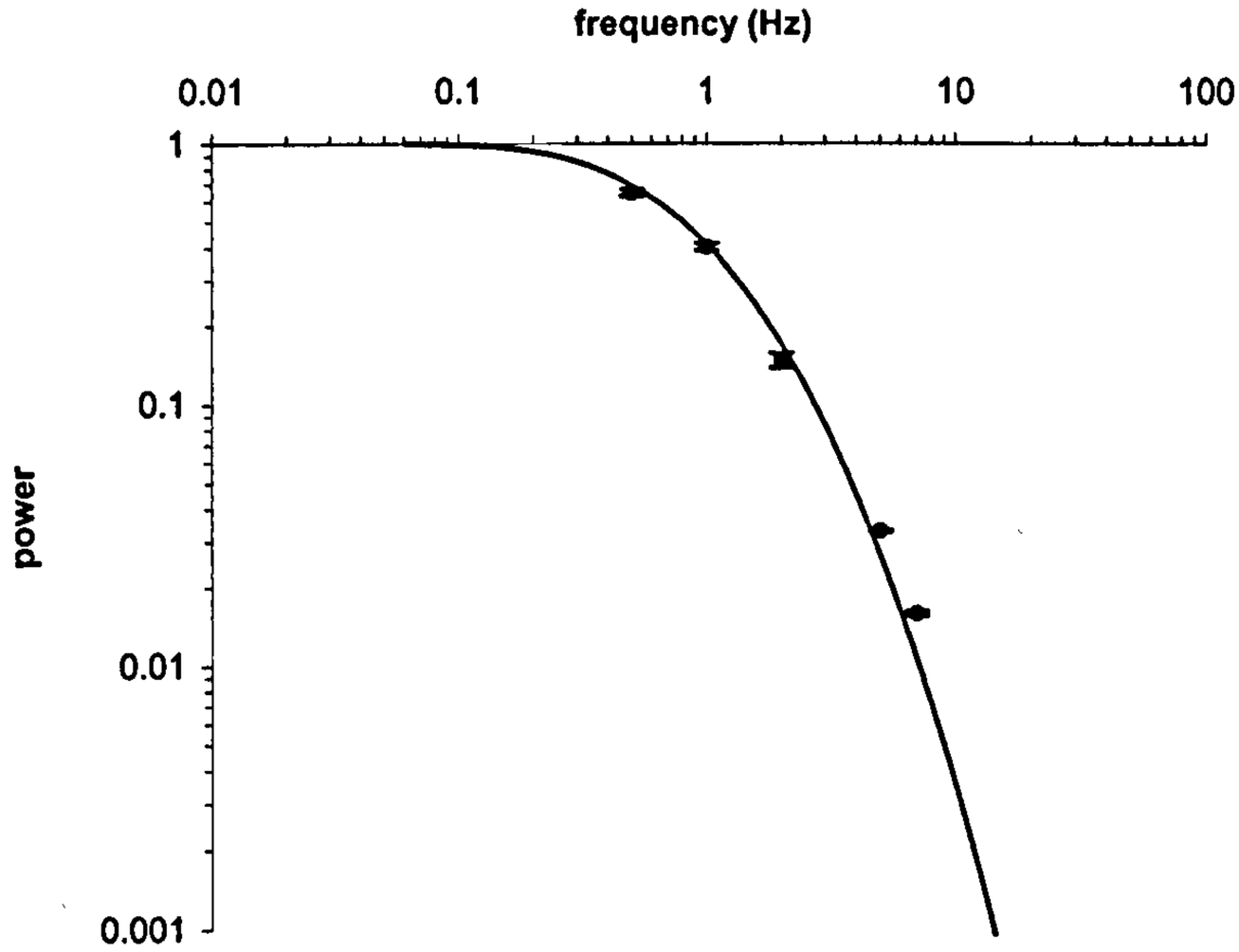

Figure 5.8. The frequency power spectra for the eye of *S. debilis* as determined by impulse response methods (line) and frequency response methods (points). The data points and associated standard deviations are the squared relative amplitude measures obtained in response to sinusoidal stimuli of differing frequencies in Chapter 4 (n=3, with associated standard deviation values). The frequency response data obtained for *S. debilis* in Chapter 4 agrees well with that obtained in the present study using the impulse response methodology.

Fig. 5.8 shows that the frequency response of the eye of *S. debilis* as determined in Chapter 4 using the frequency response methodology, agrees well with the frequency response of *S. debilis* determined in the present study using the impulse response methodology. Therefore the two methods produce comparable results and this reinforces the view that one is operating within a similar range of the VlogI curve for the species as in Chapter 4, i.e. the 50%V_{max} point.

Fig. 5.8 reveals that the eyes of *S. debilis* produce resolvable responses above the F_{10} value (2.69Hz) as the measurements taken in the study of Chapter 4 show that a resolvable response is seen at 7Hz. At a stimulus frequency of 7Hz, signal power has fallen to approximately 2.5% of the maximum, and it is apparent that the ERG recording apparatus can resolve such small

amplitude responses from the background noise in the signal. Consequently it is highly likely that the photoreceptors in the eye are capable of producing responses resolvable above the intrinsic photoreceptor noise in response to frequencies greater than 7Hz. The frequency power spectrum for the impulse response function of *S.debilis* (see Fig. 5.5c, section *5.4.3*) reveals that the frequency response of this species extends well beyond 10Hz. Beyond 10Hz, however, the signal power has dropped by more than two orders of magnitude, and therefore the signal-to-noise ratio of the photoreceptors will determine whether or not stimuli of 10Hz or more are resolvable above photoreceptor noise (see section *5.5.3.4* for detail).

5.5.5.1 Correlations

Both the values in Table 5e and the discussion in section *5.5.5* indicate that for the mesopelagic species studied here, there is no relationship between the sensitivity of the eye and the frequency response of the eye as determined by the value of F_{10}. Statistical analysis to determine the Pearson's correlation co-efficient of the relationship between these two variables was conducted using Minitab software (release 12.22) see section *5.5.4* for detail. Fig. 5.9a shows the relationship between visual sensitivity (as defined by k, values taken from Table 5e) and the value of F_{10} for each species, it is apparent that there is no significant correlation between these variables for the mesopelagic species studied (r = -0.684; p=0.316; df = 2). However, on determining the Pearson's correlation co-efficient for the relationship between the value of F_{10} for each species and the irradiance at the upper limit of the daytime depth distribution for each species, it is apparent that there is a significant positive correlation between these factors (r = 0.983; p=0.017; df = 2, see Fig. 5.9b).

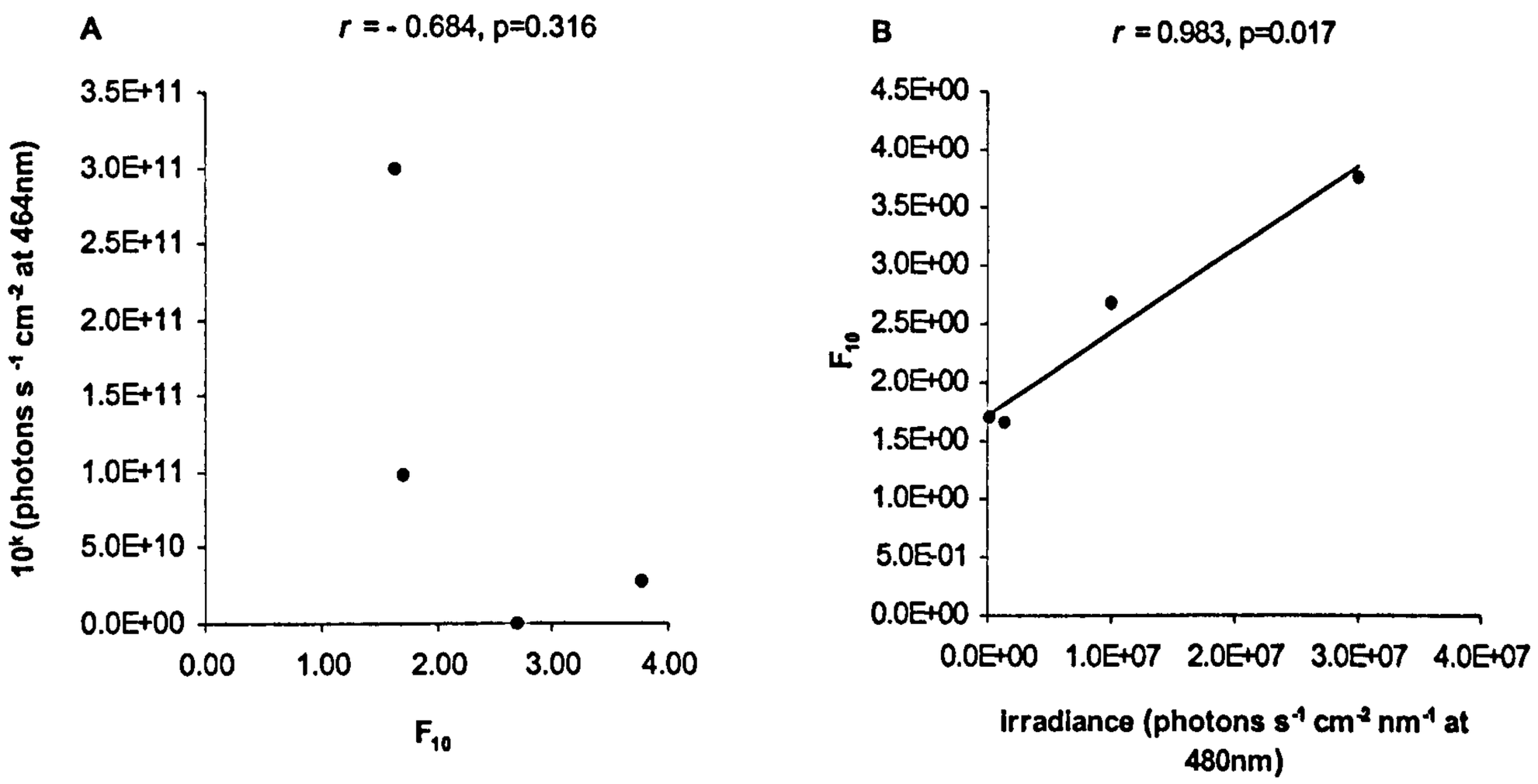

Figure 5.9. A) the correlation between F_{10} and visual sensitivity (in terms of 10^k the photon flux at the eye of 464nm light that generates a 50%Vmax response) for the mesopelagic species studied; there is no significant correlation between these variables (r = - 0.684; p=0.316; df = 2); B) the correlation between F_{10} and the downwelling irradiance levels at 480nm experienced at the upper range of the daytime depth distribution for each mesopelagic species studied. There is a significant positive correlation between these variables (r = 0.983; p=0.017; df = 2).

Therefore, the temporal resolving power of the mesopelagic species is positively correlated with the ambient light levels experienced in the natural habitat for the species studied here, i.e. as irradiance levels increase, temporal resolving power also increases.

5.5.6 Temporal Resolving Power of the Eyes of Coastal, Shallow-water Nocturnal Malacostracans in Relation to their Visual Ecology

Table 5f displays for the two coastal species studied, information on the irradiance experienced in their respective natural habitats, the relative sensitivity of each species in terms of k (the irradiance that generates a response from the eye that is 50% of the maximum), and the value of F_{10} for each species.

Justification for using surface irradiance measurements to estimate the light environments of the coastal species in this study is given in Chapter 3 section *3.5.5*.

Species	Irradiance at water surface at night (photons s^{-1} cm^{-2} nm^{-1}) at 500nm	10^k (photon flux at 464nm)	F_{10} (Hz)
Crangon crangon	$1x10^5$-$1x10^8$	$2.04x10^{12}$	4.21
Palaemon elegans	$1x10^5$-$1x10^8$	$1.05x10^{12}$	4.52

Table 5f. Displays the irradiances measured at the water surface at night (data from Dusenbery, 1992). A range of irradiances are shown as irradiance is highly dependent on weather conditions and the lunar cycle, thus on an overcast moonless night the surface irradiance at 500nm is 10^5 photons s^{-1} cm^{-2} nm^{-1}, whereas on a moonlit clear night surface irradiance at 500nm is 10^8 photons s^{-1} cm^{-2} nm^{-1} (Dusenbery, 1992). Also included are the relative sensitivities of the eyes of each species in terms of 10^k (determined via the back transformation of the value of k [the irradiance that produces a response from the eye that is 50%Vmax]; k values obtained from Chapter 3 of this thesis) and the F_{10} value for each species as determined in the present study.

The two species *C. crangon* and *P. elegans* inhabit similar environments in terms of irradiance. These two species also have similar relative sensitivities (there is no significant difference in the values of k, p=0.734, see section *3.4.1.1* Chapter 3 and appendix I), and similar values of F_{10}. The response latencies of the visual responses of these two species are also similar, as the results determined in Chapter 3 (*C. crangon* = 24.0ms, *P. elegans* = 20.3ms) show no significant difference (p=0.972, see *3.4.2.2* and appendix I) and neither do the results of response latency (*d*) determined in the present study (*C. crangon* = 24.40ms, *P. elegans* = 19.50ms, see section *5.4.2.3*). These two species, therefore, have very similar visual response dynamics and sensitivities and inhabit environments in which the background light fields are similar.

In comparison with the mesopelagic species studied (see Table 5e for details of mesopelagic species) it is clear that the eyes of coastal species are significantly less sensitive (see Chapter 3 section *3.4.2*), and with the exception of *M. norvegica*, have the shortest response latencies. The eyes of the coastal species also have greater temporal resolving power than the eyes of all the mesopelagic species studied, as determined by the value of F_{10} for each species. This is correlated with the fact that the coastal species can be exposed to nocturnal irradiances of the order of 10^8 photons s^{-1} cm^{-2} nm^{-1} (at 500nm), which is an order of magnitude more light than the brightest environment experienced by the mesopelagic species studied (i.e. *M. norvegica*). It is possible also, that the coastal species become active at twilight and surface measurements

of irradiance at 500nm at twilight yield values of 10^{11} photons s^{-1} cm^{-2} nm^{-1} (Dusenbery, 1992). Therefore it can be concluded that coastal, shallow-water nocturnal malacostracan species have eyes with higher temporal resolving powers than those of mesopelagic species and that this is correlated with these species inhabiting a relatively brighter light environment.

Figure 5.10 shows plots of the correlations between F_{10} and 10^k (see Tables 5e and 5f) and F_{10} and irradiance levels in the environment for all the malacostracan species studied.

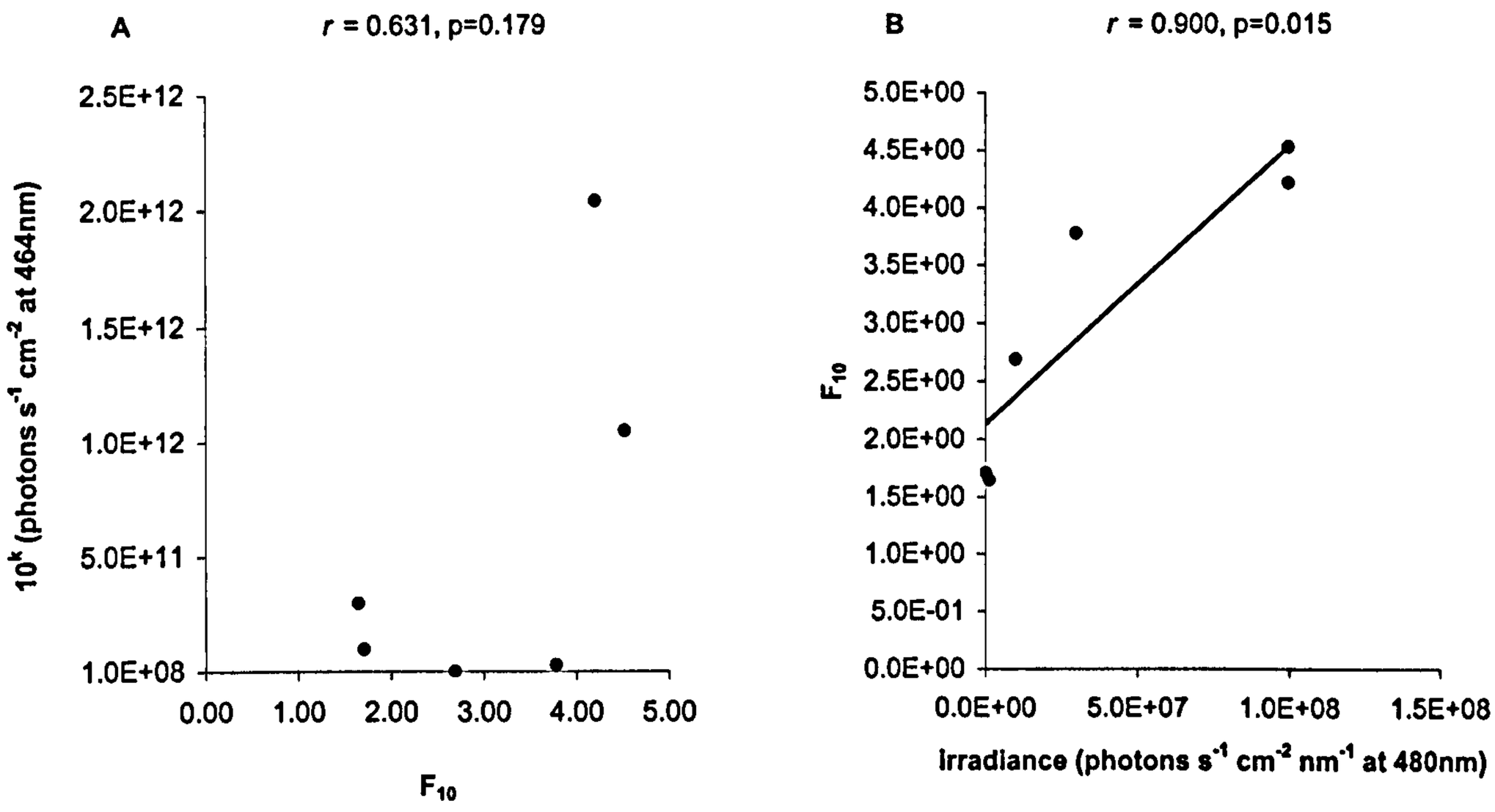

Figure 5.10. A) the correlation between F_{10} and visual sensitivity (in terms of 10^k the photon flux at the eye of 464nm light that generate a 50%Vmax response) for all the malacostracan species studied; there is no significant correlation between these variables ($r = 0.631$; $p = 0.179$; $df = 4$); B) the correlation between F_{10} and the downwelling irradiance levels (irradiance at 480nm for mesopelagic species and 500nm for coastal species, see sections *5.5.5* and *5.5.6*) experienced in the natural environment. There is a significant positive correlation between these variables ($r = 0.900$; $p = 0.015$; $df = 4$).

From the plots in Fig. 5.10, it is clear that there is no significant relationship ($r = 0.631$; $p=0.179$; $df = 4$) between F_{10} and 10^k for the malacostracan species studied (similarly there was no significant relationship between these variables for mesopelagic species, see Fig. 5.9). There is, however, a significant relationship between F_{10} and the irradiance levels experienced in the natural environment of each species ($r = 0.900$; $p=0.015$; $df = 4$). The irradiance levels for the coastal species used in determining this correlation were $1x10^8$ photons s^{-1} cm^{-2} nm^{-1} at

500nm (see Table 5f). There is a positive correlation between temporal resolving power of the eyes and the ambient irradiance in the environment inhabited. It can be concluded therefore, that coastal, shallow-water nocturnal malacostracan species have eyes with higher temporal resolving powers than those of mesopelagic species and that this is an adaptation to inhabiting a relatively brighter light environment. However, it does not necessarily follow that a higher temporal resolving power is accompanied by a less sensitive visual response for the malacostracan species in this study.

These results agree with the general findings in terrestrial arthropod species that photoreceptor response dynamics are adapted to the light environment inhabited; diurnal species have a better temporal resolving power than arrhythmic and nocturnal species (Howard *et al.* 1984; deSouza and Ventura, 1989). The results of the present study suggest that nocturnally active species of coastal malacostracan have a better temporal resolving power than mesopelagic species, which inhabit a permanently photon-limited environment.

5.5.7 Summary of Conclusions

This study has used extracellular recording techniques to determine the temporal resolving powers of the eyes of 6 species of marine malacostracan using the impulse response methodology. Of the 6 species studied, 4 are mesopelagic species with differing daytime depth distributions and 2 are coastal, shallow-water, nocturnal species. The aim of this study was threefold; it was designed to demonstrate a more convenient method (than the frequency response method used in Chapter 4) of determining the temporal resolving powers of mesopelagic species, considering that recordings are made at sea. This study was also designed for the purpose of determining and comparing the temporal resolution of the eyes of mesopelagic species with differing depth distributions, and for determining the temporal resolutions of the eyes of shallow water, nocturnally active, species in order that they can be compared with those of the mesopelagic species. The conclusions drawn from this study indicate that differences in temporal resolving power between mesopelagic and coastal species can be attributed to differences in visual ecology.

This study presents the temporal resolving powers of the dark-adapted eyes of marine malacostracans in response to light stimuli which generate a response in the middle of the

VlogI relationship for each species. Therefore the temporal resolving powers as defined here should not be considered as the maximum resolving powers of the eye, as this is greatly dependent on the irradiance of the light stimulus (Frank, 1999). However, by using a stimulus that generates a response from the eye that is close to 50%V_{max}, one is determining the frequency response of the eye in response to natural irradiance levels, similar to those likely to be encountered in the natural environment. Consequently the frequency responses as reported here are highly relevant to the functioning of the eye in its natural environment.

The following conclusions may be drawn from the results of this experiment:

a) Impulse responses obtained from the eyes of six species marine malacostracan are similar in shape and have time domain properties that are of a similar order of magnitude as those determined for terrestrial arthropod species.

b) The frequency power spectra generated by the FFT of the impulse response function of each species are comparable in shape to those determined for terrestrial arthropod species and exhibit the properties of a low-pass filter.

c) The sum of $t_p + d$ for the impulse response function of each species studied is significantly correlated (negative correlation) with the frequency response for each species studied in terms of F_{10} (r = -0.932; p=0.007; df = 4). Therefore there is a relationship between the time domain and frequency domain properties of each impulse response function.

d) The corner frequencies determined for both mesopelagic and coastal species are considerably lower than those determined for terrestrial arthropod species, even those with 'slow' eyes. This is the case despite the fact that the CF values determined for the species in the present study are for 50%V_{max} responses as opposed to threshold (as in the case of the terrestrial arthropod species) and therefore are probably an over-estimation of the temporal resolving powers of the eyes of marine malacostracans when stimulated with threshold irradiances.

e) The value F_{10} is used to compare the temporal resolving powers of the species studied as it is closer to the maximum resolvable frequency of the eye than the corner frequency, but the absolute maximum resolvable stimulus frequency will be dependent on the signal-to-noise ratio of the photoreceptors in the eye.

f) Temporal resolving power is significantly correlated (r = 0.900; p=0.015; df = 4) with downwelling irradiance in the environment inhabited for all the species (both

mesopelagic and shallow-water, coastal) studied. The brighter the light environment inhabited, the greater the temporal resolving power of the eyes.

g) Temporal resolving power is not correlated with visual sensitivity (in terms of k) for all the species studied ($r = 0.631$; p=0.179; df = 4). The eyes of the mesopelagic species *S. debilis* and *M. norvegica* have relatively high temporal resolving powers and relatively high sensitivity. It is suggested that this may be an adaptation to maintain contrast sensitivity whilst viewing moving objects in the environment, and that this will be a metabolically expensive strategy.

h) The coastal, shallow-water, nocturnal species studied have both the highest temporal resolving powers and the lowest sensitivities of all the species studied. These species also inhabit the brightest light environments of all the species studied.

i) The impulse response methodology has strong advantages over the frequency response methodology used in Chapter 4 of this thesis. It involves stimulating the eye with a quick and simple stimulus, the response from which contains information on the response of the eye to broadband frequency information. The methodologies in both Chapter 4 and the present study to determine the frequency response of *S. debilis* produce very similar results.

5.5.8 Considerations for Future Work

ERG's can be recorded from different regions of the eye in an effort to determine whether or not there is regional variation in sensitivity and temporal response dynamics across the eye. For those species that are known to possess a dual visual pigment system, for example that confers sensitivity to both blue and near-UV light (e.g. *S. debilis*), stimulating the eye with blue and near-UV light would isolate the response of each wavelength selective visual pigment, and differences in wavelength selective photoreceptor response dynamics can be identified.

The impulse responses and subsequent frequency power spectra may be determined for a number of points along the VlogI curve for these animals. This would allow one to predict the frequency response of the dark-adapted eye to a range of different stimulus irradiances and would not be a labour-intensive study.

Intracellular recording techniques may be employed in order to identify the temporal response dynamics of individual photoreceptors in the eye. This will allow one to determine whether there are regional variations in the response properties of the photoreceptors across the retina, which is possible considering that morphological variations in rhabdom structure have been identified (Gaten *et al.* 1992). Intracellular recording techniques would also allow one to determine the signal-to-noise ratios of the photoreceptors in the eye and thus reveal the absolute temporal resolving power of the eye.

5.5.9 Hypotheses Tested

Hypothesis 1: The temporal resolutions of all species will be related to visual sensitivity, i.e. visual sensitivity is the primary factor in determining temporal resolution.
H_0 = temporal resolution will not be related to visual sensitivity.

The null hypothesis is accepted. There was found to be no significant correlation between the sensitivity of the eye (as defined by k) and the temporal resolving power of the eye for the malacostracan species in this study.

Hypothesis 2: Mesopelagic malacostracan species that inhabit deeper depths during the daytime will have a lower temporal resolution than those species with a shallower daytime depth distribution.
H_0 = there will be no difference in temporal resolution between the mesopelagic species studied regardless of their daytime depth distribution.

The null hypothesis is rejected as temporal resolving power does differ between mesopelagic species as determined by the differences in the values of F_{10} for the mesopelagic species. The frequency response of the eyes of the mesopelagic species (defined by F_{10}) can be related to ambient light levels at the respective daytime depth distributions inhabited for all mesopelagic species except *Systellaspis debilis*. The temporal resolving power of *S. debilis* is explained by the potential behavioural requirements of this species and therefore required visual tasks.

Hypothesis 3: That shallower living mesopelagic malacostracans will have a temporal resolution different to that of shallow water, coastal nocturnally active, malacostracans.
H_0 = there will be no difference in temporal resolution between shallow water, nocturnally active and mesopelagic malacostracans.

The null hypothesis is rejected, as there is a difference between the temporal resolving power of the eyes of shallow-water, coastal nocturnally active species and shallower living mesopelagic species. The eyes of the shallow-water, coastal nocturnally active species have a higher temporal resolving power than those of the shallower living mesopelagic species. This can be related to the greater range of ambient irradiance levels experienced by the shallow-water coastal species in comparison with those experienced by the shallower living mesopelagic species.

CHAPTER 6: GENERAL CONCLUSIONS AND DISCUSSION

The present study considers the visual ecology of both mesopelagic and coastal, shallow-water malacostracan crustacean species in relation to the physiology of their visual response. The differences in the visual ecology of these two groups of animals have been reviewed in other sections of this thesis (sections *1.3, 1.4, 3.1*). To summarise, mesopelagic species inhabit an environment in which ambient light is very low, and in which the visual field is very uniform, being relatively constant in both spectral and spatial distribution and without solid boundaries. The uniform background of the deep-sea environment is occasionally augmented with relatively very bright bioluminescent signals and the malacostracan species in the mesopelagic environment have well-developed compound eyes. The presence of these signals and the well-developed eyes of mesopelagic animals indicate that these signals are used as a communication channel for the deep-sea inhabitants. The three major functions of bioluminescent signals are believed to be mate attraction, prey detection and predator avoidance (Herring, 1976, 1983). These signals are conservatively used however, as they are highly conspicuous against the background of the mesopelagic environment and therefore are an advertisement to all (including predators) of the location of the source of the signal. The coastal, shallow-water light environment is spectrally more diverse, potentially much brighter, and in terms of spatial distribution more complex than the mesopelagic environment. It is also an environment filled with solid boundaries that often provide visual contrasts. Therefore the visual tasks of an animal in this environment may be expected to be quite different to those of a mesopelagic animal. The differences in the light environments inhabited provide an excellent opportunity for a comparative study of visual function.

Unlike many terrestrial and shallow-water animals, e.g. birds and tropical fish such as the guppy (*Poecilia reticulata*), in which behavioural observation and studies are common and informative, it is not possible to observe the behaviour of mesopelagic animals *in situ* without introducing a relatively large amount of light into the environment to enable us to record behaviour. This is both unnatural and has been proven to cause irreversible damage to the visual systems of deep-sea animals, particularly crustaceans (Loew, 1976; Nilssön and Lindström, 1983; Shelton *et al.* 1985). Behavioural experiments in a laboratory are difficult, as once removed from their natural habitat, mesopelagic animals are often moribund, or prone to deterioration over a short time scale. Consequently, physiological rather than behavioural

studies of the visual systems of these animals are more tenable and can indicate the way in which they respond to light. The optical morphologies, spectral sensitivities and spatial acuities of mesopelagic malacostracan species have been studied previously, but there is a lack of information on the temporal response dynamics of the photoreceptors in the eye. Just as much as the optical factors, this property of the visual response ultimately determines the quality of the neural image generated because the temporal response dynamics of the photoreceptors in the eye determines the resolution of an object moving across the visual field (see section *4.1* for a review of temporal resolving power).

The present study therefore investigates the sensitivities and temporal resolving powers of the eyes of both mesopelagic and coastal, shallow-water malacostracans for comparative purposes, and in order to provide more information with respect to what marine malacostracans may be capable of seeing in their respective environments.

6.1 Summary of Findings

This study has used extracellular electrophysiological recordings (ERGs) to investigate the photoreceptor response dynamics of both deep-sea and coastal, shallow-water malacostracan species.

The species of marine malacostracan studied here have eyes with response properties similar to those of terrestrial arthropods in terms of the shape and dynamic range of the VlogI relationships, the shape of the dark-adapted frequency responses (exhibiting properties similar to those of low-pass filters), and the shape of the impulse responses. A summary of the findings from each Chapter of this thesis is given below.

6.1.1 Visual sensitivity and the speed of photoreceptor response

Chapter 3 investigates the sensitivity and speed of the photoreceptor response of the eyes of five mesopelagic and two coastal, shallow-water malacostracan species.

The species *Acanthephyra purpurea* and *Systellaspis debilis* were obtained from Jerlov type II ocean water and are the deepest living mesopelagic species studied. These two species

therefore inhabit an environment with the lowest irradiance levels in comparison with the other mesopelagic species studied. The eyes of these two species are approximately 4,400 times more sensitive to a broad blue light source than the eyes of the coastal, shallow-water species studied and this can be related to the difference in ambient irradiances in the respective environments of the two groups of animals (see sections *3.5.3, 3.5.4, 3.5.5*).

It is also established that there is a significant negative correlation ($r = -0.776$; $p=0.040$; $df = 5$) between the sensitivity of the eye (as defined by the irradiance at the eye that generates a response with an amplitude that is 50% of the maximum, i.e. k), and the speed of the response of the photoreceptors in the eye (as defined by the response latency, i.e. time between onset of light stimulus and start of response) for all the malacostracan species studied. This correlation is significant despite the eye of the mesopelagic euphausiid species *Meganyctiphanes norvegica* having a very short response latency and an eye with an intermediate sensitivity. For all the decapod malacostracan species studied (i.e. excluding the euphausiid *M. norvegica*), a very sensitive eye (e.g. the deepest living mesopelagic species, *A. purpurea* and *S. debilis*) has a relatively long response latency and conversely, a relatively insensitive eye (e.g. the coastal species *Crangon crangon* and *Palaemon elegans*) has a relatively short response latency. This correlation between the sensitivity of an eye and the speed of photoreceptor response for the decapod species provides evidence of an evolutionary adaptation to increased sensitivity at the neural level, i.e. at the level of the photoreceptor membrane (see section *6.2*). Response latency of the eye can also be related to the optical environment inhabited, for example, *A. purpurea* and *S. debilis* have eyes with the longest response latencies of all the species studied, and they inhabit an environment with the lowest ambient irradiance. Whereas the mesopelagic euphausiid species *M. norvegica* has an eye with the shortest response latency and inhabits an environment with the highest ambient irradiance of all the species studied.

For three of the mesopelagic species studied (*M. norvegica, Pasiphaea multidentata* and *Sergestes arcticus*), there are measurements of downwelling irradiance available to quantify the amount of ambient light in their natural habitats. In comparing the dynamic response ranges of the eyes of these three species with the levels of downwelling irradiance (at 480nm) available in their respective environments, it is apparent that the brightest downwelling irradiance levels at the daytime depth distributions of each species produce threshold responses from the eyes of each species. It is also acknowledged that the values for irradiance levels in the environments

of these three species quoted in Chapter 3 (Table 3h, section *3.5.4.1*) are an underestimation of total irradiance at depth in the ocean (see section *3.5.4.1*). The eyes of these mesopelagic species are also likely to be adapted, in terms of sensitivity, to viewing bioluminescent signals that occur at a distance of less than 10m (current estimates indicate that the irradiance of a bioluminescent signal at the eye of an observer that is a distance of 10m from the source will be *ca.* $8x10^2$-$8x10^4$ photons s^{-1} cm^{-2} [Herring, 2000a], and this may be below the detection range of the species in this study, see Chapter 3 section *3.5.4.1*). However, further measurements of downwelling irradiance, the irradiance of bioluminescent emissions in sea water, and modelling of the visual responses of these species to both diffuse and point sources of light are required before reliable inferences of this nature can be made.

The coastal, shallow-water decapod malacostracan species, *C. crangon* and *P. elegans* were found to have the least sensitive eyes with the fastest response latencies (with the exception of the euphausiid *M. norvegica*) of all the species studied and these animals also inhabit an environment in which ambient light levels are greater than those for the mesopelagic species.

In conclusion, the results of this experiment indicate that there is a significant correlation between the temporal dynamics of the initial stages of phototransduction in the photoreceptor and the overall relative sensitivity of the eye for decapod malacostracans (see section *6.2*), and that these factors appear to be affected by the ambient light levels experienced in the natural habitat.

6.1.2 Temporal resolving power and the frequency response method

Chapter 4 of this thesis investigates the use of the frequency response method in determining the temporal resolving powers of the eyes of four species of mesopelagic malacostracan. This study also reports the methodological considerations involved in producing a sinusoidal output from an LED.

For all four mesopelagic species studied, both the response magnitude and the phase delay in the visual response are determined for a range of different stimulus frequencies, facilitating the construction of a Bode plot for the visual response of each species. The Bode plots for each species indicate that there is a close relationship between log response amplitude of the

sinusoidal response from the eye and the phase delay in the response of the eye. The phase delay in the response leads to a reduction in the power of the visual response. This reduction in power increases until the stimulus frequency modulates too rapidly to be followed and the eye cannot resolve the modulation of light intensity.

The eyes of all four mesopelagic species studied show a maximum response magnitude in response to sinusoidal stimulus frequencies of 0.5Hz (the slowest stimulus delivered), and have frequency responses with properties analogous to those of a low pass filter, i.e. high frequencies are not processed. Stimulating the eyes with frequencies lower than 0.5Hz was impossible due to the constraints of working on board a moving vessel.

The temporal resolving powers of the eyes of the species studied are compared in terms of the maximum stimulus frequency that produces a resolvable sinusoidal stimulus from the eye. For two of the four decapod oplophorid species studied (*O. spinosus* and *S. debilis*), temporal resolving power (as defined above) can be related to both daytime depth distribution, in terms of downwelling irradiance levels, and the sensitivity of the eye, as defined by k. For the two other species (*A. purpurea* and *N. gibbosus*) temporal resolving power is not related to daytime depth distribution. The species *N. gibbosus* has a relatively high frequency response and low sensitivity considering it has the deepest daytime depth distribution of all the species studied (and therefore inhabits an environment with the lowest irradiance levels), and it is proposed that this is an adaptation to prioritise the tracking and hunting of bioluminescent prey. The species *A. purpurea* has a relatively high frequency response and yet a relatively high sensitivity that is comparable to that for the eye of *S. debilis*. It is proposed that this could be an adaptation to optimising the visualisation of moving objects in the water, be they bioluminescent or silhouettes.

It is concluded that the frequency response method is unsuitable for determining the temporal resolving powers of mesopelagic species due to the long experimental time incurred and the need to conduct experiments on board a moving vessel. It is also concluded that the results obtained from this study should be interpreted with care, as the maximum resolvable frequency of response will depend upon the intrinsic photoreceptor noise in the eye, and this can vary between species (Smola and Gemperlein, 1973; Smola, 1976, cited in Laughlin, 1981) and within a single retina (Burton *et al.* 2001).

6.1.3 Temporal resolving power and the impulse response method

Chapter 5 of this thesis investigates the use of the impulse response method in determining the temporal resolving powers of the eyes of four mesopelagic and two coastal, shallow-water malacostracan species. It is proposed that this is an effective and relatively simple method by which to determine the frequency response of an eye. In Chapter 5 of this study, the frequency response of the eye of *S. debilis* is determined and the results are compared with those obtained for the same species in Chapter 4. The results of both studies are very similar for the species *S. debilis*. The results of Chapter 5 are also comparable with those of Chapter 4 in that the frequency responses determined for the eyes of all the species studied have properties analogous to those of a low pass filter, only differing between species in the extent of roll-off in response signal power as stimulus frequency increases. It is concluded that the impulse response method has advantages over the frequency response method as it allows a complete description of the frequency response of the eye of an animal by stimulating the eye with a relatively dim light pulse of short duration. The nature of the impulse stimulus allows for adequate averaging of the impulse response as the stimulus can be repeatedly delivered to the eye over a relatively short timescale. The impulse response method also allows a description of the photoreceptor response dynamics of the eye in both the time domain and the frequency domain, and therefore the relationship between the two can be investigated.

It should be kept in mind, however, that visual systems are inherently non-linear in their response. Strictly, therefore, the temporal response to an impulse stimulus depends on the intensity of the stimulus. The stimulus used in the present study was sufficiently bright to stimulate the eye at $50\%V_{max}$ (half maximum). Further studies are required to elucidate the effect of different stimulus intensities on temporal response characteristics. Clearly, large differences are unlikely due to the underlying physiology of the photoreceptors being the determinant of temporal characteristics of an eye, but subtle differences may affect an animal's ability to track or discern bioluminescent events of different intensities. This work should be a priority for further study.

For all the malacostracan species studied, both mesopelagic and coastal, there is a significant negative correlation (r = - 0.932; p=0.007; df = 4) between the sum of the parameters t_p and d ($t_p + d$; t_p is the time-to-peak from the start of the response, and d is the time between the onset

of the stimulus and the peak of the response) and the F_{10} value for each species (frequency at which signal power has fallen to 10% of the maximum). Therefore for all species studied, there is an inverse relationship between the time to peak of the impulse response from the onset of the stimulus and the temporal resolving power of the eye. For all the species studied there is also a significant positive correlation (r = 0.900, p=0.015; df = 4) between the value of F_{10} and the irradiance levels experienced in the natural habitat for each species. Thus the temporal resolving powers of the eyes of the marine malacostracans in this study are correlated with the ambient light available in their respective natural environments; an animal inhabiting an environment with the lowest irradiance levels, e.g. *P. multidentata* has a much slower frequency response than an animal inhabiting an environment with relatively greater irradiance levels, e.g. *M. norvegica*. There is no significant correlation (r = -0.631; p=0.179; df = 4), however, between the values of F_{10} and k (sensitivity) for the malacostracan species studied. This is despite the fact that response latency and k are significantly correlated as determined by the results of Chapter 3, which investigates the sensitivity and latency of the same species as those studied in Chapter 5. It may be proposed, therefore, that whilst visual sensitivity is affected in some way by the latency in the photoreceptor response in response to a light stimulus, visual sensitivity and overall temporal resolving power are not intrinsically linked for the marine malacostracans studied here (these factors are discussed in section *6.2*).

The impulse response method also facilitates the determination of the corner frequency (CF) for the marine malacostracan species studied, which allows a comparison of the CF values for the species in the present study with those determined for other arthropod species. Such a comparison reveals that even the relatively fast eyes of the coastal malacostracan species (*C. crangon* and *P. elegans*, CF = 1.04 and 1.16 respectively) are considerably slower than the 'slow' eyes of the crane fly (*Tipula paludosus*) that have a CF value of 7Hz, this being the lowest CF value obtained in a comparative study of 20 dipteran species (Laughlin and Weckström, 1993). This comparison takes into consideration the fact that the study of Laughlin and Weckström (1993) used threshold intensities to stimulate the eyes of the dipteran species whereas the present study uses intensities that generate half maximum responses from the eye ($50\%V_{max}$), see Chapter 5, section *5.5.1*.

6.1.4 Summary of results

Table 6a presents a summary of the results obtained from all three studies in this thesis.

	Species	Irradiance (photons s^{-1} cm^{-2} nm^{-1}) in environment [§]	F_{10} (Hz) [§]	$t_p + d$ (ms) [§]	k (log photons s^{-1} cm^{-2}) [†]	Response latency (ms) [†]	Max resolvable frequency (Hz) [‡]
Mesopelagic	*S. arcticus*	$1.5x10^{5*}$	1.71	99.10	10.99	33.0	–
	P. multidentata	$1.3x10^{6*}$	1.65	126.10	11.48	30.5	–
	S. debilis	$1.0x10^{7\sim}$	2.69	99.80	8.66	48.2	7.0
	A. purpurea	–	–	–	8.66	49.5	15.0
	M. norvegica	$3.0x10^{7*}$	3.78	76.20	10.44	14.3	–
	N. gibbosus	–	–	–	9.31[3]	–	10.0
	O. spinosus	–	–	–	9.13[3]	–	15.0
Coastal	*C. crangon*	$1.0x10^{8\square}$	4.21	43.09	12.31	24.0	–
	P. elegans	$1.0x10^{8\square}$	4.52	49.22	12.02	20.3	–

Table 6a. A summary of the results obtained from all three studies in this thesis. Where available, information on the downwelling irradiance levels at 480nm, at the upper range of the daytime depth distribution of each mesopelagic species, is given (*Widder, E. A., and Frank, T. M., pers. comm.; ~Frank and Widder [1996]), and the irradiance measurements at 500nm of light at the water surface on a clear moonlit night are given for the coastal species ([□]Dusenbery, 1992). Also included for each species (where available) are: the value of F_{10} (where not available, the maximum resolvable frequency is given that indicates the maximum frequency that produces a resolvable sinusoidal response from the eye); the value of $t_p + d$; the value of k (i.e. sensitivity) and response latency.
[§]data obtained from Chapter 5.
[†]data obtained from study of Chapter 3.
[‡]data obtained from study of Chapter 4.

The results in Table 6a show that the eyes of the mesopelagic species *A. purpurea* and *S. debilis* have high sensitivities that are accompanied by relatively high frequency responses. It is suggested that for these two species sensitivity is high so as to maximise contrast sensitivity, whilst a relatively high temporal resolution is used to optimise the detection of moving objects in the water. The mechanism behind maintaining sensitivity whilst maintaining relatively fast photoreceptor response dynamics is discussed in section *6.2*. The euphausiid species *M. norvegica* has a visual response that is quite different to that of the decapod species studied in that it has a relatively high frequency response, a low value of $t_p + d$ and the shortest response latency despite having an intermediate relative sensitivity that is comparable to that of the decapod species *S. arcticus* (see Table 6a). It is possible that this is an adaptation to optimising visual function in this euphausiid species (see section *6.2*).

6.2 Phototransduction and Potassium (K^+) Channels

The frequency response of the eyes of the marine malacostracan species studied here are relatively very slow. For example, the corner frequency of the mesopelagic species *M. norvegica* and the two coastal species *C. crangon* and *P. elegans* are the fastest of all the species studied and are 1.34, 1.04 and 1.16Hz respectively. This can be compared with the 'slow' response of nocturnally active slow moving crane flies, which have a dark-adapted CF of 7Hz, or equally with the CF of the light-adapted blowfly, which is more than 100Hz, and is the fastest photoreceptor response known. Studies by Wecktsröm *et al.* (1991), Laughlin and Weckström, (1993) and Laughlin (1996) have attributed the difference in the photoreceptor response speed between the 'slow' eyes of a crane fly and the 'fast' eyes of a blowfly to different types of voltage-activated potassium channels present in the photoreceptor membrane. These voltage-activated K^+ channels produce a K^+ conductance that is responsible for repolarising the photoreceptor membrane in response to light-activated depolarisation. The photoreceptor membranes of 'fast' eyes have prominent delayed rectifying K^+ channels, which produce a sustained outward current and thus repolarise the photoreceptor membrane rapidly (Weckström *et al.* 1991; Laughlin and Weckström, 1993). Conversely, the photoreceptor membranes of 'slow' eyes lack these channels and have transient inactivating K^+ conductances that slow the repolarisation of the cell (Laughlin and Weckström, 1993). The photoreceptors of the locust (*Schistocerca gregaria*) have both of the above types of K^+ conductance and the prominence of the two conductances changes diurnally; at night the inactivating channels are prominent as fast temporal response dynamics are not required and sensitivity is maximised and during the day when light levels are high, temporal resolution is improved by using the rapidly activating delayed rectifier K^+ channels (Weckström 1994, cited in Weckström and Laughlin, 1995).

Comparative studies of the temporal response dynamics of arthropod photoreceptors have revealed that there are considerable interspecies differences in the K^+ conductances of the photoreceptor membranes and these differences can be related to the light environment inhabited and visual behaviour (Weckström and Laughlin, 1995). It is clear that the mesopelagic and nocturnally active coastal malacostracan species studied here have very slow response dynamics in comparison with terrestrial arthropods and it is probable that this is determined to some extent by the type of voltage-sensitive K^+ channel expressed in the

photoreceptor membrane. However, these repolarising conductances cannot be entirely responsible for determining the speed of the photoreceptor response, as rate-limiting steps in the phototransduction cascade will determine the time taken to initiate a light-activated conductance.

The phototranduction cascade is initiated upon photon absorption by the visual pigments in the retina, which leads to a conformational change in the visual pigment molecules. This conformational change triggers the release of second messengers (internal transmitters) that trigger light activated Na^+ conductance into the cell across the photoreceptor membrane, causing depolarisation. The temporal dynamics of the phototransduction cascade will limit the temporal response properties of the photoreceptor. The response latency represents the time taken for internal transmitters to reach threshold concentrations and so trigger depolarisations of the photoreceptor membrane. For the decapod malacostracan species studied here, response latency is correlated with sensitivity as defined by k. It is proposed, therefore, that the initial stages of phototransduction in the eyes of the species studied are related to the sensitivity of the visual response. A mechanism for increasing sensitivity involves producing relatively large quantum bumps of long duration to maximise the integration time of the photoreceptor and consequently the photon signal (Laughlin, 1990; Laughlin and Weckström, 1993). Therefore an overall slowing of the phototransduction cascade increases both response latency and the temporal properties of quantum bumps. As it is not possible to record quantum bumps using the ERG, it is suggested that long response latency may indicate a slowing of the phototransduction cascade, and also a change in the temporal properties of the quantum bumps generated in response to individual photon 'hits'. Intracellular recordings of quantum bump properties would be required to confirm this.

The values of F_{10} obtained for marine malacostracans in Chapter 5 of this thesis are not correlated with k but are correlated with $t_p + d$. The F_{10} value is a measure of the frequency response of the eye, and whilst this will, to a certain extent, depend upon the response latency of the eye and the rate of rise of the response as determined by the rate of rise of internal transmitter concentration (see Chapter 5, section *5.5.1*). It will also depend upon the speed of repolarisation of the photoreceptor. The parameter d represents response latency, and on its own is not correlated with F_{10}, however, when summed with t_p, $(t_p + d)$ represents the time course of both the phototransduction cascade and the repolarisation of the photoreceptor

membrane. The time taken to reach peak depolarisation of the photoreceptor membrane is defined by the time constant of the membrane and will depend upon a combination of the rate of rise of internal transmitter (responsible for the rate of opening of Na^+ channels), and the strength of repolarisation, e.g. a strong, rapidly activating K^+ conductance (such as the delayed rectifier) will reduce the time-to-peak of the depolarisation as repolarisation will occur quickly. It is therefore the combined temporal response dynamics of the phototransduction cascade and the repolarising K^+ conductance that define the frequency response of the photoreceptors of the species in this study and ultimately determine how well an eye will follow temporal modulations in light intensity.

Intracellular investigations would be required to determine which ion channels are present in the photoreceptor membrane and how they affect the time constant of the membrane. Laughlin's (1996) study uses intracellular techniques to determine the temporal dynamics of both the photoransduction cascade and the photoreceptor membrane on the eye of the crane fly (*Tipula paludosa*). Laughlin (1996) finds that the temporal dynamics of the phototransduction cascade and the photoreceptor membrane are matched, and this is in order to remove shot noise generated during molecular processes of phototransduction. Such techniques however, are beyond the scope of this study.

It is safe to assume, nevertheless, that the photoreceptors of the species studied here have both a relatively slow phototrandsduction cascade and weak repolarising K^+ conductance across the photoreceptor membrane in comparisons with previous findings for terrestrial arthropods. This can be related to the visual ecology of the animals studied in this thesis. All the species studied in this thesis inhabit environments in which ambient irradiance is low. The mesopelagic species are also required to see bioluminescent signals, which are rarely emitted, and may be close by or some distance away. It becomes important, therefore, for these animals to increase visual sensitivity and this can be achieved by increasing the integration time of the photoreceptor to ensure that photon capture is maximised. Weckström and Laughlin (1995) suggest that a fast visual response would be undesirable for animals using vision in an environment that is photon-limited. This is because signal-to-noise ratios are low, as are temporal modulations in light intensity (see exception below for bioluminescent signals) and high retinal velocities are rare. Fast response dynamics are also metabolically demanding, the high conductances associated with the repolarising delayed rectifier K^+ channels require high

metabolic expenditure to maintain ion concentrations across the membrane, and at rest the blowfly uses 10% of its total energy expenditure in maintaining photoreceptor ion balances (Weckström and Laughlin, 1995).

The results of the present study find that the visual responses of the species *A. purpurea* and *S. debilis* have relatively long response latencies, are relatively highly sensitive, and have relatively fast temporal resolving power. This may be related to these species prioritising the detection of both moving silhouette objects and perhaps, more significantly, bioluminescent signals, which are unusually fast, high contrast modulations in light intensity occurring against a photon-limited background space light. To achieve a relatively fast temporal response whilst maintaining sensitivity there may be specific repolarising ion channels in the photoreceptor membrane that repolarise the photoreceptor relatively rapidly, but to determine this is beyond the method of this study. If such a mechanism were to exist it would be metabolically demanding and therefore would be required to confer a distinct advantage. For example, the photoreceptors of male bibionids (love bugs) have fast response dynamics that are metabolically expensive as its reproductive success depends upon mating with a female, and the rapid response dynamics aid in visually tracking the female, which moves at high retinal velocities (Laughlin and Weckström, 1993). Interestingly, the female bibionids have slower response dynamics than the males as it does not benefit them to expend the energy required in fast response dynamics (Laughlin and Weckström, 1993).

The mesopelagic euphausiid species *M. norvegica* is unusual in having fast response dynamics, both in terms of response latency and frequency response, and yet a relatively sensitive eye. It is hard to explain this in terms of physiology and one would require a larger comparative study, with more representatives of this taxon being studied, to determine the significance of this. Frank (1999, 2000) determined the temporal resolving powers (using the critical flicker fusion method, see section *4.6.4* for detail) of three euphausiid species, *Nematobrachion flexipes*, *N. sexspinosus* and *Stylocheiron maximum*. These three euphausiid species had overall faster response dynamics than eight other mesopelagic malacostracan species studied and this is related to these euphausiid species inhabiting depths with greater irradiances than the other species studied (Frank, 2000). This in agreement with the results of the present study, where the euphausiid species *M. norvegica* has the highest temporal resolving power of the mesopelagic species studied. However, the studies of Frank (1999, 2000) indicate that there is

a correlation between temporal resolving power and visual sensitivity, which cannot be conferred by the results of the present study.

Mesopelagic species of malacostracan inhabit environments in which the ambient light levels are low in comparison with the ambient light levels in the environments of coastal, shallow-water, nocturnally active malacostracans. Consequently mesopelagic species have eyes that are relatively very sensitive to light and have slow response dynamics. The results of the present study therefore support the proposal that photoreceptor response dynamics are tuned to the habitat and lifestyle of the animal (Howard *et al.* 1984, deSouza and Ventura, 1989, Laughlin and Weckström, 1993).

6.3 Ecology and Vision

There is very little knowledge of the behaviour of mesopelagic malacostracans *in situ* due to the problems associated with obtaining behavioural data (as mentioned in the introduction to this chapter). It is therefore difficult to relate visual physiology to specific visual tasks. However, the results of this study can be used to predict visual behaviour to a certain extent. For example, the unusually fast eyes of some of the mesopelagic species studied (unusually fast when considered in relation to visual sensitivity and daytime depth distribution) may well be correlated with specific and successful predation or mating activity, particularly when one considers that a fast eye is likely to be metabolically expensive, i.e. the ability to resolve fast events has to confer a rewarding advantage. The two deep-living oplophorid species, *Acanthephyra purpurea* and *Systellaspis debilis* have faster temporal resolving powers than one might predict on the basis of their daytime depth distributions and visual sensitivities. It is suggested that this allows these animals to efficiently detect contrast (high sensitivity confers good contrast sensitivity; Laughlin, 1981) whilst also optimising temporal resolution. It is possible that this allows these animals to efficiently track objects, be they bioluminescent or silhouettes, and therefore that these animals have specific predatory or mating behaviour that may not be seen in the other species studied. The deep-living oplophorid species *Notostomus gibbosus* appears to have both a relatively insensitive and fast visual response considering that it occupies one of the greatest optical depths of the species in this study. It is proposed that this animal sacrifices contrast/visual sensitivity for the ability to resolve events in time more efficiently. It is probable that this is an evolutionary adaptation to hunting moving

bioluminescent prey, as contrast sensitivity is less important when one considers a bright bioluminescent flash against the dim ambient light of the mesopelagic zone. The euphausiid species *M. norvegica* has an unusual visual response when compared with the decapod species studied. The response dynamics of the eye are faster than those for any mesopelagic decapod studied, and yet the eye has an intermediate sensitivity. It is difficult to explain this in terms of physiology, but it is interesting that the studies of Frank (1999, 2000) also found that the three euphausiid species studied had eyes with faster response dynamics than any of the decapod species studied. As mentioned previously however, it would be necessary to obtain more data from euphausiid species before any conclusions can be drawn. Similarly, data on the visual function of more coastal, shallow-water species would be required before inferences can be made about the role of vision in their behaviour.

6.4 Further Work

6.4.1 Electrophysiology and the impulse response method

The impulse response method should be used to determine the temporal response dynamics of the eyes of mesopelagic species. Because of the convenience of the impulse response method in terms of the short timescale in which data can be obtained and the ease with which the light stimulus can be produced, it is suggested that this method has advantages over others, particularly in determining the temporal resolving powers of the eyes/photoreceptors of mesopelagic species.

This method can be used to obtain regional extracellular recordings of the temporal resolving powers of the eyes of marine malacostracans. For example, one could take extracellular recordings from the dorsal versus the ventral regions of the eye in order to look for regional variation in temporal resolving power, as has been identified in the eye of the blowfly *Calliphora vicina* (Burton *et al.* 2001). Morphological studies of the eyes of a number of oplophorid decapod malacostracans, e.g. *Oplophorus spinosus*, *Systellaspis debilis*, have shown morphological adaptations in the dorsal and ventral rhabdoms that indicate adaptation to optimising dorsal and ventral vision (Gaten *et al.* 1992). Similarly, for those marine species that possess dual pigment systems e.g. *Systellaspis debilis* (Frank and Case, 1988a) and several coastal species (Goldsmith and Fernandez, 1968; Wald and Seldin, 1968; Johnson, 1998) it

would be interesting to determine whether or not the different wavelength sensitive photoreceptors have different response dynamics.

It would also be interesting to look for both sexual dimorphism and ontogenetic differences in temporal resolving power of the eyes of marine malacostracans. It is possible that ontogenetic difference in temporal resolving power exist, as in some mesopelagic decapod species there are ontogenetic changes in compound eye structure that can be associated with the differences in the habitat of the larvae and the adults (Land, 1984; Herring and Roe, 1988, see section *1.6.1*).

Extracellular techniques can also be used to determine the extent to which the photoreceptors of mesopelagic species are able to light-adapt. Determining the temporal resolution of the light-adapted eyes of coastal species may be informative as studies on both terrestrial arthropod species (e.g. Pinter, 1972) and two coastal species (Johnson *et al.* 2000a) have shown that light adaptation introduces band-pass characteristics into the frequency response of the photoreceptors. Such band-pass characteristics contrast with the low-pass filter typical of the dark-adapted crustacean eye and that of mesopelagic species. Light adaptation also increases temporal resolution; Weckström and Laughlin's (1995) review reports a tenfold acceleration in the response dynamics of fly photoreceptors upon light adaptation. Although there is evidence to suggest that there are no optical mechanisms of light-adaptation in the eyes of mesopelagic species i.e. there is a lack of mobile screening pigment present in the eyes of mesopelagic decapod and euphausiid species (Land, 1976; Hallberg and Elofsson, 1989; Gaten *et al.* 1992), it is possible that there are mechanisms at the neural level that will alter the sensitivity of the eye upon prolonged exposure to low-level irradiances.

Intracellular recording techniques could be used to determine the following: photoreceptor noise levels, specific regional variations in photoreceptor response properties, and the specific membrane conductances present across the photoreceptor membrane, in order to elucidate the mechanisms behind the differences in temporal response dynamics. However, at present, there is no viable way of looking at the photoreceptors of deep-sea species using such delicate techniques.

6.4.2 Modelling of the visual response

There are a number of studies that have measured the time course of stimulated bioluminescent emissions, for example, Herring (1976), Mensinger and Case (1997) and Lindsay *et al.* (1999). As the present study has determined frequency response measurements from the dark-adapted eyes of mesopelagic species, one could construct a digital filter with the same low-pass properties as the frequency response of the eyes of a mesopelagic species to effectively produce a 'shrimp eye' filter. The temporal distribution of a bioluminescent signal could then be processed using the 'shrimp eye' filter and the output would indicate the frequency components of the bioluminescent signal that the eye could resolve and thus one could visualise what a mesopelagic malacostracan may be 'seeing' when observing bioluminescent signals.

In order to enhance the above analysis of the visual function of a mesopelagic shrimp, it would be possible to integrate the temporal properties of the eye with the spatial properties (where determined) and calculate the spatio-temporal response of the eye. Glantz's (1991) study of motion detection and adaptation of the photoreceptors of the crayfish (*Procambarus clarkii*) indicates that the ratio of the time constant of the photoreceptor to the acceptance angle of the ommatidium will determine the sensitivity of the eye to variations in stimulus velocity. Such modelling would require determination of both the time constant and acceptance angles of individual photoreceptors. In order to determine the time constant of the photoreceptor, one would need to measure the response of the photoreceptors using intracellular recording techniques as the time constant is the product of the membrane resistance and capacitance ($\tau = R_m C_m$; where R_m is membrane resistance and C_m is membrane capacitance). Knowledge of the spatio-temporal properties of the eyes of marine malacostracans would allow one to determine the properties of the visual response to any given stimulus.

REFERENCES

Aréchiga, H. (1977). Circadian rhythmycity in the nervous system of crustaceans. *Federation Proceedings* **36,** 2036-2041.

Armington, J. C. (1974). The Electroretinogram: Academic Press, London.

Autrum, H. (1979). Introduction. In *Handbook of Sensory Physiology*, VII/6A, Comparative Physiology and Evolution of Vision in Invertebrates: Invertebrate Photoreceptors (ed. H. Autrum): Springer-Verlag.

Autrum, H. (1981). Light and Dark Adaptation in Invertebrates. In *Handbook of Sensory Physiology*, VII/6C, Comparative Physiology and Evolution of Vision in Invertebrates: Invertebrate Visual Centres and Behaviour II (ed. H. Autrum), pp. 1-91: Springer-Verlag.

Bader, C. R., Baumann, F. and Bertrand, D. (1976). Role of intracellular calcium and sodium in light adaptation in the retina of the honey bee drone (*Apis mellifer, L.*). *Journal of General Physiology* **67,** 475-491.

Beyer, F. (1992). *Meganyctiphanes norvegica* (M. Sars) (Euphausiacea) a voracious predator on *Calanus*, other copepods, and ctenophores, in Oslofjorden, Southern Norway. *Sarsia* **77,** 189-206.

Boring, E. G. (1942). Sensation and Perception in the History of Experimental Psychology: Appleton-Century, New York.

Bradbury, J. W. and Verhencamp, S. L. (1998). Principles of Animal Communication. Sunderland, Massachusetts: Sinaur Associates, Inc.

Burton, B. G., Tatler, B. W. and Laughlin, S. B. (2001). Variations in photoreceptor response dynamics across the fly retina. *The Journal of Neurophysiology* **86,** 950-960.

Cronin, T. and Forward, R. B. (1988). The visual pigments of crabs I: Spectral characteristics. *Journal of Comparative Physiology A* **162,** 463-478.

Cronin, T. and Frank, T. M. (1996). A short-wavelength photoreceptor class in a deep-sea shrimp. *Proceedings of the Royal Society of London B* **263,** 861-865.

de Souza, J. M. and Ventura, D. F. (1989). Comparative study of temporal summation and response form in hymenopteran photoreceptors. *Journal of Comparative Physiology A* **165,** 237-245.

Denton, E. J. (1990). Light and vision at depths greater than 200 metres. In *Light and Life in the Sea* (ed. P. J. Herring, A. K. Campbell, M. Whitfield and L. Maddock), pp. 127-148: Cambridge, UK. Cambridge University Press.

Denys, C. J. and Brown, P. K. (1982). The rhodopsins of *Euphausia superba* and *Meganyctiphanes norvegica* (Crustacea, Euphausiacea). *Journal of General Physiology* **80,** 451-472.

Dodge, F. A., Knight, B. W. and Toyoda, J. (1968). Voltage noise in *Limulus* visual cells. *Science, N.Y.* **160,** 88-90.

Douglas, R., Partridge, J. C. and Marshall, N. J. (1998). The eyes of deep-sea fish I: Lens pigmentation, tapeta and visual pigments. *Progress in Retinal and Eye Research* **17,** 597-636.

Dowling, J. E. (1968). Discrete potentials in the dark-adapted eye of the crab *Limulus*. *Nature* **217,** 28.

Dusenbery (1992). Sensory Ecology: How Organisms Acquire And Respond To Information. New York: W. H. Freeman and Company.

Eakin (1972). Structure of invertebrate photoreceptors. In *Handbook of Sensory Physiology*, VII/1, Photochemistry of Vision (ed. H. J. A. Dartnall), pp. 625-684. Berlin, Heidelberg, New York: Springer-Verlag.

Fain, G. L. and Lisman, J. E. (1981). Membrane conductances of photoreceptors. *Progress in Biophysics and Molecular Biology* **37,** 91-147.

Fincham, A. A. (1984). Ontongeny and optics of the eyes of the common prawn *Palaemon* (Palaemon) *serratus* (Pennant, 1977). *Zoological Journal of the Linnean Society* **81,** 89-113.

Forward, R. B., Cronin, T. and Douglass, J. K. (1988). The visual pigments of crabs II. Environmental adaptations. *Journal of Comparative Physiology A* **162,** 479-490.

Foxton, P. (1970). The vertical distribution of pelagic decapods (Crustacea: Natantia) collected on the Sond cruise 1965. *Journal of the Marine Biological Association UK* **50,** 939-960.

Frank, T. M. (1999). Comparative study of temporal resolution in the visual systems of mesopelagic crustaceans. *Biological Bulletin* **196,** 137-144.

Frank, T. M. (2000). Temporal resolution in mesopelagic crustaceans. *Philosophical Transcripts of the Royal Society London B* **355,** 1195-1198.

Frank, T. M. and Case, J. F. (1988a). Visual spectral sensitivities of bioluminescent deep-sea crustaceans. *Biological Bulletin* **175,** 262-273.

Frank, T. M. and Case, J. F. (1988b). Visual spectral sensitivity of the bioluminescent deep-sea mysid, *Gnathophausia ingens*. *Biological Bulletin* **175,** 274-283.

Frank, T. M. and Widder, E. A. (1994a). Evidence for behavioural sensitivity to near-uv light in the deep-sea crustacean *Systellaspis debilis*. *Marine Biology* **118,** 279-284.

Frank, T. M. and Widder, E. A. (1994b). Comparative study of behavioural-sensitivity thresholds to near-UV and blue-green light in deep-sea crustaceans. *Marine Biology* **121,** 229-235.

Frank, T. M. and Widder, E. A. (1996). UV light in the deep-sea: *in situ* measurements of downwelling irradiance in relation to the visual threshold sensitivity of uv-sensitive crustaceans. *Marine and Freshwater Behaviour and Physiology* **27,** 189-197.

Frank, T. M. and Widder, E. A. (1997). The correlation of downwelling irradiance and staggered vertical migration patterns of zooplankton in Wilkinson Basin, Gulf of Maine. *Journal of Plankton Research* **19,** 1975-1991.

Frank, T. M. and Widder, E. A. (1999). Comparative study of the spectral sensitivities of mesopelagic crustaceans. *Journal of Comparative Physiology A* **185,** 255-265.

Fuortes, M. G. F. and Hodgkin, A. L. (1964). Changes in time scale and sensitivity in the ommatidia of *Limulus*. *Journal of Physiology* **172,** 239-263.

Gaten, E., Shelton, P. M. J. and Herring, P. J. (1992). Regional morphological variations in the compound eyes of certain crustaceans in relationship to their habitat. *Journal of the Marine Biological Association UK* **72,** 61-75.

Glantz, R. M. (1968). Light adaptation in the photoreceptor of the crayfish, *Procambarus clarki*. *Vision Research* **8,** 1407-1421.

Glantz, R. M. (1972). Visual adaptation: a case of nonlinear summation. *Vision Research* **12,** 103-109.

Glantz, R. M. (1991). Motion detection and adaptation in crayfish receptors - a spatiotemporal analysis of linear movement sensitivity. *The Journal of General Physiology* **97,** 777-797.

Goldsmith, T. H. and Fernandez, H. R. (1968). Comparative studies of crustacean spectral sensitivity. *Zeitshrift fur vergleichende Physiologie* **60,** 156-175.

Granit, R. (1955). Receptors and Sensory Perception. New Haven: Yale University Press.

Hallberg, E. and Elofsson, R. (1989). Construction of the pigment shield of the crustacean compound eye: a review. *Journal of Crustacean Biology* **9,** 359-372.

Hartline, H. K. (1969). Visual receptors and retinal interaction. *Science* **111,** 252-254.

Hartline, H. K. and Ratcliffe, F. (1972). Inhibitory interaction in the retina of *Limulus.* In *Handbook of Sensory Physiology,* VII/12, Physiology of Photoreceptor organs (ed. H. Autrum): Springer-Verlag.

Hartline, H. K., Wagner, H. G. and MacNichol, E. F. (1952). The peripheral origins of nervous activity in the visual system. *Cold Spring Harbour Symposium Quant. Biology* **17,** 125.

Herring, P. J. (1976). Bioluminescence in decapod crustacea. *Journal of Marine Biological Association UK* **56,** 1029-1047.

Herring, P. J. (1983). The spectral characteristics of luminous marine organisms. *Proceedings of the Royal Society of London B* **220,** 183-217.

Herring, P. J. (2000a). Species abundance, sexual encounter and bioluminescent signalling in the deep sea. *Philosophical Transcripts of the Royal Society of London B* **355,** 1273-1276.

Herring, P. J. (2000b). Bioluminescent signals and the role of reflectors. *Journal of Optics A: Pure Applied Optics* **2,** R29-R38.

Herring, P. J. and Roe, H. S. J. (1988). The photoecology of pelagic oceanic decapods. *Symposium of the Zoological Society London* **59,** 263-290.

Hiller-Adams, P. and Case, J. F. (1984). Optical parameters of euphausiid eyes as a function of habitat depth. *Journal of Comparative Physiology A* **154,** 307-318.

Hiller-Adams, P. and Case, J. F. (1985). Optical parameters of the eyes of some benthic decapods as a function of habitat depth (Crustacea, Decapoda). *Zoomorphology* **105,** 108-113.

Hiller-Adams, P. and Case, J. F. (1988). Eye size of pelagic crustaceans as a function of habitat depth and possession of photophores. *Vision Research* **28,** 667-680.

Hiller-Adams, P., Widder, E. A. and Case, J. F. (1988). The visual pigments of four deep-sea crustacean species. *Journal of Comparative Physiology A* **163,** 63-72.

Hopkins, T. L., Gartner, J. V. and Flock, M. E. (1989). The caridean shrimp (Decapoda: Natantia) assemblage in the mesopelagic zone of the eastern Gulf of Mexico. *Bulletin of Marine Science* **45,** 1-14.

Howard, J. (1981). Temporal resolving power of the photoreceptors of *Locusta migratoria. Journal of Comparative Physiology* **144,** 61-66.

Howard, J., Dubs, A. and Payne, R. (1984). The dynamics of phototransduction in insects (a comparative study). *Journal of Comparative Physiology A* **154,** 707-718.

Hubbard, B. B. (1996). The World According to Wavelets. Wellesley, Massachusetts: A K Peters.

Jerlov, N. G. (1968). Optical Oceanography: Elsevier Oceanography Series, Amsterdam.

Jerlov, N. G. (1976). Marine Optics: Elsevier, Amsterdam.

Johnson, M. L. (1998). Aspects of Visual Function and Adaptation of Deep-sea Decapods. PhD Thesis: University of Leicester.

Johnson, M. L., Shelton, P. M. J. and Gaten, E. (2000a). Temporal resolution in the eyes of marine decapods from coastal and deep-sea habitats. *Marine Biology* **136,** 243-248.

Johnson, M. L., Shelton, P. M. J., Gaten, E. and Herring, P. J. (2000b). Relationship of dorsoventral eyeshine distributions to habitat depth and animal size in mesopelagic decapods. *Biological Bulletin* **199,** 6-13.

Kent, J. (1997). The Visual Pigments of Deep-sea Crustaceans. PhD Thesis: University of Bristol.

Kirk, J. T. O. (1994). Light and Photosynthesis in Aquatic Ecosystems. Cambridge: Cambridge University Press.

Knight, B. W., Toyoda, J. and Dodge, F. A. (1970). A quantitative description of the dynamics of excitation and inhibition in the eye of *Limulus. The Journal of General Physiology* **56,** 421-437.

Knowles, A. and Dartnall, H. J. A. (1977). The Photobiology of Vision. New York: Academic Press Inc.

Land, M. F. (1976). Superposition images are formed by reflection in the eyes of some oceanic decapod crustacea. *Nature* **263,** 764-765.

Land, M. F. (1981). Optics and Vision in Invertebrates. In *Handbook of Sensory Physiology*, VII/6B, Comparative Physiology and Evolution of Vision in Invertebrates B: Invertebrate Visual Centres and Behavior I. (ed. H. Autrum), pp. 471-592: Springer-Verlag.

Land, M. F. (1984). Crustacea. In *Photoreception and Vision in Invertebrates* (ed. M. A. Ali), pp. 401-438: Plenum Press.

Land, M. F. (1990). Optics of the eyes of marine animals. In *Light and Life in the Sea* (ed. P. J. Herring, A. K. Campbell, M. Whitfield and L. Maddock), pp. 149-166: Cambridge University Press, Cambridge, UK.

Land, M. F. (1992). Locomotion and visual behaviour of mid-water crustaceans. *Journal of the Marine Biological Association UK* **72,** 41-60.

Land, M. F. (1999). Compound eye structure: matching eye to environment. In *Adaptive Mechanisms in the Ecology of Vision* (ed. S. N. Archer, M. B. A. Djamoz, E. R. Loew, J. C. Partridge and S. Vallerga), pp 51-71. Dordrecht: Kluwer Academic Publishers.

Lass, S., Tarling, G. A., Virtue, P., Matthews, J. B. L., Mayzaud, P. and Buchholz, F. (2001). On the food of northern krill *Meganyctiphanes norvegica* in relation to its vertical distribution. *Marine Ecology Progress Series* **214.**

Laughlin, S. B. (1976). The sensitivities of dragonfly photoreceptors and the voltage gain of transduction. *Journal of Comparative Physiology,* **111,** 221-247.

Laughlin, S. B. (1981). Neural principles in the peripheral visual systems of invertebrates. In *Handbook of Sensory Physiology*, VII/6B, Comparative Physiology and Evolution of Vision in Invertebrates B: Invertebrate Visual Centres and Behavior I (ed. H. Autrum), pp. 135-280: Springer-Verlag.

Laughlin, S. B. (1990). Invertebrate vision at low luminances. In *Night Vision* (ed. R. F. Hess, L. T. Sharpe and K. Nordby), pp. 223-250: Cambridge University Press, Cambridge.

Laughlin, S. B. (1996). Matched Filtering by a Photoreceptor Membrane. *Vision Research* **36,** 1529-1541.

Laughlin, S. B. and Hardie, R. C. (1978). Common strategies for light adaptation in the peripheral visual systems of the fly and dragonfly. *Journal of Comparative Physiology* **128,** 319-340.

Laughlin, S. B. and Weckström, M. (1993). Fast and slow photoreceptors - a comparative study of the functional diversity of coding and conductances in the Diptera. *Journal of Comparative Physiology A* **172,** 593-609.

Lindsay, S. M., Frank, T. M., Kent, J., Partridge, J. C. and Latz, M. I. (1999). Spectral sensitivity of vision and bioluminescence in the midwater shrimp *Sergestes similis*. *Biological Bulletin* **197,** 348-360.

Lisman, J. E. and Brown, J. E. (1975a). Light-induced changes of sensitivity in *Limulus* ventral photoreceptors. *Journal of General Physiology* **66,** 473-489.

Lisman, J. E. and Brown, J. E. (1975b). Effects of intracellular injection of calcium buffers on light-adaptation in *Limulus* ventral photoreceptors. *Journal of General Physiology* **66,** 489-506.

Loew, E. R. (1976). Light and photoreceptor degeneration in the Norway lobster, *Nephrops norvegicus*. *Proceedings of the Royal Society London B* **193,** 31-44.

Lythgoe, J. N. (1968). Visual pigments and visual range underwater. *Vision Research* **8,** 997-1012.

Lythgoe, J. N. (1979). The Ecology of Vision. Oxford: Clarendon Press.

MacFarland, W. N. and Munz, F. W. (1975). Part II: The photic environment of clear tropical seas during the day. *Vision Research* **15,** 1063-1070.

Mangel, M. and Nicol, S. (2000). Krill and the unity of biology. *Canadian Journal of Fisheries and Aquatic Science* **57,** 1-5.

Marshall, J., Kent, J. and Cronin, T. (1999). Visual adaptations in crustaceans: spectral sensitivity in diverse habitats. In *Adaptive Mechanisms in the Ecology of Vision* (ed. S. N. Archer, M. B. A. Djamoz, E. R. Loew, J. C. Partridge and S. Vallerga), pp 285-327: Dordrecht: Kluwer Academic Publishers.

Martin, F. G. and Mote, M. I. (1982). Color receptor in marine crustaceans: a second spectral class of retinular cell in the compound eyes of *Callinectes* and *Carcinus*. *Journal of Comparative Physiology* **145,** 549-554.

Mensinger, A. F. and Case, J. F. (1997). Luminescent properties of fishes from nearshore California basins. *Journal of Experimental Marine Biology and Ecology* **210,** 75-90.

Moeller, J. F. and Case, J. F. (1994). Properties of visual interneurons in a deep-sea mysid, *Gnathophausia ingens*. *Marine Biology* **119,** 211-219.

Moeller, J. F. and Case, J. F. (1995). Temporal adaptations in visual systems of deep-sea crustaceans. *Marine Biology* **123,** 47-54.

Nilssön (1989). Optics and evolution of the compound eye. In *Facets of Vision* (ed. D. G. Stavenga and R. C. Hardie): pp. 30-73. Berlin, Heidelberg, New York: Springer-Verlag.

Nilssön, H. L. and Lindström, M. (1983). Retinal damage and sensitivity loss of a light-sensitive crustacean compound eye (*Cirolana borealis*): electron microscopy and electrophysiology. *Journal of Experimental Biology* **107,** 277-292.

Partridge, J. C. (1990). The Colour Sensitivity and Vision of Fishes. In *Light and Life in the Sea* (ed. P. J. Herring, A. K. Campbell, M. Whitfield and L. Maddock), pp 167-184: Cambridge: Cambridge University Press.

Partridge, J. C. and Cummings, M. E. (1999). Adaptation of visual pigments to the aquatic environment. In *Adaptive Mechanisms in the Ecology of Vision* (ed. S. N. Archer, M. B. Djamoz, E. R. Loew, J. C. Partridge and S. Vallerga), pp 251-283: Dordrecht: Kluwer Academic Publishers.

Payne, R. and Howard, J. (1981). Response of an insect photoreceptor: a simple log-normal model. *Nature* **290,** 415-416.

Pinter, R. B. (1972). Frequency and time domain properties of retinular cells of the desert locust (*Schistocerca gregaria*) and the house cricket (*Acheta domesticus*). *Journal of Comparative Physiology* **77,** 383-397.

Roe, H. S. J. and Shale, D. M. (1979). A new rectangular midwater trawl (RMT 1+8) and some modifications to the Institute of Oceanographic Sciences' RMT 1+8. *Marine Biology* **50,** 283-288.

Rozenberg, G. V. (1966). Twilight: a study in atmospheric optics. New York: Plenum Press.

Sardou, J., Etienne, M. and Andersen, V. (1996). Seasonal abundance and vertical distributions of macroplankton and micronekton in the Northwest Mediterranean sea. *Oceanol. Acta.***19,** 645-656.

Sathyendranath, S. and Platt, T. (1990). The Light Field in the Ocean: It's modification and exploitation by the pelagic biota. In *Light and Life in the Sea* (ed. P. J. Herring, A. K. Campbell, M. Whitfield and L. Maddock), pp 3-18: Cambridge: Cambridge University Press.

Scholes, J. H. (1964). Discrete subthreshold potentials from the dimly lit insect eye. *Nature* **202,** 572-573.

Shelton, P. M. J. and Gaten, E. (1996). Spatial resolution determined by electrophysiological measurement of acceptance angle in two species of benthic decapod crustacean. *Journal of the Marine Biological Association UK* **76,** 391-401.

Shelton, P. M. J., Gaten, E. and Chapman, C. J. (1985). Light and retinal damage in *Nephrops norvegica* (Crustacea). *Proceedings of the Royal Society London B* **226,** 217-236.

Shelton, P. M. J., Gaten, E. and Herring, P. J. (1992). Adaptations of tapeta in the eyes of mesopelagic shrimps to match the oceanic irradiance distribution. *Journal of the Marine Biological Association UK* **72,** 77-88.

Smaldon, G. (1993). Coastal shrimps and prawns keys and notes for identification of the species. In *Synopses of the British Fauna*; new series no. 15 (ed. L. B. Holthuis and C. H. J. M. Fransen): Shrewsbury.

Snyder, A. W. (1979). Physics of vision in compound eyes. In *Handbook of Sensory Physiology*, VII/6A, Comparative Physiology and Evolution of Vision in Invertebrates: Invertebrate Photoreceptors (ed. H. Autrum), pp. 225-313: Springer-Verlag.

Strausfield, N. J. and Nassel, D. R. (1981). Neuroarchitecture of brain regions that subserve the compound eyes of crustacea and insects. In Handbook of Sensory Physiology, VII/6B, Comparative Physiology and Evolution of Vision in Invertebrates B: Invertebrate Visual Centres and Behavior I (ed. H. Autrum): Springer-Verlag.

Tiews, K. (1954). Synopsis of biological data on the common shrimp *Crangon crangon* (Linneaus, 1758). *FAO Fisheries Synopsis* **91,** 1167-1224.

Valeton, J. M. and van Norren, D. (1983). Light adaptation of primate cones: an analysis based on extracellular data. *Vision Research* **12,** 1539-1547.

Wald, G. and Seldin, E. B. (1968). Spectral sensitivity of the common prawn, *Palaemonetes vulgaris. Journal of General Physiology* **51,** 694-700.

Warner, J. A., Latz, M. I. and Case, J. F. (1979). Cryptic bioluminescence in a midwater shrimp. *Science* **203,** 1109-1110.

Waterman, T. H. (1950). A light polarisation analyser in the compound eye of *Limulus. Science* **111,** 252-254.

Weckström, M., Hardie, R. C. and Laughlin, S. B. (1991). Voltage-activated potassium channels in blowfly photoreceptors and their role in light adaptation. *Journal of Physiology* **440,** 635-657.

Weckström, M. and Laughlin, S. B. (1995). Visual ecology and voltage-gated ion channels in insect photoreceptors. *Trends in Neurosciences* **18,** 17-21.

Widder, E. A. (1999). Bioluminescence. In *Adaptive Mechanisms in The Ecology of Vision* (ed. S. N. Archer, M. B. A. Djamgoz, E. R. Loew, J. C. Partridge and S. Vallerga), pp 555-581: Dordrecht: Kluwer Academic Publishers.

Widder, E. A. and Frank, T. M. (2001). The speed of an isolume: a shrimp's eye view. *Marine Biology* **138,** 669-677.

Widder, E. A., Latz, M. I. and Case, J. F. (1983). Marine bioluminescence spectra measured with an optical multichannel detection system. *Biological Bulletin* **165,** 791-810.

Wild, R. A., Darlington, E. and Herring, P. J. (1985). An acoustically controlled cod-end system for the recovery of deep-sea animals at *in situ* temperatures. *Deep-sea Research* **32,** 1583-1589.

Wright, W. D. (1967). The Rays Are Not Coloured. London: Adam Hilger Ltd.

Appendix I : Comparison of relative sensitivity between species using the variable k

Appendix I displays the p-values obtained from a post-hoc Tukey test used to determine the difference of the value of k between individual malacostracan species

	Crangon crangon	*Palaemon elegans*	*Pasiphaea multidentata*	*Sergestes arcticus*	*Meganyctiphanes norvegica*	*Systellaspis debilis*	*Acanthephyra purpurea*
Crangon crangon k = 12.31		0.734	0.008	p<0.0005	p<0.0005	p<0.0005	p<0.0005
Palaemon elegans k = 12.02			0.190	0.001	p<0.0005	p<0.0005	p<0.0005
Pasiphaea multidentata k = 11.48				0.427	0.001	p<0.0005	p<0.0005
Sergestes arcticus k = 10.99					0.235	p<0.0005	p<0.0005
Meganyctiphanes norvegica k = 10.44						p<0.0005	p<0.0005
Systellaspis debilis k = 8.66							1.000
Acanthephyra purpurea k = 8.66							

For all species, result of univariate analysis of variance: $F_{6,35} = 90.6$, $p<0.0005$

Appendix II: Comparison of the response latency between species using the variable latency

Appendix II displays the p-values obtained from a post-hoc Tukey test used to determine the difference of the value of latency (lat) between individual malacostracan species (lat = latency in ms)

	Crangon crangon	*Palaemon elegans*	*Pasiphaea multidentata*	*Sergestes arcticus*	*Meganyctiphanes norvegica*	*Systellaspis debilis*	*Acanthephyra purpurea*
Crangon crangon lat= 24.00		0.902	0.064	0.008	0.038	p<0.0005	p<0.0005
Palaemon elegans lat= 20.33			0.006	0.001	0.417	p<0.0005	p<0.0005
Pasiphaea multidentata lat= 30.50				0.856	p<0.0005	p<0.0005	p<0.0005
Sergestes arcticus lat= 33.00					p<0.0005	p<0.0005	0.002
Meganyctiphanes norvegica lat= 14.30						p<0.0005	p<0.0005
Systellaspis debilis lat= 48.20							1.000
Acanthephyra purpurea lat= 49.50							

For all species, result of univariate analysis of variance: $F_{6,33} = 44.6$, $p<0.0005$

Appendix III: Comparison of the gradient of the VlogI curve between species using the variable *m*

Appendix III displays the p-values obtained from a post-hoc Tukey test used to determine the difference of the value of *m* between individual malacostracan species

	Crangon crangon	*Palaemon elegans*	*Pasiphaea multidentata*	*Sergestes arcticus*	*Meganyctiphanes norvegica*	*Systellaspis debilis*	*Acanthephyra purpurea*
Crangon crangon *m*= 0.52		0.172	0.834	1.000	0.828	0.867	0.820
Palaemon elegans *m* = 0.37			0.017	0.398	0.012	0.011	0.038
Pasiphaea multidentata *m* = 0.60				0.818	1.000	1.000	1.000
Sergestes arcticus *m* = 0.50					0.815	0.854	0.799
Meganyctiphanes norvegica *m* = 0.60						1.000	1.000
Systellaspis debilis *m* = 0.59							1.000
Acanthephyra purpurea *m* = 0.62							

For all species, result of univariate analysis of variance: $F_{6,35} = 4.0$, $p=0.004$

Appendix IV : Comparison of the time-to-peak of the impulse response functions from mesopelagic and shallow-water coastal species of malacostracan using the variable t_p

Appendix IV displays the p-values obtained from a post-hoc Tukey test used to determine the difference of the value of t_p between individual malacostracan species (t_p = time to peak in milliseconds)

	Crangon crangon	*Palaemon elegans*	*Pasiphaea multidentata*	*Sergestes arcticus*	*Meganyctiphanes norvegica*	*Systellaspis debilis*
Crangon crangon t_p = 18.69		0.707	p<0.0005	0.001	p<0.0005	0.019
Palaemon elegans t_p = 29.72			p<0.0005	0.025	0.008	0.256
Pasiphaea multidentata t_p = 106.50				0.003	0.016	0.002
Sergestes arcticus t_p = 59.00					0.990	0.982
Meganyctiphanes norvegica t_p = 64.90						0.828
Systellaspis debilis t_p = 51.80						

For all species, result of univariate analysis of variance: $F_{5,30}$=17.9, p<0.0005

Appendix V: Comparison of the width of the impulse response functions from mesopelagic and shallow-water coastal species of malacostracan using the variable σ

Appendix V displays the p-values obtained from a post-hoc Tukey test used to determine the difference of the value of σ between individual malacostracan species (σ = width factor of impulse response function)

	Crangon crangon	*Palaemon elegans*	*Pasiphaea multidentata*	*Sergestes arcticus*	*Meganyctiphanes norvegica*	*Systellaspis debilis*
Crangon crangon σ = 1.23		0.799	0.522	0.996	0.033	0.798
Palaemon elegans σ = 1.07			0.966	0.987	0.345	1.000
Pasiphaea multidentata σ = 0.92				0.808	0.954	0.995
Sergestes arcticus σ = 1.16					0.159	0.971
Meganyctiphanes norvegica σ = 0.74						0.661
Systellaspis debilis σ = 1.03						

For all species, result of univariate analysis of variance: $F_{5,30} = 2.4$, $p=0.059$

Appendix VI : Comparison of response latency between species using the variable *d*

Appendix VI displays the p-values obtained from a post-hoc Tukey test used to determine the difference of the value of *d* between individual malacostracan species (*d*= latency in millseconds)

	Crangon crangon	*Palaemon elegans*	*Pasiphaea multidentata*	*Sergestes arcticus*	*Meganyctiphanes norvegica*	*Systellaspis debilis*
Crangon crangon d = 24.40		0.507	0.812	p<0.0005	0.004	0.000
Palaemon elegans d = 19.50			1.000	p<0.0005	0.164	0.000
Pasiphaea multidentata d = 19.60				P<0.0005	0.392	0.000
Sergestes arcticus d = 40.10					p<0.0005	0.304
Meganyctiphanes norvegica d = 11.30						p<0.0005
Systellaspis debilis d = 48.00						

For all species, result of univariate analysis of variance: $F_{5,30} = 27.7$, $p<0.0005$